SIMULATION AND EXPERIMENTAL STUDIES OF HAULAGE DRIVE SYSTEM IN AN UNDERGROUND COAL MINE FOR ENERGY CONSERVATION
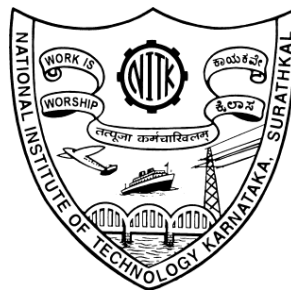
Thesis submitted in partial fulfillment of the requirements for the degree of

DOCTOR OF PHILOSOPHY

by

GANAPATHI.D.MOGER

DEPARTMENT OF MINING ENGINEERING
NATIONAL INSTITUTE OF TECHNOLOGY KARNATAKA
SURATHKAL, MANGALORE – 575025
DECEMBER , 2016

D E C L A R A T I O N

by the Ph.D. Research Scholar

I hereby *declare* that the Research Thesis entitled **"Simulation and experimental studies of haulage drive system in an underground coal mine for energy conservation"** which is being submitted to the **National Institute of Technology Karnataka, Surathkal ,** in partial fulfillment of the requirements for the award of the Degree of **Doctor of Philosophy** in **Mining Engineering,** is a bonafide report of the research work carried out by me. The material contained in this Research Thesis has not been submitted to any University or Institution for the award of any degree.

110676MN11P01, Ganapathi. D.M
(Register Number, Name & Signature of the Research Scholar)

Place: **NITK, SURATHKAL**

Date : December , 2016

C E R T I F I C A T E

This is to *certify* that the Research Thesis entitled **"Simulation and experimental studies of haulage drive system in an underground coal mine for energy conservation"** Submitted **by Mr.Ganapathi.D.Moger**,(RegisterNumber:**110676MN11P01**) as the record of the Research work carried out by him, is *accepted as the Research Thesis submission* in partial fulfillment of the requirements for the award of degree of **Doctor of Philosophy**.

Dr.Ch.S.N.Murthy   **Dr. Udaykumar .R.Yaragatti**
 Professor And Research Guide   **Professor And Research Guide**
Dept. of Mining Engineering   Dept. of Electrical and Electronics
                                                                        Engineering

(Name and Signature
With Date & seal)
Chairman-DRPC
(Signature with Date and Seal)

ACKNOWLDGEMENT

ABSTRACT

The field study is carried out in GDK 10A incline (an underground coal mine) of "The Singareni Collieries Company Limited"(The SCCL).

The man riding system is used in GDK 10A incline for transportation of men to different levels in underground by using two haulage drive systems (each 150hp). One drive system is used to transport men from surface to 8th level (8L) and another drive is used from 8L to 42nd level (42L). Energy consumption was calculated for each drive system for up the gradient and down the gradient i.e. 1 in 4.

In the Department of Mining Engineering, a laboratory set-up for mine haulage drive system was fabricated using 3hp slip ring induction motor, similarly two man riding haulage drive system used in GDK 10A incline (field). The energy consumptions is measured using conventional control with different combination of gradients and loads, for both up the gradient and down the gradient.

The experimental study in the laboratory is also carried out on 3hp motor. The laboratory set-up is suitably modified for carrying out experiments by micro controller method. The micro controller experimental setup consisting of IGBT based speed control drive unit by using AT Mega 32 micro controllers are used to implement with proper control algorithms. The energy consumption is measured using micro controller method with different gradients and loads, for both up the gradient and down the gradient. The laboratory experimental results of both methods (i.e conventional and micro controller) are presented. Experimental results are in good agreement with the simulation results.

The mathematical modeling of power requirement in general is done for haulage drive system for forward and reverse direction on inclined plane with different loads. The machine model is developed in the stator flux reference frame. Mathematical modeling of conventional drive system and micro controller (static Kramer) drive system for 3hp laboratory experimental study and 150hp underground haulage drive is also done. The principle of operation and control philosophy are explained in detail in the thesis. The dynamic equations for the power circuit which are derived from stationary and synchronous reference frames are explained in the thesis. The design of voltage controller, current controller and of rotor controller of open loop and closed loop system are also discussed in the thesis.

The computer software package MATLAB/SIMULINK is used to simulate the 3hp laboratory experimental haulage drive system (i.e. with slip ring induction motor) and micro controller haulage drive system. Similarly two man riding haulage systems in an underground coal mine (i.e. one 150hp hauler serving from surface to 8th level and another serving from 8th level to 42nd level) are modeled for both up the gradient and down the gradient and simulation is carried out using field data.

The results of simulated, experimental and field for methods, (i.e. conventional and microcontroller) are presented and compared. The slip power recovered in both methods is studied and found that the values are varied from 1.644 kWh to 3.260 kWh (for 150hp haulage drive system) and from 0.088 kWh to 0.143 kWh (for 3hp experimental). The cost for 150hp hauler drive system is calculated by taking data for energy consumption (i.e. power, time and number of trips) for 1 year for conventional method. The cost for 150hp haulage drive system is also calculated based on simulation results of both conventional and micro controller method. It is found that difference in cost for 150hp haulage drive system in an underground coal mine for conventional method based on field study results and simulation results on average is Rs.49,19,611/- and for micro controller method based on field study results and simulation results on average is Rs.45,86,661/-.

Similarly, cost for 3hp experimental haulage drive system for both methods (i.e. conventional and micro controller) is calculated by using experimental data and compared with cost estimates based on simulation results. The difference between cost analysis based on experimental and simulation results for conventional method is Rs.8437.61/ - and micro controller method is Rs.7492.13 /- .

In the present study 8% to 9% of slip power is recovered by adopting the microcontroller based control technique.

TABLE OF CONTENTS

<p style="text-align:center">CONTENTS   PAGE NO</p>

LIST OF TABLES

LIST OF FIGURES

NOMENCLATURE

T_{em}— Electromagnetic torque

ω_s— Stator speed

I_{dr}— d-axis current

I_{qr}— q-axis current

R —radius of the drum

F— Force

Ftg—force due to gravity of the loaded tubs along the incline plane.

Ftf - force due to friction of the loaded tubs along the incline plane,

Frg— force due to gravity of the rope along the incline plane .

Frf— force due to friction of the rope along the incline plane

θ—Aangle of inclination ,

Mt —total mass of the tubs.

Mr— Total mass of the rope.

μt — coefficient of friction between the tub and incline surface.

μr —coefficient of friction between the rope and incline surface.

$V_{ds}{}^s$ —d- axis stator voltage

$V_{qs}{}^s$ —q- axis stator voltage

ωm—rotor speed

T_{em} —Electromagnetic torque.

T_L —Load Torque

J —Moment of inertia

B— Coefficient of friction and wind age.

P —Output power of the Shaft

Ø − Electromagnetic flux

$\frac{n1}{n2}$ − Speed ratio

Pin − Input power

$cos\,Ø$ −Power factor

Rs − Stator resistance

Rr − Rotor resistance

Xs− Stator reactance

Xr− Rotor reactance

Rext − External resistance

S − slip per unit

ωs −slip speed

Id − Dc current

Vd − slip voltage

V_L − stator line voltage.

V_l− Inverter terminal voltage

m −Modulation index

Ton − on time of IGBT

Ts− Total switching time.

P_g − Air gap power

P_m−The mechanical output power.

P−Number of poles

P_{stator} − Stator power

P_{rotor} −Rotor power

$\cos Ø_1$ − Effective power factor of the inverter

$\cos Ø_2$ − Angle between the fundamental secondary current and the slip e.m.f

Ps−Secondary power

Pmech – Mechanical power

ωr– Rotor speed

Pgen– Generated power

kp and k_i – Proportional and integral gain

K– Gain

Gv(s)– Transfer function

P_g – The air gap power

MRS- Main receiving station

IGBT –Insulated bi-polar transistor

N_1- actually speed of the motor

N_2 – reduced speed ratio

AVR- Automatic voltage controller

PWM – Pulse Width Modulation

R0 – Zero Rotor Resistance stud

R1 – Minimum Rotor resistance stud

R2 – Maximum Rotor resistance Stud

N_1- Actual speed

N_2 – Shaft speed.

S- Slip of the machine.

Ns – Synchronous speed

f - supply frequency

i_{rd} & i_{rq} - Instantaneous values of the *d-axis* and *q-axis* rotor current reference respectively .
.

CHAPTER 1

INTRODUCTION

Coal sector is one of the prime sources of energy of our country and majority of Indian coal resources are spread over the states of Telengana, Assam, Chhattisgarh, Jharkhand, Madhya Pradesh, Maharashtra, Meghalaya, Odisha,West Bengal and in few other states. The industrial sector in India is a major energy user, accounting for about 48% of commercial energy consumption. In the process of exploration, mine development extraction of minerals, beneficiation, handling etc; enormous amount of energy is used in mining industry .Coal industry in India also accounts for employing the largest work force in its operations.

The mining sector has become increasingly energy-intensive over the time. There are wide variations in energy consumption among different units within the same industrial sector and in particular mining industry. The energy savings potential in this sector is estimated to be up to 20%. Despite the large potential for energy efficiency investments having financially attractive returns, only a small fraction is actually being tapped. Thus there is a need for concerted efforts, whether voluntary or otherwise, to promote energy efficiency in the industrial sector and mining in particular.

At present, most of the coal enterprises in India have similar problems, such as large energy consumption and low effective utilization. With the rising of energy prices, and more prominent contradictions between supply and demand of electric power, it is necessary for coal enterprises to strengthen energy management, reduce energy consumption, and change the mode of economic growth in order to achieve sustainable development through energy conservation.

Keeping in this in mind the studies carried out in an underground coal mine (i.e. GDK 10A Incline) in man riding system using conventional 150hp slip ring induction motor to study the influence of load on energy consumption during up the gradient and down the gradient. Necessary fabrication is done to carryout experimental studies in the laboratory to study the influence of the load during up the

gradient and down the gradient and also the gradient (i.e. angle with horizontal) on energy consumption using 3hp conventional method (resistance control), as well as with micro controller based drive system.

In simulation study by using MATH LAB/SIMULINK software package is used for modelling the drive system. For carrying out experimental studies in the laboratory 3hp experimental setup was made in the department of mining engineering. Which is similar to haulage drive system in the field. However, in the field the haulage drive system is used for man raiding (varying load) for both up the gradient and down the gradient. In the laboratory the haulage drive system is used for movement tubs (varying load) for both up the gradient and down the gradient. The experiments are carried out with conventional method and micro controller based method by varying load, for both up the gradient and down the gradient of the drive system. In both field and laboratory studies, energy consumption is noted by varying of electrical and mechanical parameters of drive system.

The Energy conservation means reduction or perhaps elimination of unnecessary energy usage and wastage. In many industrial applications 70% of overall electrical energy obtained is used only for electric motors driven equipments (Tripathy, S.C., 1991).The mining industry, which is the backbone of development of any country, requires huge amount of electric power. As Electric power is a major energy of coal enterprise, economy of electric power is an important direction and main thrust to reduce total energy consumption.

The main scope for power-saving of coal enterprises is electric power supply systems and electrical equipments. The coal enterprises should reinforce the technological transformation of mechanical and electrical Equipments and generalize power-saving products. In recent years energy efficient motors are available in all sizes, and thus in case of any replacement this new generation motors need to be installed. Under emergencies, the user should go for multiple winding of the motors, since every winding inherits certain losses.

The mine haulage drive system plays an important role in the underground coal mines. The energy consumption is high in conventional system used for mine hauler drive (direct rope haulage), since resistance controls pertaining to speed control connected with three phase slip ring induction motor.

2

This is not an intelligent to efficient controller with regard to precisely controlling speed in order to regulate power requirement. The conventional hauler also consumes more power for regular maintenance. Therefore, the productivity and safety of conventional hauler is not appreciable.

Simulation of the 3- Phase induction machine is well documented in the literature and a digital computer solution can be performed using various methods, such as numeric programming, symbolic programming and the electromagnetic transient program (EMTP). The main advantage of SIMULINK over other programming software's is that, instead of compilation of program code, the simulation model is built up systematically by means of basic function blocks. Through a convenient graphical user interface (GUI), the function blocks can be created, linked and edited easily using menu commands, the keyboard and an appropriate pointing device like the mouse.

A set of machine differential equations can thus be modeled by interconnection of appropriate function blocks, each of which performing a specific mathematical operation. Since SIMULINK is a model operation programmer, the simulation model can be easily developed by addition of new sub-models to cater for various control functions. As a sub-model the induction motor could be incorporated in a complete electric motor drive system.

Today more than 75% of the load in the industry of any country consists of induction motor drives. Wound rotor induction motor drives have found great applications due to the availability of slip power easily available from slip rings. Slip Ring Induction motors are widely used for high torque and variable speed applications.

Conventional methods of speed control of Slip Induction Motor from rotor side lead to wastage of energy in external resistance. Wound rotor induction motors have been popular for decades in the cement and mining industry for starting and driving large grinding mill. A wound rotor induction motor is large AC motor which has capability to control the starting characteristics and is having its own adjustable speed ability. Slip power recovery wound rotor induction motor drives are used in high power, limited speed range applications where control of slip power provides the variable speed drive system. Conventional method of speed control of slip ring induction motor is variable resistance method but more losses occur.

In this present research, conventional rotor resistance control method (Static Krammer drive) and micro controller based method (i.e. for slip power recovery) were used for the speed control of slip-ring induction motor. Furthermore, the analysis of speed and power loss has been carried out. To develop a Mathematical model for slip ring induction motor and sub synchronous converter system using data collected from field (underground mine), a simulation study was carried out using technical specifications of 150hp haulage drive system.

Matlab based Simulink model has developed with open loop operation using conventional control and micro controller (static Krammer) based methods. Similarly, simulation study was carried out for using SIMULINK/MATLAB software package and also experimental study in the laboratory has carried out using conventional based and microcontroller based methods for 3hp experimental mine haulage drive system.

1.1 ENERGY SCENARIO IN INDIA

1.1.1   Energy Need

India is equally maximum power manufacturer and a user. Presently, India rates seventh in world's maximum power producer, It is about 2.49% of the overall power generation in the world. It is also the world's fifth major electricity consumer.

There are various difficulties that are being faced by Indian Power Sector:
  i.   The increasing cost of power supply
  ii.   Less power generation

In the coming year's requirement of power supply increases to large extent and these may lead to overall impact on economy of India, because of safe guard of energy and exchange of foreign currency requirement. Industrial power requirement in India is planned to preserve the world's second highest rate associated with GDP development averaging 5.6% per year from 2006-2030. India's financial development for future 25 years is actually required to obtain additional from light industries and services when compared with large industries, in order to that the industrial share regarding the power usage declines from 72% with 2006 to 64% with 2030.

Modifications are associated with changes in India's manufacturing gas mixture with energy use raising more faster than coal use in the manufacturing sector.

Currently, almost all of the coal companies in India have the adverse effects, such as huge power requirement and low efficient usage, with the increasing of power tariffs, extreme scarcity of water day by day, and much more visible contradictions among supply along with requirement of energy, it is crucial for coal companies to improve power operations, lower the power usage, along with adjustment of the actual function of financial progress in order to achieve eco friendly growth.

In our country the following are the main problems:

  i. Optimum demand general shortage close to 14% and a generation shortage of 8.4%.

 ii. 6%raisein India's GDP imposes a higher requirement of 9% on its power sector. Therefore, power generation capacity will be increased to 115,794MW and implemented in the next 11years.

iii. The sector-wise electricity usage in India is presented in the chart 1.1.The electricity available in different sources according to different country wise is presented in Table 1.1.Sector wise ultimate electricity usage (past and projected) is presented in pie chart 1.2.The source of electricity demand for the year 2011-2012 is 1067.88 billion units and coal demand is 173.47million tons (Planning commission BUA). The natural source of energy in different countries are presented in Table1.2 (Putri ZalilaYaacobet al.,1993).

Table 1.1 Natural source of energy

COUNTRY	OIL	NATURAL GAS	COAL	NUCLEAR ENERGY	HYDRO ELECTRIC	TOTAL
China	275.2	29.5	799.7	9.8	64.0	1178.3
India	113.3	27.1	185.3	4.1	15.6	345.3
Japan	248.7	68.9	112.2	52.2	22.8	504.8
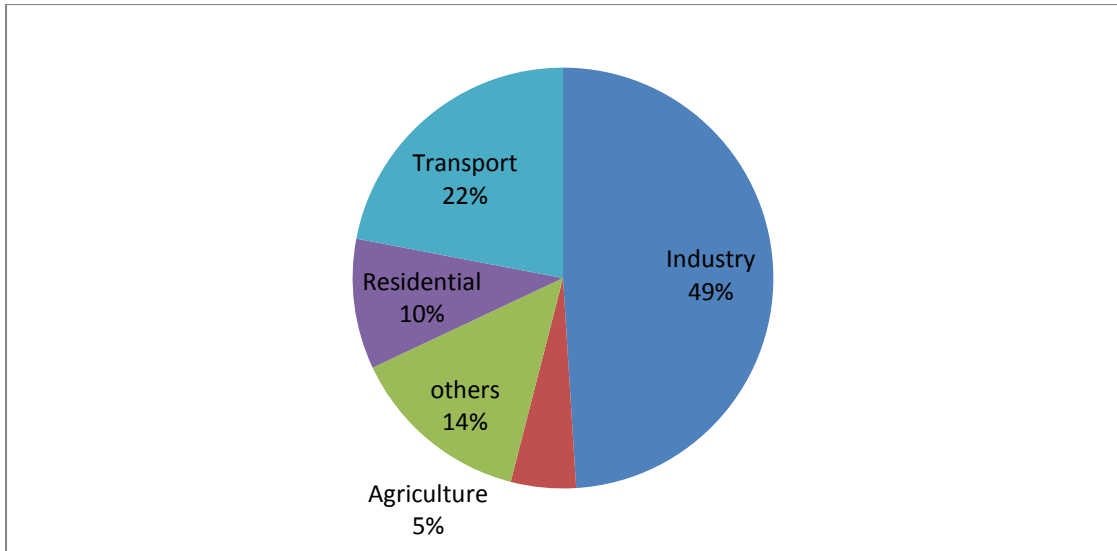
Chart 1.1 Sector wise ultimate electricity usages (past and projected)

Table 1.2 Requirement of final electricity usage (CEA, 2009)

Source	Units	1994-95	2001-02	2006-07	2011-12
Electricity	Billion Units	289.36	480.08	712.67	1067.88
Coal	Million Tones	76.67	109.01	134.99	173.47
Lignite	Million Tones	4.85	11.69	16.02	19.70
Natural Gas	Million Cubic Meters	9880	15730	18291	20853
Oil products	Million Tones	63.55	99.89	139.95	196.47
Source : Planning Commission BAU: Business As Usual					

Following tips are initiated for energy conservation policy in energy sectors:

i. Various energy sector reforms undertaken by Government

ii. Coal policy initiatives and other reforms

iii. Private investment allowed for import and marketing

iv. Liberal framework of development for the power sector

v. Industrial appetite for energy is insatiable

vi. Ever-increasing energy needs - huge investments

vii. Non-renewable energy sources finite and dear

viii. Sustainable development - adopt energy efficiency measures

ix. Energy conservation potential for economy - 23%

x. Energy management and conservation is need of the hour.

All India energy consumption sector-wise till end of 1st year of 12th plan is presented in chart 1.2(CEA , 2009).

Chart 1.2 Indian sector-wise Energy consumption
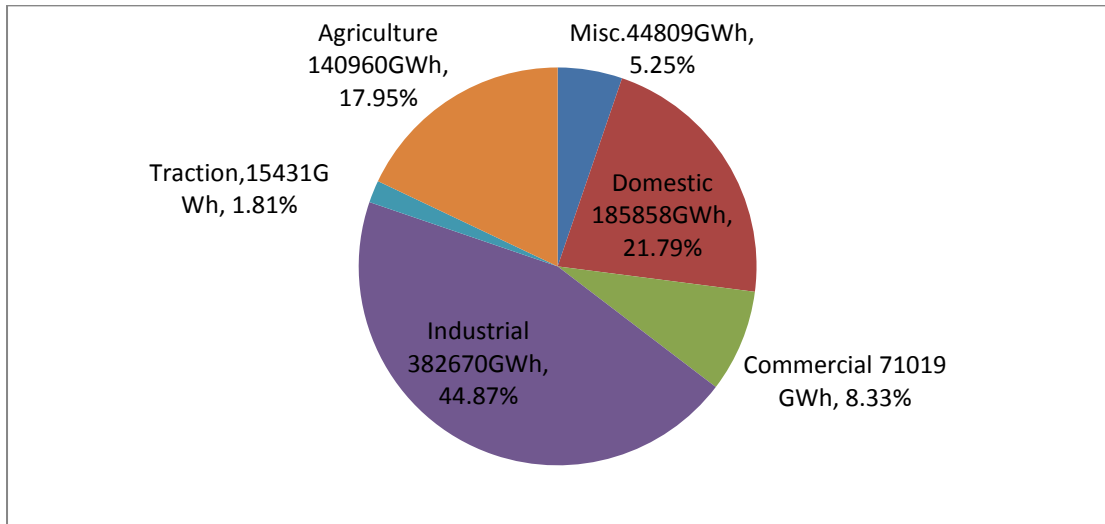
Source: CEA, 2009

Electricity usage prospective in Indian sector is given in Table 1.3 and energy saving potential in Indian sector is also given in Table1.4 (CPRI Bangalore, 2007). According to the collected energy conservation data percentage of energy conservation potential of many industries are lagging because of different drive methods and type of drives used. In particular, industries will depend upon the induction motor drive. And most of the modern industrial drive systems are of static controlled. In some of the process industry energy consumption varies on the type of drive used. The energy saving potential in Indian industrial sector will conserve more energy than other energy sector. One of the main reasons the industries are following the energy conservation policy in their sector (Energy Audit Report for HOCL by CPRI, 2007). Sector-wise energy saving potential is given in the following section. In this the agriculture sector consumes more energy compared to the industrial sector.

Table 1.3 Electricity usages prospective in Indian sector (Energy audit report
for HOCL by CPRI, 2007)

	%Share of Energy price	Conservation Potential (%)
Steel and Iron	15.8	8-10
Pesticides andFertilizers	18.3	10-15
Textile	10.9	20-25
Cement	34.9	10-15
Chlor-alkali	15.0	10-15
Pulp and paper	22.8	20-25
Aluminum	34.2	8-10
Ferrous Foundry	10.5	15-20
Petrochemical	12.7	10-15
Ceramics	33.7	15-20
Glass	32.5	15-20
Refineries	1.0	8-10
Ferro - Alloys	36.5	8-10
Sugar	3.4	25-30
Industries Potential(%)		
Economy as a whole		up to 23
Agricultural		up to 30
Industrial		up to 25
Transport		up to 20
Domestic and commercial		up to 20

1.1.2 Electrical energy conservation at GDK 10A incline

In industrial process like prime movers, compressors, water pumping and many other applications, the induction motor is used as a main drive. But induction motor consumes huge amount of energy for industrial applications. As per survey, the maximum industrial motor loaded up to 50% or even less than 50%. So that in under loading condition, the induction motor leads to low power factor and efficiency of the motor decreases. As per an estimate by adding 1.1KMW power capacity with low investment, the efficiency of the motor can improved by 2% (Chakarbarthi et al.,1992).Economic proposal can be obtained by selecting correct size of motor particularly fluctuating speed drive for fluctuating load application such as blowers, fans, compressors etc.

The energy conservation process can be implemented in various mining aspects and tools like, illumination, haulers, conveyors, winding system, transformer,

drilling and blasting equipments, cutting tools, crushers, refrigeration and other electrical equipments (Pradhan et al, .2010).An attempt is made in this thesis to study the consumption of energy in GDK 10A incline, underground coal mine of "M/s The Singareni Collieries Company Limited" (The SCCL).

By adding the external resistance to rotor is very commonly adopted in rotor circuit. The resistance can be in two forms, that is, liquid rheostat and discrete resistors with contactors**.** External resistance reduces the high starting current for smooth start and changing the speed at which the motor develops high torque. By selecting proper resistance, at low speed maximum torque can be developed **.**This method of control causes more energy to be wasted.

Implementation of energy conservation technology in mines improves the overall efficiency of mining machineries and lighting systems will lead to energy saving and also improve the generation of energy with existing resources.

SLIP RING INDUCTION MOTOR WITH CONVENTIONAL CONTROL SETUP → **REDUCTION GEAR WITH FORWARD & REVERSE MECHANI** → **ROPE DRUM** ↔ **TUB OR CAR**
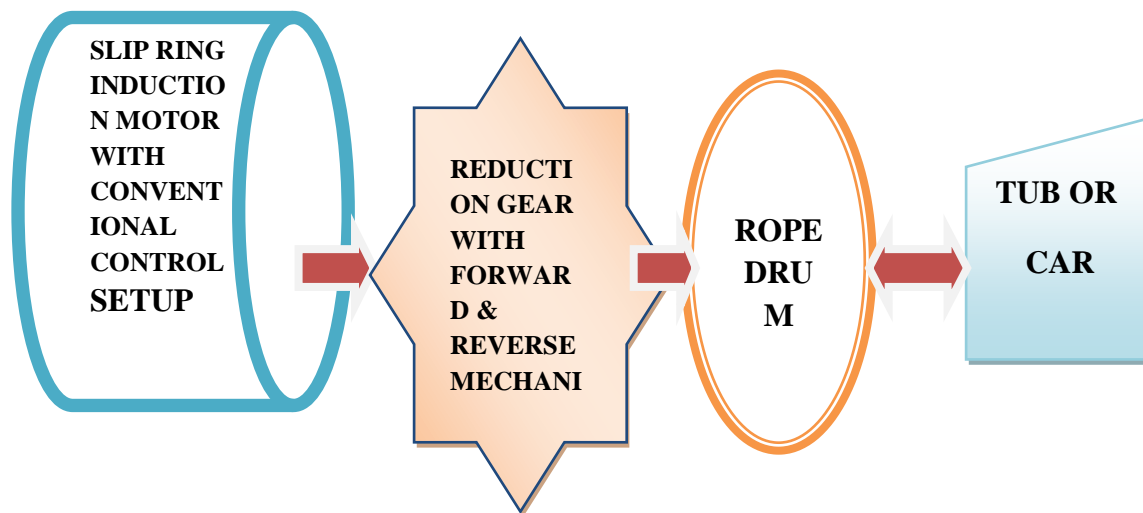
Figure 1.1 Block diagram of Direct Rope Mine Hauler

"Mine hauler is a mechanism used to move up and down load from one level to another level through track as means". Mine haulers act as a very important transportation system in an underground coal mines to transport the coal and materials and consumes huge amount of electrical energy**.**

Conventional hauler works on nonlinear resistance controls with brush gear three phase slip ring induction motor. The some parts of the hauler which requires regular maintenance and it needs replacement due to high power requirement. Caliper

type brakes with hydraulic cylinders were introduced with 87hp and 150hp haulers which are being used for man driving application. The block diagrams of mine haulers are shown in Figure 1.1. Each block represents the different components used for haulage drive in the visited mine. The slip ring induction motor, reduction gear system (1:29), rope drum and tub or car with rail track are the main components of direct rope haulage drive system in mine.

1.1.3 Overview of Energy Conservation in Underground Coal Mines

In this section various equipments considering energy in underground mines are listed. In Any under Ground Coal Mining Operations the major areas of energy use are   (Mahto, 2009)

      i.   Winding /transportation of men and material (shaft or incline, with rope haulages' or conveyor etc.)

     ii.   Pumping/de watering

    iii.   Use of LHDs/SDLs, coal drills, etc.

    iv.   Illumination

     v.   Ventilation system.

As per literature review of the energy conservation pattern of mechanized mines of coal India, the energy share in total power (percentage) (Chakrabarti et al.,1992) is presented in Table1.4. According to the content in the table mine dewatering requires more consumption compared to other purposes.

Table1.4 Energy consumption for different purposes in mines (Pradhan et al., 2010)

Consumption purpose	Average	Range
Mine Dewatering	35	20-50
Ventilation	20	15-35
Winding	10	5-20
Horizontal transport(rope haulages/conveyors)	15	10-30
Coal face(SDLs/HDL, ,coal drill)	10	2-15
Others	10	5-15

In mine dewatering purpose, the methodology adopted to install pumps in old underground mines resulted in improper pumping load distribution. By having a

proper planning, a lot of electrical power can be saved. This opens wide scope for reorganization of the total system, especially in old mines. Following are the main methods used for conservation of energy in underground coal mines for dewatering purpose:

i. Lack of standardization (head and discharge and type of water to be handled).

ii. Inadequate sump capacity or gradual decrease of sump capacity due to silting etc. Poor sump layout.

iii. Using higher capacity pumps at suitable location reducing too many intermediate pumps leading to multi stage operation. This will reduce the energy consumption.

iv. Staggering the operation timing of pumps to reduce the peak demand and wrong selection of pumps.

v. Pump foundation– reduction of vibration in the pump can help in having better life of bearing. This will help to prevent overloading of motor and reducing the energy consumption.

vi. Foot valve position – care is to be taken to stop sucking of slush and other unwanted material inside the suction pipe, choking the impellers and reducing the discharge of water.

vii. Maintenance of pumps and pipe line network (below and above ground).

viii. Controlling leakages in delivery lines for reducing working hours of pump.

ix. Proper selection and size of suction and delivery pipes, avoiding sharp bends, non –return valve on delivery lines etc.

x. Using microprocessor or micro controller based soft starter for machinery to reduce energy losses during starting and operation of the electric motors.

Proper Ventilation systems in underground coal also improve the energy conservation by selecting the following criteria.

i) The correct choice of main fan for a given mining condition.

ii) Correct calculation of pressure and quantity of air.

iii) Large variation in the actual performance curve from the theoretical curve stipulated by the manufacturer.

Total number of winding engines used in Coal India Limited (CIL) as on 1992 were 268, distributed over 123 mines, and having total power connected to the tune of 33MW (Chakrabarti et al.,1992).

Following measures are taken to improve the energy conservation in the winder system:

  i.   Speed control.
 ii.   Selection of motor vis-à-vis motor rating.
iii.   Switching over from A.C to D.C system.
 iv.   Use of thyristor drives, filtering system.
  v.   Reducing peak load through friction system of winding over the drum system.
 vi.   Reduction of dead weight by proper design of skips/cage etc; reduction in the rope size.
vii.   Pit bottom bunkers to help in the reduction of overloading factor of loaded skip or tubs to minimum. This will reduce the drive size in the same proportions. Also,
viii. It can improve the winder utilization factor considerably.

Winder system is used in mine shafts for movement of men and materials. Winder should be operated with totally enclosed air cooled motor having control thyristor drive, Programmable Logic Controller (PLC) for interlock and signaling system along with Human Machine Interface (HMI).One end of rope is attached to cage and other end is anchored to the drum. This is with two drums, one of the drums is keyed to main shaft known as fixed drum and another is driven via multi toothed clutch. While clutch slides on hexagonal shape drum shaft the actuation is operated by hydraulically operated cylinders with necessary inter locking.

Direct Current (DC) Winder comprises double drums driven by a 350hp DC motor through gear box and having facilities of a brake.

Hoisting speed of 3.6m/s is achieved by Thyristor fed DC Drive system - 1400A (max) Thyristor Converter with digital drive regulator.

Transportation system has essential part in underground coal mines to carry the men and material to different levels of coal mines. In this regard the following measures have to be applied to reduce the electricity use in transport systems.

  i.   Replacing mine tubs by mine cars can improve the haulage capacity.

ii.   Proper laying and maintenance of the tracks.

iii. Lubrication of the friction pulleys.

iv.   Proper rope guides.

v.   Proper layout/alignment of the conveyors, idlers, quality of bearings, housekeeping, etc.

Primary task of a mine winder is to move a loaded conveyor by means of rope from an underground station through the shaft to surface or vice versa for a loaded cage to move down the shaft. During each wind, the motor is accelerated according to the duty cycle and again decelerated after a constant speed phase, and this alternately in both directions of rotation.

Closed loop control system of 3 phase 6-pulse thyristor- fed D.C. winder is by continuous Armature reversal and unidirectional single phase field control. Automatic control of winder should follow the duty cycle closely. A prerequisite for this is the correct guidance of the speed reference value according to the duty cycle.

Energy conservation opportunities in pumping systems: In underground mines for pumping the ground water to outside, following steps are followed to reduce the energy conservation (Singh, 1994).

1.1.4 Selection of higher efficient motors:

In most mines and industries, right selection of motors is not done. This leads to running at under load resulting in heavy energy losses. Due to variable production planning of the mine, many a times, the motors are bound to operate at under load condition. One study indicates that mines having beneficiation system and fluctuating production plan give rise to 95% of their motors to operate at under loading condition. The average running is within 55-60% load. This can be rectified by proper selection of size and energy efficient motors. When there is a substantial cut in production, it is advisable to install a low capacity motor to effect energy saving.

1.1.5 Energy conservation in lighting:

In this method, new energy efficient lamps are used to conserve electrical energy in underground mines:

i.   Installation of energy efficient fluorescent lamps in place of "Conventional" fluorescent lamps

ii.   Installation of Compact Fluorescent Lamps (CFL's) in place of incandescent lamps.

iii.   Installation of metal halide lamps in place of mercury / sodium vapour lamps. Installation of High Pressure Sodium Vapour (HPSV) lamps for applications where colour rendering is not critical. Installation of light emitting diode (LED) panel indicator lamps in place of filament lamps. For example, from 54 Underground Mines and minimum 100 kms roadway lighting expected savings are of Rs.51.6 Lakhs per year (Annual report SCCL , 2009).

1.1.6 Energy conservation by power factor methods:

Following are measures taken in energy conservation by power factor methods:

i) Installation of capacitor banks at the Main Receiving Station (MRS) on the secondary side transformer to maintain the 'Unity Power Factor' and use the advanced power factor correction method to improve the energy conservation.

ii) Use of Automatic power factor controllers: Various types of automatic power factor controls are available with relay / microprocessor logic. Two of the most common controls are: Voltage Control and Kilovolt Ampere Reactive (KVAR) Control.

iii) Intelligent Power Factor Controller (IPFC): This controller determines the rating of capacitance connected in each step during the first hour of its operation and stores them in memory. Based on this measurement, the IPFC switches on the most appropriate steps, thus eliminating the hunting problems normally associated with capacitor switching.

vi) Energy conservation by energy efficient transformers: Most energy loss in dry-type transformers occurs through heat or vibration from the core. The new high-efficiency transformers minimise these losses.

The conventional transformer is made up of a silicon alloyed iron (grain oriented) core. Iron loss of any transformer depends on the type of core used in the transformer. However, the latest technology is to use amorphous material – a metallic glass alloy for the core. Expected reduction in energy loss over conventional (Si Fe core) transformers is roughly around 70%, which is quite significant. By using

amorphous core with unique physical and magnetic properties - these new types of transformers have increased efficiencies even at low loads - 98.5% efficiency at 35% load. Electrical distribution transformers made with amorphous metal cores provide excellent opportunity to conserve energy right from the installation.

1.1.7 Light distribution system in underground mines

In any opencast and underground coal mines lighting constitutes an important requirement for better safety of men and machinery and also productivity. Due to low investment in every mine lighting modifications get higher priorities to contribute effective energy saving potential without compromising the Directorate General of Mines Safety (DGMS) standards (Website of SCCL).

Power should not be transmitted to mine at a voltage beyond 11KV and should not be used therein at voltage beyond 6.6KV. Providing where handheld portable device is needed, this voltage should not meet or exceed 125 volts. Wherever electric lighting is used in underground coal mines, the lighting system will employ a middle of or even neutral position linked to earth and also the voltage should never go beyond 125 volts between phases. On the surface of a mine, the voltage should not increased to 250 volts, if the neutral or the midpoint of the system is connected with earth and the voltage between the phases should not increased to 250 volts; In which portable hand-lamps are employed in underground working of mine, the particular voltage should not go beyond 30 volts.

In which virtually any circuit is employed for that remote control device or electric powered inter-locking device, the circuit voltage should not go beyond 30 Volts. In fixed plants, the mentioned voltages may be allowed around 650 volts, when the bolted type plug has used.

1.1.8 Field study on energy conservation in a coal company (The SCCL)

Following measures were being implemented in this company for reducing energy conservation in underground operations (Sagar et al., 2002):

i.   Variable Speed Drives for Underground machinery (Haulers, Conveyor drives and Fans).

ii. Fibre reinforced plastic [FRP] runners for mine ventilation fans (under trial).

iii. Use of Compact Flourcent Lamps (CFL) & Sand Powder in underground illumination.

iv. Use of Variable Frequency Drives (VFD) over conventional drives.

v. Replacement of tub system by belt conveyor system.

vi. Stage pumping using pumps of low rating.

vii. Use of drill compressors for pneumatic bolting.

viii. Installation of Capacitor Banks in Surface sub-station.

In this company, specific energy consumption for coal production reduced from 25.19 kWh/T in 2003-04 to 17.76 kWh/T in 2008-09.Table1.5 presents the production of coal (million tonnes) output per man shift and specific energy consumption in 2003-04 to 2008-09(up to Feb). The Chart 1.1 presents the Production in million tonnes and specific energy consumptions kWh/tonne.

Table 1.6 represents energy consumption 2012-13 to 2015-16 (up to April 15) and the corresponding energy chart is also presented in chart 1.2. The following observations are made from the specific energy consumption of The SCCL (Annual report of The SCCL, 2009). Energy consumption depends upon coal production in the mine. Due to high productivity of coal the energy consumption requirement is also increased.

Table 1.5 Production of coal and energy consumption (million tonnes)

Years	2003-04	2004-05	2005-06	2006-07	2007-08	2008-09 (upto Feb)
Production (million tones)	28.941	27.326	29.556	30.274	30.811	29.942
Output per man shift (tones) overall including mines & departments	1.17	1.14	1.24	1.25	1.34	1.48
Specific energy consumption (kWh/tones of coal)	25.19	25.00	23.30	22.45	20.27	17.76

(Annual report of SCCL , 2009).
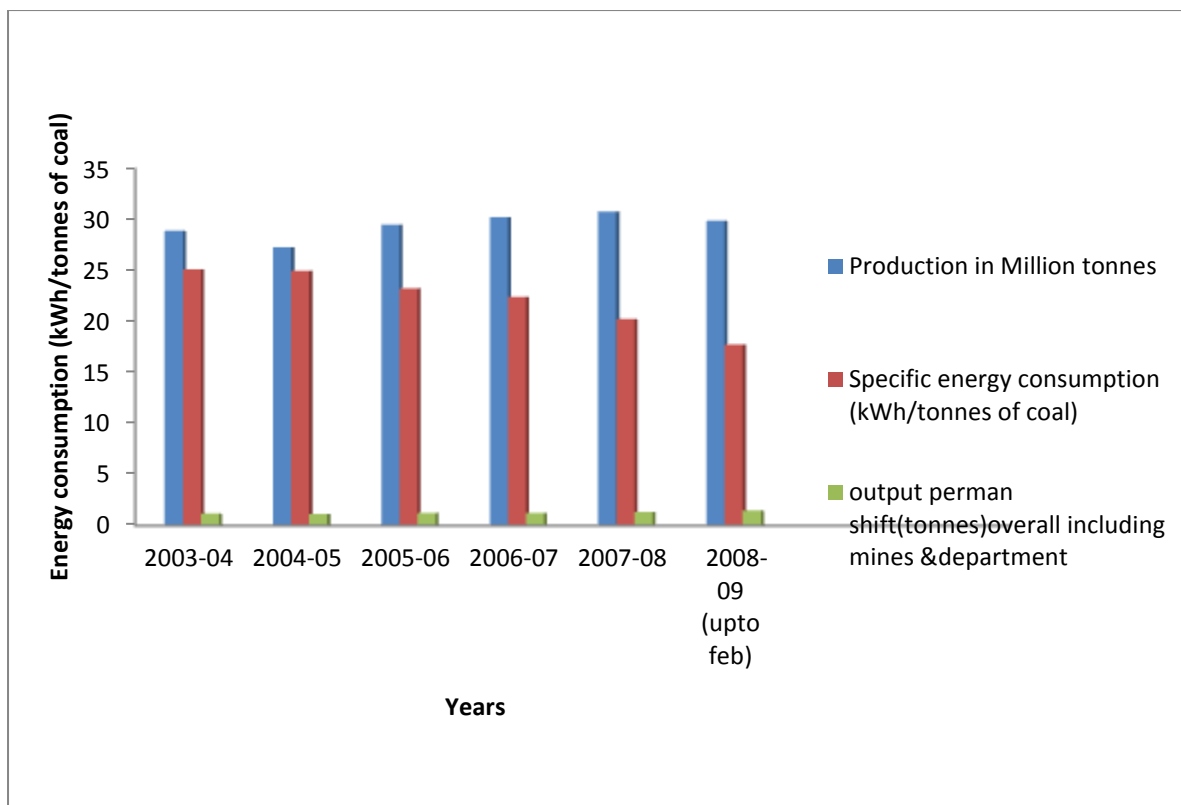
Chart 1.1(Annual report of SCCL, 2009).

Table 1.6 Electrical energy consumption in 2012-13 to 2015-16(up to April 2016)

(Annual report of SCCL, 2015-2016)

Years	2012-13 April12	2013-14	2014-15	2015-16
Coal output million Tones	3.17	2.90	2.37	4.32
Specific energy consumption (kWh tonnes of coal)	13.63	24.80	19.91	18.21
Total electrical Energy consumpation(million kWh)	57.71	57.81	58.77	58.87
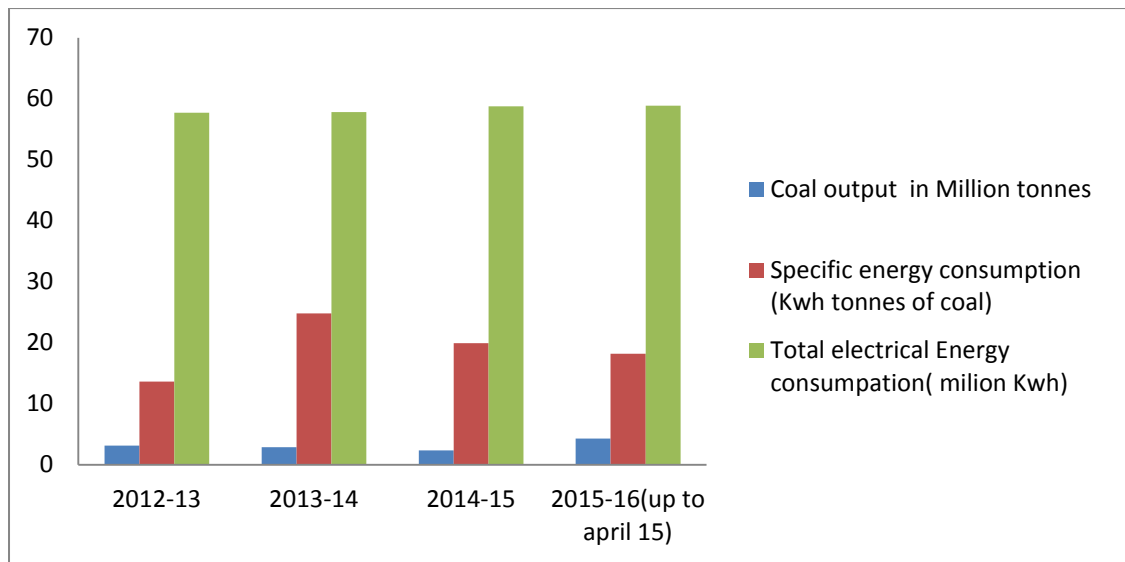
Chart 1.2 Energy consumption chart from 2012-13 to 2015-16 (up to April 15)

1.1.9. Haulage Drive System in an Underground Coal Mine

1.2.1 Rope haulage

Main roads feeding the shaft must supply a continuous stream of coal through the working shift. The rope haulage is successfully applied as main haulage. Rope haulage is applicable in all existing installations, and especially, where the road ways are driven in a seam of varying gradients in shallow mines where coal has to be hauled up an inclined drift to surface. Rope haulage may be classified under the following heads (Ghatak,1995):

i.   Direct rope haulage
ii.   Main and tail rope haulage
iii. Endless rope haulage
iv.   Gravity haulage

In these, direct ropes haulage is used for mine drive application because this is very popular and the simplest form rope haulage and has several variations. The equipment for this type of haulage consists of a single drum mounted on shaft, a jaw clutch being used to enable the drum to either run freely or to clutch to the shaft when a full set is being drawn up. Power is supplied by a motor which drives the gear

18

through the shafts. Lengths of rope, equal to the length of the haulage road plus a few extra coils on the drum are required for this type of haulage.

1.2.2 Endless Hauler

Instead of rope drum, a clifton wheel is connected to output of gear box. The rope of hauler connects to coal tubs in different directions to facilitate the tubs to travel in both directions on almost level/horizontal plane**.**

1.2.3 Tugger Hauler and Double Drum Scraper Hauler

These haulers consist of a rope drum driven by electric motor through internal and planetary gears system. The drum fitted on main shaft is supported by cast steel pedestals on either end. Planetary gears are mounted on the shaft and facilitate to transmit power to the drum. Drum starts rotating when applying clutch lever. After attaining maximum speed the clutch is pulled down to extreme lock position. For changing the rotation, one has to release the clutch, press brake lever and select push button in reverse direction.

In underground coal mines two different types of systems are used for the transport of men and they are,

 i.   Car type with multiple sitting arrangement
 ii.   Chair type with single sitting arrangement for each chair.

1.3 Method of Speed Control used in Underground Coal Mine

3-phase induction motor drive used for transportation of material and water pumping purpose, ect for both underground and surface mines. Most of the drives uses conventional speed control methods. This proposed method of control requires huge amount of energy to run the motor. Type of speed control for drive application is conventional method of speed control and static speed control method. Static control drive system consumes less energy compared to conventional control drive system. The conventional method of control is used for direct haulage man riding system in the concerned underground coal mine.

1.3.1 Conventional Method (Rotor Resistance Starter or Rheostatic Control)

Starter unit consists of three variable resistances connected in star. It is connected to the three slip ring terminals so that each phase of rotor winding has a variable resistance with it. The resistance of the rotor circuit can be varied by an external control. Figure 1.2 shows the rotor resistance starter for slip ring induction motor.

To start the motor, the resistances are set at their highest value. When the supply to the stator winding is switched on, the motor starts slowly with a high starting torque and relatively low starting current. Resistances are progressively reduced, thereby permitting the motor to speed up, until the three terminals are, in effect, short circuited and the motor runs at full speed.
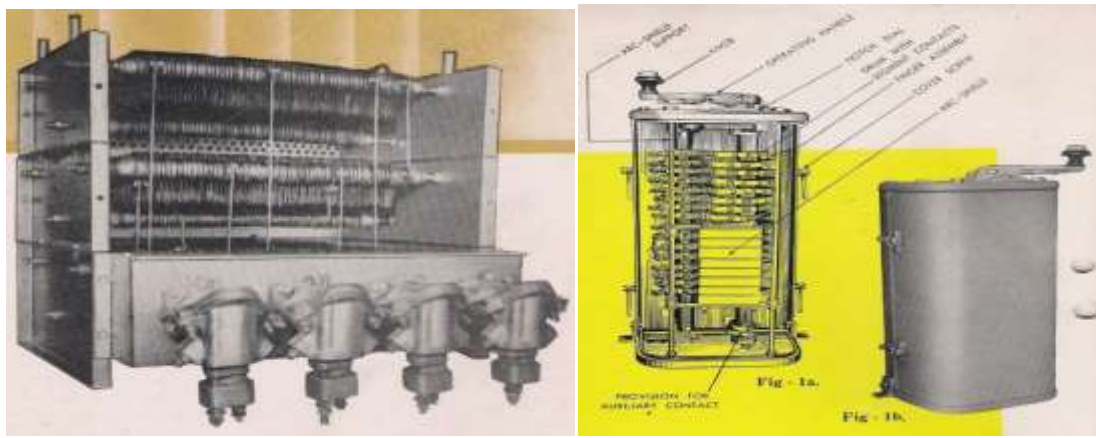
Figure 1.2 Rotor resistance starters or rheostatic control (BHEL, 2008)

1.3.2 Problems of rheostatic control in slip ring induction motor

Following problems associated with starter are discussed in this section.

i.   **External Cooling:** A portion of the input power has to be dissipated in the external rotor resistors. These resistors require cooling fans to dissipate the heat generated by them. The cooling fans form an additional load.

ii. **Maintenance:** Because of many contactors and other moving parts, it requires regular maintenance.

1.3.3 Static method of speed control:

This method of drive system is used for very few applications such as pumping the water in the underground mine and belt conveyer system, etc. Slip power wasted in the slip ring induction motor is recovered back and fed into the supply. This method is known as slip recovery method or modified Krammer method speed control discussed in the next section. This method is adopted in experimental mine drive haulage system using micro controller technique to reduce energy consumption.

1.4 General introduction to Slip Power Recovery

Efficient control of electric power, both at the generation and utilization ends, has been an important contributing factor for industrial growth in the twentieth century. Bulk of this power is generated and utilized through electromechanical energy conversion. Variable speed operation of electrical machines enables this conversion of power in a controlled manner. With the availability of power semiconductor devices the efficiency of conversion is high and, if desired, fast dynamic response can also be achieved.

Even though, Direct Current machines can be easily controlled and are inherently suitable for high dynamic performance, several disadvantages associated with the mechanical commutator have restricted their use in the recent past. On the other hand, squirrel cage induction machines have become increasingly popular due to their rugged construction and maintenance-free operation. Using field oriented control techniques, the flux and torque of an induction machine can be controlled in a decoupled manner and hence, fast dynamic performance, similar to that possible with Direct Current machines, can also be achieved.

While cage rotor induction machines are mainly used for medium power drive applications, the wound rotor or slip-ring induction machines are commonly used in large power drives having limited range of operating speeds. The increased cost of a slip-ring machine is justified by the reduced size of power electronic converter in the rotor circuit. So far, such machines were used as slip power recovery drives with pump or fan type of mechanical loads and mine drive application.

1.4.1 Basic concept of rotor side control

Speed of a cage rotor induction machine is primarily determined by the supply

frequency. Short circuited rotor offers very low resistance and the nominal slip is within 5%. A small part of the power fed from the stator (Ps) is lost in the rotor circuit (due to rotor resistive loss) (Pr) and the rest appears as mechanical output (Pm). Power flow diagram is shown in Figure1.3.Rotor power loss, being proportional to the slip speed, is commonly referred to as the slip power.

In case of a wound rotor induction machine it is possible to introduce additional resistance in the rotor circuit (Figure1.4). Thereby the rotor power loss increases with a corresponding decrease in the shaft output power. For the same load torque this results in an increased slip and a reduction in the shaft speed. Using variable rotor resistance it is, therefore, possible to vary the slip power and, hence the rotor speed.
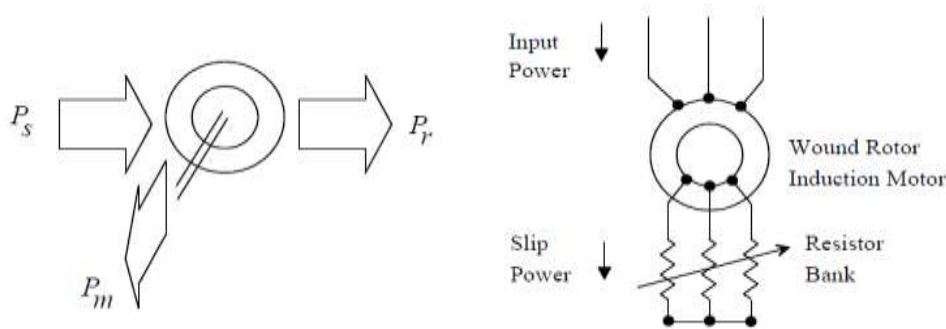
Figure1.3 Power flow in cage rotor induction motor. Figure1.4 Speed control of slip
ring induction motor with
external rotor Resistance

With the availability of thyristors this concept was utilized to introduce a dynamically varying resistance in the rotor circuit as shown in Figure1.5 (Sen et al. ,1975). It is shown that the torque produced by the machine is approximately proportional to the dc link current. Therefore, a speed controlled drive can be designed whose inner loop controls the dc link current by adjusting the duty ratio of the switch.

High starting torque is available at low starting current. Also improved power factor is possible over a wide range of speed. However, the method is inefficient because of the power lost in the external resistors and, is only used in intermittent speed control applications where the efficiency penalty is not of great concern.

If the slip power is absorbed by an appropriate electrical source instead of being

22

wasted in the resistive elements, the same objective can be achieved. The rotor power, in this case, is regenerated back in electrical form. It is possible to control the amount of power absorbed by the source and hence the shaft speed can be varied. If the source has both sourcing and sinking capabilities, power can be absorbed from or injected into the rotor circuit. Slip can, therefore, be positive or negative enabling sub synchronous and super synchronous operation.
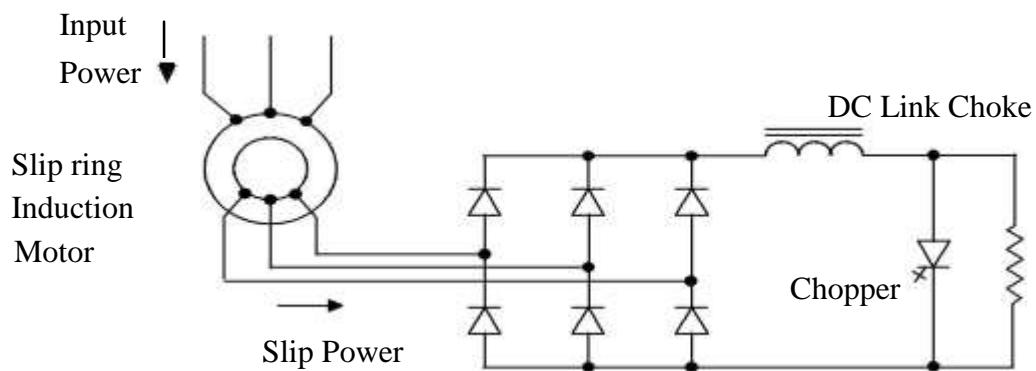
Figure 1.5 Wound rotor induction machine control with dynamic rotor resistance

1.4.2 Background of slip power recovery

Historically the controllable electrical source in the rotor circuit was another auxiliary machine. Slip power was recovered back either in mechanical form or in electrical form. Former was proposed by Krammer and the latter by Scherbius in the same year (1906). These schemes can be viewed in simplified forms as in Figure 1.6(a) and Figure 1.6(b). In Krammer drive the torque contribution of the dc motor reduces the mechanical load taken by the induction motor. On the other hand, electrical recovery by Scherbius scheme uses another induction generator which feeds back the slip power to the grid at power frequency. In both cases, slip is controlled by controlling the field of the dc machine.

With the availability of thyristors this concept was utilized to introduce a dynamically varying resistance in the rotor circuit (Sen et al., 1975) as shown in Figure 1.4. It is shown that the torque produced by the machine is approximately proportional to the dc link current. Therefore, a speed controlled drive can be designed whose inner loop controls the dc link current by adjusting the duty ratio of

the switch. High starting torque is available at low starting current. Also improved power factor is possible over a wide range of speed control.

(a) Krammer System

(b) Scherbius system
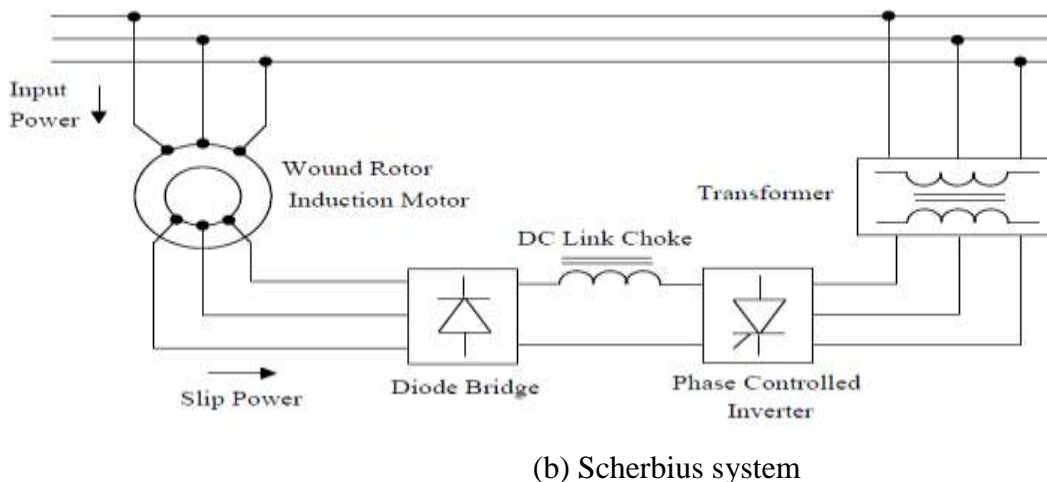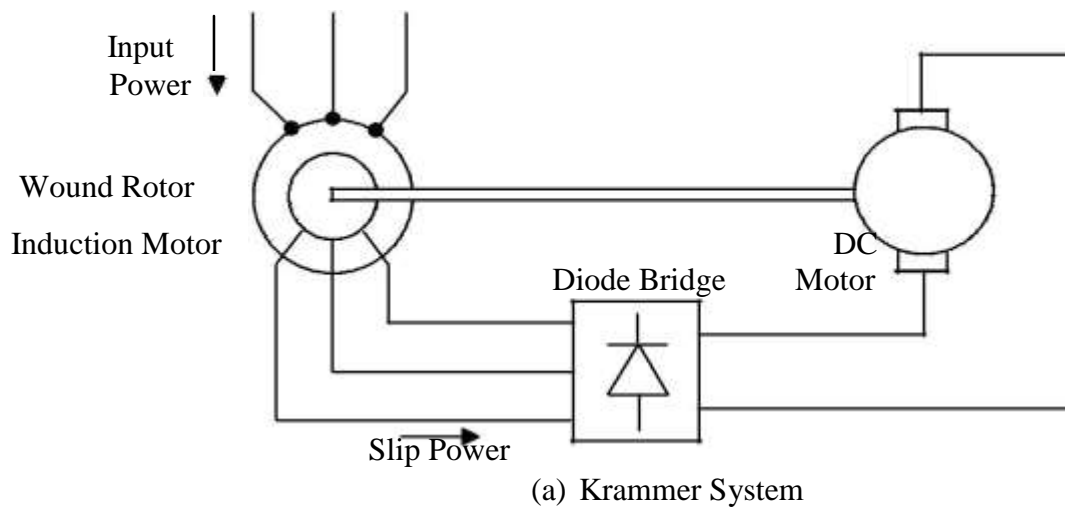
Figure1.6 (a) and (b) Slip power recovery schemes using auxiliary machines

With the advent of controllable power devices like SCRs, it was possible to dispense with the additional machines. Variable frequency slip power could be recovered by introducing a phase-controlled converter at the grid interface. This was proposed by several researchers in the 1960s. Erlicki (1965) proposed a scheme in 1965 where the rotor circuit was fed by an inverter operating at a frequency greater than the grid frequency. Inverter is the power source of the drive and part of the slip power is fed back from the stator to the grid.

A phase-controlled rectifier is provided between the inverter and the network, which permits continuous voltage control of the dc inverter supply. However, the

rating of the inverter and the rectifier in the rotor circuit has to be more than the mechanical output obtained from the drive.

More conventional scheme where the rotor power is rectified and fed back to the grid by a phase-controlled inverter (Figure 1.7) was subsequently proposed by Lavi and Polge (Lavi et al.,1966), and Shepherd and Stanway (Shepherd *et al*, 1969). This method of control became popularly known as the Static Scherbius system. A large dc link choke is used to interface the diode bridge output with the grid-side inverter. This ensures that the rotor current is continuous and proper control over the speed can be exercised by varying the inverter firing angle.

However, the inverter consumes reactive power because of phase control and the overall system power factor is poor. The reactive power demand of the inverter also depends on the slip range, being ideally zero when the rotor runs at the synchronous speed. To improve the system power factor a transformer with proper turn's ratio is connected between the inverter and the grid. The drive is started through external resistors in the rotor circuit which are subsequently cut-off when the designed slip range is reached.

With the diode bridge and inverter arrangement, a commutatorless Krammer drive for large capacity induction machines was proposed by Wakabayashi et.al.in 1976. (Wakabayashi et al.,1976) In this scheme the inverter in the rotor circuit drives a synchronous motor whose shaft is coupled to the main motor shaft; hence the slip power adds to the mechanical output. The inverter is load commutated; hence control at low speeds is not possible because of insufficient back EMF.
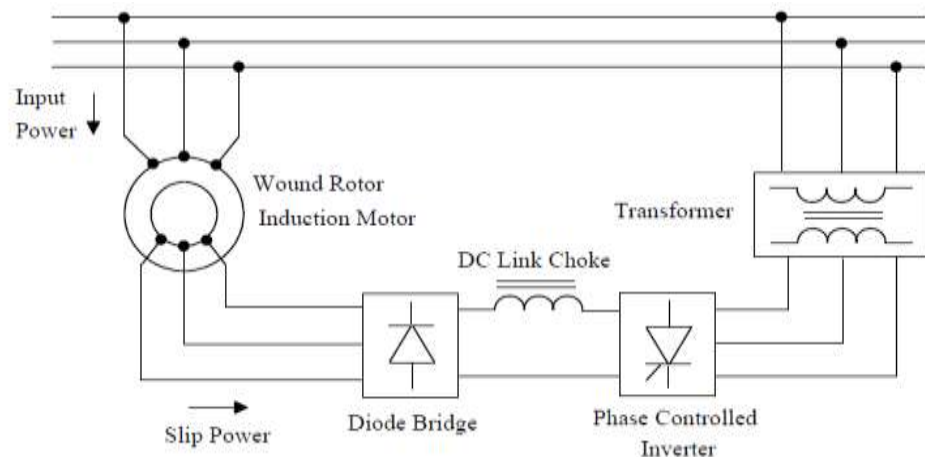
Figure.1.7 Static slip power recover scheme

Wind energy recovery using *Static Scherbius* induction generator was proposed *(*Smith et al.,1981).In their scheme a current source inverter is used on the rotor side and a fully-controlled rectifier on the line side. A novel signal generator concept, which is locked in phase to the rotor EMF, controls the secondary power to provide operation over a wide range of sub synchronous and super synchronous speeds.

The volt ampere (VA) rating of the current source is determined as a function of the gear ratio and the operating range. However, the need for a large dc link choke and commutation capacitors were the major disadvantages. Subsequently, Holmes et al., (1984) proposed a cyclo converter-excited divided-winding doubly-fed machine as a wind power converter. System was conceptually similar to the previous scheme, except that, the current source inverter was replaced by a cyclo converter in the rotor circuit. Krammer drive (micro controller) method is used to reduce the energy consumption in 150hp underground haulage drive system to GDK 10A incline mine.

1.5 INDUCTION MOTOR DRIVING TECHNIQUES

1.5.1. Frequency Control (V/F)

The 3hp micro controller based experimental haulage drive is implemented by variable frequency control method to reduce energy consumption in underground coal mine. Whenever AC supply is given to induction motor coil, a rotating magnetic field is produced and it rotates at synchronous speed (Patel,.2014) given by $Ns = \frac{120f}{p}$ where, N is the speed of rotor of induction motor Ns is the synchronous speed, S is the slip of the machine and p is the number of pole pairs of the motor.

In three phase induction motor EMF is induced by induction like that of transformer which is given by E or V= 4.44$\emptyset$KTf Now by modifying frequency, synchronous speed changes but with reduction in frequency and flux increase. Where E is the induced emf , $\emptyset$ is the flux per pole, K is the distribution factor, T is the turns per phase and f is the supply frequency.

1.5.2. Controlling Supply Voltage

The torque produced by running induction motor depends on number of poles (B. S.Cunha, 2001) rotor resistance, induced EMF, etc. Since rotor induced EMF $E_2 \propto$ V So, $T \propto sV_2$. From the equation given it is clear that by decreasing supply voltage

torque also decreases. Where E_2 is rotor output voltage, V is the output voltage of generator, T is the torque of the machine and s is the slip of the machine.

But for supplying the same load, the torque must remain the same and it is only possible if we increase the slip and if the slip increases the motor will run at reduced speed.   This method of speed control is rarely used because small change in speed requires large reduction in voltage, and hence the current drawn by motor increases, which cause over heating of induction motor. Hence driving efficiency is reduced.

1.5.3. Multiple Stators Winding Method

In multiple stators winding method of speed control of induction motor, stator is provided by two separate windings (Deepali et al., 2013). These two stator windings are electrically isolated from each other and are wound for two different pole numbers. The supply is given to one winding only and hence speed control is possible. A disadvantage of this method is that the smooth speed control is not possible. This method is more costly and less efficient as two different stator winding are required. This method of speed control can only be applied for squirrel cage motor.

1.5. 4. Adding Rheostat in the Stator Circuit

In this method of speed control of induction motor technique, rheostat is added in the stator circuit due to this voltage gets dropped .In case of three phase induction motor torque produced is given by $T \propto sV_2$ (Deepali et al.,2013). Where T is the torque ,S is the slip and V_2 is the rotor voltage of the motor . If there is decrease in supply voltage torque also decreases. But for supplying the same load, the torque must remain the same and it is only possible if there is increases the slip and if the slip increases motor will run at reduced speed.

1.5.5. Adding external resistance on rotor side

In this method of speed control of induction motor, external resistance is added on rotor side. If there is increase in rotor resistance, torque decreases. So if there is increase in slip, which will further result in decrease in rotor speed. Thus by adding additional resistance in rotor circuit the speed of three phase induction motor is deduced.

The main advantage of this method is that with addition of external resistance starting torque increases but this method of speed control of induction motor also suffers from some disadvantages like, the speed above the normal value is not possible, large speed change requires large value of resistance and if such large value of resistance is added in the circuit it will cause large copper loss and hence reduction in efficiency, presence of resistance causes more losses, this method cannot be used for squirrel cage induction motor.

1.5.6. Cascade control method

In cascade control method of speed control of induction motor, the two three phase induction motors are connected on common shaft and hence called cascaded motor. One motor is called the main motor and another motor is called the auxiliary motor. The three phase supply is given to the stator of the main motor while the auxiliary motor is derived at a slip frequency from the slip ring of main motor.

1.5.7. Injecting slip frequency EMF in to rotor side

When the speed control of induction motor is done by adding resistance in rotor circuit, some part of power, called the slip power, is lost as I^2R losses. Therefore the efficiency of three phase induction motor is reduced by this method of speed control. This slip power loss can be recovered and supplied back in order to improve the overall efficiency of three phase induction motor and this scheme of recovering the power is called slip power recovery scheme and this is done by connecting an external source of EMF (Electromotive Motive Force) of slip frequency to the rotor circuit.

The injected EMF can either opposes the rotor induced EMF or aids the rotor induced EMF. If it oppose the rotor induced EMF, the total rotor resistance increases and hence speed decreases and if the injected EMF aids the main rotor EMF the total resistance decreases and hence speed increases. Therefore by injecting induced EMF in rotor circuit speed can be easily controlled. The main advantage of this type of speed control of three phase induction motor is that wide range of speed control is possible whether it is above normal or below normal speed.

1.6 MICRO CONTROLLER DRIVE

Slip power recovery wound rotor induction motor drives are used in high power, limited speed range applications where Control of slip power provides the variable speed drive system. Simulation of the scheme is carried out using MATLAB/SIMULINK environment and experimental set-up is prepared in the laboratory for a 3-hp wound rotor induction motor. Microcontroller technique is used for the generation of Pulse Width Modulation (PWM) pulses for the inverter bridge (Ajay Kumar et al., 2013).

Advantages of static control method over conventional method:

    i.   In the recent development in electrical power semiconductor technology, induction motors are now being widely used in lots of fluctuating speed in industrial drives.

    ii.   It improves the power factor and controls starting torque current.

    iii.   Variable speed control can be achieved without much power loss.

    iv.   This scheme provides contactless and continuous variation of rotor resistance.

    v.   The control scheme for constant torque operation of induction motor is simple elegant and inexpensive.

    vi.   The torque is directly controlled and remains constant over a wide range of speed.

Disadvantages of conventional control method:

    i.   The deterioration causes large oscillating torque

    ii.   The formation of air bubbles always leads to different resistance in the induction machine rotor phases

    iii.   Around 20-30% of the power is wasted in the rheostatic control of slip ring induction motors.

    iv.   Requires frequent maintenance of various parts and sometimes replacement of components beside high power consumption.

1.6.1 Methodology in wound rotor induction motor drive using various Pulse Width Modulation (PWM) concepts

Micro controller plays a role in induction motor driving mechanism (Deepali et al.,2013). The controlling signals for the Insulated Gate Bi-polar Transistor (IGBT) switching will be taken care by micro controller. In Pulse Width

Modulation (PWM) technique, the amplitude is maintained constant but the ON and OFF time of each pulse is varied. The width of each pulse is made directly proportional to the amplitude instantaneous value of modulating signal.

The information being carried on the pulse train by encoded the width of pulses (Brig, 2012; Gajare,2012; Patel et al.,2014). Initiation of high power, fast switching devices and fast microcontroller has facilitated the expansion of variable speed induction motor drive systems.

Classic variable frequency converter consists of a rectifier, direct current (DC) link, and Insulated gate bipolar transistor (IGBT) inverter. There are two fundamental classifications of inverters used in variable speed induction motor drives

    i.   Current-source-inverter: Suitable for high power levels.

    ii.   Voltage-source-inverter: Suitable for lower levels hence pulse width modulation (PWM) inverter is popular.

The present job makes use of Microcontroller, in order to activate slip ring induction motor using variable frequency (V/F) method. The various factors which make the microcontroller based system smart are

    i.   Simplicity of execution in variable speed drives

    ii.   Better reliability and bigger flexibility.

    iii.   Little cost and high precision

1.6.2. Microcontroller based pulse width modulation (pwm) inverters

Speed control of open loop variable frequency (V/F) control of wound rotor (slip - ring) induction motor consists of rectifier with a capacitor bank, converter, insulated gate bipolar transistor (IGBT) driving module, microcontroller, three -phase pulse width modulation (PWM) inverter and 3-phase phase wound rotor induction motor (Patel,2014; Cunha,2001). Different probes for speed control, direction of rotation is given at the microcontroller side. In this the reference speed is set.

This frequency and amplitude are used to update the PWM duty cycle. IGBT based inverter gives the supply to the induction motor. Below are the different methods of designing inverter drive along with their features.

Advantage of using microcontroller based pwm inverter for wound rotor induction motor drive:

i. Change of pulse width modulation (PWM) frequency at any time.

ii. The speed of the motor can be controlled smoothly.

iii. 50 Hz and 60 Hz base frequency both are equally applicable for constructed inverter.

iv. Motor acceleration or deceleration can be controlled and can change the direction of motor at any time.

v. In online and off line it is possible to change the modulation index and voltage boost therefore it is achievable to control the output voltage.

vi. It is possible to monitor the dc bus voltage of the inverter.

Above all these reasons micro controller haulage drive system is very much suitable for man riding haulage drive system in an underground coal mine for reducing the energy consumption at approximately 8 to 9 percent as compared to conventional drive in mine.

1.7 Thesis Outline

Present work aims at experimental studies (in the field and laboratory) modelling and simulation studies haulage drive system used in an underground coal mine for energy conservation. With particular reference to energy conservation in mine haulage drive system in GDK 10A incline underground coal mine; the thesis is organized in the following chapters. To address the various issues discussed in the literature survey, the thesis is written and consists of 8 chapters.

Chapter -1

Introduction includes the different sources of energy, energy demand and coal production of energy in India. Energy consumption by various operation and equipment in underground coal mines was discussed. Different energy conservation techniques used in underground mine were discussed. Types of conventional haulage drive system used in underground coal mine and different methods slip power recovery systems were discussed.

Chapter -2

Present comprehensive survey of literature on energy consumption by various operations and equipments in mining industry and different methods of slip power

recovery. Microcontroller method for slip power recovery for energy conservation, aspects of mathematical modelling and simulation was also discussed.

Chapter -3

Field studies were carried out on 150hp haulage drive systems (two no.) in an underground coal mine GDK 10A incline in Ramagundam area of the "Singareni Collieries Company Limited" (The SCCL). Data obtained for two 150hp haulage drive systems, one from surface to 8th level (8L) and another one from 8L to 42level (42L) was used to calculate energy consumption.

Chapter -4

i) Necessary fabrication was done to carryout experiments in laboratory using 3hp motor to represent conventional haulage drive system. The laboratory set-up consists of 2.202kW, 600rpm, 10 poles, slip-ring induction motor with its stator connected to the415V, 50Hz, gear reduction 1:40 drum with rope connected to tub which moves on rail with provision to vary the gradient (i.e. angle with horizontal). Experiments were carried out with different combinations of loads and gradients for up the gradient and down the gradient. The results are given in tables.

ii) Experimental set up of 3hp haulage drive system was suitably modified using micro controller circuitry to study the energy consumption with different combinations of loads and gradients, by considering up the gradient and down the gradient.

Wireless technique i.e. implementation of RF-433MHz transmitter and receiver was used to control the tub movement and changing the direction gear system. ATMega-32 micro controller was used to control the motor speed as well as generation of pulse to drive the IGBT using Pulse Width Modulation (PWM) technique in rotor side of slip ring induction motor and control of tub movements.

Chapter -5

Mathematical modelling of power requirement of haulage drives system was done for up the gradient and down the gradient with combinations of different loads and gradients, for both conventional and micro controller (static Krammer) method. Machine model was developed in the stator flux reference frame. Design of voltage

controller, current controller and of rotor controller of open loop and closed loop system are discussed and used for simulation purpose.

Chapter -6

Present the MATLAB /SIMULINK simulation of the 3hp haulage drive system used in the laboratory and 150hp haulage drive system-1 and haulage drive system-2 used in an underground coal mine with conventional method. Simulation model was also given for open loop control and closed loop control of micro controller (static) haulage drive system for 3hp used in laboratory and 150hp used in an underground coal mine. Simulated results were tabulated and discussed.

Chapter -7

Field study Results of 150hp haulage drive systems and 3hp laboratory experimental haulage drive system were presented. Simulation studies for conventional method and microcontroller method for both up the gradient and down the gradient were given in the form of figures and comparative study of results and analysis done for energy consumption and energy conservation.

Chapter –8

Presents the summary of important results obtained from the studies carried out in this research work with suggestions for scope of future studies.

CHAPTER 2

2.0 LITERATURE REVIEW

Number of studies carried out by different researchers regarding slip power recovery method and energy conservation in mining is limited. A summary of the relevant work carried out by different researchers worldwide has been presented in this chapter

2.1 Literature Survey

Park (1920) studied and implemented a new approach to electric machine analysis. He formulated a change of variables which, in effect, replaced the variables (voltages, currents, and flux linkages) associated with the stator windings of a synchronous machine with variables associated with fictitious windings rotating with the rotor.

Park's transformation, which revolutionized electric machine analysis, has the unique property of eliminating all time-varying inductances from the voltage equations of the synchronous machine which occur due to i) electric circuits in relative motion and ii) electric circuits with varying magnetic reluctance.

Lavi et al.,(1966) studied and analyzed the chopper-controlled resistor in rotor circuit was relatively simple and less expensive control and it has the advantages of controlled starting torque, current, and improved power factor. Slip-power recovery system is an efficient method of speed control of wound rotor induction motor.

Shepherd et al., (1969) carried out an experimental studies on slip power recovery in an induction motor by the use of thyristor inverter and found that poor efficiency and low speed of induction motor performance can be improved by converting slip frequency power, inverting this to supply frequency, feeding it back in to mains directly**.**

Samathy et al.,(1969)designed static Krammer drive modelling and implemented speed control scheme for the static Krammer drive was introduce the hybrid model of the Krammer drive system only d,q transformation is applied to only to the stator circuits is kept in its abc form. That allows exact examination of the rotor

circuit and its energy recovery elements and this shows the successful implementation of the proportional integral (PI) controller in to the static Krammer system.

Weiss at el., (1974) studied and proposed schemes the rotor power can flow in one direction only; so the machine can operate either at sub synchronous or at super synchronous speeds. However, instead of dual converter system, use of a cycloconverter in the rotor circuit permits power flow in both the directions.

Cycloconverter permits a reversible power flow naturally and speed control is possible for sub synchronous as well as super synchronous operation by controlling the injected rotor voltage. Long and Schmitz described cycloconverter control of a doubly-fed induction motor giving speed torque characteristics similar to that of a dc series motor. Weiss reported the application and performance of an ac drive using a cycloconverter and a doubly-fed wound rotor motor for pump and compressor applications.

Chattopadhyay (1978) studied and examined a simple rotor position-detector used to control the switching of thyristor configuration in a sequential manner to generate an output voltage having a predominant slip-frequency component.

Wani (1978) carried out experimental studies on silicon controlled rectifier (SCR) chopper circuit which is used on the rotor side for the speed control of wound rotor induction motor drive. This type of control system gives contactless and continuous variation of rotor resistance. It should be noted though that the limited speed range is not an inherent defect of slip energy recovery drives; the KVA ratings and hence cost of the rectifier/inverter combination is considerably reduced however by limiting the speed range.

Mayer (1979) studied the speed-torque characteristics obtained were similar to that of a dc shunt motor, and the drive is reported to be inherently stable. A15000hp cycloconverter-fed wound rotor induction motor drive with high dynamic response of stator active and reactive powers which were presented in orthogonal control scheme employed to determine the rotor voltages. However, in the absence of proper current control loops, the stator power flow can be smoothly controlled only above 35% slip.

However, the use of cycloconverters in industrial drives has been restricted because of the large number of thyristors used in the power circuit, the complexity

involved in the firing and commutation circuits and the complex interaction with the grid.

Bose (1982) studied and implemented the concept of Variable – frequency induction motor drives by using gadget device which was commonly used in industrial sector**.**

Heising (1982) studied the failure of motor winding in manufacturing sector, motor failure was due to winding insulation.

Smith et al., (1984) studied the major drawback of gadget device drives was high cost and difficulty, as well as the harmonic distortion introduced on motor and supply sides.

Schmidt et al., (1988) studied the energy conservation reduction techniques in underground mines. Parts used in electrical power system shows shorter life when compared to manufacturing devices. This is due to hard environment, continuous operations and poor maintenance. Induction motor is an important part in electrical power system in mines, the motor failure requires more time for its maintenances. One large U.S. coal producer, for example, reported that 49 electric motors required replacement during a one year period in an underground coal mine operating three continuous miner sections.

Akpinar and Pillai (1990) designed the method of modelling on **r**eference analyses of slip power recovery drive and studied the performance of slip power recovery scheme for induction motor. A new energy recovery scheme for variable speed double fed induction motor was proposed by Fan et al., 1990.

Akpinar et al.,(1990)carried out experimental studies on slip power recovery method and observed the problem of getting limited speed and also suggested that the limited speed can be overcome by choosing proper kilo volt- amp (kVA) rating of rectifier and inverter combination. It is possible to control the speed from high to low with low frequency by adopting the required rectifier /inverter ratings**.**

In slip recovery method, induction motor drive is more difficult in rotor side control compared to stator side control of induction motor drives. The Krammer drives are more commonly used in industries because of its reliable and efficient drive system. It is mainly used in limited speed application such as fan and pumps.

Sen (1990) discussed and compared the recent advancement in power semiconductor technology, induction motors were being widely used in many variable speed industrial drives. Three important methods commonly employed for induction motor speed control, supply voltage control, supply frequency control and rotor resistance control. With proper control strategies, the induction motor drive can be operated in constant torque and constant horsepower modes. Perhaps the most important control is the torque control.

A direct control of torque can provide rapid acceleration and retardation such as in foundry or steel mill hoists, cranes, and traction systems. A constant torque operation of the induction motor can be obtained by using a static adjustable frequency converter. In such a system, the slip frequency is maintained constant, and the motor is operated at a constant flux level by changing the supply voltage with the frequency.

Paresh (1990) studied the common speed control system for slip ring induction motor was obtained by changing the resistance of rotor. It has been established that this rheostatic rotor resistance control method can give maximum starting torque and low starting current and changing (variation) of speed over a wide range below the synchronous speed of the motor

Singh (1994) studied and suggested the energy conservation opportunities in pumping systems: In underground mines for pumping the ground water to outside, steps are followed to reduce the energy conservation. Make sure the availability of standard instruments such as flow meters and pressure gauges.

Papathanassiou et al., (1998) studied and implemented the commutation angle analysis, harmonic analysis and performance improvement of slip power energy recovery drive. The more conventional system, where the rotor power is rectified and fed back to the grid by a phase-controlled inverter, was subsequently proposed by Lavi and Polge, and shepherd and Stanway. This method of control became popularly known as the *Static Scherbius* system. A large DC link choke is used to interface the diode bridge output with the grid-side inverter

Singh et al., (2001) designed an accurate method of wound rotor induction motor on closed-loop control slip power recovery scheme using micro processor technique and found that microprocessor based closed loop operation of the drive

provides greater flexibility and accuracy, the improved dynamic response and the speed control independent of load variation.

Chengwu et al., (2009) reviews about the energy conservation project on motor system were one of the top ten energy saving projects of national eleventh five year plan. The energy – saving system and can achieve double –fed motor speed control to run energy control, reactive power compensation control and motor reserve capacity.

Mahto (2009) studied about the energy efficient motors which were available in all sizes, and thus in case of any replacement, this new generation motors need to be installed. Except for emergencies, at no other time the user should go for multiple winding numbers of the motors, since every winding inherits certain losses

Energy Efficient Motors additionally contribute to:

i.   Higher efficiency at operating level and consequently reduction in electricity bill.

ii.   Can take care of wider supply variation and higher ambient.

iii. Lower slip which enhances output of the end product.

In rheostatic (conventional control) method of speed control external cooling is required, speed adjustment and maintenance is required manually, and energy consumption in these methods of control will be more. Hence it is better to be replaced by variable frequency drive.

The advantages in the Variable Frequency Drive (VFD) like, energy savings, reduction in motor current at start, (low motor starting current, reduction of thermal and mechanical stresses on motors and belts during starts), easy installation and high power factor, less kilo volt- amp rating will make variable frequency drive (VFD) is most important drive**.**

Kumar et al., (2009) carried out an experimental investigation on steady state modelling of static slip energy recovery controlled slip ring induction motor drive and also studied that the good degree of agreement of the computed results with experimental work, proves the validity of the developed model of the drive. Torque of the drive varies linearly with the dc link current irrespective of the delay angle of the controlled converter.

Pradhan and Chakraborti (2010) discussed about energy conservation in different mining industries and broadly highlight some of the energy saving measures adopted in some of the Indian mines technique for conservation of electricity in underground coal mines.

Steibler et al., (2010) carried out experimental studies on slip power recovery drive and investigated that induction motor drives with control of speed have huge applications in the modern industrial set up. More than 75% of the load today in the industry of any country consists of induction motor drives. Wound rotor induction motor drives have found great applications due to the availability of slip power easily available from slip rings and can be utilized mechanically or electronically for better speed control.

 Slip power can be recovered from static converters instead of wasting power in the resistance. High performance induction motor drive application requires low cost, high efficiency and simple control circuitry for the complete speed range. Slip power recovery drives (SPRD), also known as Static Scherbius system, are widely used for the limited speed range applications such as large-capacity pumps and fan drives, variable-speed wind energy systems, ship-board variable speed/constant frequency system.

Many researchers (Zahawi et al., 1987, Brown et al., 1986, Doradla et al., 1998) presented motor performance using slip recovery systems, analysis of transient state of Krammer drives, and proposed new slip recovery scheme for improved power factor presented (Krause et al., 1988).

Singh (2010) studied about the impact of the principle of slip power recovery drive particularly to reduce the power losses at output terminals of slip ring induction motor due to the output. Power losses are more during speed control due to use of variable resistance (Rheostat) in previous methods.

As the slip power can flow only in one direction, modified static Krammer drive offers speed control below synchronous speed only and improves overall poor drive efficiency of the system.

Rakesh et al., (2011) carried out experimental and simulation studies on slip ring induction motor which were suitable for cement and mining industries for starting and driving large grinding mills. Slip power recovery wound rotor induction

motor drives were used in rotor resistance starters for Slip-ring (wound rotor) induction motor.

Kumar et al.,(2011)carried out an experimental investigation on wound rotor induction motor by using microcontroller technique was used for the generation of firing pulses for the inverter bridge and also studied the steady state performance analysis of conventional slip power recovery scheme using static line commutated inverter in the rotor circuit. The simulation and experimental results are analyzed.

Abhishek et al., (2014) studied new circuit design for the slip power recovery scheme and different Pulse Width Modulation (PWM) control technique was employed here to reduce the injection of the harmonics to the supply by using slip power recovery system for variable speed drive system in which the power across the slip rings of induction motor was recovered and controlled.

Srivatsa et al., (2015) studied about the different methodologies of induction motor drive. Induction motor drive is a process of controlling the speed, power and efficiency of the induction motor using various techniques.

2.2 Origin of Present Research work

Mining industry is energy intensive i.e. lot of electrical energy required for different operations like drilling, transportation of men, ore or material, pumping convening, haulage and winding etc. Direct haulers are used for transportation of coal or ore from underground to surface i.e. up the gradient. Empty tubs are cars are sent inside the mine (i.e. higher level to lower level for down the gradient) by gravity. However, in man riding system direct hauler is used for transportation of men in both directions i.e., up the gradient (lower level to higher level) as well as down the gradient (higher level to lower level).

Speed control conventional haulage drive system which requires more energy, in which energy being wasted in the form of excessive heat and that this power can be recovered back through slip power recovery scheme of the drive.

Economy of electric power is an important aspect and main thrust to reduce total energy consumption. The coal enterprises should reinforce the technological transformation of mechanical and electrical equipments and generalize power-saving products. In recent years energy efficient motors are available in all sizes, and thus in case of any replacement this new generation motors need to be installed.

Mine haulage drive system plays an important role in the underground coal mines. Energy consumption is high in conventional system used for mine hauler drive (direct rope haulage), since resistance control was connected with three phase slip ring induction motor. This is not an intelligent and efficient controller with regard to precisely controlling speed in order to regulate power requirement.

Therefore, the productivity and safety of conventional hauler is not appreciable. The conservation of electrical energy in mines includes replacement of conventional systems with the improved technology, which leads to reduction in energy consumption per annum, i.e. about 10-15%. Therefore, microcontroller based mine haulage drive system by using slip energy recovery mechanism with control system should be interfaced to the conventional mine haulers used in an underground coal mine can reduce electrical energy consumption.

Keeping this in mind the present research proposal has formulated, a 3hp haulage drive system (similar to the haulage drive system used in the field) is fabricated with necessary accessories to study the energy consumption by conventional method and micro controller method.

2.3 Definition of the Problem

The implementation of energy conservation technology in mines improves the overall efficiency of mining machineries and lighting systems. This will lead to energy saving and also improve the energy conservation with existing resources. Slip power recovery wound rotor induction motor drives are used in high power, limited speed range applications, where control of slip power provides the variable speed drive system.

In this thesis, the steady state performance analysis of conventional slip power recovery scheme using IGBT inverter in the rotor circuit is presented. Simulation of the scheme is carried out using MATLAB/SIMULINK environment and 3hp experimental set-up is prepared in the laboratory for a 3-hp wound rotor induction motor. Microcontroller technique is used for the generation of Pulse Width Modulation (PWM)pulses for the inverter bridge and the aim is to study the influence of micro controller technique on energy consumption and there by the saving of energy in percentage.

In field, every coal seam is having a specific gradient i.e. 1 in 4 or 1 in 8 or 1 in 10 etc, and it is not possible to vary this gradient in the field. Hence the experimental studies are planned in the laboratory using 3hp haulage drive to study the influence different combination loads and gradients on energy consumption. Mathematical models were developed to predict the energy consumption in haulage drive system and compare the experimental results.

2.4 Research objectives

1. To study the influence of load (up the gradient and down the gradient) on energy consumption of a 150hp hauler used for man riding system in an underground coal mine.

2. To do necessary fabrication work for a laboratory experimental set- up for 3hp conventional haulage drive system, similar to direct hauler in the field (i.e.in an underground coal mine) to study the influence of different combination loads and gradients, for up the gradient and down the gradient.

3. To study the influence of different combination loads and gradients for up the gradient and down the gradient on energy consumption using same laboratory experimental set-up with micro controller (static Krammer) based drive system.

4. To develop a mathematical model for slip ring induction motor and sub synchronous converter system, using data collected from field and laboratory experiments for different combination loads and gradients for up the gradient and down the gradient.

5. To develop simulation model for i) 150hp haulage drive system(field studies) ii) 3hp haulage drive system (laboratory studies) for both conventional method and micro controller (static Krammer) methods using SIMULINK/MATLAB software.

6. To compare the data of energy consumption from slip power recovery method and with the data of energy consumption obtained from the conventional method (rheostatic control) for both field and laboratory experiments done with different combination of loads and gradients, for up the gradient and down the gradient.

CHAPTER 3

FIELD STUDIES

To achieve the above objectives, the following methodology was adopted. The experimental studies are done both in field and laboratory. Also mathematical model and simulation are done to predict the energy consumption and compare these results with experimental results.

3.1 Field studies

Field studies are carried out in GDK 10A incline of The Singareni Collieries Company Limited, on man riding system which is used for transportation of men with two direct haulers (each 150hp slip ring induction motor drive).One direct hauler (150hp) is used to transport of men from surface to 8th level (8L) and another direct hauler (150hp) is used to transport of men from 8L to 42nd level (42L).

The gradient of coal seam is 1 in 4 (i.e. 14.04° with horizontal). Gradient of a coal seam is generally defined as 1 in x, where x is horizontal distance and 1 is vertical distance (or drop).In other wards coal seam making an angleθ with horizontal and gradient is $\tan^{-1}\theta$ and is equal to 1 in x. Therefore, in this thesis, the gradient of coal seam is considered as an angle (θ) with horizontal. The entrance of GDK 10A incline (an underground coal mine) is shown in Figure 3.1.

Both haulers are used for transport of men for up the gradient and down the gradient. The parameters namely ,voltage, current, speed, number of persons travelling in one trip , total load (weight) and time taken for each trip (using stop watch) are measured for both up the gradient and down the gradient. Based on these parameters, the other parameters like electrical shaft output power, efficiency, input power and energy consumption are calculated and tabulated.

43

Figure 3.1 Entrance of GDK 10A incline (an underground coal mine).

3.1.1 The Singereni Collieries Company Limited (The SCCL)

The Singareni Collieries Company Limited (The SCCL) is public sector Company with 51% shares, held by state government (Telangana) and 49% shares are held by central government. The SCCL is having both opencast coal mines and underground coal mines in four districts.

3.1.2 Man riding car system

Modern mines are extensive. The distance between the pit bottom and faces is usually several kilometers with haulage ways which include horizontal as well as inclined section. Under such conditions, it becomes essential to transport miners from underground to the surfaces and vice-versa .Transport of men should be done in special man – riding cars at controlled haulage speed. Man – riding needs special track equipment, terminal station and winches. To decrease jerking during the running as well as shunting, the man –riding cars are equipped with spring loaded bumpers and couplings.

The travelling speed of man riding cars along horizontal roadways and braking distance for car moving down the prevailing gradient should not exceed 3.0 m/s (10.8 km/h and 20 m respectively (Kerelin, 2001).

Currently, due to increasing areas from which individual mines draw coal, travelling on foot to reach the working face creates the following problems.

i.   Travelling time on foot becomes greater.

ii.   After walking a long distance the workmen may not be ready to begin work immediately.

iii. Actual working time during shift is reduced.

iv.   The return journey may require longer time because the work men being tired after a shifts work.

v.   Heavy gradient may add to travelling time further.

3.1.3. Salient features of man riding car system

This system is used for transportation of   men in an underground mine.

i.   The Man riding car system is used to increase the work efficiency of man power and eliminate the drudgery of walking in uphill gradient of 1 in 4 (i.e.14.04°)

ii.   The prime mover of the system is Direct Hauler and the cars are moved on track.

iii. The system is approved by DGMS and has many safety features like over speed trip, emergency brake, service brake, signaling and telephone communication system and emergency brake in cars. The technical specification of man riding car are given as follows. Drive power: 150hp or 87hp Car Speed : 8 Kmph max. Rope size: Ø 26 mm, Maximum persons travel at a time: 35 (depending on gradient), Operating Voltage of Hauler: 3.3 kV or 550V or 440 V at 3 Phase 50 Hz.

150hp direct haulage system along with man riding car is shown in Figure 3.2 and underground mine car is shown Figure 3.3.
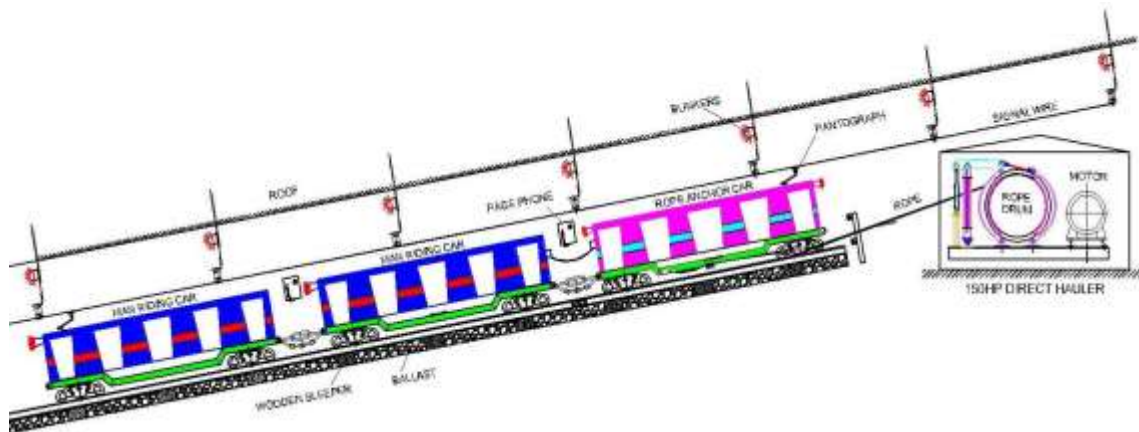
Figure 3.2 150hp direct hauler with mine cars.

Figure 3.3 Underground mine car.

3.2 Mine hauler and slip ring induction motor drive

Mine haulers perform an important function in underground mining operations to transport coal and materials. Specific electric power will be used by this haulage machines. Conventional hauler works on non linear resistance controls with brush gear three phase induction motor. It needs regular servicing of numerous components of the hauler and occasional replacement in addition to large electric power usage. Figure 3.4 (a) shows the 150hpMine hauler and Figure 3.4(b) shows the rotor resistance control for slip ring induction motor used in underground mine.

These are purely conventional method of control. These types of electric equipments consume a large amount of electrical power because of particular

rheostatic characteristics. These have been replaced by variable frequency drive in which the by using gadget device the energy usage can be reduced in induction motor.
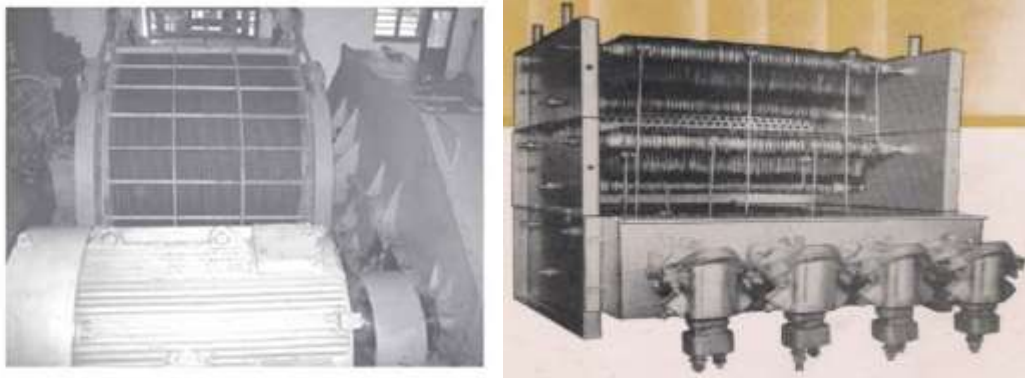
a) 150 hp Hauler   b) Rotor resistance starter

Figure 3.4 Mine hauler and rotor resistance starter for slip ring induction motor.

3.3 Field study on energy consumption

Field study data collection procedure of 150hp underground coal mine haulage drive system the electrical and mechanical parameters for different levels are indicated in Figure 3.5. The collected data is pertaining to 150hp conventional control man ride haulage drive system in GDK 10A underground incline coal mine.
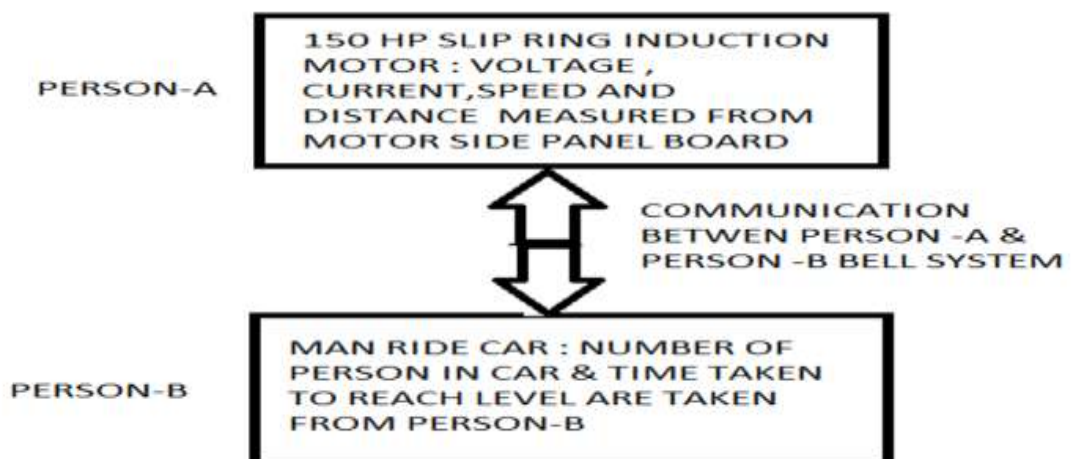
Figure 3.5 Field study procedure for collection of data of150hp underground mine haulage drive system

In the field study the collection data is based on the above Figure 3.5 to find energy consumption details of direct rope haulage drive system in GDK 10A incline

underground coal mine. The following are the main parameters to decide the energy consumption in concerned mine i.e. voltage, current, time, speed, distance of each level and number of persons in each trip. Based on these parameters the other parameters like electrical shaft power output, efficiency, input power and energy consumption are calculated for 1 trip and tabulated.

These parameters are different from each level of underground mine. The tabulated results on energy consumption for 150hp underground haulage drive system -1 (from surface to 8th level (8L) are presented in Table3.1.Theparameters namely, voltage, current, speed, number of persons travelling in one trip , total load (weight), time taken for each trip (using stop watch), speed and distance of each level are measured for both up the gradient and down the gradient. Based on the inputs, electrical parameters like efficiency of the drive system, output shaft power, and energy consumption are calculated for each level of the mine.

Similarly the up the gradients of drive system -1 from 8th level to the surface up the gradient the same observations are followed as per previous case. The tabulated up the gradient (8th level to surface) energy consumptions are presented in Table 3.2. The drive system -2 has also same specification as that of drive system- 1, but it is located in 8th level of the underground mine. The similar procedure is followed in drive system-2 to collect data of energy consumption. The collected data are pertaining to the total distance of underground mine about 4.2km away from surface drive system.

 In all the tables in field study electrical and mechanical parameters indicating the measured values of various N_1(Actual speed) $,N_2$ (1:29)(Shaft speed) , Input power , Output power, Distance of each level , Efficiency , Torque , Energy consumption for each level, and yearly energy consumption each level are measured and calculated parameters procedure are illustrated in APPNDIX-II. The load of man riding system (using cars) depends upon the number of persons sitting in the car at given time. There are different levels to which the man riding system serves and each level are separated from each other depending upon the pillar size.

 Energy consumption from 8th level to 42nd level (down the gradient) and also from 42nd level to 8th level (up the gradient) are given in Table 3.3 and Table 3.4 respectively.

Table 3.1 Energy consumption (surface to 8th level) of 150hp underground haulage drives system-1 (down the gradient)

Sl. No.	Load (kN)	Voltage (V)	Current (A)	N_1 (rpm) (Actual speed)	N_2 (rpm) (1:29) (Shaft speed)	Torque (Nm)	Input power (W)	Output power (W)	Efficiency (%)	Time (s)	Distance (km)	Energy Consumption (kWh)	Yearly energy Consumption (kWh)
1	33.32	3000	20	400	13.80	6668	144000	97785.3	67.90	18.75	0.10	0.509	1465.8
2	32.65	3050	19	410	14.14	6521	139080	98040.4	70.49	37.5	0.18	1.021	2940.4
3	30.38	3100	18.5	415	14.32	6081	133920	924366	69.10	56.00	0.28	1.437	4138.5
4	28.71	3110	17.5	420	14.5	5641	130200	86895.5	66.74	75.00	0.38	1.810	5212.8
5	24.50	3010	16	425	14.72	4908	115584	76360.2	66.06	94.00	0.47	1.993	5739.8
6	20.09	2990	16	430	14.82	4028	114816	63496.2	55.30	112.5	0.56	1.984	5713.9
7	18.62	2990	15.8	430	14.82	3734	113380	58861.6	51.91	131.0	0.66	2.141	6166.0
8	17.64	3000	15.5	440	15.18	3539	111600	57096.1	51.16	150.0	0.75	2.379	6851.4

Table 3.2 Energy consumption (8[th]level to surface level) of 150hp underground haulage drive system-1(up the gradient)

.

Sl. No.	Load (kN)	Voltage (V)	Current (A)	N_1 (rpm) (Actual speed)	N_2 (rpm) (1:29) (Shaft speed)	Torque (Nm)	Input power (W)	Output power (W)	Efficiency (%)	Time (s)	Distance (km)	Energy consumption (kWh)	Yearly energy Consumption (kWh)
1.	36.7	2990	17	430	14.9	4572	121992	72071.67	59.07	180.0	0.75	3.603	10376.0
2.	33.0	2990	17.5	415	14.32	5573	125580	84817.85	67.54	157.5	0.66	3.710	10685.0
3.	31.6	3010	18	410	14.14	6067	130032	90914.06	69.91	135.0	0.56	3.409	9817.9
4.	29.4	3100	18.5	410	14.14	6047	137640	90914.06	66.05	112.5	0.47	2.841	8182.0
5.	27.9	3150	19	405	13.96	6363	143640	94488.7	65.78	90.00	0.38	2.362	6802.5
6.	25.7	3100	20	405	13.96	6837	148800	101527.5	68.23	67.5	028	1.903	5480.6
7.	22.0	3100	20.5	400	13.8	7153	152520	104939.8	69.67	45.00	0.18	1.311	3775.6
8.	21.0	3150	22	400	13.8	7943	166320	116483.0	70.03	22.5	0.10	0.728	2096.6

Table 3.3 Energy consumption (8th L to 42nd level) of 150hp underground haulage drive system-2 (down the gradient)

Sl. No.	Load (kN)	Voltage (V)	Current (A)	N_1 (rpm) (Actual speed)	N_2 (rpm) (1:29) (Shaft speed)	Torque (Nm)	Input power (W)	Output power (W)	Efficiency (%)	Time (s)	Distance (km)	Energy consumption (kWh)	Yearly energy Consumption (kWh)
1	39.2	3150	20	415	14.3	7841	151200	119174.4	78.81	84	0.15	2.780	8006.4
2	36.2	3200	19.5	420	14.5	7254	149760	111742.6	74.61	169	0.20	5.245	15105.6
3	34.8	3110	19	415	14.3	6961	141816	105799.4	74.60	253	0.27	7.435	21412.8
4	32.6	3100	18.5	410	14.14	6521	137640	98040.45	71.22	338	0.38	9.205	26510.4
5	30.4	3110	18	405	14.00	6081	133920	90301.15	67.42	422	0.46	10.585	30484.8
6	28.2	3090	17.5	400	13.8	5641	129780	82724.53	63.74	507	0.56	11.650	33552
7	23.0	3010	17	400	13.8	4614	122808	67663.7	55.09	592	0.66	11.126	32042.88
8	20.2	3000	16.5	400	13.8	3941	118800	57794.0	50.00	676	0.76	10.82	31161.6
9	19.8	3000	16	405	14.00	3734	115200	55448.86	48.13	720	0.85	11.06	31852.8

Table 3.4 Energy consumption (42nd to 8th level) of150hp underground haulage drive system-2 (up the gradient)

Sl. No	Load (kN)	Voltage (V)	Current (A)	N_1 (rpm) (Actual speed)	N_2 (rpm) (1:29) (Shaft speed)	Torque (Nm)	Input power (W)	Output power (W)	Efficiency (%)	Time (s)	Distance (km)	Energy Consumption (kWh)	Yearly energy Consumption (kWh)
1.	17.6	3200	22.5	400	13.8	9523	175500	139653	79.57	840	0.85	32.53	93686.4
2.	19.5	3250	22.5	405	13.96	9313	175500	138295	78.80	716	0.76	27.50	79200
3.	24.0	3250	22	410	13.98	8786	171600	132093	76.97	617	0.66	22.63	65174.4
4.	29.3	3250	22	415	14.32	8259	171600	125697	73.25	518	0.56	18.05	51984
5.	33.9	3210	21.5	420	14.5	7332	165636	112944	68.18	422	0.46	13.23	38102.4
6	38.2	3100	21	428	14.75	6342	148800	99518	66.88	321	0.36	8.873	25554.2
7	40.6	3100	20	430	14,8	5204	148800	81767	54.95	222	0.26	5.042	14520.9
8	43.1	3140	19	435	15.0	4235	143184	67412	47.08	123	0.16	2.303	6632.64
9	44.1	3150	18	440	15.18	3834	136080	61816	45.42	48	0.10	0.824	2373.1

Table 3.5 Total energy consumption of 150hp underground haulage drive system- 1and haulage drive system- 2 in an underground coal mine

Sl.No	Levels of mine haulage drive system	Daily Energy consumption kWh	Monthly Energy consumption kWh	Yearly Energy consumption kWh
1.	Surface to 8th level (drive system-1)	105.72	3171.6	38228.6
2.	8thlevel to surface level (drive system-1)	149.808	4494	57216.2
3.	8th level to 42nd level (drive system-2)	*640.28*	*21831.6*	*230128.8*
4.	42nd level to 8th level (drive system-2)	1047.93	31437.9	377228.8
5.	**Total energy consumption kWh**	**1954.738kWh**	**58566kWh**	**702801.64kWh**

Energy consumption calculation steps for down the gradient drive and up the gradients are presented in APPENDIX II. The total energy consumption of haulage drive system -1 and haulage drive system-2 also presented in Table 3.5. The total energy consumption results table will represents the overall energy consumption in haulage drive system – 1 and haulage drive system–2. This will help us to study energy consumption in each drive system of the underground mine. The above study results gives planning to implement the static drive system to reduce energy consumption in the mine haulage drive system in the concerned mine.

The similar electrical and mechanical parameters i.e. load , speed , Torque, Power, efficiency and energy consumption variation are observed in all the field study tabulated results of Table 3.1 , Table 3.2 ,Table 3.3 and Table 3.4 of haulage drive system-1 , drive system-2 of underground mine .

CHAPTER 4

LABORATORY EXPERIMENTAL STUDIES

4.1 CONVENTIONAL CONTROL METHOD

Speed control of induction motor for conventional control is achieved by adding resistance at rotor side. The rotor also has a three-phase winding, usually connected in a wye (or star) circuit. The three terminals of the rotor winding are connected to separate slip rings. Brushes ride on these slip rings and the rotor winding is connected to an external liquid rheostat or resistor bank. This resistance, when inserted into the rotor circuit, overall rotor resistance will increase and reduces starting currents. The motor speed can be adjusted by changing the resistance. The continuous power flowing into the resistor is lost as heat. Slip ring induction motor drives have found great applications due to the availability of slip power easily available from slip rings. Slip ring induction motors are widely used for high torque and variable speed applications like for haulers in underground coal mines.

Conventional methods of speed control of slip ring induction motor from rotor side, lead to wastage of energy, in external resistance. Slip ring induction motors have been popular in the cement and mining industry for starting and driving large grinding mill. Figure 4.1 shows that by increasing the rotor resistance from R_0 , R_1 and R_2, the breakdown torque peak is shifted left to zero speed. The R_0 , R_1 and R_2 are represented as Zero rotor resistance stud, Maximum rotor resistance stud and Minimum rotor resistance stud values of rotor starter resistance of slip ring induction motor. This torque peak is much higher than the starting torque available with no rotor resistance (R_0) Slip is proportional to rotor resistance, and pullout torque is proportional to slip. Thus, high torque is produced while starting. Depending on the rotor resistance and the load, the operating speed of the motor can thus be manipulated. At full load, the speed can be effectively reduced to about 50% of the motor synchronous speed, particularly when driving fluctuating torque and speed loads. Reducing speed below 50% results in very low efficiency. By inserting external resistance in the rotor circuit, not only the starting current is reduced, but at same time starting torque is increased.
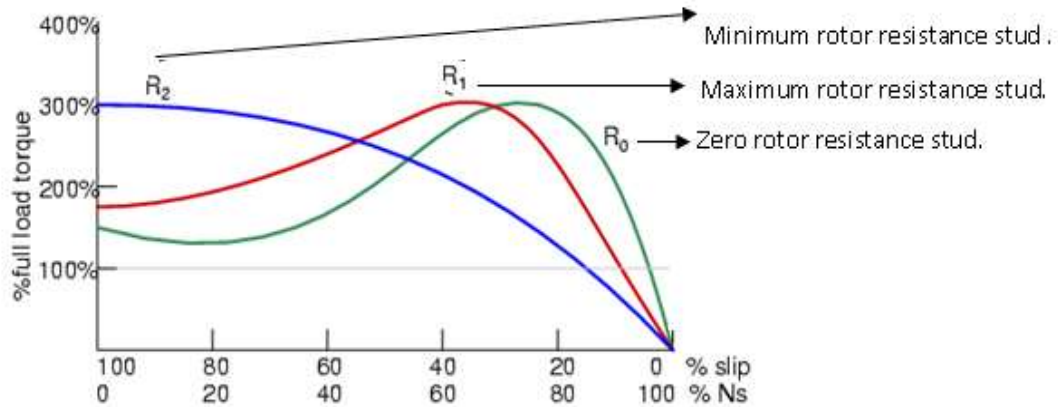
Figure.4.1 Torque speed characteristic of slip ring induction motor

Figure 4.2 shows the conventional method of speed control unit for slip ring induction motor used for 3hp haulage drive system laboratory experimental work. These electrical equipments consume huge amount of electrical energy due to the rheostat nature. It can be replaced by variable frequency drive due to which the electrical energy consumption can be reduced.

4.2 HARDWARE DESCRIPTION

The 3hplaboratory experimental haulage drive system set-up consists of the following components by using conventional method are explained in this section.

4.2.1 Liquid rheostat

It is used to start the slip ring induction rotor for smooth starting and it acts as an external resistance in starting of slip ring induction motor. The solution for liquid rheostat is prepared by water mixed with washing soda (sodium carbonate). Figure 4.3 shows the Liquid Rheostat rotor starter for three-phase slip ring motor. The excellent properties of slip ring motors make them particularly suitable for special application.
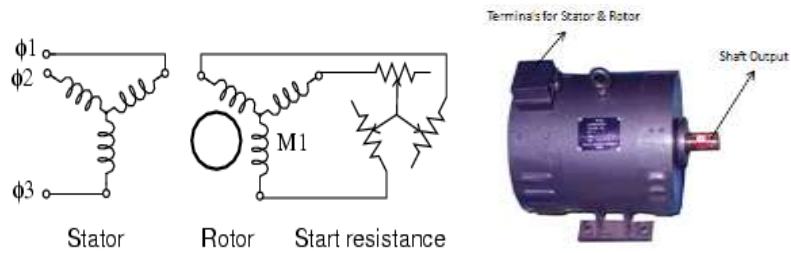
Figure 4.2 Slip ring induction motor with external rotor resistances.
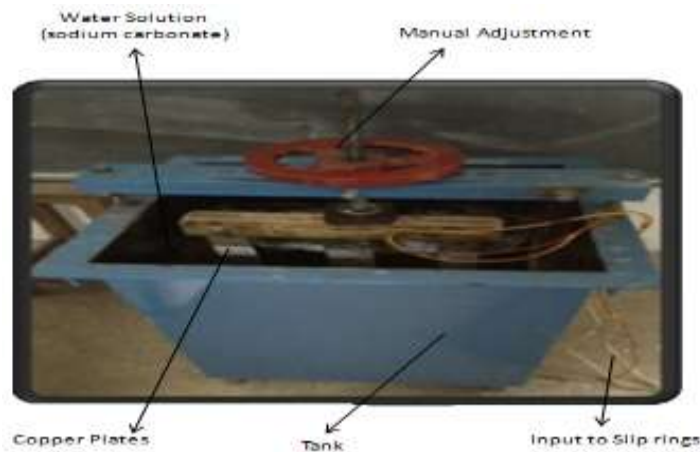
Figure 4.3 Liquid rheostat rotor starter for 3-phase slip ring induction motor

4.2.2 Reduction gear drive system (1:40)

Conventional gear drives are more commonly used with stepping motors. The fine resolution of a micro stepping motor can make gearing unnecessary in many applications, where gears are used only for increase system precision. Gears generally have undesirable efficiency, wear characteristics, backlash, and can be noisy. (Mohammad,. 2001).The double fed induction motor (DFIM) based mine haulage drive is driven by the gearbox system to attain a suitable speed range for the rotor by means of the gearbox.

The actual gearbox ratio is chosen considering the optimum speed of the operations of the motor. The optimum speed of induction motor is selected based on the speed of the man riding car or tub. Another aspect to be considered, when selecting a gearbox ratio is the weight of the gearbox, which increases along the gearbox ratio. The gears are generally intended to control power transmission with different methods namely changing the direction through which power can be

transmitted (i.e. parallel, right angles, rotating, linear etc.),changing the amount of the load or maybe torque and by changing the rpm.

The forward and reverse movement of man riding car or tub can be changed mechanically by using the levers of reduction gearbox in drive system. Reduction gear (1:40) was achieved in 3hp haulage drive system, for laboratory experiments, by manual forward and reverse direction control and is shown in Figure 4.4.Using compound gear concept, the reduction gear is designed for 600rpm and the drum side speed is 15rpm.

The maximum loading capacity of gear system is about 1960N with 1: 40 speed ratio at load side. The design of the gear system consists of 3- stage speed reduction with different dimension of drive gear and driven gear. Idler gear changes the direction of driven gear rotation for both forward and reverse direction of the motor manually as shown in   Figure 4.5.Compound reduction gear design mainly based on the speed of the man riding car or tub which is 8-15km/hr in the present case (Kerelin, 1999).

4.2.3. Technical and fabrication details of laboratory experimental set-up of 3hp conventional haulage drive system

Technical and fabricationdetails for laboratory experimental set-up of 3hp conventional haulage drive system are given in Table 4.1.
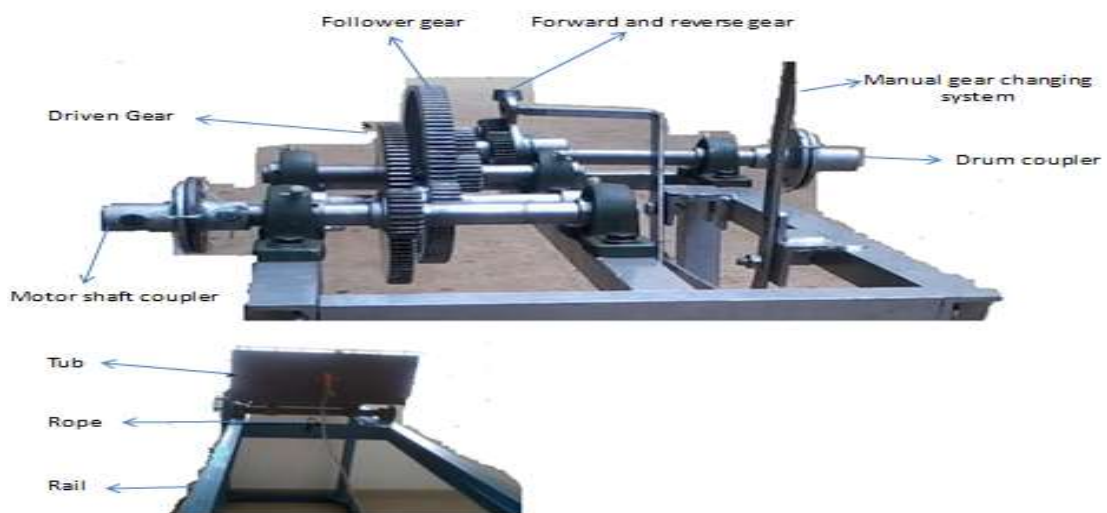
Figure 4.4 Reduction gear (1:40) system with manual forward and reverse direction control and tub with rail arrangement.

Figure 4.5 Idler gear changes the direction of the driven gear rotation

Table 4.1 Technical and fabrication details of 3hp Conventional haulage drive system

Sl. No.	Equipments	Particulars
1.	3-Ø Slip ring motor	3hp,415V, 10-pole, 600rpm,6.5Amps
2.	Reduction gear with forward and reverse direction with mechanical control	Base length =0.0635m, height = 0.0381m, speed ratio = 1:40
3.	Drum	Drum diameter=0.2m.Lengthofdrum =0.195m. Shaft diameter = 0.038m.Coupling = 0.03m.
4.	Tub	Length= 0.7493m,height = 0.254m, width = 0.508m, weight of the tub: 196N
5.	Inclined rail track	Length = 5 m, Angular adjustments 27^0, 29^0, 32^0 and 35^0
6.	Foundation table	L=2 m ,W= 0.609m,H= 1.524m

4.3 Experimental studies with 3hp haulage drive by conventional method

Experimental set-up for 3hp laboratory haulage drive system EMFor conventional method and line diagram for the same is shown in Figure 4.6 and Figure 4.7 respectively. The slip ring induction motor is started by using the liquid rheostat rotor starter. The simplest speed control scheme for wound rotor induction motors is achieved by changing the rotor resistance. This rotor resistance control method can provide high starting torque and low starting current and variation of speed over a wide range below the synchronous speed of the motor.

Following procedure is adopted for conducting experiments in the laboratory with 3hp experimental haulage drive system. 3-phase supply is given to the 3-phase auto transformer. Output is connected to the stator side of the machine and the slip ring terminals are connected to liquid rheostat starter. The respective stator and rotor side measurement parameters are noted down for different combinations of loads and gradients. Experiment are conducted with different combination of loads (i.e. 1079 N, 1275 N, 1471N and 1765.8 N) and gradients (angle with horizontal i.e. 27º, 29º, 32º and 35º) for both up the gradient and down the gradient.

The set of parameter such as speed (N_1/N_2), input power, voltage, current and time are noted for all combinations of loads and gradients used for up the gradient and down the gradient.

Using the experimental data the energy consumption are calculated and presented in Table 4.2 and Table 4.3 for down the gradient and up the gradient different combination of loads and gradients.

The experimental results are tabulated by considering different combination of loads (i.e. 1079N, 1275N, 1471N and 1765.8N) and gradients (angle with horizontal i.e. 27º, 29º, 32º and 35º) for both up the gradient and down the gradient. Tabulated results are based on measurement of speed, input power; output power, torque, efficiency and energy consumption presented in the above Tables and calculation procedure is given in APPENDIX –III. The results table of energy consumption and conservation are presented in chapter 7 (results and discussion) and explanation for various parameters are discussed for both up the gradient and down the gradient of 3hp laboratory conventional method haulage drive system.
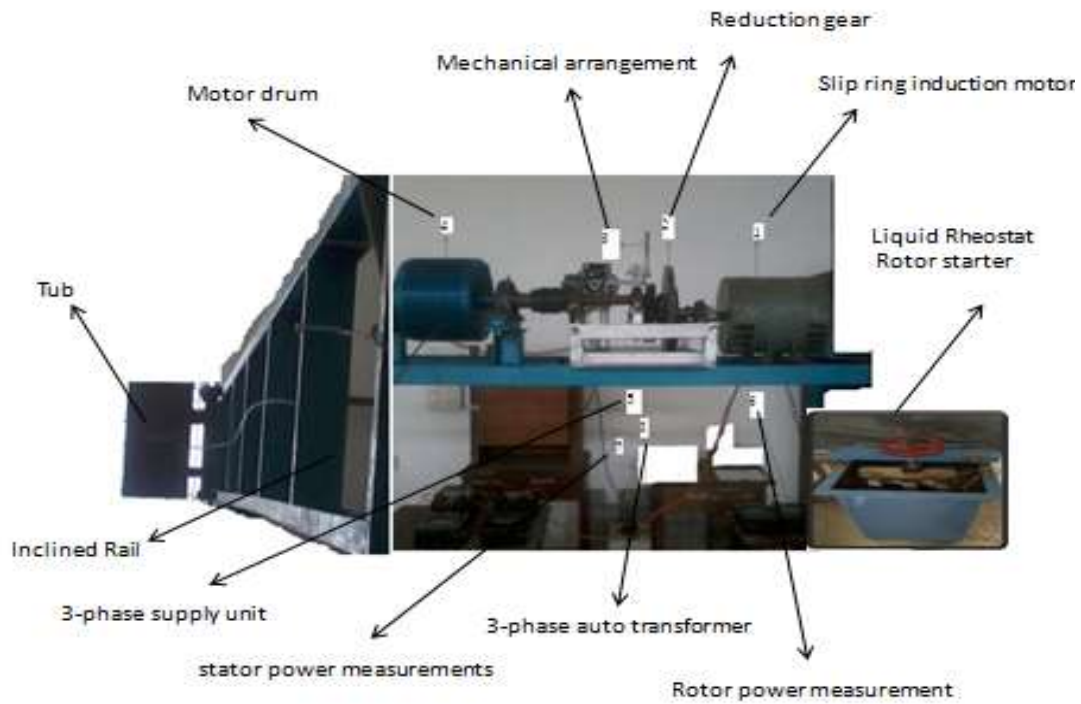
Figure 4.6   Experimental set-up for 3hp laboratory experimental haulage drive
system for conventional method
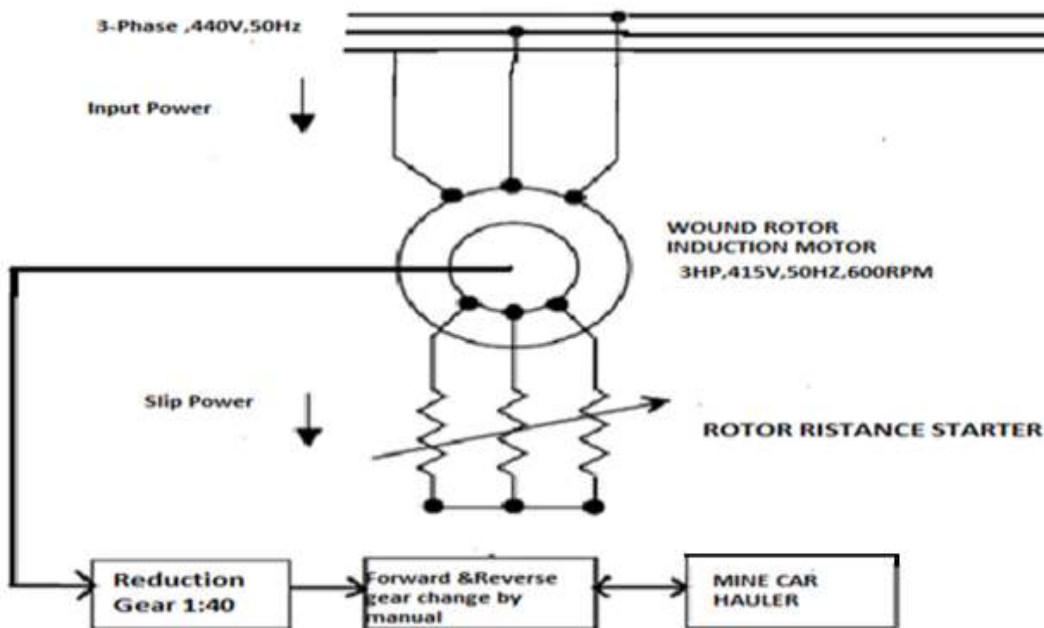
Figure 4.7 Line diagram of conventional mine haulage drive system

Table 4.2 Results of energy consumption of 3hp laboratory haulage drive system by conventional method for different combination of loads and gradients for down the gradient

Angle with horizontal	Load (N)	Voltage (V)	Current (A)	N_1 (rpm) (Actual speed)	N_2 (rpm) (1:40) (Shaft speed)	Torque (Nm)	Input power (W)	Output power (W)	Efficiency (%)	Time (s)	Energy consumption (kWh)	Yearly Energy consumption (kWh)
27^0	1079	390	3.0	549	13.73	69.13	1621.2	937.1	57.80	22.5	0.005856	25.297
	1275	390	3.2	543	13.58	76.58	1729.3	1026.3	59.34	24.25	0.00691	29.851
	1471	395	3.3	533	13.33	91.49	1806.7	1195.0	66.16	25	0.008298	35.847
	1765	395	3.5	521	13	106.4	1915.6	1393.1	72.72	27	0.01044	45.100
29^0	1079	395	3.2	546	13.6	73.34	1751.2	1016.8	58.06	20	0.005648	24.399
	1275	390	3.4	539	13.47	82.04	1837.3	1106.9	60.24	21.5	0.006610	28.581
	1471	395	3.6	528	13.2	98.00	1970.4	1295.7	65.75	23	0.008278	35.760
	1765	400	3.7	518	12.95	114	2050.3	1497.2	73	25.25	0.010511	45.36
32^0	1079	390	3.4	542	13.54	78.42	1837.4	1076.3	58.57	19	0.005680	24.537
	1275	395	3.5	537	13.42	86.87	1915.6	1170.9	61.12	21	0.006830	29.505
	1471	400	3.6	526	13.14	103.8	1995.3	1359.1	68.11	22.5	0.008494	36.694
	1765	405	3.7	512	12.8	119.6	2076.4	1535.2	73.93	23	0.009808	42.370
35^0	1079	396	3.5	541	13.51	82.19	1920.5	1100.1	57.28	22	0.006722	29.039
	1275	400	3.6	535	13.38	91.04	1995.3	1215.6	60.92	23	0.007766	33.549
	1471	400	3.8	522	13.04	108.7	2106.1	1359.9	64.56	24	0.009066	39.165
	1765	404	3.9	510	12.74	126.4	2188.6	1613.5	73.72	25	0.01120	48.384

Table 4.3 Results of energy consumption of 3hp laboratory haulage drive system by   conventional method for different combination of loads
          and gradients for up the gradient

Angle with horizontal	Load (N)	Voltage (V)	Current (A)	N_1 (rpm) (Actual speed)	N_2(rpm) (1:40) (Shaft speed)	Torque (Nm)	Input power (W)	Output power (W)	Efficiency (%)	Time (s)	Energy consumption (kWh)	Yearly Energy consumption (kWh)
27^0	1079	390	3.2	548	13.7	70.65	1729.2	979.45	56.62	24	0.00652	28.1664
	1275	390	3.4	542	13.5	78.22	1837.3	1045	57	26	0.00754	32.5728
	1471	395	3.5	531	13.3	93.38	1915.6	1243.0	64.88	27.7	0.00958	41.3856
	1765	395	3.7	520	13	108.5	2025.1	1389.3	68.60	29	0.01119	48.3408
29^0	1079	395	3.3	546	13.6	75.4	1806.1	1045.3	57.87	22	0.00638	27.5616
	1275	400	3.4	541	13.5	83.5	1884.5	1114.4	60	23.5	0.00727	31.4064
	1471	400	3.5	529	13.2	99.69	1939.9	1325.7	67.93	25	0.00920	39.744
	1765	415	3.7	523	13.1	115.9	2076.4	1490.7	71.79	26.5	0.01097	47.3904
32^0	1079	390	3.5	541	13.5	79.6	1891.4	1080.5	57.12	20	0.00600	25.92
	1275	400	3.6	537	13.4	88.14	1995.3	1174.1	58.84	22	0.00717	30.9744
	1471	400	3.7	524	13.1	105.2	2076.4	1377.4	66.33	23.5	0.00899	38.8368
	1765	410	3.8	516	12.9	122.3	2130.4	1570	73.69	25	0.01090	47.088
35^0	1079	400	3.5	541	13.5	83.18	1939.9	1174.8	60.55	23	0.00750	32.4
	1275	400	3.6	537	13.4	92.12	1995.3	1277.4	64	24	0.00851	36.7632
	1471	400	3.8	521	13	110.4	2158.8	1408.5	65.3	26	0.01017	43.9344
	1765	405	3.9	509	12.7	127.8	2188.8	1614.8	73.77	27	0.01211	52.3152

4.4 EXPERIMENTAL STUDIES WITH 3HP HAULAGE DRIVE BY MICRO CONTROLLER METHOD

4.4.1 Introduction

A major emphasis of the present work is to develop a generalized hardware platform for high-performance ac drives. The system organization for rotor side control of doubly-fed slip ring induction machine presents a versatile case where rotor side converters are necessary. In order to illustrate the application of such a system to direct rope haulage drive system, slip ring induction motor drive characteristics also need to be simulated with a direct rope haulage drive.

4.4.2 Control technique of slip ring induction motor

In earlier days, the squirrel cage induction motor(SCIM) was used for essentially constant speed drive, and the slip ring induction motor (SRIM) was used for variable-speed drive systems. Although the SRIM is more expensive and less rugged than the SCIM, it has been favored for use in high-power applications in which a large amount of slip power could be recovered. It may be noted that an attractive feature of SRIM control is that only the slip power is handled by power electronics, which may be only a fraction of the rated machine power.

Classically, speed of the SRIM was changed by mechanically varying external rotor circuit resistance. The Krammer drive provides sub synchronous speed control. Field-oriented control can also be applied in SRIM's to provide decoupled control of real power and reactive power. These features are extremely beneficial in high-power applications.(Takahashietal.,1989)

Pulse width modulated (PWM) drives is presently widely available for both low voltage and medium voltage squirrel cage induction motors. These drives power the motor through the stator. However, low voltage PWM drives are suitable for use as an slip power recovery (SPR) drive. The inherent characteristics of the PWM converters can overcome the disadvantages of old current source SPR drive. The power circuits were unchanged, but the control in the rotor converter needed for some modifications.

4.4.3 Pulse Width Modulation (PWM) technique

With advances in solid-state power electronic devices and microprocessors, various inverter control techniques employing pulse-width-modulation (PWM) techniques are becoming increasingly popular in AC motor drive applications. These PWM-based drives are used to control both the frequency and the magnitude of the voltages applied to motors (Salehfar, 2005).Various PWM strategies, control schemes, and realization techniques have been developed in the past two decades (Pongiannan et al., 2011).PWM strategy plays an important role in the minimization of harmonics and switching losses in converters, especially in three-phase applications.

The main aim of any modulation technique is to obtain a variable output with a Maximum fundamental component and minimum harmonics (Kumaretal.,2010). Three-phase voltage source pulse-width modulation inverters have been widely used for DC to AC power conversion since they can produce outputs with variable voltage magnitude and variable frequency. Typical solutions employ microcontrollers or DSPs (Giesselmann, 2001)

4.4.4. Types of Control

Alternating Current (AC) drives that use PWM (Pulse Width Modulation) techniques have varying levels of performance based on control algorithms. There are four basic types of control for AC drives today. These are volts per hertz, sensor less vector control, flux vector control, and field oriented control. Volts/hertz control is a basic control method, providing a variable frequency drive for applications like fan and pump. It provides fair speed and starting torque, at a reasonable cost.

Sensor less vector control provides better speed regulation and the ability to produce a high starting torque. Flux vector control provides more precise speed and torque control with dynamic response. Field oriented control drives provide the best speed and torque regulation available for AC motors. It provides DC (Direct Current) like performance for AC motors, and is well suited for typical DC applications.

The varieties of these control approaches are numerous. One of the methods is using microcontroller for speed control of three phases motor which in turn control speed of direct rope haulage system (Singh et al., 2001). Microcontroller based method uses pulse width modulation technique. In this speed of the motor is

controlled by sensing the current value of the rpm. The current value of rpm is sensed by inductive magnetic switch and its output is fed to the microcontroller.

The micro controller compares the current value of the rpm with set values and adjusts the time period of the pulses applied to the stator to control the frequency of the stator. But the drawbacks of this method are it requires skilled programmers and sensitivity of sensor.

4.4.5 Inverter control

In present research work Insulated Gate Bi-polar Transistor (IGBT) based slip recovery method of speed control is used in direct rope haulage drive system. An inverter control provides a means for both speed control as well as torque control. A variable Frequency drive is used to vary the speed of the motor.

A variable frequency drive will introduce harmonic current into the motor, which will be approximately five to six per cent of normal motor amps. Because of its superior insulation, an inverter duty motor should always be used with the inverter drive. An inverter control works by changing the voltage and frequency of the AC power supplied to the stator windings. Below base speed, the voltage and frequency are reduced in a fixed V/Hz ratio in order to maintain a constant level of magnetizing current.

This control method is not very effective at very low speeds and is not recommended for hoisting and bridge applications and for applications requiring full torque at zero speed. A closed loop or vector control is recommended for greater speed control and developing full torque at zero speed. An encoder feedback is required for closed loop control. With closed loop control, the motor speed can be precisely controlled. This control method is very effective at very low speeds and can provide up to 200% of full torque at zero speed depending on the motor design. With the vector control, the slip of the motor is constantly monitored and adjustments made to keep the motor at rated slip and develop full torque over the whole range of speed. Vector control is also used for applications requiring precise torque control.

Three phase voltage source inverters are widely used in variable speed AC motor drive applications since they provide variable voltage and variable frequency output through pulse width modulation control. Many different PWM methods have been developed to achieve the following aims: wide linear modulation range; less

switching loss; less Total Harmonic Distortion (THD) in the spectrum of switching waveform; and easy implementation and less computation time. Space vector pulse width modulation (SVPWM) is one of the most important PWM methods for three phase inverter; it uses the space vector concept to compute the duty based design of PWM based Inverter scheme

The following needs to be defined for the design of the PWM inverter system:

i. A model that defines different processes of pulses.
ii. Implement zero order hold and relational operator to the sine wave.
iii. A periodic scalar signal having waveform that we specify using the Time values and Output values.

Following parameters need to be defined to implement a PWM Inverter

i. Sine wave operates in time-based or sample-based mode.
ii. Repeating sequence a periodic scalar signal having a waveform that we specify using the time values and Output value parameters.
iii. Zero order hold holds the input for the sample period.

Relational Operator compares two inputs cycle of the switches. It is simply the digital implementation of PWM modulators.

4.4.6 The Rotor-Side Converter (RSC)

The rotor-side converter (RSC) applies the voltage to the rotor windings of the doubly-fed induction generator. The purpose of the rotor-side converter is to control the rotor currents such that the rotor flux position is optimally oriented with respect to the stator flux in order that the desired torque is developed at the shaft of the machine. The rotor-side converter uses a torque controller to regulate the motor output power and the voltage measured at the machine stator terminals.

Usually, a Proportional-Integral (PI) regulator is used at the outer control loop to reduce the power error (or rotor speed error) to zero. The output of this regulator is the Quadrature-axis Rotor Reference Current (irqref) that must be injected in the rotor winding by rotor-side converter. This q-axis component controls the electromagnetic torque Te. The actual Quadrature-axis Rotor Current (irq) component of rotor current is compared with Irqref and the error is reduced to zero by a current PI regulator at the inner control loop. The output of this current controller is the Quadrature-axis Rotor Voltage (vrq) generated by the rotor-side converter.

With another similarly regulated direct –axis rotor current and rotor voltage (Ird and Vrd) component the required 3-phase voltages applied to the rotor winding are obtained. The dc-link model describes the dc-link capacitor voltage variations as a function of the input power to the dc-link (Ledesma & Usaola,2005). The energy stored in the dc capacitor is Wdc = ∫Pdcdt = CVdc. Power flow of slip ring induction motors are given in Figure 4.8.
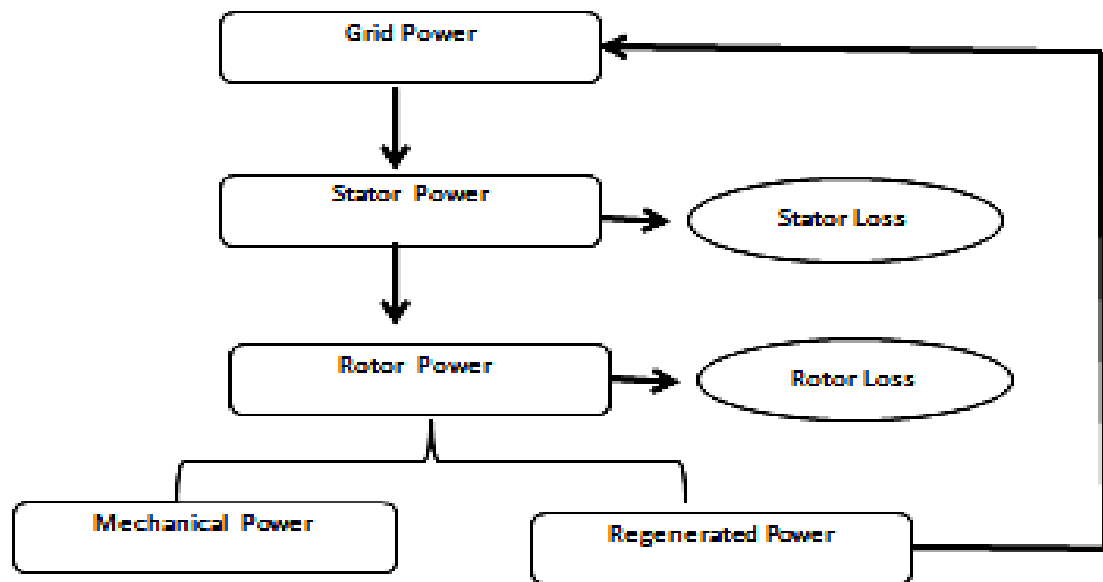
Figure 4.8 Power flow of slip ring induction motor

4.5 Hardware description of micro controller based haulage drive system

4.5.1 Insulated Gate Bi-polar Transistor (IGBT) Converter

The IGBT converters use the conventional three phase bridge topology. The converters are fabricated in-house in a modular fashion. Physically, the machine side converters and diode bridge rectifier with filter units are connected together through cables. The electrolytic capacitors are seated directly on the bus and, are physically close to the device terminals. Apart from these electrolytic capacitors, polypropylene capacitors with low ESR are connected directly at the device terminals.

The inverter design is, therefore, snubberless; the polypropylene capacitors only absorb the small switching spikes that appear on the dc bus. The devices are mounted on an appropriate heat sink and, forced air-cooling is employed. The other hardware subsystems of the inverter are described below.

4.5.2 Speed Measurement IR (infra red) Sensor

The working of sensor rotor of the induction motor white and black disc is mounted on the rotor machine. The black and white surfaces are reflecting and non reflecting surface. Infra red (IR) sensor has Emitter (LED) and collector (photo diode). When light strikes on black surface PN diode does not receive photon and when light strikes on white surface PN diode receives photon. On receiving light from white surface, comparator gives one pulse which is denoted as one revolution.

When no light receives from black surface comparator gives low pulse and it is denoted as rotating. The speed measurement using infra red (IR) is given in Figure 4.9. The AT Mega 32 micro controller ports a connected to IR Light Emitting Diode (LED) and Photo diode of speed sensor which is mounted on the machine side shaft.

The 3pin connectors are connected to port A of the micro controller. Machine starts when 3-phase supply is given to stator of the motor control relay–A, which is shorted to the slip ring of motor. As speed of motor reaches 600rpm, it is measured by speed sensor. Once speed reaches the desired rpm the PWM pulse generated from microcontroller drives the IGBT inverter with proper sequence. The detailed explanations are given in section 4.5.
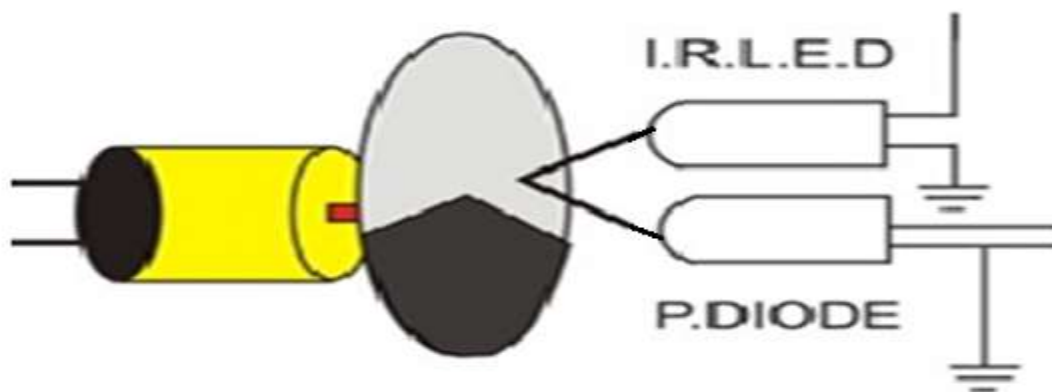
Figure 4.9 Speed measurement using IR (Infra red) sensor

4.5.3 Control relay

A relay is an electrically operated device. The principle of operation is similar to that of the contactor but differs in application. Figure 4.10 shows the motor control

power relay which is used for automatic connection of rotor terminal and grid connection according to instruction command of micro controller. In this experimental work, the separate control unit is designed for connectivity of slip rings, and closing grid terminal after performing synchronization process.
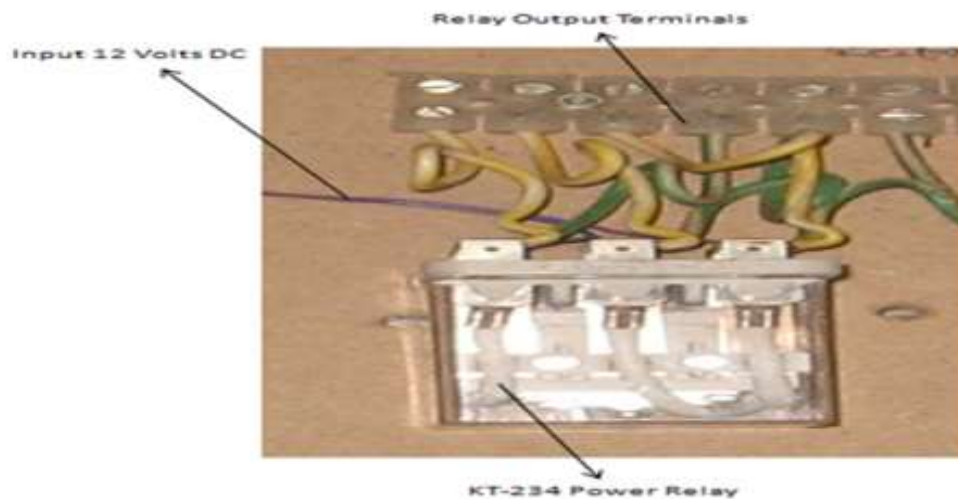
Figure 4.10 Motor control power relay unit

4.5.4 Slip ring induction motor speed Control unit

The speed control unit of the 3hp experimental micro controller based haulage drive system for slip ring induction motor is shown in Figure 4.11. The speed control unit consists of 3- phase diode rectifier, LC filter and insulated gate bi-polar transistor (IGBT) inverter with IGBT gate drive unit. The PWM control pulses from the microcontroller are directly fed to control circuit unit.
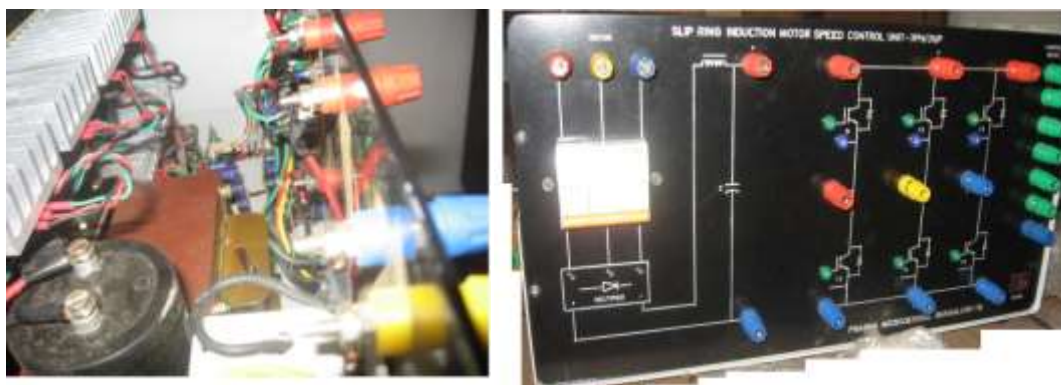
Figure 4.11 3hp experimental micro controller based haulage drive speed
control unit for slip ring induction motor

4.5.5 The AT Mega 32 micro controller and control relay unit

The 8 bit microcontrollers have their own role in the digital electronics market dominated by 16-32 & 64 bit digital devices. Although powerful microcontrollers with higher processing capabilities exist in the market, 8bit microcontrollers still hold its value because of their easy-to-understand-operation, very much high popularity, ability to simplify a digital circuit, low cost compared to features offered, addition of many new features in a single IC and interest of manufacturers and consumers.

At present some of the major manufacturers are Microchip, Atmel, Hitachi, Phillips, Maxim, NXP, Intel etc. Our interest is upon ATmega32. It belongs to Atmel's AVR series micro controller family. The pin diagram of ATmega32 is shown in Figure 4.12.

PIN count: Atmega32 has got 40 pins. Two for Power (pin no.10: +5v, pin no. 11: ground), two for oscillator (pin 12, 13), one for reset (pin 9), three for providing necessary power and reference voltage to its internal ADC, and 32 (4×8) I/O pins.

About I/O pins: ATmega32 is capable of handling analogue inputs. Port A can be used as either DIGITAL I/O Lines or each individual pin can be used as a single input channel to the internal ADC of ATmega32, plus a pair of pins AREF, AVCC & GND (refer to ATmega32 datasheet) together can make an ADC (Analog Digital Converter) channel.

Digital I/O pins: ATmega32 has 32 pins (4portsx8pins) configurable as Digital I/O pins.

Timers: 3 Inbuilt timer/counters, two 8 bit (timer0, timer2) and one 16 bit (timer1).**ADC:** It has one successive approximation type ADC in which total 8 single channels are selectable. They can also be used as 7 (for TQFP packages) or 2 (for DIP packages) differential channels. Reference is selectable, either an external reference can be used or the internal 2.56V reference can be brought into action.There external reference can be connected to the AREF pin. Communication Options: ATmega32 has three data transfer modules embedded in it. They are

  i.   Two Wire Interface
  ii.   USART
  iii. Serial Peripheral Interface

Analog comparator: On-chip analog comparator is available. An interrupt is assigned for different comparison results obtained from the inputs.

External Interrupt: 3External interrupt is accepted. Interrupt sense is configurable.

Memory: It has 32Kbytes of In-System Self-programmable Flash program memory, 1024 Bytes EEPROM, 2Kbytes Internal SRAM. Write/Erase Cycles: 10,000 Flash / 100,000 EEPROM.

Clock: It can run at a frequency from 1 to 16 MHz . Frequency can be obtained from external Quartz Crystal, Ceramic crystal or an R-C network. Internal calibrated RC oscillator can also be used.

More Features: Up to 16 MIPS throughput at 16MHz, most of the instruction executes in a single cycle. Two cycle on-chip multiplication. 32×8 General Purpose Working Registers

Debug: JTAG boundary scan facilitates on chip debug.

Programming: In ATMega-32 in system programming can be either interfacing of serial peripheral or parallel programming method and also programming through joint test action group. Programmer need to make sure that Serial Peripheral Program encoding and joint test action group are not being disabled using fusebits;
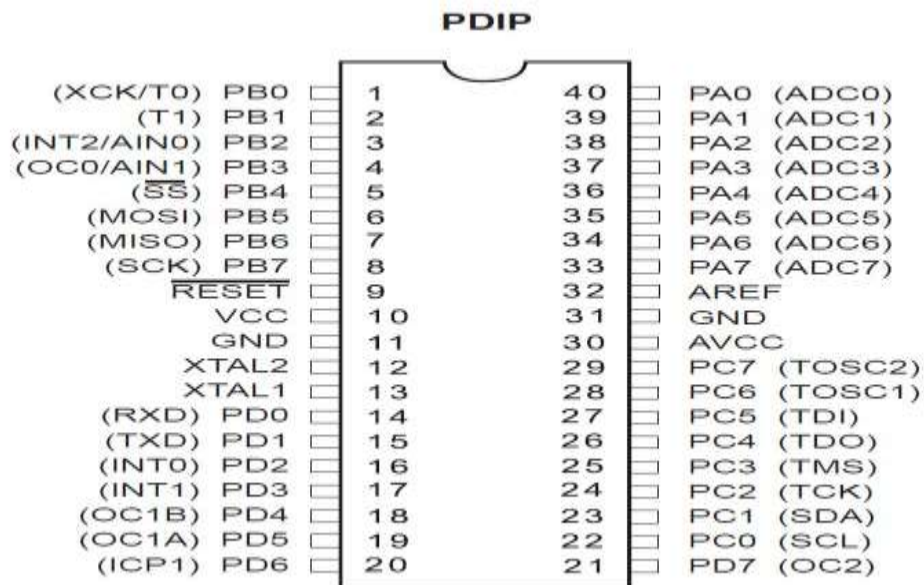
Figure 4.12 Pin out of AT Mega 32

Interfacing of IGBT base drive control unit, speed sensor and control relay unit with AT Mega 32 micro controller are presented in Figure 4.13.

i. Using AT Mega 32 micro controller the following procedure is followed to 3hp experimental haulage drive system for power recovery of slip ring induction motor.

ii. Make the connection of downloading serial cable and connect power supply (+12V) to both EM_P02 as well as SDM Board.

iii. Connect the IGBT gate driver unit to Port B to J5 connector of SDM Board.

iv. Set the microcontroller (EM_P02) board in programming mode.

v. Write the program in Keil Compiler.

vi. Create the HEX file.

vii. Program the HEX file by using flash magic down loader by selecting the Device.

viii. Come out from programming mode and press reset switch for execution of Program.

ix. Observe the haulage drive motor operation.

The block diagram of AVR micro controller 32 is as shown in APPENDIX IV. In this assembly language programming c code is written for PWM generation and control of bi- directional motor and control of tub in both directions. The typical programming code for generation of PWM pulses for IGBT switching action to control the slip ring induction motor, bi-directional motor control and control of tub direction are given in APPENDIX V.

4.5.6 Bi-directional motor

For automatic control of reduction gear system for 3hp experimental micro controller based haulage drive unit the bi-directional motor (wiper motor) with rack and pinion arrangement is used to change the direction. The required operating voltage for operation of bi-directional motor for which the separate bridge rectifier circuit is designed for operating voltage of 12 Volts and current of 5amps dc supply to drive the bi-directional motor.

The bi- directional motor is shown in Figure 4.14. Micro controller based wireless RF433MHz transmitter and receiver system is designed for controlling tub movement in forward and reverse direction by connecting the four proximity sensor (two sensor fixed on reduction gear system and other two sensor are fixed on the rail track to control the movement of the tub) on both end of the tub movement one is fixed on the starting and other one dead end of the rail track. The operational characteristics of transmitter and receiver are explained in the next section.
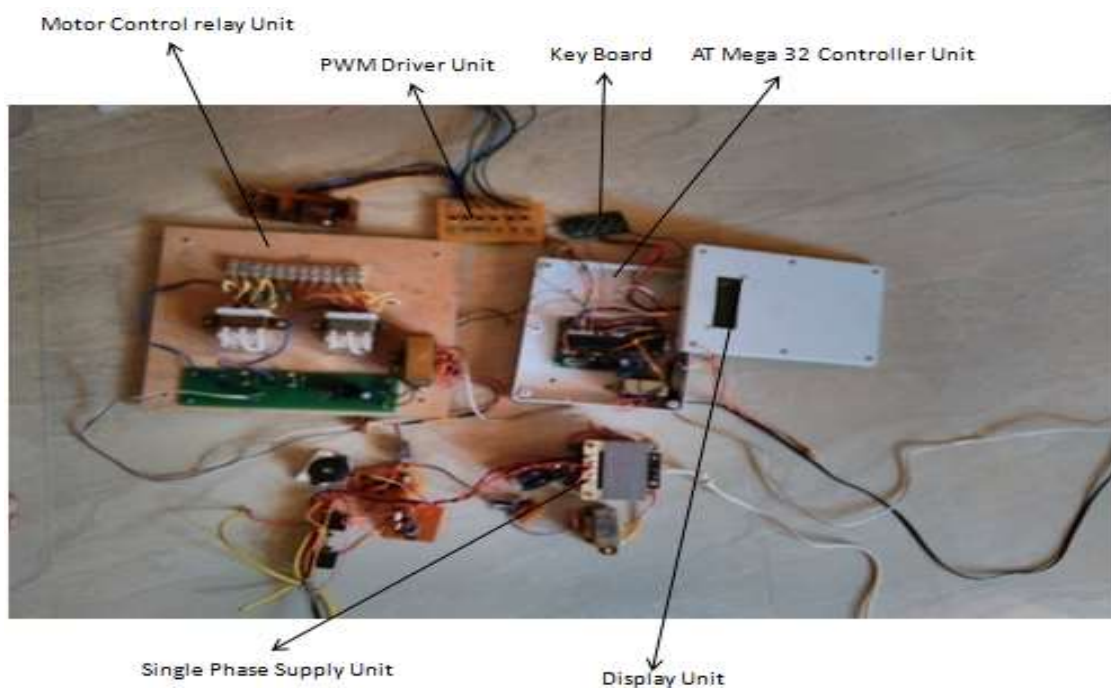
Figure 4.13 Interfacing IGBT base drive control unit, speed sensor and control relay unit with AT Mega 32 micro controller.

Figure 4.14 Bi-directional motor with rack and arrangement

4.5.7 Wireless (RF 433MHz) transmitter and receiver

A wireless radio frequency (RF) transmitter and receiver can be easily made using HT12DDecoder, HT12E Encoder and ASK RF Module. Wireless transmission can be done by using 433 MHz or 315MHz ASK RF Transmitter and Receiver modules. In these modules digital data is represented by different amplitudes of the carrier wave, hence this modulation is known as Amplitude Shift Keying (ASK). Radio Frequency (RF) transmission is stronger and more reliable than Infrared (IR) transmission due to the following reasons:

Radio frequency signals can travel longer distances than infrared. Only line of sight communication is possible through Infrared while radio frequency signals can be transmitted even when there is an obstacle. Infrared signals will get interfered by other IR sources but signals on one frequency band in RF will not get interfered by other frequency RF signals. The wireless (RF 433MHz) transmission and receiver circuit technique is used for controlling the gear and tub movement of the drive system.

This is a simple type remote control by using RF communication with microcontroller. The radio frequency Transmitter and Receiver operating specification details are shown in APPENDIX VI. In this thesis work a remote control has been designed for position of car movement for both directions. It gives a lot of comfort to the user, since we can operate it in same working place. By using this remote control technique the movement of the car can be controlled within the range of 150meters. The (RF 433MHz) wireless radio frequency control consists of two sections, transmitter (remote) and receiver section.

Whenever car reaches end by pressing limit switch transmitter it generates the corresponding RF signals and these signals are received by the receiver unit. ASK transmitter and receiver is used as transmitter and receiver. HT12E, HT12D encoders and decoders are used in this electronic circuit.

Automatic Contact control relay wireless transmission and receiver circuit for RF 433MHz for controlling the gear and tub movement are presented in Figure 4.15.The fabricated 3hp laboratory experimental micro controller based haulage drive system for different circuit connection diagram of RF 433MHz Wireless (RF) transmitter and receiver circuit for control of tub are presented in Figure 4.16.

The various circuit connection diagram for fabricated 3hp experimental haulage drive system such as Bi-directional motor power supply converter, power supply for PC817 opt coupler circuit for changing the direction of bi-directional motor and ICs circuit connection diagram of RF 433MHz Wireless (RF) transmitter and receiver circuit for control of tub movement direction are presented in Figure 4.16(a), Figure 4.16(b) and Figure 4.16(c) respectively.

4.5.8 Remote Section

Remote section consist of an encoder (HT 12E) and a ASK transmitter. The encoder generates 8 bit address and 4bit data. Address can be set by using the DIP switch connected in A0 to A7 (pin1to 8) of encoder. And also set an address in the remote section, the same address will be required in the receiver section.

So always set the same address in transmitter and receiver section of the remote controller. Whenever car reaches the end by pressing the limit switch press the encoder generates corresponding 4bit data and send this data with 8bit address by using ASK transmitter. The transmitting frequency is 433MHz.The transmitter output is up to 8mW at 433.92MHz with a range of approximately 400 foot (open area) outdoors. The serial data flow process for the movement bi- directional motor is shown in APPENDIX VII.

4.5.9 Receiver Section

At the receiver section ASK receiver is present. The receiver also operates at 433.92MHz, and has a sensitivity of 3uV. The ASK receiver operates from 4.5 to 5.5 volts-DC, and has both linear and digital outputs. It receives the data from transmitter. Then the decoder (HT 12D) decodes the data and it will enable the corresponding output pin (pin 10, 11, 12, 13). Each output pins are connected to separate flip flops.

The output of encoder will change the state of the flip flop. So its output goes to set (high) from reset (low) state. This change makes a high signal in the output of the flip flop. This output signal is not capable to drive a relay directly. So using this, BC54 transistor will act as a current driver. Relay will be re-energized when the same switch is pressed in the remote. This is because of pressing same switch in the remote control. The output of the decoder again goes to high so this signal will again change

the state of the flip flop. So, the relay gets re-energized and the motor relay goes to OFF state.
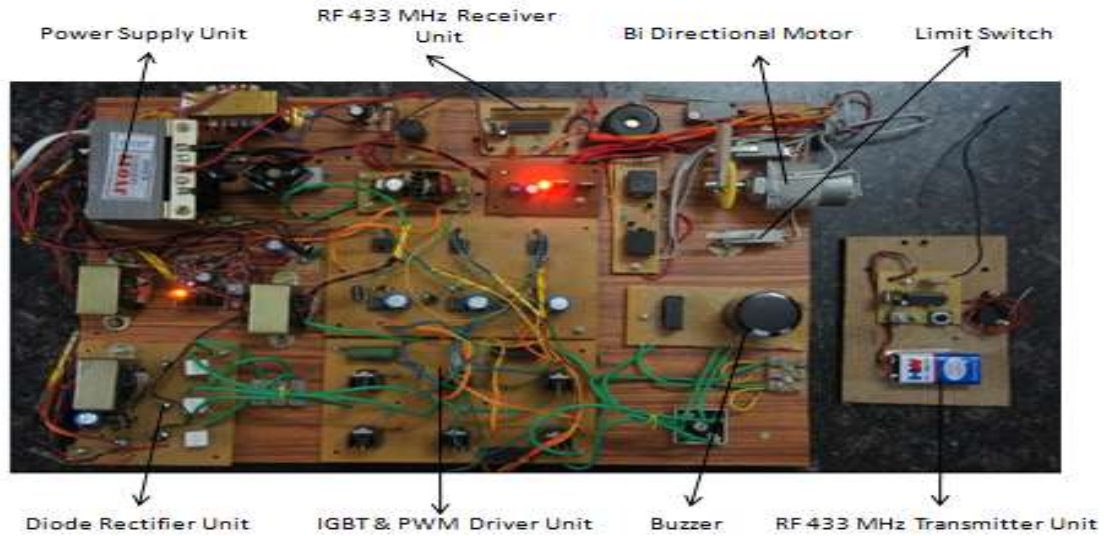
Figure 4.15 3hp laboratory experimental micro controller based haulage drive system
for automatic contact control relay wireless transmission and receiver
circuit for RF 433MHz for controlling the gear and tub movement
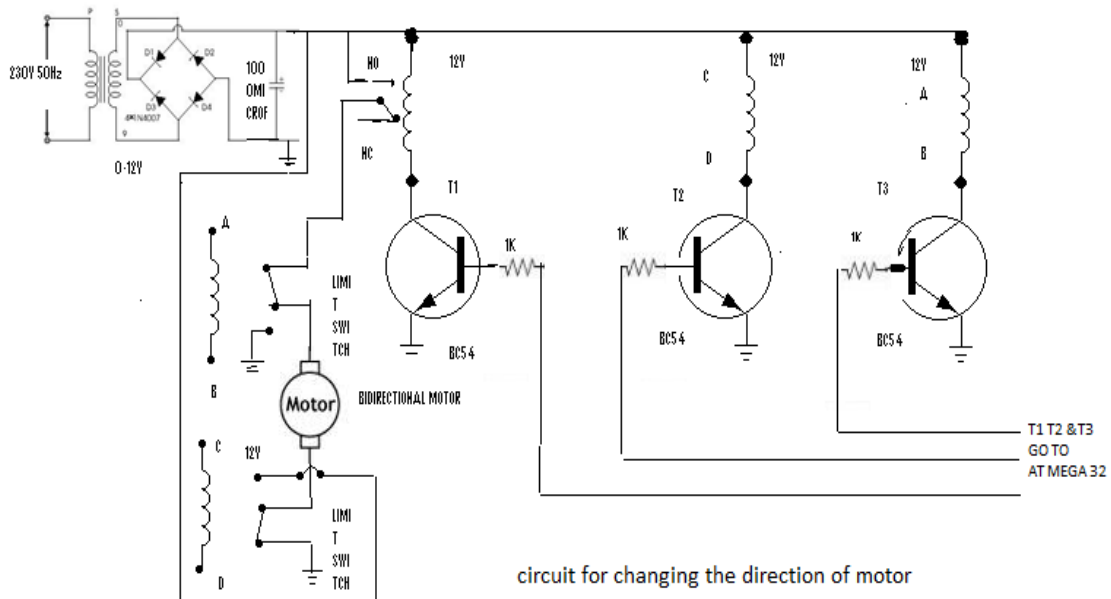
Figure 4.16(a) Circuit connection for bi-directional motor power supply converter
and control of motor direction to change the reduction gear position
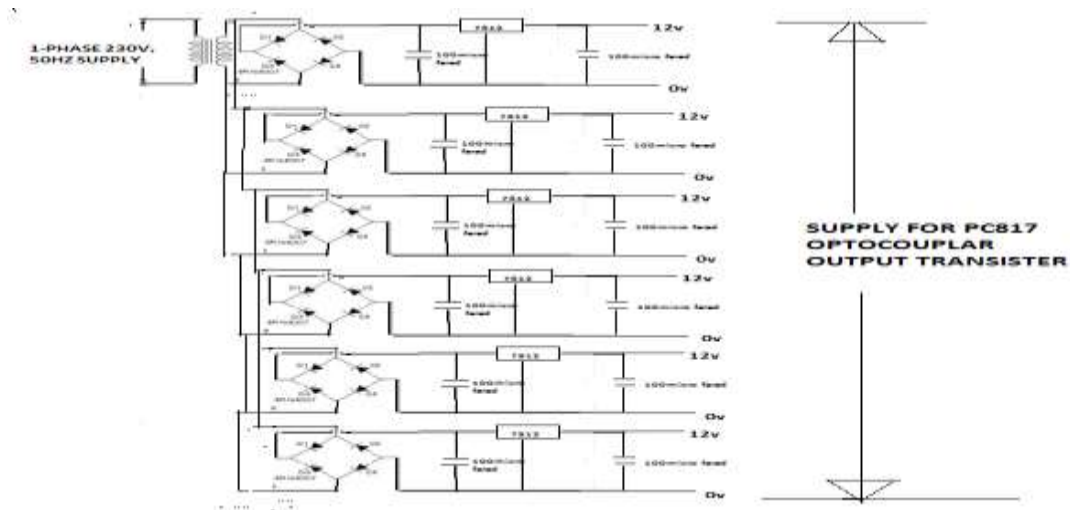
Figure 4.16(b) Generation of power supply for operation of PC 817 optcouplar.
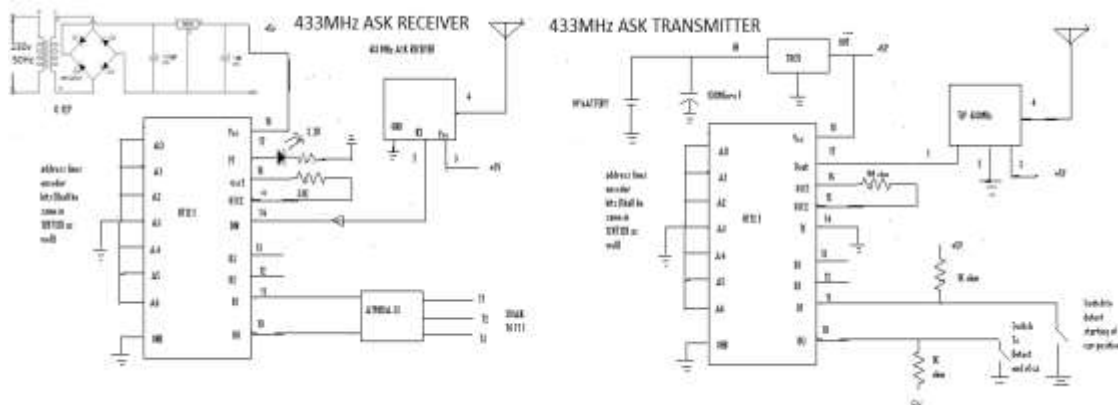
Figure4.16(c) IC circuit connection diagram of RF 433MHz Wireless (RF) transmitter and receiver circuit for control of tub

4.6 EXPERIMENTAL SET-UP FOR MICRO CONTROLLER BASED HAULAGE
   DRIVE SYSTEM

The design of AT MEGA 32 micro controller based slip power recovery controlled slip ring induction motor is described. The ATMega32 micro controllers is used to implement the speed sensing of induction motor and to generate the firing pulses to drive 3 phase IGBT inverter to recovery slip power for open loop control. The microprocessor based closed loop operation of the drive provides greater flexibility and accuracy, improved dynamic response and speed control independent of load variation.

In this thesis the microprocessor based slip power recovery control of slip ring induction motor is presented in Figure 4.17 consists of a slip ring induction motor, three phase uncontrolled bridge rectifier, three phase IGBT inverter, smoothing reactor and recovery transformer(1:n). The speed and current feedback signals are obtained by connecting speed sensor to the motor shaft. After digitizing, these signals are fed to the Port A, Port B, Port C and Port D of AT Mega 32 micro controllers. The generated pulses from the microcontroller are switching on the IGBT inverter phase difference of 600, 1200, 1800, 2200, 2800, 3600 degrees with delay of 5 milli seconds of each leg of IGBT.

The switching operation of 3-phase IGBT inverter is presented section 4.5.7. The firing pulses generated by the microcontroller are fed to the inverter through driver circuit. The static slip power recovery controlled slip ring induction motor drive is gaining importance because of higher efficiency, low cost and simple control circuitry (Bose,1987). Technical and fabrication details of laboratory experimental 3hp micro controller haulage drive system are given in Table 4.4.The description of various components required for conduction of experimental work is presented in this section. The detailed 3hp experimental microcontroller based haulage drive system block diagram and circuit diagram for the same is shown in Figure 4.17 and Figure 4.18 respectively. In Figure 4.18 there are two converters in cascade, usually called the "sub-synchronous cascade" because they provide speed control below the synchronous speed of the machine.

The first converter is the diode rectifier bridge, which rectifies the slip frequency voltage of the rotor. The output of this rectifier is connected in series with a smoothing inductor to the DC terminals of the second converter, which is a 3-phase Insulated Gate Bipolar transistor (IGBT) controlled bridge, operating in the inversion mode. The AC side of this bridge is connected to the 3-phase AC power system bus. The inverter serves to feed back power from the DC side to the AC power bus by phase controlled inversion.

The DC bus voltage may be expected to be small, because the DC is obtained by rectification of the slip frequency voltage from the rotor. Therefore a large angle of advance device conduction angle (β) will be needed for the inverter to feed to the power. The large value of device conduction angle (β) will adversely affect the power

factor. Therefore it will be advisable to use a transformer between the AC system bus and the inverter to match the voltages. The power fed back can be adjusted by adjustment of the firing angle of advance β of the inverter. The scheme is pertaining to closed – loop version of the slip power recovery. There is an outer speed control loop from which the speed controller provides the reference for an inner current control loop.

The inner loop senses the DC current and automatically adjusts the firing angle of the inverter to maintain the DC current at reference value. The speed of the slip ring induction motor is reduced in the scale of 1:40 using reduction gear system. The actual speed of the Induction motor is 600 RPM which is reduced to 15 RPM using reduction gear system. Forward and reverse direction of the hauler can be done by using forward/reverse gear system with help of sensors. A sensor may be required to sense the stopping point of the hauler for reverse direction actuation. Speed limiter switch to limit the speed for both forward and reverse direction of mine hauler.

4.6.1 Introduction to Micro Controller Haulage Drive System

The micro controller based speed control is attached to the 3hp laboratory haulage drive system by providing separate automatic gear drive system arrangement. The line diagram and 3hp laboratory experimental set-up for micro controller based haulage drive system are shown in Figure 4.19 and Figure 4.20 respectively After digitizing, the signals are fed to the Port A, Port B, Port C and Port D of AT Mega 32 micro controllers.

The firing pulses generated by the microcontroller are fed to the inverter through driver circuit. The movement of the gear system with bi-directional motor is attached by mechanical lever. The specification of bi-directional motor is 12V, 5 amp direct supply (DC) supply. The automatic gear changing drive unit system consists of bi-directional with rack and pinion arrangement with limit switch on both sides of the gear. The complete gear and tub or car movement depends on the wireless communication technique adopted in the fabrication of 3hp laboratory experimental haulage drive system. The entire experimental set-up is developed for open loop control of slip power recovery by micro controller technique. The speed of the motor is sensed by IR sensor which is connected to the port –D of AT mega 32 controllers.

Table 4.4 Technical and fabrication details of laboratory experimental 3hp micro
controller haulage drive system

Sl. No	Equipments	Particulars
1.	Bidirectional dc motor 12 V, 5 A mounted on the gear system with limit switch on both sides.	Forward and reverse movement of tub is controlled by wireless communication technique RF433 MHz.
2.	AT Mega -32 micro controller.	AT MEGA -32 is a low-power CMOS 8-bit microcontroller based on the AVR boosted RISC architecture, The supply voltage 4.4 to 5.5V .
3.	IGBT inverter module with heat sink, 3phase diode bridge rectifier, inductor and capacitor. IGBT drive circuit.	10 A , 600 V
4.	Automatic contact control relay.	230V , 50Hz.
5.	Transformer.	2KVA, 3 phase 50Hz with tapping on the primary and secondary sides.
6	RF 433MHz wireless transmitter and receiver.	Operating distance=121.92m,12V DC, 9V DC, frequency 433MHz.

.
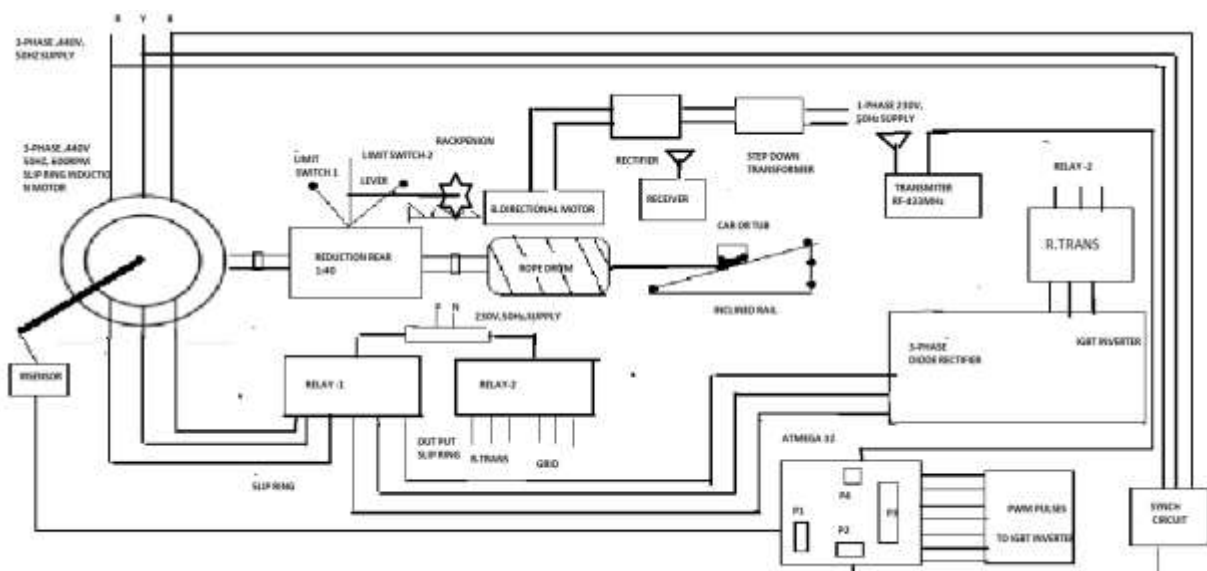
Figure 4.17 The block diagram of 3hp laboratory experimental set-up for micro
controller based haulage drive system
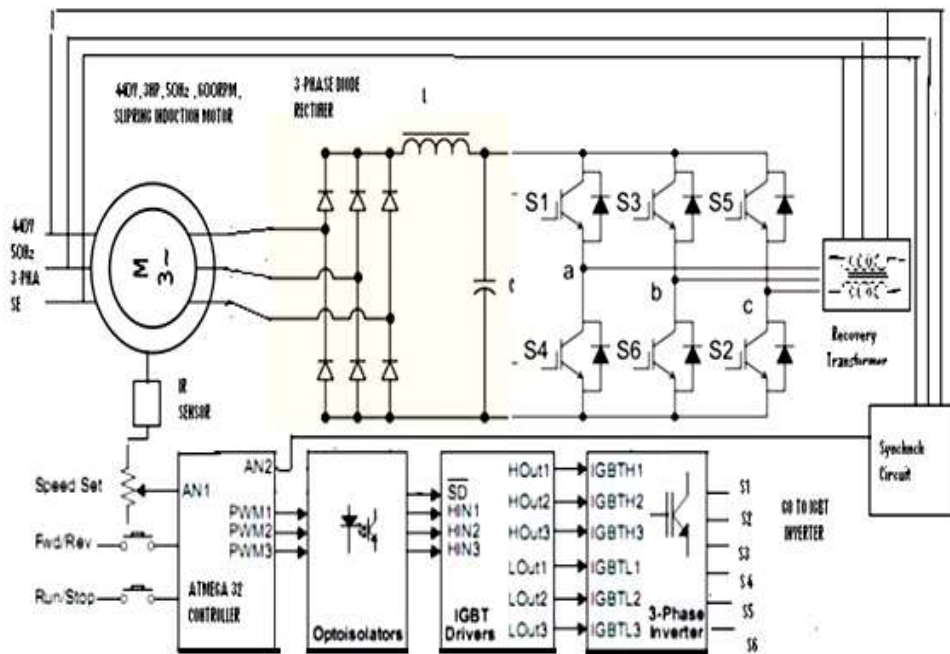
Figure 4.18 Circuit diagram for micro controller based 3hp laboratory
experimental haulage drive system
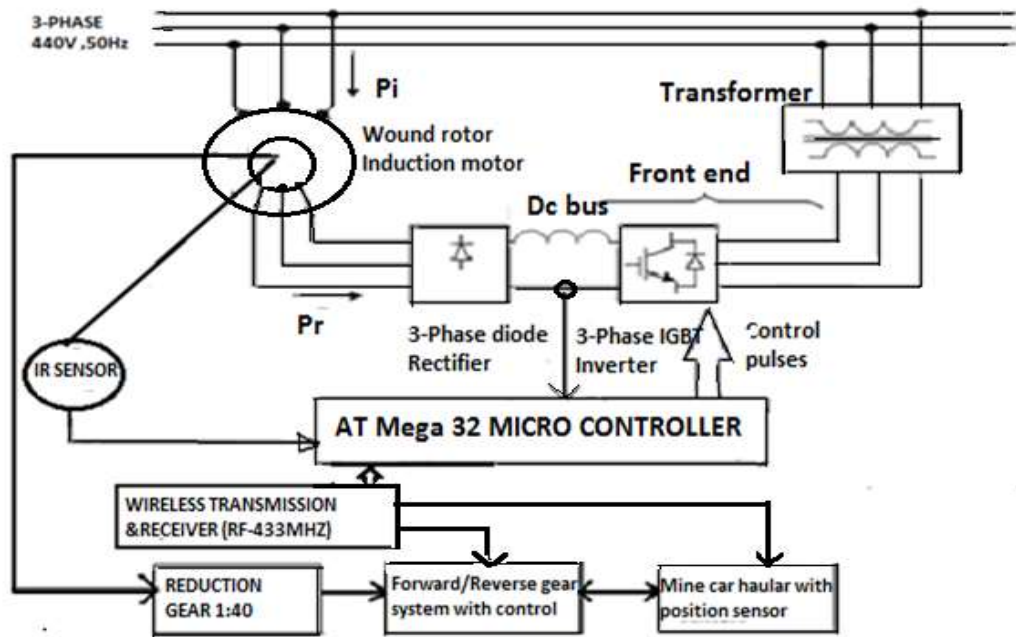
Figure 4.19 Line diagram of 3hp micro controller based haulage drive system
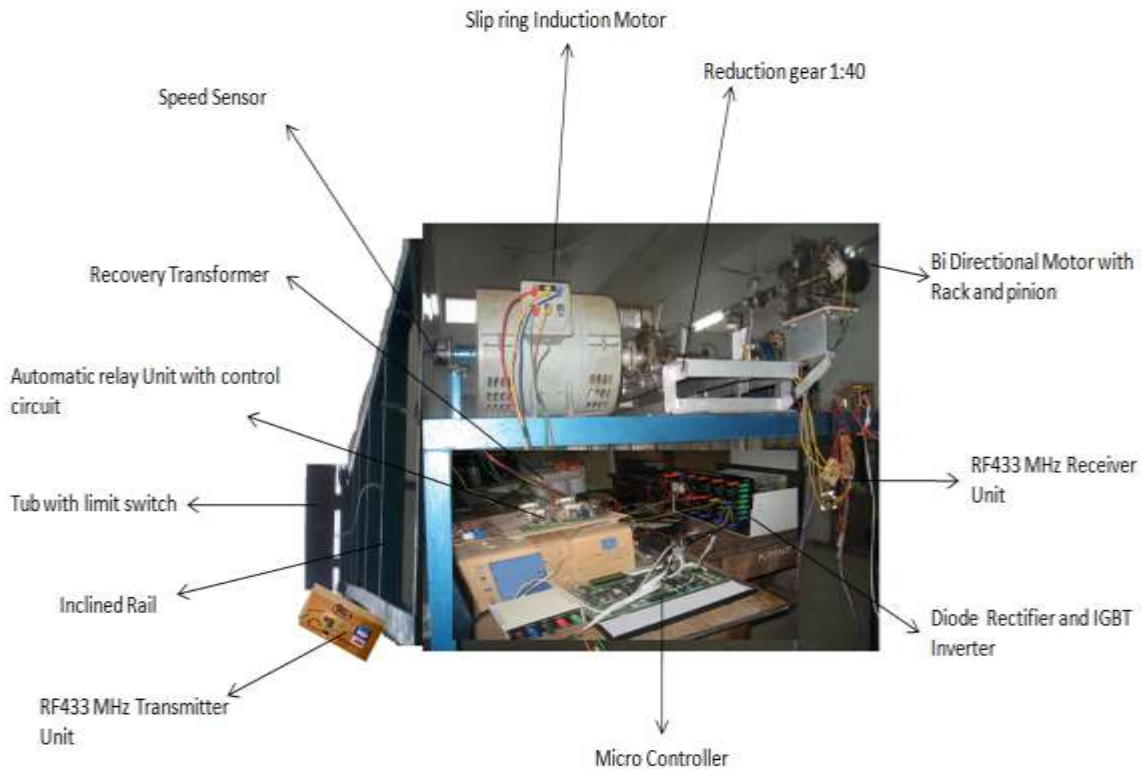
Figure 4.20 3hp laboratory experimental set-up for micro controller based haulage
drive system

4.6.2 Experimental procedure

The control circuit generates complementary pulses for IGBT switching on and switching off. Complementary pulses are needed for triggering the IGBTs. These are square wave pulses of magnitude 12V (approx.). In order to ensure proper commutation of the IGBTs, a blanking time of approximately 100μSec (for an insulated gate bipolar transistor (IGBT)) has been introduced. This is to make sure that both the IGBT are not switched on simultaneously (short-circuited).

The following procedure is used for conducting experiments in the 3hp laboratory experimental set- up, 3-phase supply is given to the 3-phase auto transformer. The slip ring terminal is connected to input of automatic power relay A and output is connected to 3-phase bridge rectifier of control unit. Automatic power relay B input is connected to primary and secondary of recovery transformer.

The motor side automatic power relay A will get the signal from micro controller so that the motor rotor terminals get shorted and the induction motor will start. The speed sensor (IR) senses the speed, once the motor speed reaches the rated

speed (600RPM). After time delay of 10 seconds the pulse width modulation (PWM) action will start according to switching sequence table (mentioned in section 4.5.7). The power supply connected to the primary terminal of power recovery transformer from automatic power relay B, and secondary terminal power recovery transformer gets connected to supply grid after the proper synchronization.

The experiment is conducted based on conventional control experimental input data. Respective stator and rotor side measurement parameters are noted down. The movement of the tub depends on the wireless control technique by sensing the dead end and start of the tub with required time delay. The experiments are carried out with different combination of loads (i.e. 1079N, 1275N, 1471N and 1765.8N) and gradients (angle with horizontal i.e. 27º, 29º, 32º and 35º) for both up the gradient and down the gradient.

The set of parameters such as actual speed (N_1), shaft speed (N_2), input power, voltage and current, time and power recovery for up the gradient and down the gradient and time are measured. The data obtained from the 3hp laboratory micro controller experimental based haulage drive system the calculated energy consumption for different combination of loads and gradients for down the gradient and up the gradient is tabulated for one trip (5m) and yearly energy consumption are given in Table 4.5 and Table 4.6.

The experimental results are tabulated by considering different combination of loads (i.e. 1079N, 1275N, 1471N and 1765.8N) and gradients (angle with horizontal i.e. 27º, 29º, 32º and 35º) for both up the gradient and down the gradient. Tabulated results are based on measurement of speed, input power; output power, torque, efficiency and energy consumption presented in the above Tables and calculation procedure are given APPENDIX –IV. The results table of energy consumption and conservation are presented in chapter 7 (results and discussion) and explanation for various parameters are discussed for both up the gradient and down the gradient of 3hp laboratory haulage drive system.

Table 4.5 Results of energy consumption of 3hp laboratory haulage drive system by microcontroller method for different combination of loads and gradients for down the gradient

Angles with horizontal	Load (N)	Voltage (V)	Current (A)	N_1 (rpm) (Actual speed)	N_2 (rpm) (1:40) (Shaft speed)	Torque (Nm)	Input power (W)	Output power (W)	Efficiency (%)	Power recovery (W)	Time (s)	Energy consumption (kWh)	Yearly Energy consumption (kWh)
27^0	1079	390	2.9	568	14.2	69.10	1567	1007	64.75	69.9	18	0.00503	21.729
	1275	390	3.0	560	14	77.50	1621	1114.6	69.00	88.3	20	0.00619	26.740
	1471	395	3.1	562	14.05	91.44	1697	1309.4	77.74	114.	21	0.00763	32.961
	1765	395	3.2	554	13.9	106.2	1751	1516	86.57	123	22	0.00926	40.003
29^0	1079	395	3.0	562	13.85	75.30	1642	1071	65.49	54.2	16	0.00476	20.563
	1275	400	3.2	565	14.17	82	1729	1193.2	69	86.3	18	0.00596	25.747
	1471	400	3.3	563	14.12	97.80	1806	1418.2	78.2	123	19	0.00748	32.313
	1765	415	3.5	560	14	115	1940	1653.4	85.22	156	21	0.00964	41.644
32^0	1079	390	3.2	564	14.1	78.32	1729	1134.8	65.59	58.5	16	0.00504	21.772
	1275	400	3.3	562	14.05	86.8	1829	1252.4	68.5	81.5	18	0.00626	27.043
	1471	400	3.4	560	14	103.2	1884.5	1483.7	78.73	125	20	0.00824	35.596
	1765	410	3.6	559	13.97	119.1	2020	1709.3	84.61	174	21	0.00997	43.070
35^0	1079	400	3.3	564	14.1	82.1	1811	1188.8	65.64	88.7	18	0.00594	25.660
	1275	400	3.4	562	14.05	90.44	1884	1319.3	70	104	19	0.00696	30.067
	1471	400	3.6	560	14	108.3	1995	1557	78.00	141	21	0.00908	39.225
	1765	405	3.7	558	13.95	126	2076	1805	86.95	192	22	0.0110	47.52

Table 4.6 Results of energy consumption of 3hp laboratory haulage drive system by microcontroller method for different combination of loads and gradients for up the gradient

Angles with horizontal	Load (N)	Voltage (V)	Current (A)	N₁ (rpm) (Actual speed)	N₂ (rpm) (1:40) (Shaft speed)	Torque (Nm)	Input power (W)	Output power (W)	Efficiency (%)	Power recovery (W)	Time (s)	Energy consumption (kWh)	Yearly Energy consumption (kWh)
27^0	1079	390	3.0	566	14.15	70.00	1621	1017.2	62.75	41.7	20	0.00565	24.408
	1275	390	3.1	564	14.1	77.56	1675.2	1123	67.0	78	22	0.00686	29.635
	1471	395	3.3	563	14.07	93.18	1806.1	1344.7	74.43	101	24	0.00896	38.707
	1765	395	3.5	548	13.7	108.0	1915.6	1519.2	79.32	130	26	0.0109	47.088
29^0	1079	395	3.2	570	14.25	75.1	1751.4	1099	62.74	53.7	18	0.00549	23.716
	1275	400	3.3	564	14.1	83	1829	1202	65.71	87.6	19	0.00634	27.388
	1471	400	3.4	562	14.1	99.3	1884.4	1470.5	78	145	20	0.00816	35.251
	1765	415	3.6	558	13.95	115.4	2070	1653.2	80	163	22	0.0101	43.632
32^0	1079	390	3.4	565	14.12	79.1	1837.4	1147.4	62.45	70	16	0.00509	21.988
	1275	400	3.5	563	14.02	88.0	1940	1267.5	65.33	93.4	18	0.00633	27.345
	1471	400	3.6	560	14	105.0	1995.3	1509.6	75.65	132.	19	0.00796	34.387
	1765	410	3.6	559	13.97	122.0	2045.2	1751	85.6	181	20	0.00972	41.990
35^0	1079	400	3.4	570	14.25	85.0	1884.5	1243.9	64.5	69	20	0.00691	29.851
	1275	400	3.5	566	14.15	94	1940	1380.5	70.41	88.5	21	0.00805	34.776
	1471	400	3.5	562	14.05	109	1940	1515	78	107	22	0.00925	39.96
	1765	405	3.6	555	13.87	124	2076	1766.8	85.10	152	23	0.0112	48.384

4.6.3 Software organization of laboratory 3hp experimental haulage drive system

The requirement for fast real-time control demands that the software has to be efficient in terms of execution time. This has prompted the use of assembly language for programming the AT MEGA 32 micro controller. The software organization for AT Mega 32 is used for writing the c code for generation of pwm pulses for drive IGBT with proper switching sequence. The complete sequence of operations of the haulage drive system are presented in flow chart and given in Figure 4.21.

The control sequence of tub moment and bi-directional motor operation for movement of gear changing process is also described in flow chart and given in Figure 4.22 along with flow chart; the operation sequence algorithm is also presented in the next section. Slip ring induction motor speed is sensed by IR sensor at Port D and PWM pulses to turn ON the IGBT for each operation will be generated. Movement of the tub control also controls bi-directional motor operation by RF 433MHz transmitter signal in each direction with a time delay of 5minutes or depends upon the job. Entire experimental procedure is given below.

4.6.4 The experimental procedure algorithm for slip power recovery of slip ring Induction motor

The induction motor is maintained at the required speed by maintaining the current required to run it.

i.   The current used by the motor is rectified using a three phase bridge rectifier and is controlled by the inductor in the LC filter circuit.

ii. The IR sensor senses the current value in terms of speed and sends this value to the microcontroller through universal asynchronous receiver/transmitter (UART) (speed sensor).

iii. The microcontroller decodes the value received and computes the error between the received value and the reference value. The error is then used in a PI Controller used to control the system.

iv. The microcontroller sends signals to the gate drive control circuit. This pulse turn On the insulated-gate bipolar transistors (IGBTs)with time delay of 5ms.

v.   The controlling of the IGBTs lead to the controlling of the system.

vi. The output of the IGBT inverters connected to the recovery transformer secondary terminal is connected to relay B in relay unit.

vii.   After synchronization the relay –B is connected to supply grid terminal.

viii.   The algorithm for generation PWM to IGBT switching sequence is as follows:

The following steps illustrate the algorithm to obtain the three phase PWM waveforms using microcontroller.

i.   Access the three phase synchronous PWM pulse width data values from look up table using three different pointers to look up table.

ii.   Send the desired PWM code pattern at port pins.

iii.   Set the timer value with lowest pulse width value first.

iv.   Start the timer and wait until timer flag set.

v.   Send the next desired PWM code pattern at port pins.

vi.   Set the timer value with next higher pulse width value.

vii.   Start the timer and wait until timer flag set.

viii.   Send the next desired PWM code pattern at port pins.

ix.   Set the timer value with next higher pulse width value.

x.   Start the timer and wait until timer flag set.

xi.   Increment pointer by one and loop back step 1.

xii.   The operation of the 6 pulse IGBT is each device ON at 60° phase displacement with time delay of 5ms.

4.6.5 The algorithm for operation of bi-directional motor

i.   Tub senses dead end of the proximity switch and then RF transmitter sends coded 10.

ii.   Receiver gets decode signal 10 when the frequency are equal to input port D signal.

iii.   The transistor 1 ON the relay gets energized motor starts run for forward direction.

iv.   The gear handle reaches and presses the proximity switch with 5 minutes delay.

v.   The second operation starts when RF 433MHz transmitter sends coding 01 the motor rotates in reverse direction.

vi.   Receiver gets decoded signal and Transistor-2 will ON the motor, and with reverse relay gets energized motor starts run.

vii.   The operation will repeat the above said procedure.

4.6.6 Pulse Width Modulation (PWM) Generation using microcontroller

Modified maximum constant boost PWM control method is most advantageous over the other PWM control methods. It also reduces voltage stress across switching

devices and improves performance. In this work maximum constant boost with third harmonic injected PWM signal is generated digitally through programming microcontroller (Srichander etal.,1994).
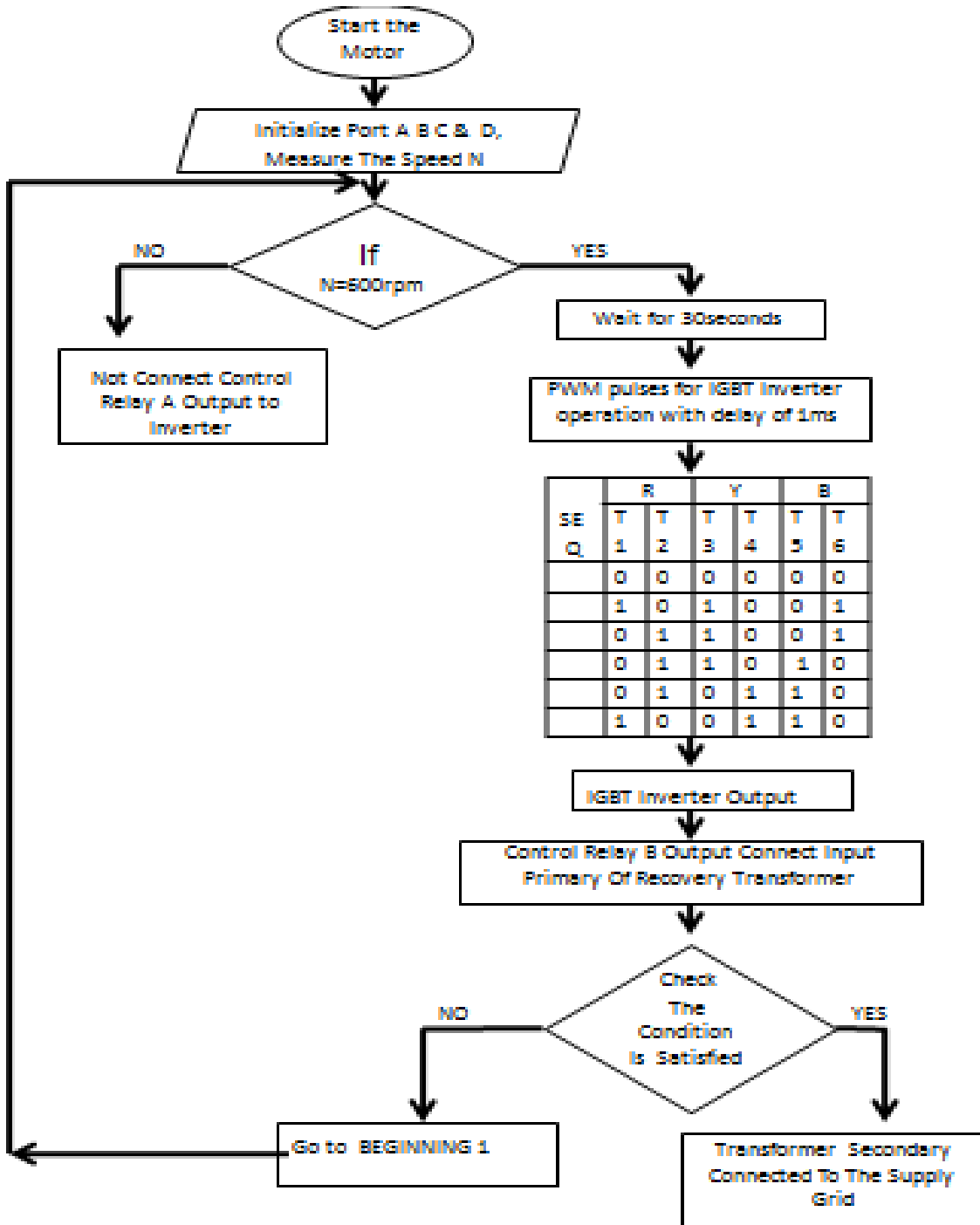
Figure 4.21 Flowchart for AT Mega 32 micro controller of slip power recovery and generation of pulse to control of IGBT switches
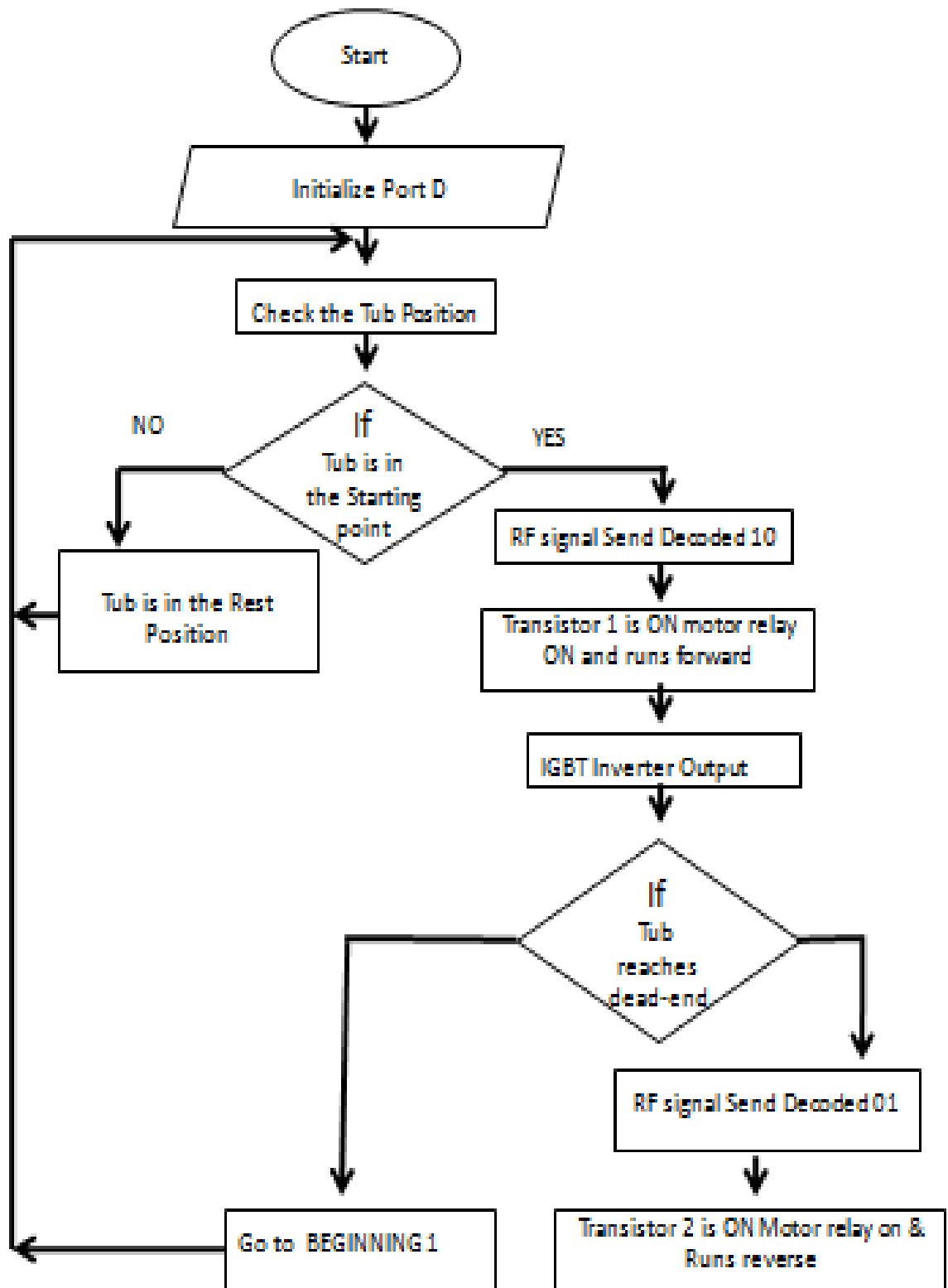
Figure 4.22 Flowchart for movement of the tub, reduction gear and bi-directional
motor control

4.6.7 Pulse width modulation (PWM) switching pattern

Table 4.7 shows all possible PWM states for inverter and respective PWM code pattern. The letters T_1, T_2, and T_3 indicates upper three switching devices and T_4, T_5, and T_6 indicate lower three switching devices in three arms of the main inverter circuit. Two devices in the same arm cannot switch on simultaneously in traditional inverters. This state is called shoot-through state inverter.

As shown in Table 4.7 Pulse Width Modulation (PWM) techniques for inverter consists of six active states (S1, S2,....S6) and two are zero states (S0, S7). PWM code is depicted on the right side last column. Microcontroller sends this PWM code at the port A at regular time instances provided by timer. All PWM code bit are complemented when passed through gate drive circuit. Thus bit 0 in Table 4.7 implies that particular switch is OFF and bit 1 implies ON switch in each PWM state.

Table 4.7 PWM switching table

R		Y		B	
T_1	T_2	T_3	T_4	T_5	T_6
0	0	0	0	0	0
1	0	1	0	0	1
0	1	1	0	0	1
0	1	1	0	1	0
0	1	0	1	1	0
1	0	0	1	1	0
1	0	0	1	0	1

4.6.8 Voltage vectors and their effects

Figure 4.23 shows the 8 possible switching states of a three phase voltage source inverter (VSI) of which six are active states (S1, S2,....S6) and two are zero states (S0, S7). Assuming that the orientation of the three phase rotor winding in space at any instant of time is as given in Figure 4.24, the six active switching states would correspond to the voltage space vectors U1, U2 ....U6 (Figure 4.25) at that instant. In order to make an appropriate selection of the voltage vector the space phasors plane is first subdivided into six 60^0 sectors I,II,III and VI.

The instantaneous magnitude and angular position of the rotor flux space phasors can now be controlled by selecting a particular voltage vector depending on its present location. The effect of the different vectors as reflected on the stator side active and reactive powers, when the rotor flux is positioned in sector 1 is illustrated in the Figure 4.25.

S1
(1 0 0)

S2
(1 1 0)

S3
(0 1 0)

S4
(0 1 1)

S5
(0 0 1)

S6
(1 0 1)

S0
(0 0 0)

S7
(1 1 1)
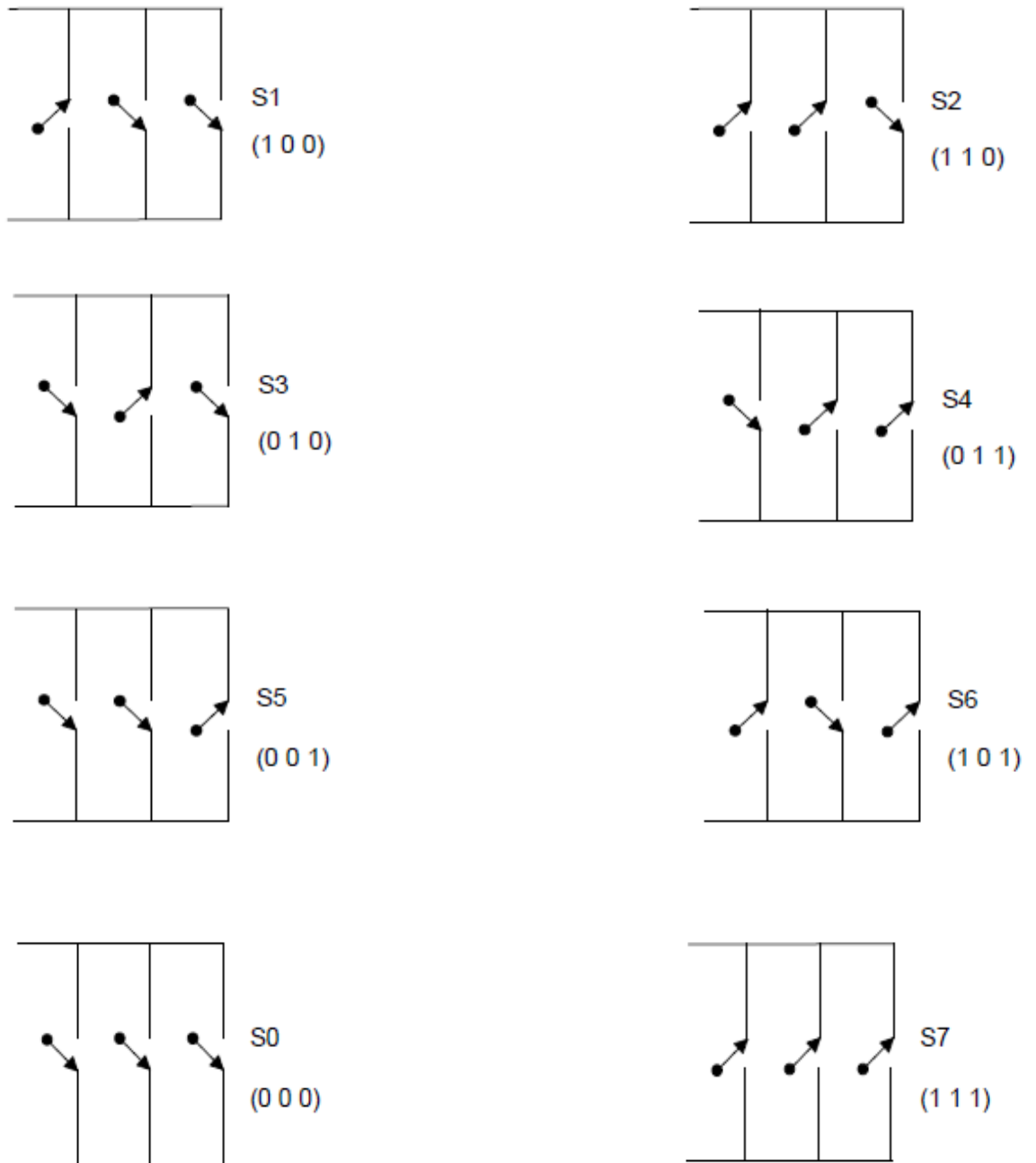
Figure 4.23 Possible switching states of a three phase voltage source inverter (VSI)
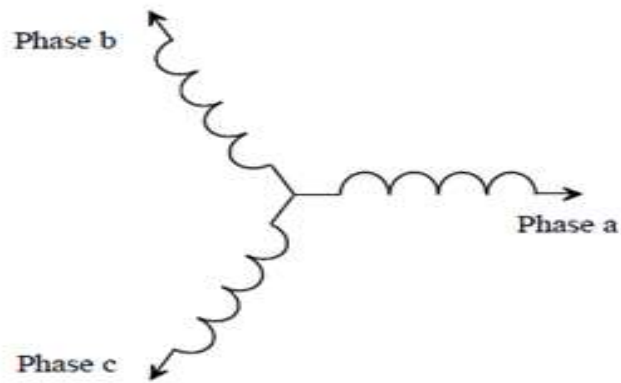
Figure 4.24 Orientation of the rotor winding in space with respect to which the voltage
space phasors are drawn
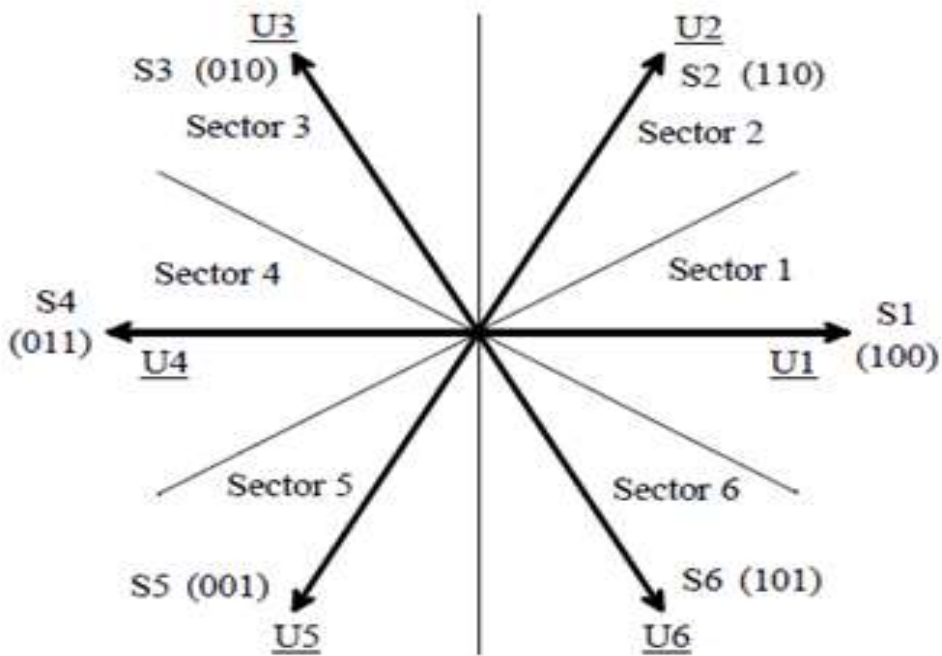
Figure 4.25 Voltage space phasors

CHAPTER 5

MATHEMATICAL MODELLING

5.1 Introduction

To solve the problems with induction motor, many mathematical models have been implemented over the years. These range from the simple equivalent circuit models to more complex Direct- axis, Quadrature –axis (D,Q)models and abc models which allow the inclusion of various forms of impedance and/or voltage unbalance.

When air gap in synchronous machines of the cylindrical rotor construction is partial uniform length that of salient – pole machine is much longer in the quadrature axis (i.e . in the region between poles) then in the direct axis or at the pole centre. Since the air gap is of minimum length in the direct axis , a given armature magneto motive force (mmf) directed along that axis produces maximum value of flux , and the same armature mmf directed along the quadrature- axis where the gap has its greatest length produces a minimum value of flux. The synchronous reactance associated with the direct axis is therefore a maximum and is known as direct - axis synchronous reactance x_d (D).The minimum reactance x_q (Q) is called as quarature- axis synchronous reactance.

This thesis examines the slip ring induction motor electrical and mechanical parameters of motors which are calculated on the basis of a mathematical model (Krause,1965). Induction machines are the major electromechanical conversion devices in industry. There is a mathematical model of induction motor which is designed from the parameters taken from Machine lab. Through this model we can calculate major features of induction motor very easily.

This mathematical model can be used to simulate the complete haulage drive system for concerned mine problem. Using this mathematical model simulation of 3hp slip ring induction motor and two 150hp slip ring induction motor is done. In this chapter mathematical model related to mine haulage drive system and all the required mechanical and electrical parameters are derived.

Rheostat starter is designed for the start of slip ring induction motor by using conventional control technique and other required parameters for this drive are also

discussed in this section. The mathematical equation for mechanical load modeled for both forward and reverse direction of the drive is presented. Because of advances in control technique, induction motor can be used as variable speed drive. Whenever a motor power is usually manifested as being a numerical style along with inputs and also outputs, it is usually analyzed and also identified often, considering unique research support frames and also state-variables.

This statistical models of induction motors with squirrel cage, dual squirrel cage, and also wound rotors tend to be formulated in the spinning organize method rigidly linked with rotating magnetic field. Induction machines with wound rotor construction, where the rotor winding terminals are accessible via slip rings can be started with external resistance introduced to limit the starting current. The maximum torque developed does not depend on rotor circuit resistance, but the slip at which the maximum torque is developed can be varied by rotor external resistance (Dhaval D.Mer1 et al., 2014). The mathematical model equation of Krammer drive slip recovery method with pwm control is also derived in this section.

5.2 MATHEMATICAL MODELLING OF HAULAGE DRIVE SYSTEM

5.2.1 Power requirement of the motor to run haulage

The force diagram of an ascending tub in a haulage system is shown in Figure 5.1.Total force equations are used for calculating the power requirement of the motor for up the gradient and down the gradient of mine haulage drive system. The same procedure is also used for modelling of 3hp experimental mine haulage drive system. The factors are considered to obtain total force which acts on the performance of energy consumption (Thomason, 2011).

ROPE

TUB

Mt=mue1 * Mt*g*costheta

Nr

Ftg + Ftf   Mt*g   Mt*gcostheta   Mrg + Frf   Mr*g   Mr*g*costheta

Force diagram of the ascending tubs and rope
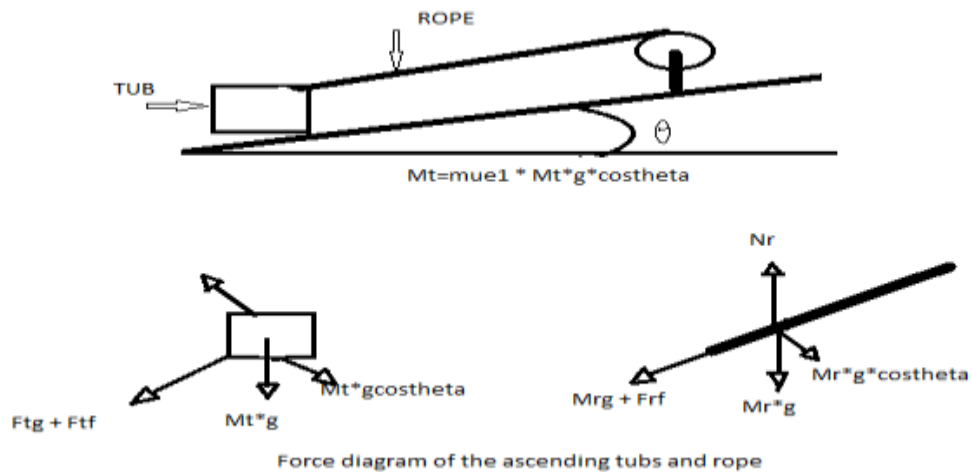
Figure 5.1 Force diagrams of the ascending tubs and rope.

Total Force along the incline plane,

$$F = F_{tg} + F_{tf} + F_{rg} + F_{rf} \qquad 5.1$$

Where F_{tg} = force due to gravity of the loaded tubs along the incline plane.
 F_{tf} = force due to friction of the loaded tubs along the incline plane.
   F_{rg} = force due to gravity of the rope along the incline plane.
   F_{rf} = force due to friction of the rope along the incline plane.

   θ = Aangle of inclination,
   M_t = total mass of the tubs.
   M_r = Total mass of the rope.
   μ_t = coefficient of friction between the tub and incline surface.
   μ_r = coefficient of friction between the rope and incline surface.

$$F = Mt \times g \times \sin\theta + \mu t \times Mt \times g \times \cos\theta + Mr \times g \times \sin\theta + \mu r \times Mt \times g \times \cos\theta. \qquad 5.2$$

If the down the gradient (negative), then the total force along the incline plane,

$$F = F_{tg} - F_{tf} + F_{rg} - F_{rf} \qquad 5.3$$

 The torque equation of the experimental model pertaining to both up the gradient and down the gradient along with simple mechanics force diagram are presented in the above diagram.

    Load torque equation of the experimental model for both up the gradient and down the gradient by using force diagram simple mechanics of load is

95

T_L = Total Force X radius of the drum

   = FXR

$= [(Mt \times g \times \sin\theta \pm \mu t \times Mt \times g \times \cos\theta + Mr \times g \times \sin\theta \pm \mu r \times Mt \times g \times \cos\theta) \times R]N/m^2$ 5.4

5.2.2 Mathematical modelling of conventional haulage drive system

     The d-q axis equivalent circuit model for a no-load, three phase symmetrical induction machine are presented Figure 5.2. Per-unit stator and also rotor voltage equation using Krause transformation according to stationary reference frame are also given. The simulink implementation of mechanical system equation and load torque equation of the experimental model for both up the gradient and down the gradient by using force diagram simple mechanics of load are also given (Krause, P.C., 2009).
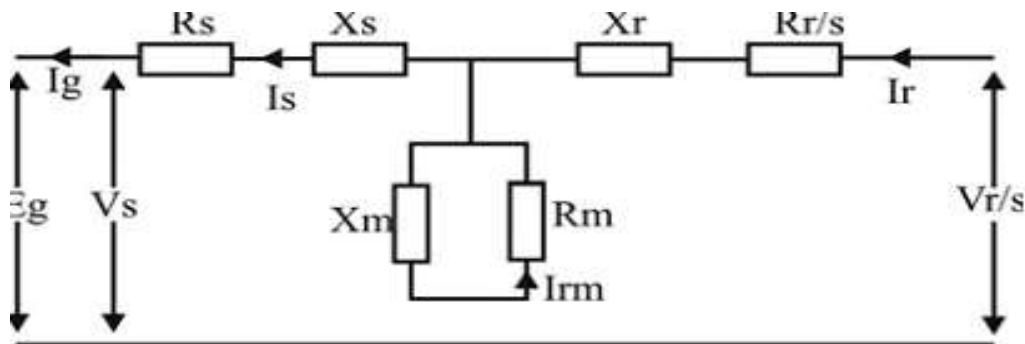
Figure 5.2 D-Q Equivalent Circuit of double fed induction generator(DFIG)

5.2.3 Induction Motor Model

     In a doubly-fed wound rotor induction machine, control is exerted on the rotor side while the stator remains connected to a constant voltage constant frequency source. In order to formulate the dynamic modelling in the field coordinates, it is assumed that the rotor side converter is equipped with fast-acting current loops. It is the stator voltage equation, which determines the dynamic behavior of the machine. This equation, in the stationary reference frame, is furnished below

Stator circuit equations**:**

$$Vds^s = \frac{d}{dt}(\psi ds^s) + rsids^s \qquad\qquad 5.5$$

$$Vqs^s = \frac{d}{dt}(\psi qs^s) + rsiqs^s \qquad\qquad 5.6$$

Rotor circuit equations

$$Vqr^s = \frac{d}{dt}(\psi qr^s) + rriqr^s \qquad 5.7$$

Mechanical System.

The electromagnetic torque developed is:

$$Te = \frac{2Hd}{dt}(\omega m) + Bm\,\omega m + Tl \qquad 5.8$$

Where $Te = Tg$ and $Tshaft = Tl)$

$$Te - Tl = \frac{2Hd}{dt}(\omega m) \qquad 5.9$$

Neglecting the torque due to friction (Bmωm)

$$Te - Tl = \frac{2Hd}{dt}(\omega m) \qquad 5.10$$

From the above equation, the rotor speed (ωm) is

$$\omega m = \frac{Te - Tl}{(2Hg)}dt$$
$$= \left(\frac{0.5}{Hg}\right)(Te - -Tl)dt \qquad 5.11$$

The sum of the instantaneous input power to all six windings of the stator and rotor is given by:

$$Pin = VasIas + VbsIbs + VcsIcs + VarIar + VbrIbr + VbrIbr \qquad 5.12$$

The electromagnetic torque developed by the machine is given by the sum of the (ω.ψi) terms divide by mechanical speed, that is.

Using the flux linkage relationships, Tem can also be expressed as follows:

$$Tem = \left(\frac{3}{2}\right)\left(\frac{p}{2}\omega r\right)[\omega(\psi dsiqs - \psi qsids) + (\omega - \omega r)(\psi driqr - \psi qridr)] \qquad 5.13$$

Using the flux linkage relationships, one can show that

$$Tem = \left(\frac{3}{2}\right)\left(\frac{p}{2}\right)[(\psi qridr - \psi driqr)]$$

$$= \left(\frac{3}{2}\right)\left(\frac{p}{2}\right)[(\psi dsiqs - \psi qsids)]$$

$$= \left(\frac{3}{2}\right)\left(\frac{p}{2}\right)Lm[(idriqs - iqrids)] \qquad 5.14$$

One can rearrange the torque equations by inserting the speed voltage terms given below:

$Eqs = \omega\psi ds \quad Eds = -\omega\psi qs$

$Eqr = (\omega - \omega r)\psi dr \quad Edr = -(\omega - \omega r)\psi qr.$ 　　　　　　　　5.15

The equation for the mechanical motion is

$Te = T_L + JP\omega r + B\omega r$ 　　　　　　　　5.16

Where T_L is the load torque, J is the moment of inertia constant and B is the coefficient of friction and wind age. Load torque equation of the proposed model for both up the gradient and down the gradient by using force diagram simple mechanics of load is:

T_L= Total Force X radius of the drum

= FXR

= [(Mt × g × sin θ ± μt × Mt × g × cos θ + Mr × g × sin θ ± μr × Mt × g × cos θ) × R] N/m^2

　　　　　　　　5.17

Output power of the Shaft = $P = \dfrac{2\pi NT}{4500}$ N/m^2 　　　　　　　　5.18

Where $N = \dfrac{n1}{n2} = \dfrac{n1}{40}$ 　　　　　　　　5.19

T=Te 　　　　　　　　5.20

$InputPower = Pin = 3 \times V \times I \times \cos \emptyset\, watts$ 　　　　　　　　5.21

Energy consumption 　　= Output power ×Time taken for completion work

　　　　　　　　= (P ×T) watt/sec. 　　　　　　　　5.21a

% Efficiency (η) 　　　　$= \dfrac{output power of the shaft}{Input power} \times 100$ 　　　　　　　　5.22

The energy consumption is obtained from the Equation (5.21a) of the drive system.

5.2.4 Rotor Resistance Control

The rotor resistance starter usually formulated depends on rating of induction machines. The Equation associated with speed control variation with rotor resistance (Rashid ,M.H. 1994) is understood by Equation (5.22) which provides   the torque developed by the motor as

$$Td = 3\frac{(Rr+Rext)}{s\omega s}\frac{Vs^2}{\left[\left(Rs+\frac{(Rr+Rext)}{S}\right)^2+(Xs+Xr)^2\right]}$$

5.23

In equation 5.23 Rr (Rotor resistance), Rext (External resistance), Xs (Stator reactance) and Xr (Rotor reactance) are constants therefore the torque developed (internal) is a function of rotor resistance and rotor speed.

5.2.5 MODELLING OF STATIC DRIVE SYSTEM

The mathematical model developed for drive system it mainly depends on the power recovery and rotor side power control. The mathematic model for static Krammer drive system is also developed to mine haulage drive system**.**

The thesis is to formulate a mathematical model of the direct rope haulage wound rotor induction machine drive system in underground coal mine. A design methodology is evolved for developing the current controllers.

5.2.6 Mathematical model static (micro controller) drive controller based technique

The following assumptions were made:

    i.   Stator drops and supply voltage fluctuation are neglected

    ii.   The dc link current is considered as harmonic free.

    iii.   Commutation overlap angle of the diode rectifier is neglected.

    iv.   Stator and rotor drops are neglected.

In steady – state   the slip voltage Vd and inverter voltage V_1 will balance for a certain dc current Id

$$V_d \propto S \propto I_d$$

5.24

$$V_d = \frac{1.35}{n1}SV_L$$

5.25

$$\left(Vd = \frac{3}{\pi}\sqrt{2}Vrms|m|\right)$$

V_L the stator line voltage and S the per unit slip .The inverter terminal voltage V_l

$$V_l = \frac{1.35}{n2}SV_L|m|$$

5.26

Modulation index $m = \frac{T_{on}}{T_s}$

5.27

Where T_{on} is on time of IGBT and Ts is the total switching time.

The voltage there is three phase legs, hence three modulation indices, ma, mb and mc. The voltages between the mid-point of each phase leg and the 0V node of the dc.

$$Va0 = maV_{dc} \qquad\qquad 5.27a$$

$$Vb0 = mbV_{dc} \qquad\qquad 5.27b$$

$$Vc0 = mcV_{dc} \qquad\qquad 5.27c$$

Now, if each modulation index varies sinusoidal according to the resultant output line voltages will take the form.

$$V_{ab} = V_{a0} - V_{b0} = \sqrt{3}mV_{dc}\sin\left(\omega t - \frac{\pi}{6}\right) \qquad\qquad 5.28a$$

$$V_{bc} = V_{b0} - V_{c0} = \sqrt{3}mV_{dc}\sin\left(\omega t - \frac{5\pi}{6}\right) \qquad\qquad 5.28b$$

$$V_{ca} = V_{c0} - V_{a0} = \sqrt{3}mV_{dc}\sin\left(\omega t + \frac{\pi}{2}\right) \qquad\qquad 5.28c$$

n_2 is the transformer line side to inverter ac side turns ratio and m is the modulation index of IGBT inverter V_d and V_l must balance in the ideal case, the Equation (5.24) and (5.25) give

$$S = \frac{n1}{n2}|m| \qquad\qquad 5.29$$

That is

$$\omega_r = \omega_e(1 - |m|) \qquad\qquad 5.30$$

Assuming that $\frac{n1}{n2}$ = 1. Equation (5.29) indicates that ideally speed can be controlled between zero and synchronous speed ω_e by controlling inverter firing angle α.

Again neglecting losses, the following power equation can be written:

$$SP_g = V_lI_d \qquad\qquad 5.31$$

$$P_m = (1 - S)P_g = T_e\omega_m = T_e\omega_e(1 - S)\left(\frac{P}{2}\right) \qquad\qquad 5.32$$

Where P_g is the air gap power and P_m the mechanical output power. Combining the equation gives.

$$T_e = \frac{V_lI_d}{S\omega_e}\left(\frac{P}{2}\right) \qquad\qquad 5.33$$

Substituting Equation (5.24) and (5.25) gives

$$T_e = \frac{1.35 V_L I_d}{\omega_e n_1} \left(\frac{P}{2}\right)$$
5.34

Equation (4.34) indicates that the torque is proportional to current I_d , but from higher load torque I_d will increase and fixed V_l , V_d should slightly increase to overcome the dc link drop.

So the more accurate torque equation relating slip and modulation index for the proposed drive system is. (Bimal.K.Bose,1982)

$$T_e = \frac{3V_s^2}{\omega R'_r} \left[\frac{1}{S n_2} |m| \left(\frac{S^2}{n_1} - \frac{|m|}{n_2}\right) + S \left(\frac{S}{n_1} - \frac{|m|}{n_2}\right) 2 \right] \left(\frac{P}{2}\right)$$
5.35

  From above Equation (5.35) we obtain the T_L which depends on the proposed drive load system.Shaft output of the proposed drive system:

The output shaft power Equation (5.18) is used for calculating the power in proposed drive system. Determining the power to be regenerated starts with recognizing the stator power passes to the rotor, and in per unit quantities, is given by

$$P_{stator} = P_{rotor} = T \cdot \omega_s$$
5.36

$$P_{genr} = \omega_r^2 (1 - \omega_r)$$
5.37

$$Pnewgen = P_{newrotor} - P_{newmech}$$
5.38

The fundamental inverter power transmitted to the supply is

If $\cos \emptyset_1$ is the effective power factor of the inverter, then the inverter power

Transmitted to supply Ps is then

$$P_{1F} = \sqrt{3} V_1 I_{2F} \cos \emptyset_1 \text{ Watts}$$
5.39a

The secondary power Ps is given by

$$P_s = \sqrt{3} S E_s I_{2F} \cos \emptyset_2 \text{ Watts}$$
5.39b

Where, $\cos \emptyset_2$ is the angle between the fundamental secondary current and the slip e.m.f.

5.2.7 Pulse Width Modulation (PWM) slip power recovery for 3hp laboratory experimental haulage drive system:

    When the PWM algorithm was applied to the actual IGBT module and actual induction motor, it was observed that the motor started to rotate slowly to its desired speed depending on the reference frequency provided. The speed of the motor increased steadily

based on the frequency supplied by the control signal until it reached the desired speed and remained constant at the speed. The speed of the motor was captured using a small taco generator attached to the rotor. A infra red speed sensor or tachometer was connected to the taco generator to observe the speed of the motor.

The source converter must be selected with regard to the maximum power to be regenerated to the power system. This power can be determined from the controlled speed range, the motor nameplate power, and the type of load being driven. Determining the power to be regenerated starts with recognizing the stator power passes to the rotor, and in per unit quantities, is given by

$$P_{stator} = P_{rotor} = T \cdot \omega_s \qquad\qquad 5.40$$

For any operating condition, motor losses are neglected. T = motor output torque and ωs is the stator electrical frequency. But in per unit, the stator electrical frequency is constant and always equal to 1. Therefore, we recognize the power going into the motor is always proportional to the output torque. Next, neglecting loss in the rotor, the rotor power can be divided between the power regenerated to the power system and the mechanical power transmitted to the load:

Pgen = Protor − Pmech

Next, substituting for P rotor and recognizing the output mechanical power is proportional to rotor speed, ωr, and output torque, T, the following results:

$$P_{gen} = T(1 - \omega_r). \qquad\qquad 5.41$$

Then ωr = 1−S, where s is the slip between the stator and rotor frequencies in per unit. So an alternate form for the regenerated power is in per unit of the motor rated power. The result means the regenerated power is equal to the slip at minimum speed (in per unit) Times the load torque at that speed (also in per unit).

$$P_{regen} = s \times T \qquad\qquad 5.42$$

The recovered slip power calculated is given as,

Total Power recovered= Shaft output power conventional method− Output power micro controller method

The other electrical parameters are calculated as per simulation output and data obtained from conduction of 3hp laboratory experimental on conventional method haulage

drive system and micro controller based haulage drive system also the field study on 150hp underground haulage drive system-1 and haulage drive system-2.

5.2.8. Modelling of IGBT inverter

The following steps are considered for modelling of IGBT inverter and controller for haulage drive system.

Steps in modelling: FIRST: Mathematical modelling.

SECOND: Decision making

THIRD: Design of controller

The modelling is carried out with the following assumptions:

    i.   All switches are ideal.

    ii.   The source voltages are balanced.

    iii.   Rs represent the converter losses and Ls represents losses of the coupling inductor.

    iv.   The harmonic contents caused by switching action are negligible.

The primary modelling in the IGBT inverter may be presented by making use of (d-q) transformation. On the other hand, for uncomplicated reference, the modelling of the above is briefly revisited here. The 3-phase grid voltage, Vsabc lagging with the phase angle difference 'a' to the IGBT inverter terminal voltages Voabc can be expressed as

$$V_{s,abc}(t) = \begin{bmatrix} V_{sa}(t) \\ V_{sb}(t) \\ V_{sc}(t) \end{bmatrix} = \sqrt{\frac{2}{3}} V_s \begin{bmatrix} \sin(W_1 t - \alpha) \\ \sin\left(W_1 t - \frac{2\pi}{3} - \alpha\right) \\ \sin\left(W_1 t + \frac{2\pi}{2} - \alpha\right) \end{bmatrix}$$

5.43

In the (d-q) reference frame of (5.43) is

$$V_{s,dq0}(t) = K V_{s,abc}(t) = V_s \begin{bmatrix} \cos\alpha & -\sin\alpha & 0 \end{bmatrix}^T$$

5.44

Where:

$$K = \sqrt{\frac{2}{3}} \begin{bmatrix} \sin(w_1 t) & \sin\left(w_1 t - \frac{2\pi}{3}\right) & \sin\left(w_1 t + \frac{2\pi}{3}\right) \\ \cos(w_1 t) & \cos\left(w_1 t - \frac{2\pi}{3}\right) & \cos\left(w_1 t + \frac{2\pi}{3}\right) \\ \frac{1}{\sqrt{2}} & \frac{1}{\sqrt{2}} & \frac{1}{\sqrt{2}} \end{bmatrix}$$

The above voltages and currents are transformed into dq frame as, the relationship between the grid voltage and IGBT inverter current i_{cabc}, in the series inductor Ls,in dq frame is given by

$$L_s d(i_{cd}(t)) = wL_s i_{cq}(t) - R_s(t)i_{cd}(t) + v_{sd}(t) - v_{od}(t)$$ 5.45

$$L_s d(i_{cq}(t)) = wL_s i_{cd}(t) - R_s(t)i_{cq}(t) + v_{sq}(t) - v_{oq}(t)$$ 5.46

The voltage and current related in dc side is,

$$dv_{dc}/dt = i_{dc}/c$$ 5.47

$$i_{dc} = m_{[0\ 1\ 0]}[i_{cq}\ i_{cd}\ i_{co}]^T$$ 5.48

Now by comparing (4.45) and (4.46), $dv_{dc}/dt = m/c(i_{cd})$

The complete mathematical model of inverter

$$\frac{d}{dt}\begin{bmatrix} i_{cq} \\ i_{cd} \\ v_{dc} \end{bmatrix} = \begin{bmatrix} -\dfrac{R_s}{L_s} & -w & 0 \\ w & -\dfrac{R_s}{L_s} & -\dfrac{m}{L_s} \\ 0 & \dfrac{m}{c} & 0 \end{bmatrix}\begin{bmatrix} i_{cq} \\ i_{cd} \\ v_{dc} \end{bmatrix} + \frac{v_s}{L_s}\begin{bmatrix} -\sin\alpha \\ \cos\alpha \\ 0 \end{bmatrix}$$

5.49

The state space modelling of the IGBT is given in Equation. (5.49). It is found to be non-linear in α. Here the control task taken up is to keep m (mc) constant since α is related to qc of the IGBT inverter. This control task is best achieved through small signal model of the IGBT inverter. The active power (losses plus change of steady state) is indirectly controlled by controlling the dc-link voltage. It may be noted that a controller is able to perform the control task.

5.3 DESIGN OF CONTROLLERS FOR ROTOR

5.3.1. Phase-locked loop

A phase-locked loop or (PLL) is a control system that generates an output signal whose phase is related to the phase of an input signal. While there are several differing types, it is easy to initially visualize as an electronic circuit consisting of a variable frequency oscillator and a phase detector.

The oscillator generates a periodic signal. The phase detector compares the phase of that signal with the phase of the input periodic signal and adjusts the oscillator to keep the phases matched. Bringing the output signal back towards the input signal for comparison is called a feedback loop since the output is 'fed back' toward the input forming a loop. Keeping the input and output phase in lock step also implies keeping the input and output frequencies the same.

Consequently, in addition to synchronizing signals, a phase-locked loop can track an input frequency, or it can generate a frequency that is a multiple of the input frequency. These properties are used for computer clock synchronization, demodulation, and frequency synthesis.

Phase-locked loops are widely employed in radio, telecommunications, computers and other electronic applications. They can be used to demodulate a signal, recover a signal from a noisy communication channel, generate a stable frequency at multiples of an input frequency (frequency synthesis), or distribute precisely timed clock pulses in digital logic circuits such as microprocessors.

Since a single integrated circuit can provide a complete phase-locked-loop building block, the technique is widely used in modern electronic devices, with output frequencies from a fraction of a hertz up to many gigahertz's. Figure 5.3 shows the block diagram of Phase-Locked Loop (PLL) controller. This is used for design of closed loop control of micro controller based (static control) mine haulage drive system.
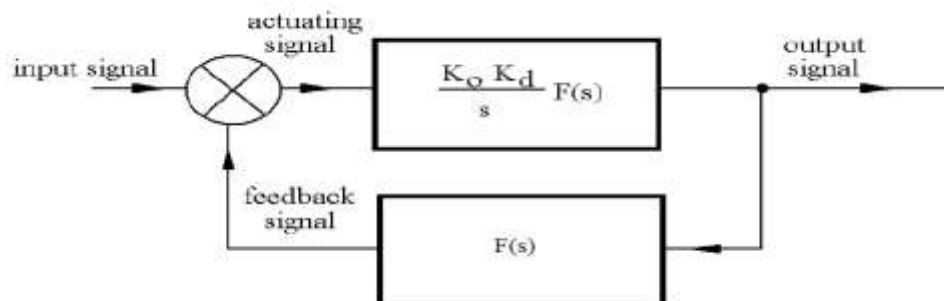
Figure 5.3. Block diagram of PLL controller

The dc-link capacitor has slow dynamics compared to the compensator, since the capacitor voltage is sampled at every zero crossing of phase a supply voltage. The sampling

can also be performed at a quarter-cycle depending upon the symmetry of the dc link voltage wave form.

5.3.2 Proportional- integral (PI) control

To regulate the system voltage and reactive power compensation PI control is employed. The combination of proportional and integral terms is important to increase the speed of the response and also to eliminate the steady state error and offset error produced by P-mode which is eliminated by I-mode, and hence the system considers the history of errors with full gain of the system. The PID controller block is reduced to P and I blocks only as shown in block. The various characteristics of the composite PI mode are, When the error is zero, the controller output is fixed at the value that integral mode had when the error went to zero.

- It improves the steady state accuracy.
- It increases the rise time so response becomes slow.
- It decreases bandwidth of the system.
- It filters out the high frequency noise.
- It makes the response more oscillatory.
- When the error is not zero, proportional mode adds the correction while the integral term starts increasing or decreasing from its initial value depending upon reverse or direct action.

Auxiliary control method is used to regulate the system voltage and to regulate the reactive power current effectively. Figure 5.4 shows the controller for IGBT. The output of the phased lock loop (PLL) is the angle that is used to measure the direct axis and quadrature axis component of the ac three-phase voltage and current.

The outer regulation loop comprising the ac voltage regulator provides the reference current (Iqf) for the current regulator that is always in quadrature with the terminal voltage to control the reactive power. The voltage regulator is a PI controller. A supplementary regulator loop is added using the dc capacitor voltage. The dc side capacitor voltage charge is chosen as the rate of the variation of this dc voltage. The current regulatory controls the

magnitude and phase of the voltage generated by the converter (Vq (quadrature voltage) ,Vd (direct voltage)) from the reference currents produced, respectively, by the dc voltage.
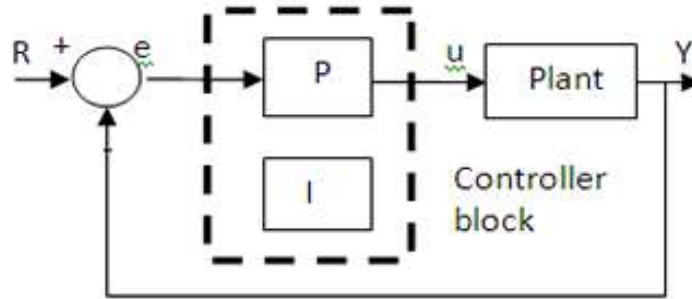
Figure 5.4. Block diagram of PI controller

The drawback of this conventional controller is that its transient response is slow, especially for fast changing loads. Also, the design of PI controller parameters is quite difficult for a complex system and hence, these parameters are chosen by trial and error. With the assumption of the system voltage and IGBT inverter output voltage are in phase and hence the Eqn.(5.43) and (5.44) can be modified as,

$$
\frac{d}{dt}\begin{bmatrix} i_{cq} \\ i_{cd} \end{bmatrix} = \begin{bmatrix} -\dfrac{R_s}{L_s} & -w \\ w & -\dfrac{R_s}{L_s} \end{bmatrix}\begin{bmatrix} i_{cq} \\ i_{cd} \end{bmatrix} + \frac{1}{L_s}\left[\begin{bmatrix} v_{sq} \\ v_{sd} \end{bmatrix} - \begin{bmatrix} v_{oq} \\ v_{od} \end{bmatrix}\right]
$$

5.50

So Eqn.(5.50) is multi input multi output (MIMO) system, its input and output are given in Eqn.(5.52). Both active and reactive currents are coupled with each other, through reactance of coupled inductor, so it is very essential to decouple both active and reactive current from each other and design the controller for tracking the required value.

5.3.3. Design of current controller

The current controller design for the above system can be done using the d and q axes equations, so that the MIMO system reduces to two independent Single Input Single Output (SISO) systems as,

$$
\begin{bmatrix} i_{cq} \\ i_{cd} \end{bmatrix} = \begin{bmatrix} -\dfrac{R_s}{L_s} & 0 \\ 0 & -\dfrac{R_s}{L_s} \end{bmatrix}\begin{bmatrix} i_{cq} \\ i_{cd} \end{bmatrix} + \frac{1}{L_s}\left[\begin{bmatrix} v^*_{oq} \\ v^*_{od} \end{bmatrix}\right]
$$

5.51

Taking Laplace transform on both side of above equation, we get

$$G_i(s) = \frac{I_{cq}(s)}{V_{oq}^*(s)} = \frac{I_{cd}(s)}{V_{od}^*(s)} = \frac{1}{R_s + sL_s}$$

5.52

The T.F of a PI controller is,

$$G_{pi}(s) = K\left(1 + \frac{1}{s\tau_i}\right) = K_P + \frac{K_i}{s}$$

5.53

With $k_p = k$ and $k_i = \dfrac{k}{\tau_i}$, The transfer function in open loop of PI controller associated with the transfer function on the a.c. system is

$$[G_{pi}(s).G_i(s)] = K\left[1 + \frac{1}{s\tau}\right]\left[\frac{1/R_s}{1 + s\dfrac{L_s}{R_s}}\right] = K/sL_s$$

5.54

The closed loop transfer function is given,

$$T = \frac{1}{1 + s\dfrac{L_s}{K}}$$

5.55

The gain of K can be adjusted in such a way that if it is increased too high then the system behaves as second order, otherwise responses are very slow.

5.3.4. Design of voltage controller

Voltage and current mode are the two regulatory conditions that handle the output of the supply. Most applications call for a supply to be used as a voltage source. A voltage source is generally modeled as providing a low output impedance of the supply.

These two regulating modes work together to provide continuous control of the supply, but with only one mode regulating at a time. These are fast acting electronic regulating circuits, so automatic crossover between voltage modes to current mode is inherent in the design. With the programming of the voltage mode and current mode set points available to the customer, the maximum output voltage and current of the supply can be controlled under all operating conditions.

The relation between dc voltage V_{dc} and dc current idc is

$$V_{dc} = \frac{1}{c}\int i_{dc}dt$$

5.56

The transfer function can be written as,

$$G_v(s) = \frac{V_{dc}}{I_{dc}} = \frac{1}{sc}$$

5.57

Neglecting the power loss in the source resistance and power losses in the switches, balancing the power on both sides,

$$V_{sd} \times i_{cd} = V_{dc} \times i_{dc}$$

The bus voltage is maintained at 400 volts. With V_{dc} as the reference, the voltage control loop is shown and it consists of inner d - axis current control loop. The active power is supplied by the d -axis current which is nothing but the ripple current of the capacitor. To make the steady state error of the voltage loop zero proportional control is adopted here and it produces the reference d - axis current for the control of the d -axis current. The design of voltage controller is as follows, the proportional integral controller is considered for the voltage control. Hence, the transfer function of PI controller is associated with the transfer function on dc side is

$$\left[G_v(s).G_{pi}(s) \right] = K\left(1 + \frac{1}{s\tau} \right)\left(\frac{1}{sc} \right)$$

5.58

After taking C=τ_v and on simplification

$$\left[G_v(s).G_{pi}(s) \right] = K\left(\frac{1 + s\tau_v}{s^2\tau_v^2} \right)$$

5.59

The transfer function in closed loop

$$\left[G_v(s).G_{pi}(s) \right] = \left(\frac{1 + s\tau_v}{1 + s\tau_v + \dfrac{s^2\tau_v^2}{K}} \right)$$

5.60

The value of K can be determined form root locus with approximate settling time as 1/200 and 1/400.

CHAPTER 6

SIMULATION STUDIES

6.1 INTRODUCTION OF MATLAB/SIMULINK

Simulink is a software package for modelling, simulating, and analyzing dynamical systems. It supports linear and nonlinear systems, modeled in continuous time, sampled time, and hybrid of the two systems can also be multirate (Parlos,2001). For modelling, simulink provides a graphical user interface for building models as block diagrams, using click-and-drag mouse operations. Simulink includes a comprehensive block library of sinks, sources, linear and nonlinear components, and connectors.

We can prepare our own model blocks with reduced size. These parts gives an idea for developing the model and inter connection of various parts. After define a model, we can simulate it, using a choice of different methods, either from the simulink menus or by entering commands in MATLAB's command window.

The simulation results can be observed by scopes and display device when simulation is running and also in addition, we can change parameters and immediately see what happens, for "what if" exploration. The simulation results can be put in the MATLAB workspace for post processing and visualization. Matlab and Simulink tools are integrated type therefore we can repeat these block model for both environment at any point.(Parlos, 2001) The development of specific software dedicated to simulation of power electronic systems allows simulating fast and accurately the converter behavior.(MATLAB7.10, "Simulink 7.10 /SimPowerSystems,"2010).

Simulation of the three-phase induction machine is well documented in the literature and a digital computer solution can be performed using various methods, such as numeric programming, symbolic programming and the electromagnetic transient program (EMTP). This chapter discusses the use of the SIMULINK software of MATLAB, in the dynamic simulation of the wound rotor induction motor.

The main advantage of SIMULINK over other programming software is it gives the simulation model which built a system for basic function blocks where as other programming software gives the complication of program code only. With the help of a

convenient graphical user interface, the function blocks can be created, linked and edited easily using menu commands, the keyboard and mouse. A set of machine differential equations can thus be modeled by interconnection of appropriate function blocks, each of which performing a specific mathematical operation. SIMULINK is a model operation programmer; the simulation model can be easily developed by addition of new sub-models to cater for various control functions (Smolleck, 1990).

In this thesis the proposed work based on the comparison of the conventional rotor resistance method and slip power recovery system(micro controller) method used for the speed control of slip-ring induction motor and analysis of speed and power loss are carried out. MATLAB/SIMULINK is used to simulate both methods (conventional and static control) for slip-ring induction motor.

This thesis introduces specialized computational tools as a part of laboratory experiments to enhance the classroom teaching of courses related to induction motor (IM)which provides an opportunity to compare the results of laboratory experiments by those obtained through computer simulation (Nehrir, 1995).

Such a comparison will help us to realize the superiority of simulation tools over hardware experiments. To make the simulation even more efficient and user friendly, the special features are incorporated in the model. The proper arrangements for the measurement of power, voltage, current, phase angle, power factor, speed, torque and efficiency have been provided fora complete understanding of state of the machine.

This section also explains the MATLAB/SIMULINK model of 3-phase 3hp laboratory experimental (conventional control and micro controller method)haulage drive slip ring induction motor and field study of 150 hp underground haulage drive system-1 and drive system -2 (conventional control and micro controller (simulation) slip ring induction motors drive for direct haulage drive system in an underground mine.

6.2 Simulation of 3hp experimental and 150hp underground haulage drive system
6.2.1Simulation model description of conventional method

The computer software package MATLAB/SIMULINK is used to implement the 3hp laboratory experimental haulage drive slip ring induction motor and 150hp underground coal mine haulage drive system model as shown in Figure 6.1(a) and Figure

6.1 (b). Each model consists of the conventional asynchronous machine block available in the Sim Power Systems block set.

In this model, a 3-phase wound rotor induction motor power is measured by the help of the two wattmeter method. The load on the motor is simulated by a separate mechanical sub model to study the influence of combination of different loads and different gradients (for both up the gradient and down the gradient).The values used for creating MATLAB data file are given in APPENDIX IX.

The 3hp laboratory experimental haulage drive model is simulated using the required design data obtained from the simulation without loading condition. The no load electrical parameters simulation data for 3hp slip ring induction motor are given in Table 6.1. The starter resistance for slip ring induction motor requires starting inrush current during staring of induction motor. The experimental arrangement for conventional control 3hp laboratory haulage drive system associated with slip ring induction motor, reduction gear (1:40) with mechanical gear change mechanism for forward and reverse gear changing, rope drum, tub with inclined rail arrangement and different inclined changing angle (angle with horizontal) are provided in fabricated experimental study .

The technical and fabrication details of 3hp conventional experimental drive system is given in Chapter 4 in Table 4.1.In the simulation study simulink model consists of rotor resistance starter with circuit breaker arrangement. Mechanical load model with different load angles are simulated using the power required for haulage drive system for up the gradient and down the gradient and load torque equation is given in Equation 5.4 in section 5.1.1.The Simulink model for Mechanical load arrangement of 3hp and 150hp haulage drive system is shown in Figure 6.2.

The simulation has been carried out for different combination of loads and gradients for both the direction of drives, and simulated results are presented in tabulation form. In simulation the electrical parameters like electromagnetic torque, efficiency, rotor current, and power loss during the starting of induction motor are investigated. The conventional drive system simulation study shows energy consumption variation in starting of induction motor are more and also during loading condition of the machines. The effect of such electrical parameter characteristics are discussed and are given in section 7.2.2.

Simulation is carried out as per mathematical Modelling of 150hp underground mine haulage drive system. The similar SIMULINK flat form (modelling 3hp motor) is arranged for modelling of 150hp drive system -1 and drive system-2 of underground coal mine. The entire drive is simulated by using field study data obtained from 150hp underground haulage drive system-1 and haulage drive system-2 of GDK 10A inclined coal mine.

The 150 hp haulage drive system technical data specifications (APPENDIX I) are used for simulation of 150hp slip ring induction motor at no- load condition .The no-load electrical simulation parameters of 150hp haulage drive are given Table 6.1.

The MATLAB/SIMULINK model for3hp laboratory experimental mine haulage drive system and 150 hp underground mine haulage drive system are as shown in Figure 6.1a and Figure 6.1b.

The simulated results for 150hp underground haulage drive system- 1 and haulage drive system- 2 for up the gradient and down the gradient are given in Table 6.4 and Table6.5.The Similar simulation study procedure is carried out on 3hp laboratory conventional experimental haulage drive system for different combination of gradient such as 27^0, 29^0, 32^0 and 35^0 up the gradient drive of different combination of loads respectively. The simulation study is also carried out with different combination of loads (i.e. 1079 N, 1275 N, 1471N and 1765.8N) and gradients (angle with horizontal i.e. 27º, 29º, 32º and 35º) for both up the gradient and down the gradient.

The set of parameters such as speed (N_1/N_2), input power, voltage and current, time and power recovery for up the gradient and down the gradient and time are measured. The simulated results are presented in Table. The same steps which have been carried out for up the gradient and are also followed for down the gradients study of drive system. These simulated parameters are displayed on the workspace screen and to run the drive system by clicking the run button on the main menu.

The entire behavior of the machine parameters is plotted with the help x-y plotter. It is easy to make separate md.file in simulation study by putting all unknown parameter related to drive and to run the SIMULINK. The MATLAB DATA FILES for run the

simulation are presented in APPENDIX IX. Tabulated simulation results of 3hp laboratory haulage drive system by conventional method for different combination of loads and gradients for up the gradient and down the gradients are given in Table 6.2 and Table 6.3.

The advantage of using simulation is, to avoid manual calculation. The 3hp and 150hp drive system rotor starter modeled and SIMULINK block model are also given in Figure 6.3 and Figure 6.4. The speed of a slip ring induction motor can be varied by regulating resistance in rotor circuit. The following equation is used for deciding the resistance required for the rotor starter for 3 hp slip ring induction motor and 150 hp slip ring induction motor , $\alpha = (Sm)^{1/n}$ .The Rm = R_1*sm.Therefore R_1= Rm/sm where n = number of resistance elements.

The total resistance is nearly equal to R_1(Sawhney,2014) Simulation results pertaining to experimental and 150hp underground haulage drive system are discussed in section 7.6.1 Input data obtained from field study on energy consumption results are used for simulation of two 150hp underground haulage drive system in an underground coal mine**.** The conventional method simulation field study results of150hp surface hauler drive system -1 (down the gradient) from surface to 8L and 8L to surface (up the gradient) tabulated simulation results are presented in Table 6.4 and Table 6.5 respectively. Similarly conventional method simulation field study results of 150hp underground hauler drive system-2 (down the gradient) from 8L to42nd level and up the gradient (i.e.42nd to 8L) tabulated simulation results are given in Table 6.6 and Table 6.7, respectively.
The procedure for calculation of energy consumption for conventional control method of drive system is presented in APPENDIX IV.

Explanation of simulation process with physical haulage drive system of Figure 6.1a represents SIMULINK model for 3hp conventional control experimental haulage drive system. These Simulinks blocks are connected to physical laboratory 3hp experimental haulage drive system for slip ring induction motor. The slip ring induction motor is simulated at no load condition. And Figure 6.1b represents Simulink model for 150 hp conventional control underground mine haulage drive system of slip ring Induction motor are simulated at no load condition. The simulated no load electrical parameters of 150 hp and 3hp are presented in Table 6.1.The available 3 phase voltage source of 3.3 KV, 440V, are connected to 150hp and 3hp simulated slip ring induction

motor. Conventional rotor starter are designed for required current rating by using available simulink blocks and separately connected to rotor of the slip ring induction motor. The mathematical modeling equation (5.3) and (5.4) for both up the gradient and down the gradient drive system are derived.

The equation for power requirement of the motor to run haulage drive by using available parameters in MATLAB/SIMULINK blocks are connected to make the mechanical load systems for 150hp and 3hp slip ring induction motor. For each equipment of the physical haulage drive system are created by using MATLAB/SIMULINK tools and connected together to make physical 150hp and 3hp haulage drive system for simulation process. The various meters like Ammeters , voltmeters and wattmeter's are connected for measurement of current ,voltage and power for loads for up the gradient and down the gradient of the drive system by using MATLAB/SIMULINK tools .

The electrical and mechanical internal behaviors of drive system are observed by connecting scope and xy plotter for required terminal of the drive system in simulink blocks. By creating md.file in MATLAB the different parameters required for the simulation are enter in the program and run the file and after that run the simulink name.mdl file by entering run in workplace. After each iteration note down the various electrical parameter required for energy consumption calculation (i.e. Speed, Torque, current , voltage , time ,ect). According to simulation the various cases Tabulated results are presented in Table 6.2 up to Table 6.7 in the thesis.
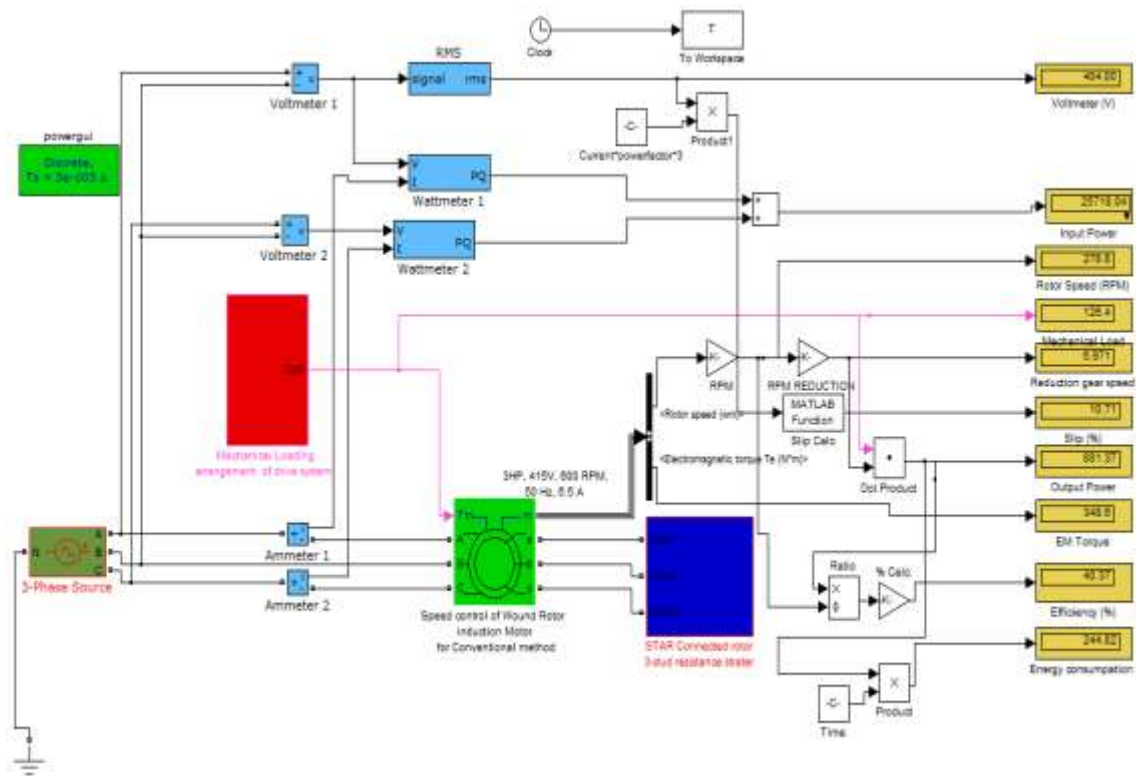
Figure6.1a Simulink model for 3hp conventional control experimental haulage
        drive system
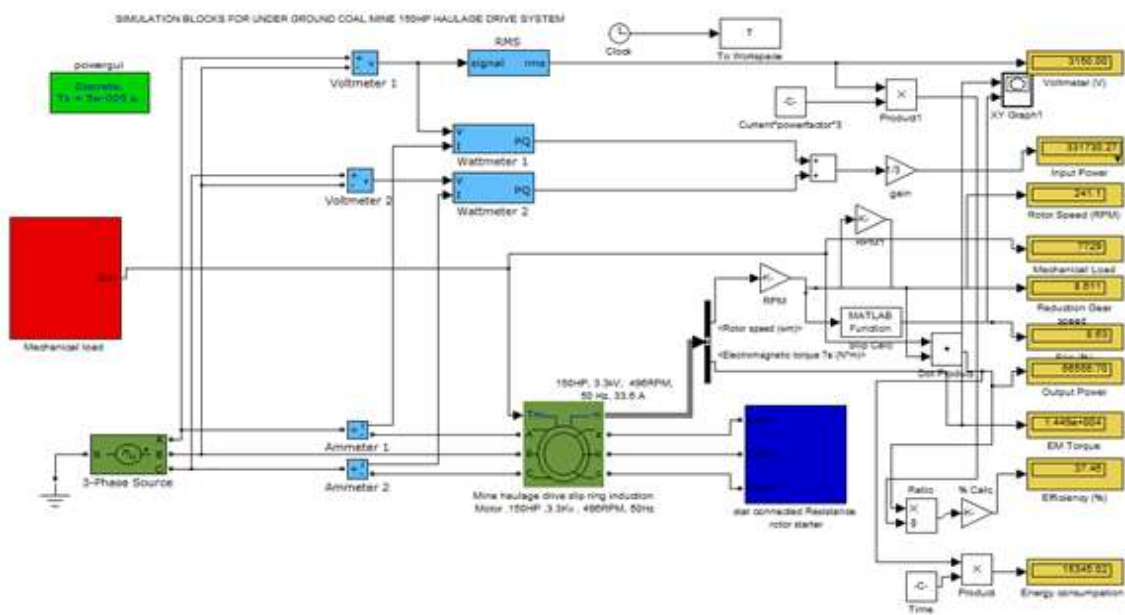
Figure 6.1b Simulink model for 150 hp conventional control underground mine
        haulage drive system
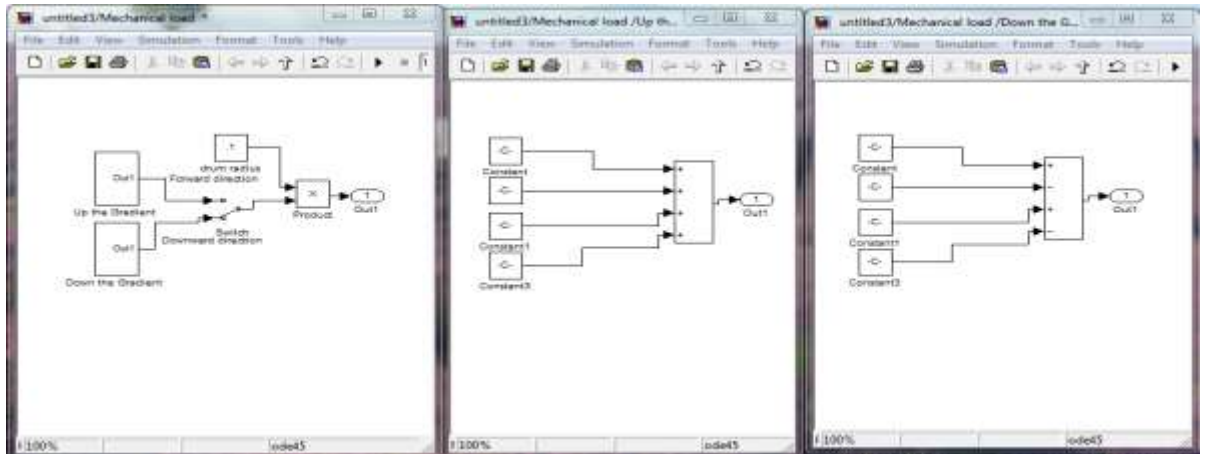
Figure 6.2 Simulink model for mechanical load arrangement of 3hp and 150hp
            haulage drive system
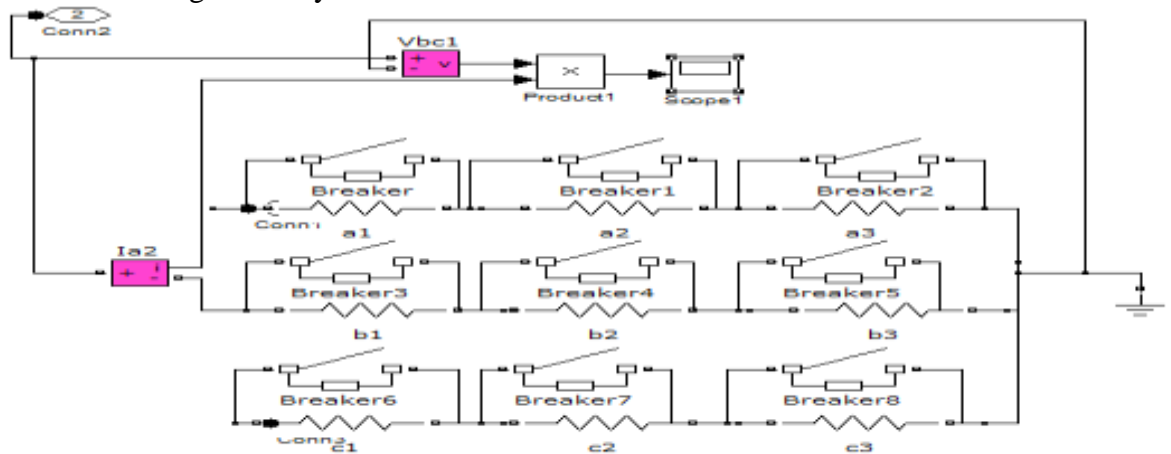
Figure 6.3 Simulink model for star connected 3step rotor resistance starter of 3hp
           haulage drive system
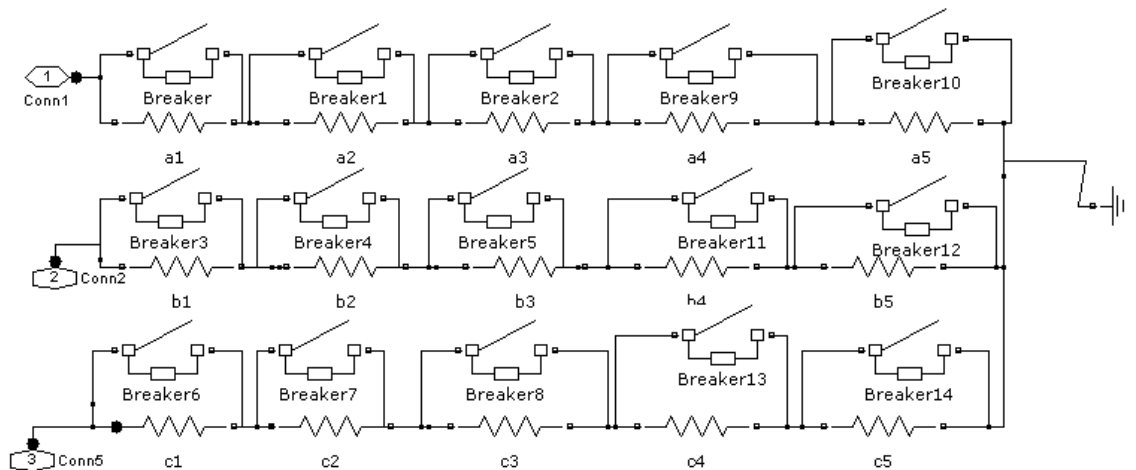
Figure 6.4 Simulink model for star connected 5 step rotor resistance starter for
           150hp underground haulage drive system

117

Table 6.1 Simulation study results of electrical parameters of 3hp and 150hp slip ring
         induction motor

Sl.No.	3hp slip ring Induction motor		150hp slip ring Induction motor	
1.	Nominal Parameters	Values in SI Units.	Nominal Parameters	Values in SI Units.
2.	Stator Resistance(Rs)	0.83131Ω	Stator Resistance(Rs)	1.950Ω
3.	Rotor Resistance(Rr)	0.700Ω	Rotor Resistance(Rr)	0.78Ω
4.	Stator Inductance(Ls)	0.0021H	Stator Inductance(Ls)	0.0041H
5.	Rotor Inductance(Lr)	0.0021H	Rotor Inductance(Lr)	0.0041H
6.	Mutual inductance(Lm)	0.38H	Mutual inductance(Lm)	0.22H
7.	Inertia(J)	10kgm^2	Inertia(J)	141kgm^2
8.	Friction Factor (F)	0.0021Nm^2	Friction Factor (F)	0.00314Nm^2
9.	Pole pairs (p)	5	Pole pairs (p)	6

Table 6.2 Simulation results of 3hp laboratory haulage drive system by conventional method for different combination of loads and gradients for down the gradient

Angles with horizontal	Load(N)	Voltage (V)	Current (A)	N_1 (rpm) (Actual speed)	N_2 (rpm) (1:40) (Shaft speed)	Torque (Nm)	Input power (W)	Output power (W)	Efficiency (%)	Time (s)	Energy consumption (kWh)
27^0	1079	390	3.0	549	13.73	69.13	1621.2	949	58.53	22.5	0.00593
	1275	390	3.2	543	13.58	76.58	1729.3	1040	60.14	24.25	0.00700
	1471	395	3.3	533	13.33	91.49	1806.7	1220	67.53	25	0.00847
	1765	395	3.5	521	13	106.4	1915.6	1387	72.4	27	0.01040
29^0	1079	395	3.2	546	13.6	73.34	1751.2	1012	57.8	20	0.00562
	1275	390	3.4	539	13.47	82.04	1837.3	1105	60.15	21.5	0.00660
	1471	395	3.6	528	13.2	98.00	1970.4	1294	65.7	23	0.00826
	1765	400	3.7	518	12.95	114	2050.3	1475	71.92	25.25	0.01034
32^0	1079	390	3.4	542	13.54	78.42	1837.4	1062	57.8	19	0.00560
	1275	395	3.5	537	13.42	86.87	1915.6	1166	60.86	21	0.00680
	1471	400	3.6	526	13.14	103.8	1995.3	1364	68.34	22.5	0.00852
	1765	405	3.7	512	12.8	119.6	2076.4	1545.5	75.35	23	0.00987
35^0	1079	396	3.5	541	13.51	82.19	1920.5	1111.0	57.9	22	0.00679
	1275	400	3.6	535	13.38	91.04	1995.3	1218	61.05	23	0.00778
	1471	400	3.8	522	13.04	108.7	2106.1	1418	67.35	24	0.00945
	1765	404	3.9	510	12.74	126.4	2188.6	1612	73.81	25	0.01119

Table 6.3 Simulation results of 3hp laboratory haulage drive system by conventional method for different combination of loads and gradients for up the gradient

Angles with horizontal	Load(N)	Voltage (V)	Current (A)	N_1 (rpm) (Actual speed)	N_2 (rpm) (1:40) (Shaft speed)	Torque (Nm)	Input power (W)	Output power (W)	Efficiency (%)	Time (s)	Energy consumption (kWh)
27^0	1079	390	3.2	548	13.7	70.65	1729.2	967.8	56	24	0.00645
	1275	390	3.4	542	13.5	78.22	1837.3	1060	57.6	26	0.00765
	1471	395	3.5	531	13.3	93.38	1915.6	1240	64.8	27.75	0.0087
	1765	395	3.7	520	13	108.5	2025.1	1410	69.7	29	0.01358
29^0	1079	395	3.3	546	13.6	75.4	1806.1	1028.7	56.95	22	0.00650
	1275	400	3.4	541	13.5	83.5	1884.5	1129	60	23.5	0.00737
	1471	400	3.5	529	13.2	99.69	1939.9	1317.8	67.93	25	0.00915
	1765	415	3.7	523	13.1	115.9	2076.4	1514	71.17	26.5	0.01115
32^0	1079	390	3.5	541	13.5	79.6	1891.4	1076	56.9	20	0.0060
	1275	400	3.6	537	13.4	88.14	1995.3	1184	59.36	22	0.00724
	1471	400	3.7	524	13.1	105.2	2076.4	1380	67.3	23.5	0.00900
	1765	410	3.8	516	12.9	122.3	2130.4	1577	74	25	0.01095
35^0	1079	400	3.5	541	13.5	83.18	1939.9	1126	58	23	0.00719
	1275	400	3.6	537	13.4	92.12	1995.3	1231	61.7	24	0.00821
	1471	400	3.8	521	13	110.4	2158.8	1432	68	26	0.0103
	1765	405	3.9	509	12.7	127.8	2188.8	1627.4	74.4	27	0.0122

Table 6.4 Conventional method simulation field study results of 150hp underground hauler drive system -1from surface to 8L (down the gradient)

Sl.No	Load(kN)	Voltage (V)	Current (A)	N₁ (rpm) (Actual speed)	N₂ (rpm) (1:29) (Shaft speed)	Torque (Nm)	Input power (kW)	Output power (kW)	Efficiency (%)	Time(s)	Distance (km)	Energy consumption (kWh)
1	33.3	3000	20	410	14.13	6668	144.000	97.500	67.71	18.75	0.10	0.507
2	32.6	3050	19	415	14.31	6521	139.080	96.738	69.56	37.5	0.18	1.008
3	30.4	3100	18.5	425	15.18	6081	133.920	92.337	67.09	56.00	0.28	1.437
4	28.1	3110	17.5	432	15.43	5641	130.200	87.034	66.63	75.00	0.38	1.813
5	24.5	3010	16	437	15.6	4908	115.584	76.697	66.36	94.00	0.47	1.898
6	20.1	2990	16	449	16	4028	114.816	64.636	56.31	112.5	0.56	2.020
7	18.6	2990	15.8	430	16.19	3734	113.380	60.474	53.34	131.0	0.66	2.200
8	17.6	3000	15.5	456	16.3	3539	111.600	57.487	51.7	150.0	0.75	2.403

Table 6.5 Conventional method simulation field study results of 150hp underground hauler drive system 1from 8L to surface level

(up the gradient)

Sl.No	Load (kN)	Voltage (V)	Current (A)	N₁ (rpm) (Actual speed)	N₂ (rpm) (1:29) (Shaft speed)	Torque (Nm)	Input power (kW)	Output power (kW)	Efficiency (%)	Time(s)	Distance (km)	Energy consumption (kWh)
1	36.7	2990	17	441	15.20	4572	121.992	72.098	59.1	180.0	0.75	3.605
2	33.0	2990	17.5	427	14.72	5573	125.580	85.112	65.45	157.5	0.66	3.832
3	31.6	3010	18	425	14.65	6047	130.032	91.926	66.8	135.0	0.56	3.498
4	29.4	3100	18.5	425	14.65	6047	137.640	91.926	66.8	112.5	0.47	2.8727
5	27.9	3150	19	423	14.58	6363	143.640	96.347	67	90.00	0.38	2.4088
6	25.7	3100	20	414	14.28	6837	148.800	102.573	67.91	67.5	0.28	1.894
7	22.0	3100	20.5	409	14.10	7153	150.620	104.466	69.70	45.00	0.18	1.305
8	21.0	3150	22	400	13.79	7943	153.846	113.541	73.80	22.5	0.10	0.709

Table 6.6 Conventional method simulation field study results of 150hp underground hauler drive system -2from 8L to42nd L

(down the gradient)

Sl. No	Load (kN)	Voltage (V)	Current (A)	N_1 (rpm) (Actual speed)	N_2 (rpm) (1:29) (Shaft speed)	Torque (Nm)	Input power (kW)	Output power (kW)	Efficiency (%)	Time (s)	Distance (km)	Energy consumption (kWh)
1	39.2	3150	20	418	13.9	7841	151.200	118.532	77.5	84	0.15	2.626
2	36.2	3200	19.5	414	14.3	7254	149.760	109.333	74	169	0.20	5.039
3	34.8	3110	19	413	14.2	6961	141.816	102.578	72.4	253	0.27	7.209
4	32.5	3100	18.5	412	14.5	6521	137.640	97.497	71	338	0.38	9.154
5	30.4	3110	18	406	14.7	6081	133.920	91.460	68	422	0.46	10.83
6	28.1	3090	17.5	411	14.9	5641	129.780	83.826	65.0	507	0.56	12.22
7	23.0	3010	17	412	15.2	4614	122.808	71.813	55.5	592	0.66	11.97
8	19.8	3000	16.5	409	15.6	3979	118.800	64.003	53	676	0.76	12.01
9	18.6	3000	16	413	15.7	3734	115.200	59.0520	52.5	720	0.85	12.104

Table 6.7 Conventional method simulation field study results of 150hp underground hauler drive system -2from 42ndL to 8L

(up the gradient 1 in4 or 14^0)

Sl.No	Load (kN)	Voltage (V)	Current (A)	N$_1$ (rpm) (Actual speed)	N$_2$ (rpm) (1:29) (Shaft speed)	Torque (Nm)	Input power (kW)	Output power (kW)	Efficiency (%)	Time (s)	Distance (km)	Energy consumption (kWh)
1	17.64	3200	22.5	379	13.06	9523	175.500	128.80	74.54	840	0.85	30.05
2	19.50	3250	22.5	387	13.32	9313	175.500	128.72	73.34	716	0.76	25.60
3	24.01	3250	22	395	13.6	8786	171.600	124.01	72.3	617	0.66	21.25
4	29.30	3250	22	403	13.9	8259	171.600	118.92	69.3	518	0.56	17.11
5	33.90	3210	21.5	414	14.3	7332	165.636	108.36	65.5	422	0.46	12.70
6	38.22	3100	21	421	14.5	6342	148.800	99.287	61	321	0.36	8.509
7	40.67	3100	20	437	15.12	5204	148.800	81.333	54.66	222	0.26	5.042
8	43.12	3140	19	452	15.6	4235	143.184	68.537	47	123	0.16	2.279
9	44.10	3150	18	457	15.78	3834	136.080	62.619	46	48	0.10	0.835

6.3 SIMULATION STUDY ON SLIP POWER RECOVERY OF HAULAGE DRIVE SYSTEM

6.3.1 Static control (micro controller) of haulage drive system:

In this section the entire system is simulated on the MATLAB-SIMULINK platform. The simulation model comprises different functional modules or subsystems. Each of these modules, in turn has several levels of subsystems which are developed by using the standard SIMULINK library. For the Simulation of energy recovery of haulage drive system using static Krammer (micro controller) method for open loop and closed loop control study, the following drive methods are considered.

- Experimental 3hp mine haulage drive system
- 150hp underground haulage drive system.

When operated from the fixed frequency grid, the slip ring induction motor (SRIM) operates at a constant speed. In earlier days, speed control of the SRIM below synchronism was done by dissipating the slip power through the external resistor banks. This type of control has a very poor efficiency considering the large amount of slip power lost. Instead of wasting the slip power, the electrical energy can be recovered by feeding it back to the supply system.

Many authors have presented many methods for slip recovery from the secondary rotor circuit, which utilized either mechanical or electrical methods. Variable speed control for slip ring induction motor (SRIM) may be achieved by simply dissipating the rotor power into resistor banks. However, the drive efficiency is very low and speed regulation is poor. When the drive requirements include good efficiency, dynamic response and accurate speed or torque regulates. Then such open loop control is unsatisfactory. It is necessary to operate the SRIM in a closed loop mode, especially when the dynamic operation of the drive has an important effect on the overall performance of the system.

In simulation study, the micro controller (Static Krammer) sub-synchronous slip recovery system is designed for experimental 3hp laboratory haulage drive system and two 150hp underground haulage drive system are simulated. For sub-synchronous operation, a static converter replaces the DC machine of the early

Krammer drive. This system consists of a three-phase rectifier bridge connected to the rotor, and cascaded with the DC link and a mains side converter.

The rectified slip power returns to the AC supply via the DC link and the frequency matching converter. Both the rectifier and the inverter are naturally commutated by the alternating Electromagnetic force (EMF). at the secondary output terminals and the AC supply, respectively. The performance characteristics of the Static Krammer system have been analyzed in detail by many authors. The torque developed by the system was shown to be proportional to the fundamental component of the secondary current from the DC link. The static Krammer drive is common in situations where limited sub-synchronous speed range is adequate. The system is particularly advantageous at high power levels because of better overall efficiency.

The sub model for controller is designed for active power, reactive and active power load side of the system. The speed controller is used by proportional integral (PI) controller. The entire system controller is used to drive the IGBT using PWM technique. The simulated design parameters for fabricated 3hp laboratory experimental haulage drive and 150hp underground haulage drive system of different simulink blocks are presented in APPENDIX X.

In static Krammer drive system both open loop variable frequency control and closed loop control are designed for speed and slip power recovery in both the experimental and field study 150hp underground coal mine haulage drive. It is also simulated as per the data obtained from GDK 10A incline mine.

This is to analyze the performance of slip power recovery work in laboratory environment using microcontroller as IGBT PWM controller for the inverter circuit. The advantages of using microcontroller over digital and microprocessor techniques are: it is simple, flexible, economical, and consumes less hardware.

In this work, steady state relationships between torque, speed, power and energy for the slip power recovery are derived in section 5.1.5. By using dynamic model library in MATLAB/SIMULINK, a simulation model of the mine haulage drive system is implemented. The simulated results are compared with an experimental set-up developed in the mining laboratory.

To study the performance of the 3hp and 150hp underground haulage drive system, a simulation block-set in MATLAB/SIMULINK has been implemented. Variable frequency (V/f) control method of SIMULINK model for open loop control and closed loop control is shown in Figure 6.5 and Figure 6.6.

Explanations of simulation process with physical haulage drive system of Figure 6.5. Represents Simulink model of the 3hp experimental haulage drive system for open loop control of slip ring induction motor is simulated at no load condition. And Figure 6.6 represents Simulink model of the 150hp underground haulage drive closed loop control system slip ring Induction motor are simulated at no load condition. The no load simulated electrical parameters of 150 hp and 3hp are presented in Table 6.8.The available 3 phase voltage source of 3.3 KV , 440V , are connected to 150hp and 3hp simulated slip ring induction motor. 3 phase diode bridge rectifier and 3phase IGBT (Insulated Gate Bipolar Transistor) inverter and 2 KVA recovery transformer are designed and simulated for 150hp and 3hp experimental haulage drive system by MATLAB/SIMULINK tools and separately connected to rotor of the slip ring induction motor. The separate PI controllers are designed for closed loop control system of 150hp and 3hp haulage drive systems are simulated.

The simulated blocks are presented in the Figure 6.9. The mathematical modeling equation (5.3) and (5.4) for both up the gradient and down the gradient drive system are derived. The equation for power requirement of the motor to run haulage drive by using available parameters in MATLAB/SIMULINK blocks are connected to make the mechanical load systems for 150hp and 3hp slip ring induction motor. For each equipment of the physical haulage drive system are created by using MATLAB/SIMULINK tools and connected together to make physical 150hp and 3hp haulage drive system for simulation process. The various meters like Ammeters , voltmeters and wattmeter's are connected for measurement of current ,voltage and power for loads for up the gradient and down the gradient of the drive system by using MATLAB/SIMULINK tools .

The electrical and mechanical internal behavior of drive system is observed by connecting scope and xy plotter for required terminal of the drive system in simulink blocks. By creating md.file in MATLAB the different parameters required for the simulation are enter in the program and run the file and after that run the

simulink name.md file by entering run in workspace. After each iteration note down the various electrical parameter required for energy consumption calculation (i.e. Speed, Torque, current, voltage, time, ect). Based on the above simulation model the various loads and gradients are simulated for both down the gradient up the gradient of the drive system. The entire drive system results tabulated and presented in Table 6.9, 6.10, 6.11, 6.12, 6.13 and Table 6.14 in the thesis.
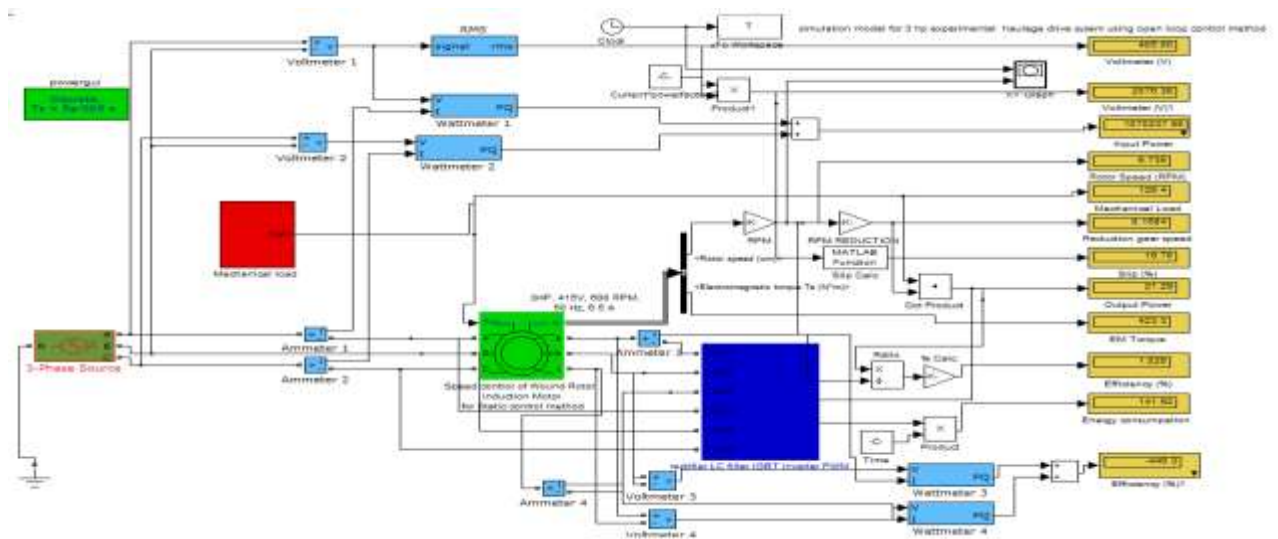
Figure 6.5 Simulink model of the 3hp experimental haulage drive system for open loop control slip ring induction motor
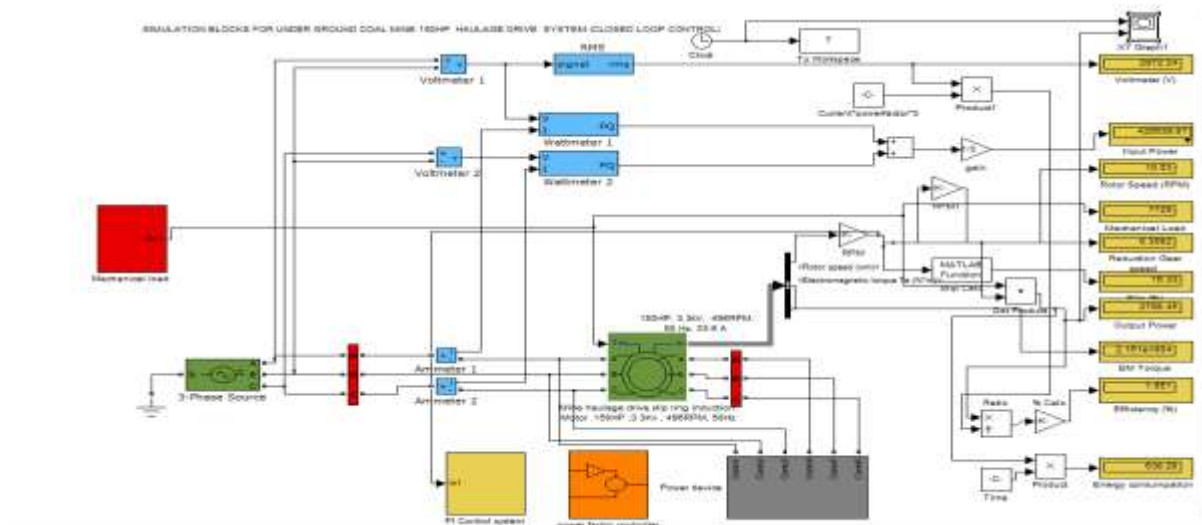
Figure 6.6 Simulink model of the 150hp underground haulage drive closed loop control system

The technical details of drive system and simulation electrical parameters of drive system are given in Table 6.8.Provision has been made to measure stator current, speed and torque of the motor and also different voltages and currents of the scheme wherever required.

The active and reactive power input of the motor, the recovery transformer and the source have been measured using P-Q block. The data has been saved to the workspace for further analysis. The SIMULINK controller blocks related open loop control drive for different sub system blocks related to 150hp underground haulage drive system and experimental 3hp laboratory haulage drive are given in Figure 6.7 and Figure 6.8.

 The controller for closed loop haulage drive system is designed and given in Figure 6.9.The same technical specification and simulation procedure are adopted in simulation slip power recovery control of drive system also. The various simulation results of drive system are tabulated and discussed in the next section.
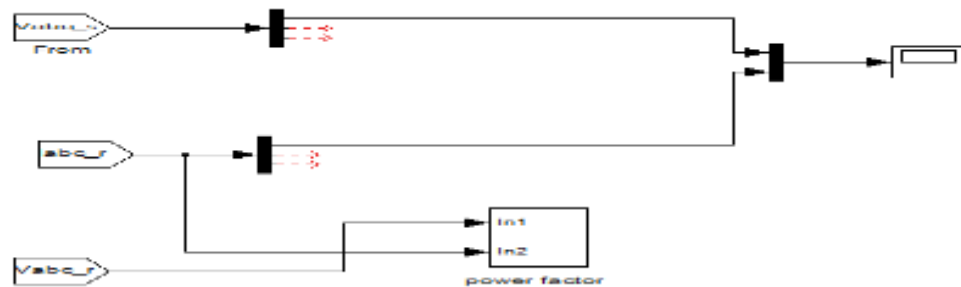
Figure 6.7 Simulink model for active, reactive power control of 3hp experimental
        and 150hp underground haulage drive system
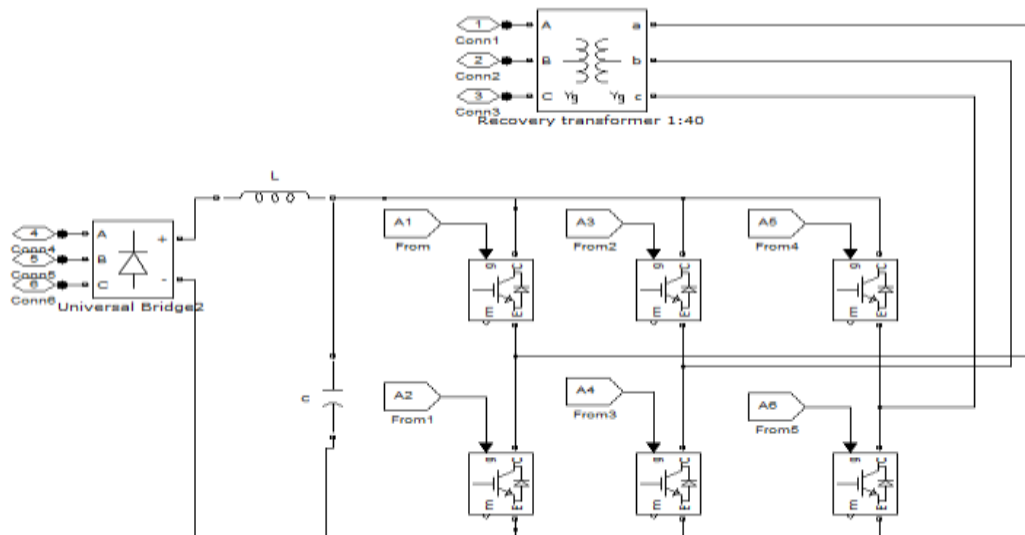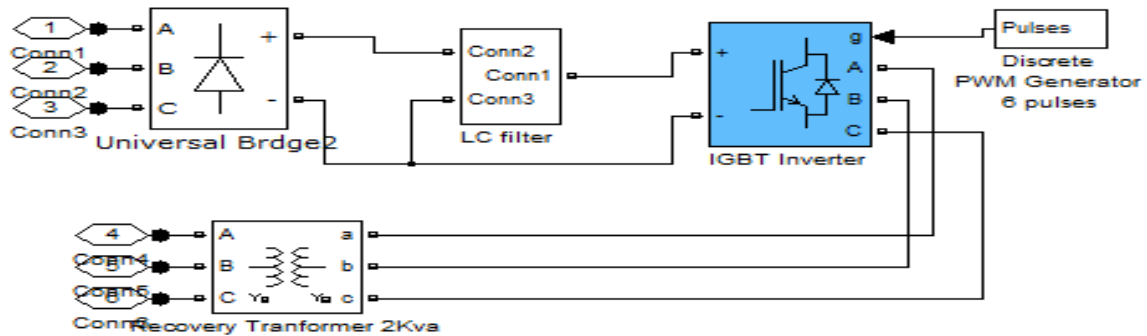
Figure 6.8 Simulink model for slip power recovery of static Krammer (micro
controller) open loop control of 150hp underground haulage drive system
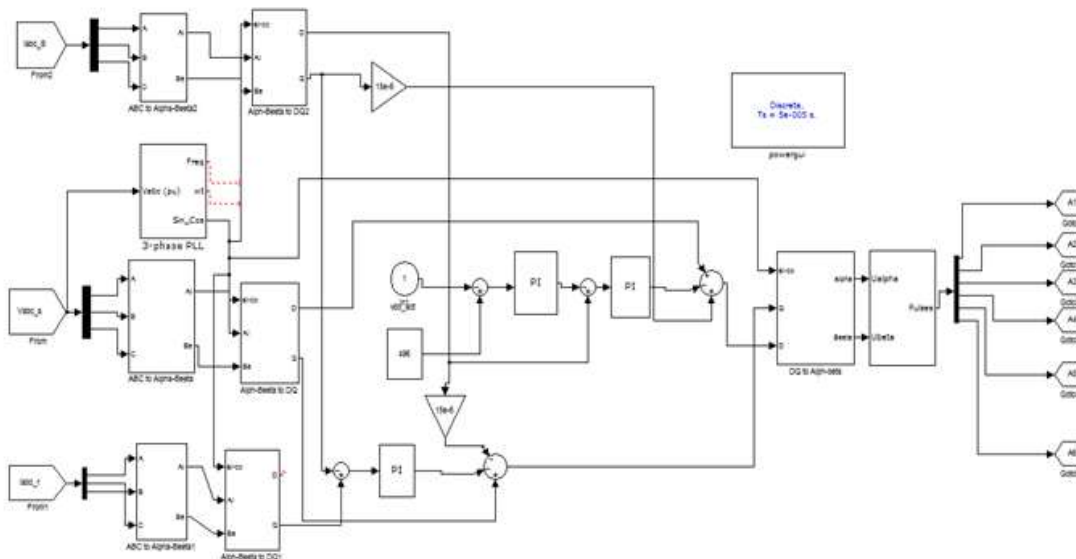
Figure 6.9 Simulink model for closed loop controller of 150hp underground haulage
drive system

6.3.2 Simulation procedure

In chosen technical details the 3hp laboratory experimental haulage drive model and 150hp underground haulage drive slip ring motor are simulated for no-load condition. The 3hp laboratory experimental static control (micro controller method) model was developed using MATLAB/SIMULINK. The simulation work is carried out using an experimental data obtained from 3hp laboratory experimental micro controller based haulage drive system.

The simulations are carried out for different combination of loads and gradients for up the gradient and down the gradient of the drive haulage system using microcontroller (static Krammer) method. The simulation results of 3hp laboratory

130

haulage drive system by micro controller method for different combinations of loads and gradients for down the gradient and up the gradient on energy consumption are tabulated and presented in Table 6.9 and Table 6.10 respectively. Similarly the MATLAB /SIMULINK model was developed for 150hp underground micro controller based haulage drive system. The simulation work is carried out the field data obtained from conventional 150hp haulage drive system -1 and haulage drive system-2 surface to 42nd level of underground GDK 10A incline coal.

The tabulated simulation results of micro controller method field study results of 150hp drive from surface to 8L(down the gradient)and 8L to surface (up the gradient) are given in Table 6.11 and Table 6.12 respectively for haulage drive system -1. Similarly simulation results of micro controller method field study results of 150hp haulage drive system from 8L to 42nd level(down the gradient) and 42nd to 8L (up the gradient) are given in Table 6.13 and Table 6.14 respectively for haulage drive system -2.

The detailed technical specifications for both the drive system are given in APPENDIX I. As per available data 150hpunderground mine haulage drive system and laboratory experimental 3 hp haulage drive system are simulated. The entire system simulation is carried out by experimental data obtain from the laboratory experimental haulage drive system with respect to different combination of loads and gradients for both up the gradient and down the gradient.

The micro controller (static Krammer) method of control (slip power recovery) is used for simulation of150hp underground haulage drive system- 1 and haulage drive system- 2 of underground coal mine GDK-10A incline. The results obtained from simulations are tabulated. The procedure for calculation of energy consumption for slip power recovery method of drive system is presented in APPENDIX X.

The results obtained from the drive system for different cases are also presented in results and discussion chapter 7 in the thesis. The 150hp underground mine haulage drive system is simulated by using the field study data obtained from mine. The No-load Electrical simulation parameter of 3hp and 150hp slip ring (wound rotor) induction motor are presented in Table6.8.The Open loop control simulation

graphical results for various parameters variation with time are presented in result and discussion chapter.

The field study results are simulated by using Simulink model of 150hp slip ring induction motor drive system. The tabulated simulation results are applicable up to 4.2 kilometers distance of underground coal mine. The input data used for simulation is based on the 150hp underground haulage drive system field study report discussed in chapter 3 of this thesis. The conventional drive system input data is also used in simulation of 3hp experimental slip power recovery haulage drive system. So this helps to compare the results in easy way.

Table 6.8 No-load electrical simulation parameters of 3hp and 150hp haulage drive system

Sl.No.	3hp slip ring induction motor		150hp slip ring induction motor	
1.	Nominal Parameters	Values in SI Units.	Nominal Parameters	Values in SI Units.
2.	Stator Resistance(Rs)	0.83131Ω	Stator Resistance(Rs)	1.950Ω
3.	Rotor Resistance(Rr)	0.700 Ω	Rotor Resistance(Rr)	0.78 Ω
4.	Stator Inductance(Ls)	0.0021H	Stator Inductance(Ls)	0.0041H
5.	Rotor Inductance(Lr)	0.0021H	Rotor Inductance(Lr)	0.0041H
6.	Mutual inductance(Lm)	0.38H	Mutual inductance(Lm)	0.22H
7.	Inertia(J)	10 kgm^2	Inertia(J)	141kgm^2
8.	Friction Factor (F)	0.0021Nm^2	Friction Factor (F)	0.00314Nm^2
9.	Pole pairs (p)	5	Pole pairs (p)	6
10.	LC filter	1.5e^{-3}, 33e^{-3}	LC filter	151e^{-5}, 175e^{-6}
11.	Switching frequency Carrier	1.16 kHz	Switching frequency	1.90 kHz
12.	Recovery transformer	1:40 2kVA	Recovery transformer	50 kVA
13.	Modulation index	0.85	Modulation index	0.85

Table 6.9 Simulation results of 3hp laboratory haulage drive system by microcontroller
method for different combination of loads and gradients for down the gradient

Angles with horizontal	Load (N)	Voltage (V)	Current (A)	N_1 (rpm) (Actual speed)	N_2 (rpm) (Shaft speed)	Torque (Nm)	Input power (W)	Output power (W)	Efficiency (%)	Power recovery (W)	Time (s)	Energy consumption (kWh)	Yearly Energy consumption (kWh)
27^0	1079	390	3.0	570	14.25	70.13	1621	1024	63.17	20	41.75	0.00568	20.48
	1275	390	3.2	567	14.17	77.66	1729	1129.6	65.5	22	78	0.00690	24.851
	1471	395	3.4	565	14.12	93.38	1861	1344.7	72.3	24	101	0.00896	32.27
	1765	395	3.5	561	14	108.5	1916	1551	81	25	129.9	0.01098	39.50
29^0	1079	395	3.2	574	14.35	75.4	1751	1105	63	18	53.7	0.00552	19.89
	1275	400	3.3	567	14.17	83.5	1829	1208	66	19	87.6	0.00637	22.95
	1471	400	3.4	564	14.1	99.69	1884	1433.5	76	20	144.8	0.00796	28.67
	1765	415	3.6	562	14	115.9	2070	1659	80.1	22	162.5	0.0113	36.49
32^0	1079	390	3.4	567	14.17	79.6	1837	1153	62.75	16	70	0.00512	18.44
	1275	400	3.5	565	14.12	88.14	1940	1272	65.6	18	93.4	0.00636	22.89
	1471	400	3.6	563	14.07	105.2	1995	1513.3	75.85	19	132.2	0.00798	28.75
	1765	410	3.7	561	14.02	122.3	2102	1754	83.3	20	181	0.00974	35.08
35^0	1079	400	3.4	568	14.2	83.18	1884	1208	64.18	20	69	0.00671	24.18
	1275	400	3.5	566	14.15	92.12	1940	1339	69	21	88.5	0.00781	28.11
	1471	400	3.6	562	14.05	110.4	1995	1580	79.19	22	106.5	0.00965	34.75
	1765	405	3.7	558	13.95	127.8	2076	1824	87.87	23	152	0.0116	41.63

Table 6.10 Simulation results of 3hp laboratory haulage drive system by micro controller method for different combination of loads and gradients for up the gradient

Angle with horizontal	Load (N)	Voltage (V)	Current (A)	N₁ (rpm) (Actual speed)	N₂ (rpm) (Shaft speed)	Torque (Nm)	Input power (W)	Output power (W)	Efficiency (%)	Power recovery (W)	Time (s)	Energy consumption (kWh)	Yearly Energy consumption (kWh)
27^0	1079	390	2.8	570	14.25	69.13	1513	1010	66.75	18	69.9	0.00505	18.18
	1275	390	3.0	566	14.15	76.58	1621	1101	68	20	88.3	0.00611	22.02
	1471	395	3.1	565	14.12	91.49	1697	1327	78.2	21	114.4	0.00774	27.867
	1765	395	3.2	557	13.9	106.4	1751	1521	87	22	122.9	0.00920	33.46
29^0	1079	395	3.0	568	14.2	73.34	1642	1079	65.7	16	54.2	0.00479	17.26
	1275	400	3.2	567	14.17	82.04	1729	1194	69	18	86.35	0.00597	21.478
	1471	400	3.3	564	14.1	98.00	1806	1419	78.5	19	122.5	0.00748	26.94
	1765	415	3.5	561	14	114	1940	1642	84.7	21	156.1	0.00957	34.48
32^0	1079	390	3.2	567	14.17	78.42	1729	1141	66	16	58.5	0.00507	18.256
	1275	400	3.3	565	14.12	86.87	1829	1262	69	18	81.5	0.00631	22.716
	1471	400	3.5	563	14.075	103.8	1940	1500	77.4	20	124.6	0.00833	30.00
	1765	410	3.6	560	14	119.6	2020	1735.	86	21	174.1	0.01012	36.43
35^0	1079	400	3.3	567	14.17	82.19	1811	1196.	66	18	88.7	0.00598	21.53
	1275	400	3.4	565	14.12	91.04	1884	1320	70	19	103.7	0.00696	25.06
	1471	400	3.6	562	14.05	108.7	1995	1568.	78.6	21	140.9	0.00914	32.93
	1765	405	3.7	560	14	126.4	2076	1792	86.3	22	191.5	0.0109	39.40

Table 6.11 Micro controller method simulation field study results of 150hp drive from surface to 8L(Down the gradient or Angle 14^0)

Sl. No	Load (kN)	Voltage (V)	Current (A)	N_1 (rpm) (Actual speed)	N_2 (rpm) (Shaft speed)	Torque (Nm)	Input power (kW)	Output power (kW)	Efficiency (%)	Time (s)	Distance (km)	Power recovered (W)	Energy consumption (kWh)	Yearly energy consumption (kWh)
1	33.3	3000	19	450	15.6	6668	136.80	110.05	80.44	16	0.10	12265	0.489	1408
2	32.6	3050	18	454	15.65	6521	131.76	108.58	82.40	30	0.18	10542	0.904	2606
3	30.4	3100	17.5	452	15.58	6081	130.20	100.81	77.42	46	028	8373.4	1.288	3710
4	28.2	3110	16.5	454	15.65	5641	123.56	93.930	76.26	65	0.38	7034.5	1.695	4881
5	24.5	3010	15	457	15.75	4908	108.36	82.264	76	84	0.47	5903.8	1.919	5515
6	20.1	2990	15	461	15.89	4028	107.64	68.105	63.3	102	0.56	4608.8	1.929	5526
7	18.6	2990	14.4	463	15.96	3734	100.46	63.408	63	118	0.66	4546	2.07	5961
8	17.7	3000	14	465	16.04	3539	100.80	60.357	60	130	0.75	3260.9	2.17	6249

135

Table 6.12 Micro controller method simulation field study results of 150hp surface hauler (up the gradient or Angle 14^0) from 8l to surface level

Sl. No	Load (kN)	Voltage (V)	Current (A)	N_1 (rpm) (Actual speed)	N_2 (rpm) (shaft speed)	Torque (Nm)	Input power (kW)	Output power (kW)	Efficiency (%)	Time (s)	Distance (km)	Power recovery (W)	Energy consumption (kWh)	Yearly energy consumption (kWh)
1	36.7	2990	15	459	15.82	4572	107.64	73.716	68.48	156	0.75	1644.3	3.194	9199
2	33.0	2990	15.5	455	15.70	5573	111.28	86.992	78.17	137	0.66	2174.9	3.310	9532
3	31.6	3010	16	454	15.65	6067	115.58	93.457	80.85	116	0.56	2542.9	3.012	8674
4	29.4	3100	16.5	457	15.75	6047	122.76	94.391	76.89	96	0.47	3477.5	2.517	7249
5	27.9	3150	17	453	15.62	6363	128.52	105.71	82.25	74	0.38	11230	2.173	6258
6	25.7	3100	18	452	15.6	6837	133.92	113.34	84.63	56	028	11815	1.763	5077
7	22.1	3100	18	452	15.6	7153	133.92	117.67	88.54	31	0.18	12730	1.01	2909
8	21.2	3150	20	445	15.34	7943	151.20	129.63	85.74	17	0.10	13156	0.612	1763

Table 6.13 Micro controller method simulation field study results of 150hp underground hauler (down the gradient or Angle 14^0) from 8L to42^{nd} level

Sl. No	Load (kN)	Voltage (V)	Current (A)	N_1 (rpm)(actual speed)	N_2 (rpm)(Shaft speed)	Torque (Nm)	Input power (kW)	Output power (kW)	Efficiency (%)	Time (s)	Distance (km)	Power recovery (W)	Energy consumption (kWh)	Yearly energy consumption (kWh)
1	39.2	3150	19	445	15.3	7841	151.20	127.97	89	76	0.15	8799.6	2.701	7780.88
2	36.2	3200	18.5	450	15.5	7254	149.76	119.72	84.2	152	0.20	7981.4	5.05	14918
3	34.8	3110	18	450	15.6	6961	141.81	114.88	85.51	227	0.27	9088.6	7.244	20863.1
4	32.6	3100	17.5	456	15.7	6521	137.64	109.06	83.75	280	0.38	11020	8.482	24429.6
5	30.3	3110	17	458	15.8	6081	133.92	102.14	80.51	315	0.46	11848	8.93	25741.8
6	28.2	3090	16.5	459	15.8	5641	129.78	94.964	77.60	406	0.56	12239	10.70	30844.3
7	23.0	3010	16	458	15.8	4614	122.80	77.506	67	493	0.66	9842.3	10.61	30568.3
8	19.9	3000	15.5	463	15.9	3979	118.80	67.569	60.50	528	0.76	9780	9.91	28541.3
9	18.6	3000	15	465	16.0	3734	115.20	63.682	59	582	0.85	8233.1	10.29	29650.6

Table 6.14 Micro controller method simulation field study results of 150hp underground hauler (up the gradient or Angle 14^0)

from 42nd level 8L

Sl. No	Load (kN)	Voltage (V)	Current (A)	N_1 (rpm) (Actual speed)	N_2 (rpm) (Shaft speed)	Torque (Nm)	Input power (kW)	Output power (kW)	Efficiency (%)	Time (s)	Distance (km)	Power recovery (W)	Energy consumption (kWh)	Yearly energy consumption (kWh)
1	17.6	3200	23.5	441	15.20	9403	180.48	152.08	85	745	0.85	12435	31.47	90639
2	19.5	3250	23	440	15.17	9313	179.40	150.29	83.7	602	0.76	11997	25.13	72379
3	24.0	3250	22	443	15.27	8786	171.60	142.75	83	556	0.66	10660	22.04	63495
4	29.3	3250	21	447	15.41	8259	163.80	135.40	82.6	449	0.56	9705	16.88	48635
5	33.9	3210	20	449	15.5	7332	154.08	120.74	78.4	379	0.46	7798	12.71	36608
6	38.2	3100	20	452	15.86	6342	148.80	105.13	70.6	289	0.36	5619.5	8.432	24306.
7	40.6	3100	19	458	15.8	5204	141.63	87.416	62	172	0.26	5648.9	4.16	12028
8	43.2	3140	18	463	15.98	4235	135.64	71.916	53	92	0.20	4504.3	1.83	5293
9	44.1	3150	17	467	16.1	3834	128.52	65.669	51	38	0.15	3852.9	0.693	1996.5

CHAPTER 7

RESULTS AND DISCUSSION

7.1 FIELD STUDIES IN UNDERGROUND HAULAGE DRIVE SYSTEM

Data collected for haulage drive system -1 and haulage drive system -2 in an underground coal mine are used to calculate efficiency, torque, and power output and energy consumption. The figures for influence of power output on torque of haulage drive system -2 and influence of power output on efficiency for haulage drive system-1 for up the gradient are give in Figure 7.1 and Figure 7.2, respectively.

The field study results clearly show that energy consumption for up the gradient drive consumes more power than the down the gradient drive and on average varies 21.20% (from 1.033kWh to1.311kWh). From the field study results the following observations are made on power output of haulage drive system

1) Field study results on conventional method the power output was varied 41.12% (from 57096.1W (minimum load, 17.64 kN) to 98040.4W (maximum load, 32.65 kN)) of down the gradient of haulage drive system-1. Similarly the power output varied 38.14% (from 72071.67 W (minimum load, 21 kN) to 116483 W (maximum load, 36.7kN)) for up the gradient of haulage drive system-1.

2) The power output was varied 53.47% (from 55448.86 W (minimum load, 19.8kN) to 119174.4 W(maximumload,39.2kN)) for down the gradient of haulage drive system-2.Similarly the power output was varied 55.73% (from 61816.1W (minimum load,17.6 kN) to 139653.0 W (maximum load,44.1kN)) for up the gradient haulage drive system-2.

The energy consumption was varied for different levels in an underground mine haulage drive system. The energy consumption for down the gradient and up the gradient for 150hp haulage drive system -1 (i.e. serving from surface to 8th level and 8th level to surface) was varied from 0.509 kWh to 2.379 kWh and from 0.728 kWh to 3.603 kWh respectively. Similarly the energy consumption for 150hp haulage drive system -2 for down the gradient and up the gradient (i.e. serving from 8th level to 42nd level and 42^{nd}level to8^{th} level)was varied 78.6% (from 2.780 kWh to11.06 kWh) and 97.4% (from 0.824 kWh to 32.53 kWh) respectively.

Field data collected from the mine for different measured electrical parameters of 150hp underground haulage drive system -1 and haulage drive system-2 are calculated and also energy consumption calculation steps are given in APPENDIX II.

Influence of power output on efficiency for both up the gradient(8th to surface level) and down the gradient of haulage drive system-1 and haulage drive system-2 are given in Figure 7.1(a) , Figure 7.1(b) , Figure 7.1(c) and Figure 7.2(d), respectively. The efficiency changes linearly as the power output of the drive is also increases.

It is observed that efficiency is decreased non-linearly in both the drive system -1 and drive system -2.The influence of power output on torque for 150hp haulage drive system -1 and 150hp haulage drive system-2 for both down the gradient and up the gradient are shown in Figure 7.2 (a), Figure 7.2(b), Figure 7.3(a) and Figure 7.3(b), respectively.

It is observed that the torque decreases nonlinearly as the output increases for down the gradient. Also the torque increases nonlinearly as power output is increases. Because the total load acting on the motor will be more for up the gradient than the down the gradient. Also for up the gradient torque required is more and hence more power is required.

Similarly influence of load on energy consumption of 150hp underground haulage drive system -1 and haulage drive system-2 for both down the gradient and up the gradient are shown in Figure 7.4(a) , Figure 7.4(b) , Figure 7.4(c) and Figure7.4(d), respectively. It is observed that energy consumption changes when the load increases and also gradients increases (up the gradient and down the gradient) of the haulage drive system.

The influence of distance (km) on energy consumption of 150hp haulage drive system-1 and haulage drive system-2 for up the gradient and down the gradient are shown in Figure7.5 and Figure 7.6 respectively. From graphical results the up the gradients of the drive system consumes more energy than the down the gradient of drive system and energy consumption increases asymptotical discussed in the literature. The cost analysis for total energy consumption in 150hp haulage drive system GDK 10A mine is calculated based on the following assumptions:

i. The total weight of empty car is 18250 N, average weight of each person is 736 N; number of persons in one car travelling at a time are 35.

ii. Number of trips per day are 8.

Based on the above assumptions, daily, monthly and annual energy consumption are calculated. The cost analysis is done according to the data obtained from GDK 10A incline for both haulage drive system -1 and haulage drive system -2.The total energy consumption per year and total cost of energy per year for both haulage drives are 7,02,801kWh and Rs.49,19,611/- respectively.

The field study results clearly show that energy consumption of up the gradient drive system consumes more power than the down the gradient drive system. The energy consumption chart in Figure 7.7(a) indicates the down gradient of the drive system and also energy consumption chart in Figure 7.7(b) indicates up the gradient of the drive system. The plotted results also show that the difference of energy consumption for both the drive systems. In this results the up the gradient of the drive system consumes more power than the down the gradient drive system of concerned mine haulage drive system.
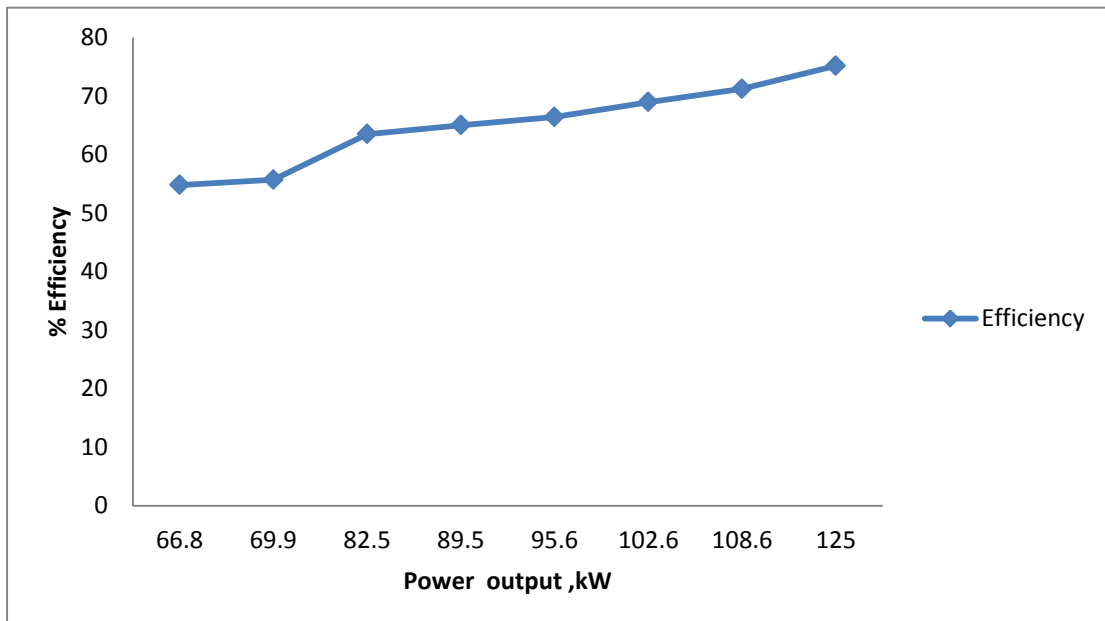
Figure 7.1(a) Influence of efficiency variations with output power up the gradient (8th to surface level) of haulage drive system-1
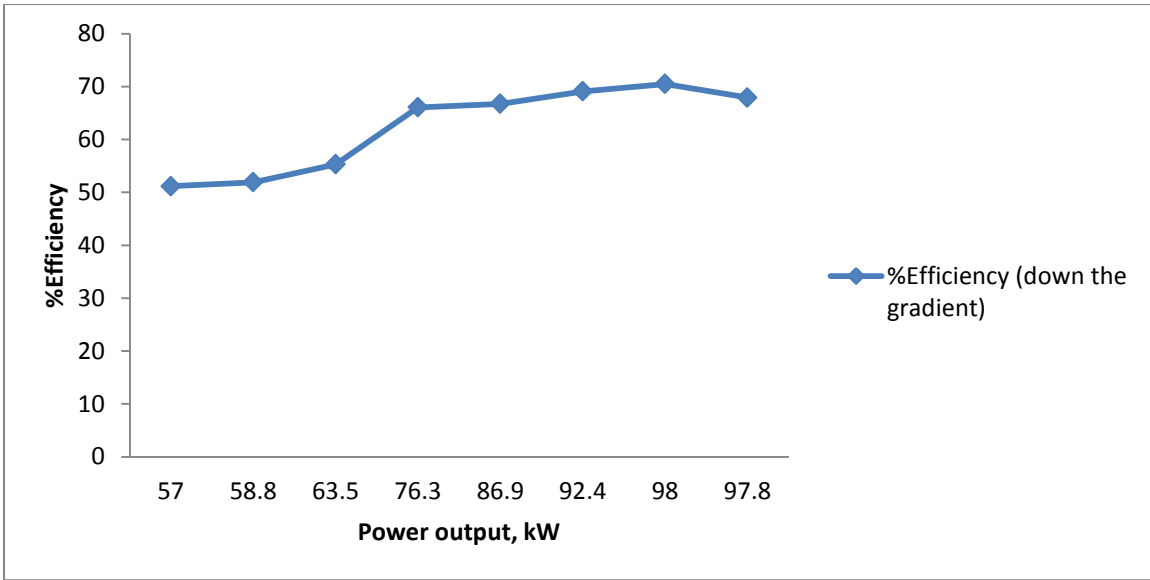
Figure 7.1(b) Influence of efficiency variations with output power down the gradient (8th to surface level) of haulage drive system-1
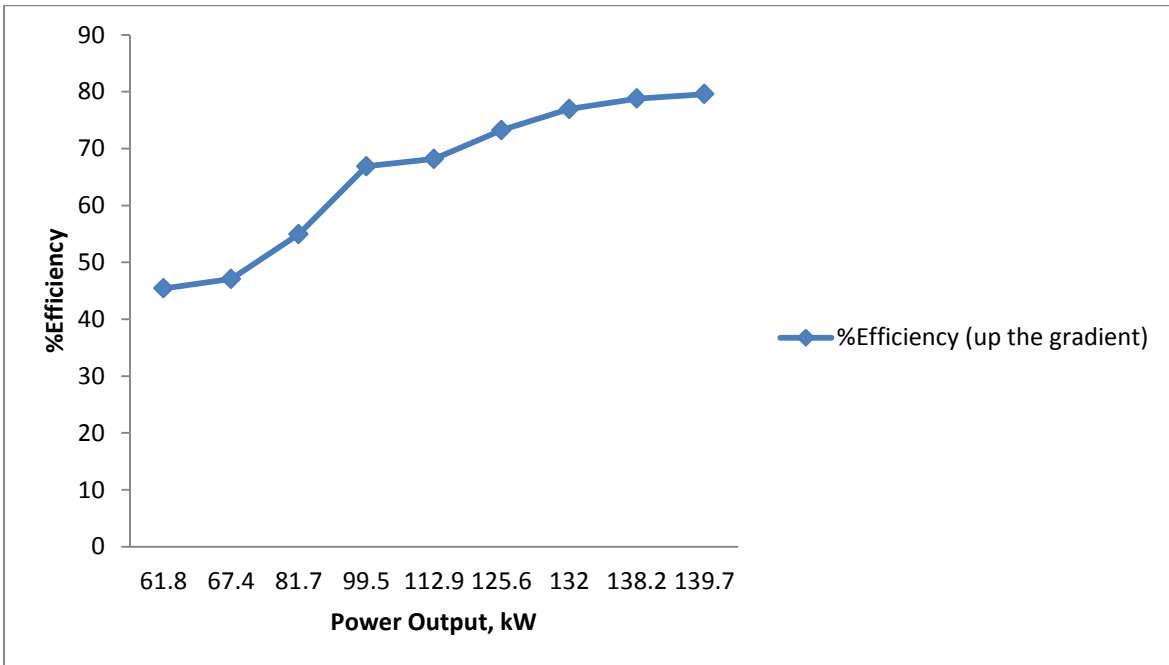
Figure 7.1(c) Influence of efficiency variations with output power up the gradient of haulage drive system-2
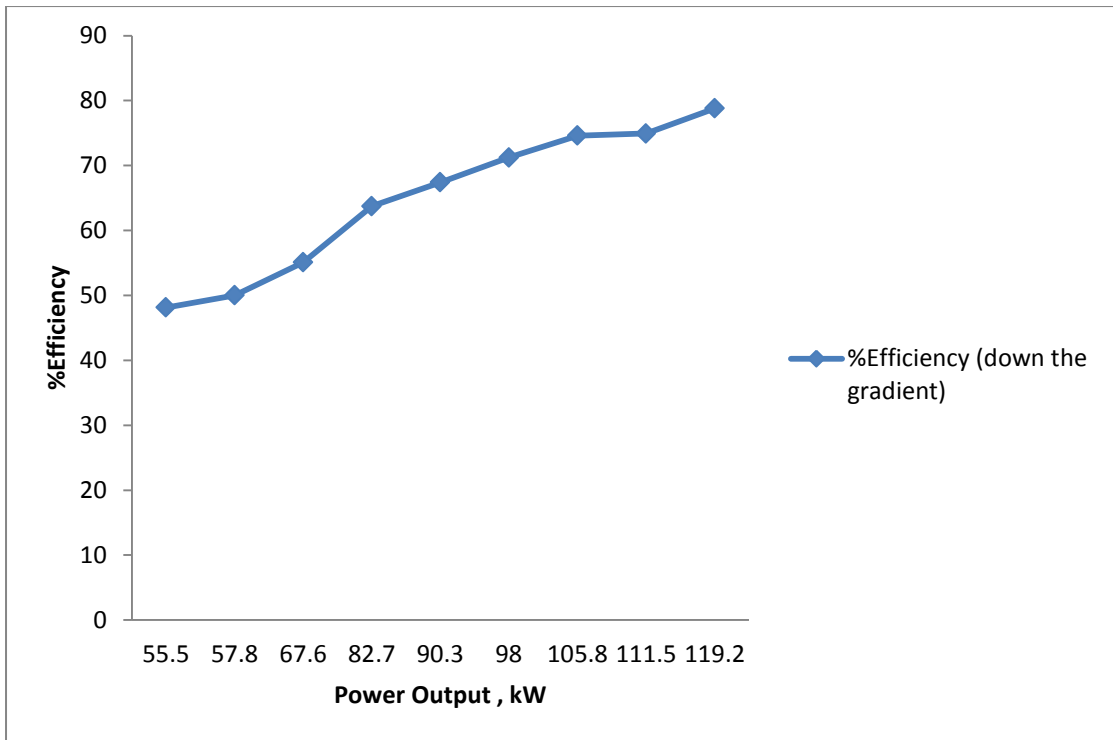
Figure 7.1(d) Influence of efficiency variations with power output for haulage drive system-2 for down the gradient
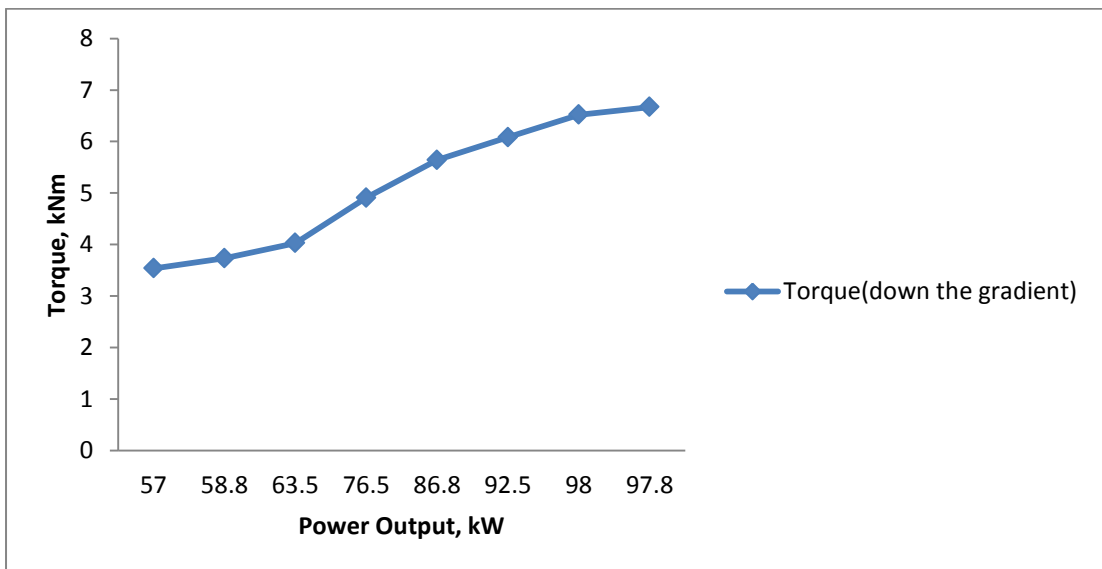
Figure 7.2(a) Influence of power output on torque for 150hp haulage drive system -1 for down the gradient
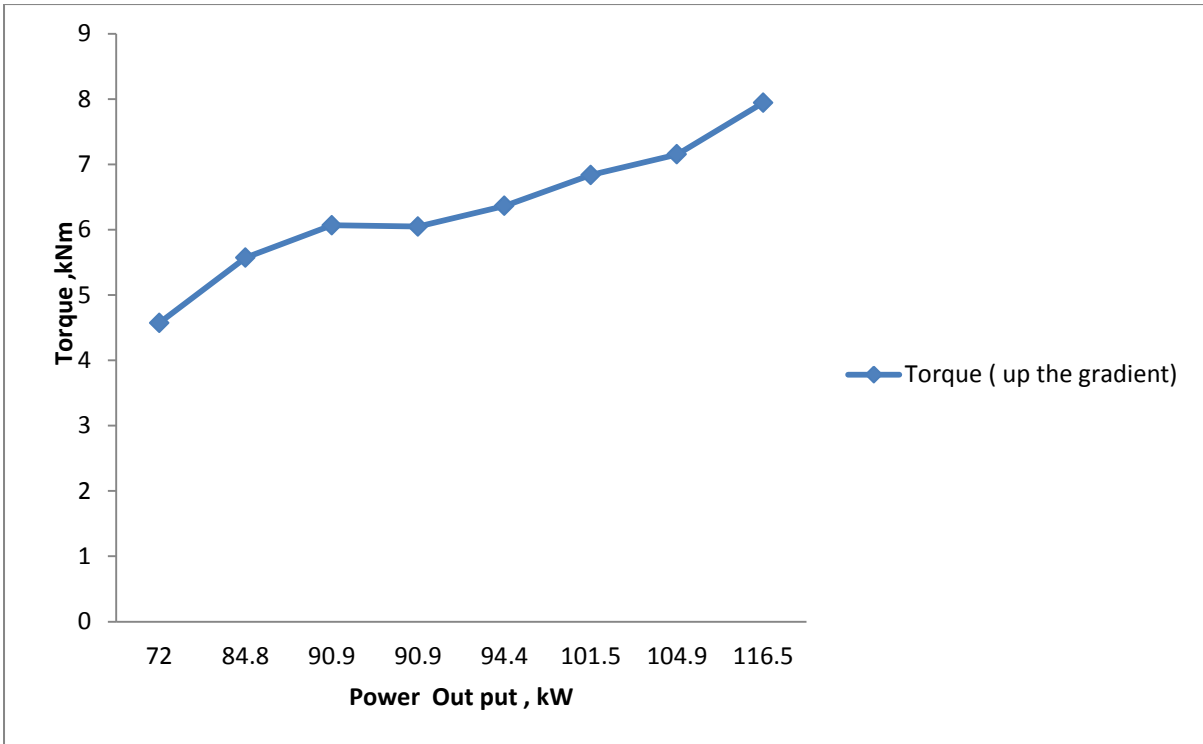
Figure 7.2(b) Influence of power output on torque for 150hp haulage drive system -1
for up the gradient
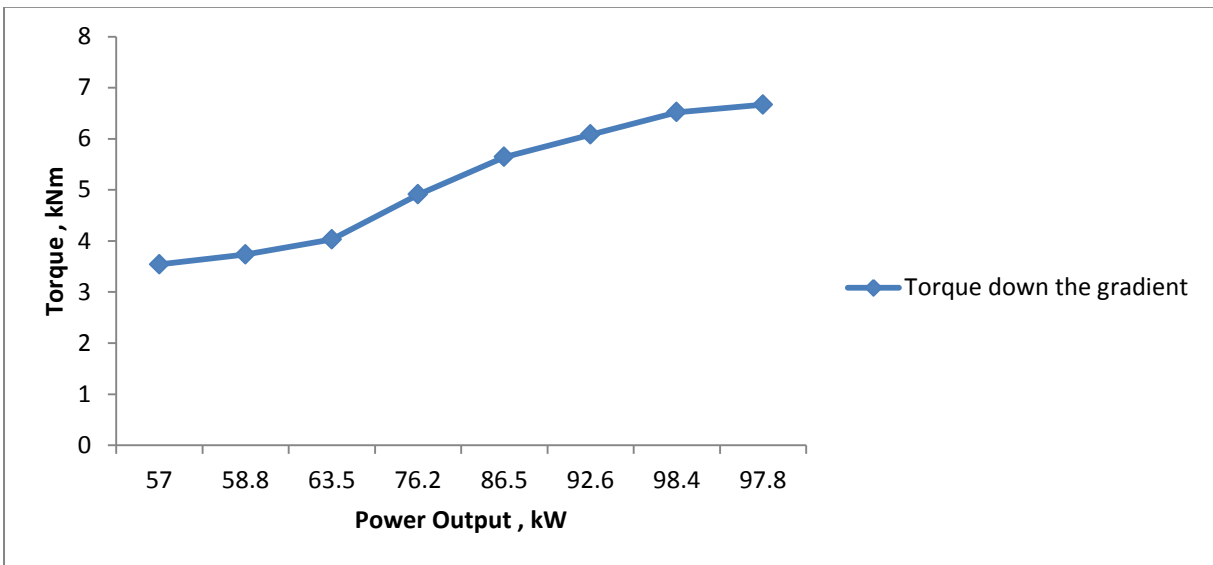
Figure 7.3(a) Influence of power output on torque for 150hp haulage drive system -2
for down the gradient
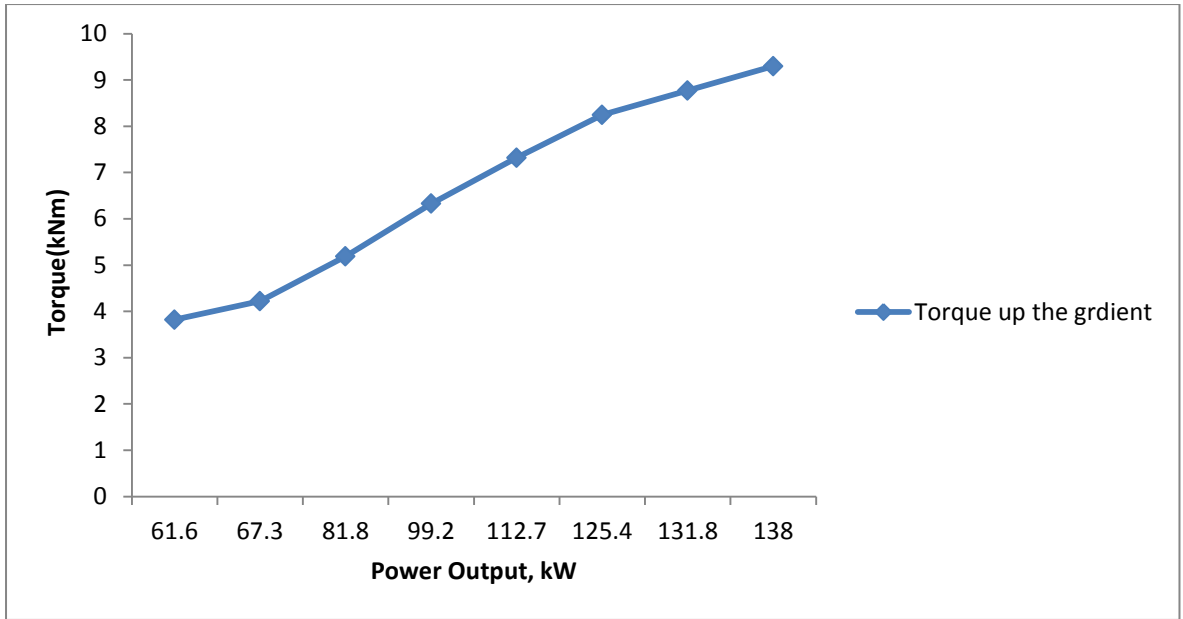
Figure 7.3(b) Influence of power output on torque for 150hp haulage drive system -2
for up the gradient
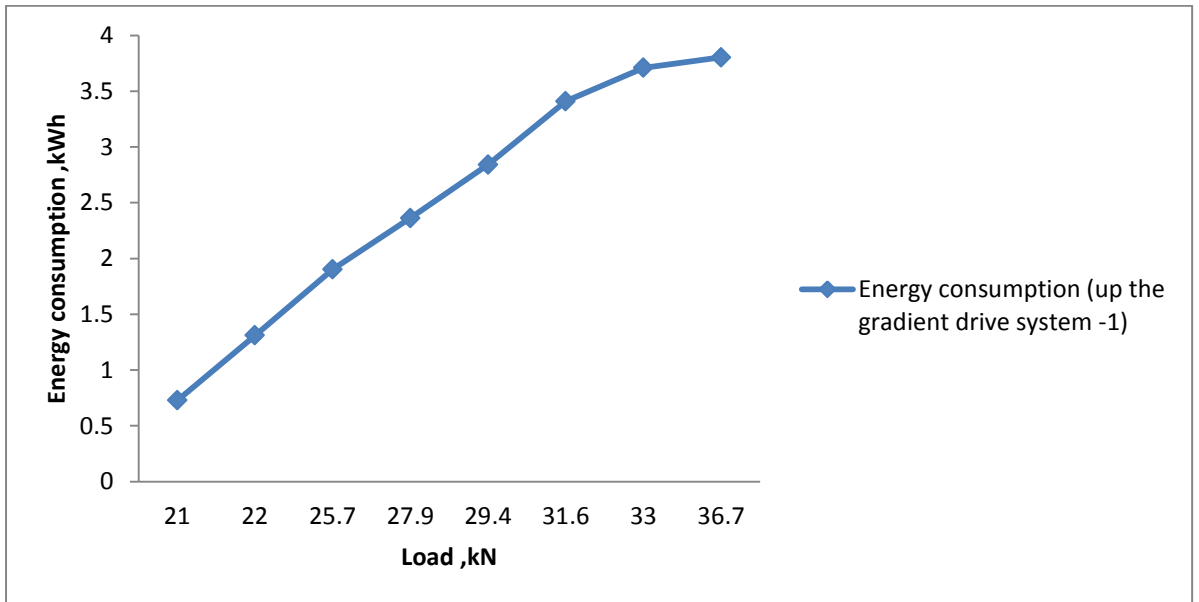
Figure 7.4(a) Influence of load on energy consumption for 150hp haulage drive
system -1 for down the gradient
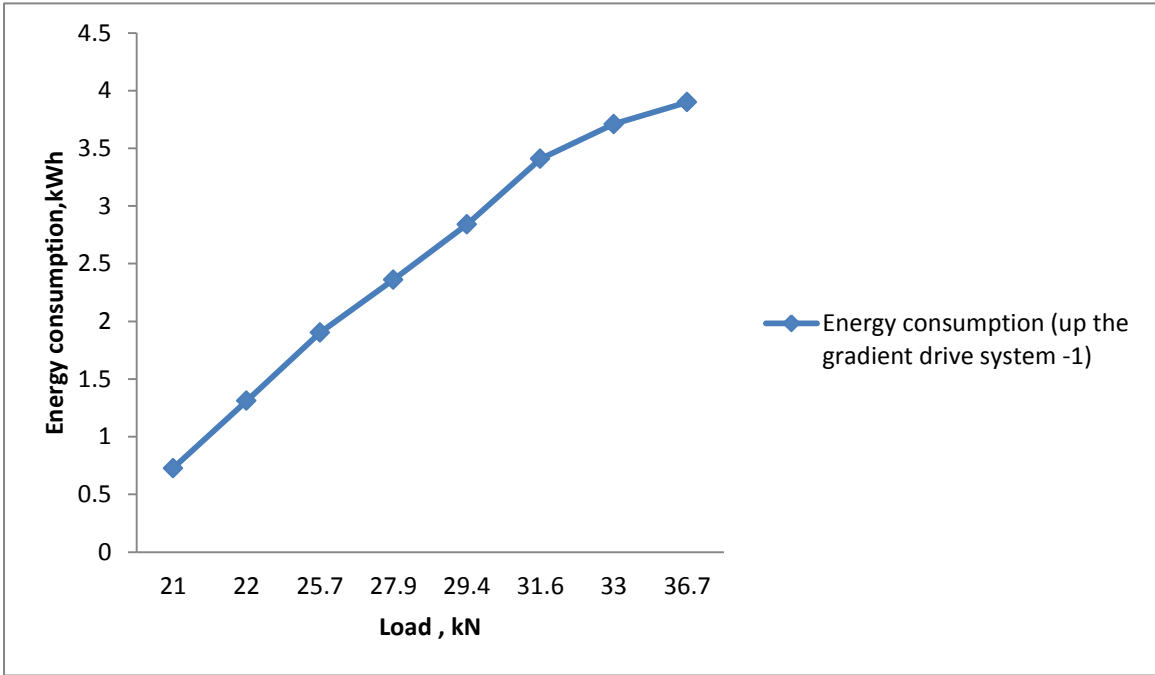
Figure 7.4(b) Influence of load on energy consumption for 150hp haulage drive
        system -1for up the gradient
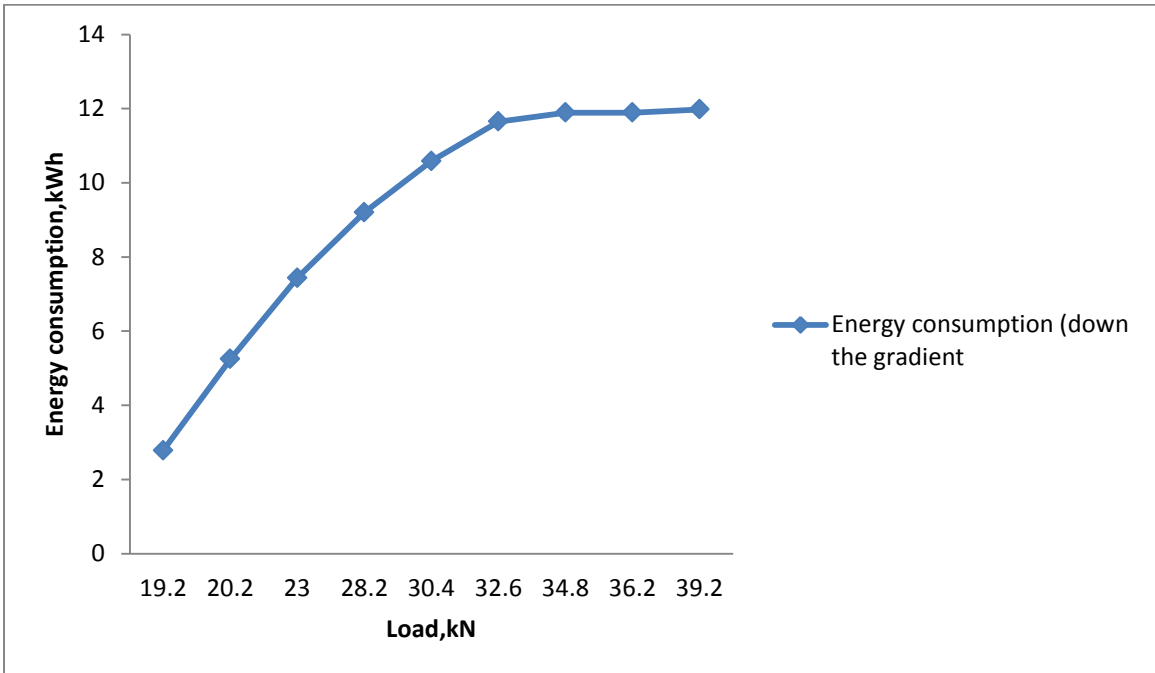
Figure 7.4(c) Influence of load on energy consumption for 150hp haulage drive
        system -2 for down the gradient
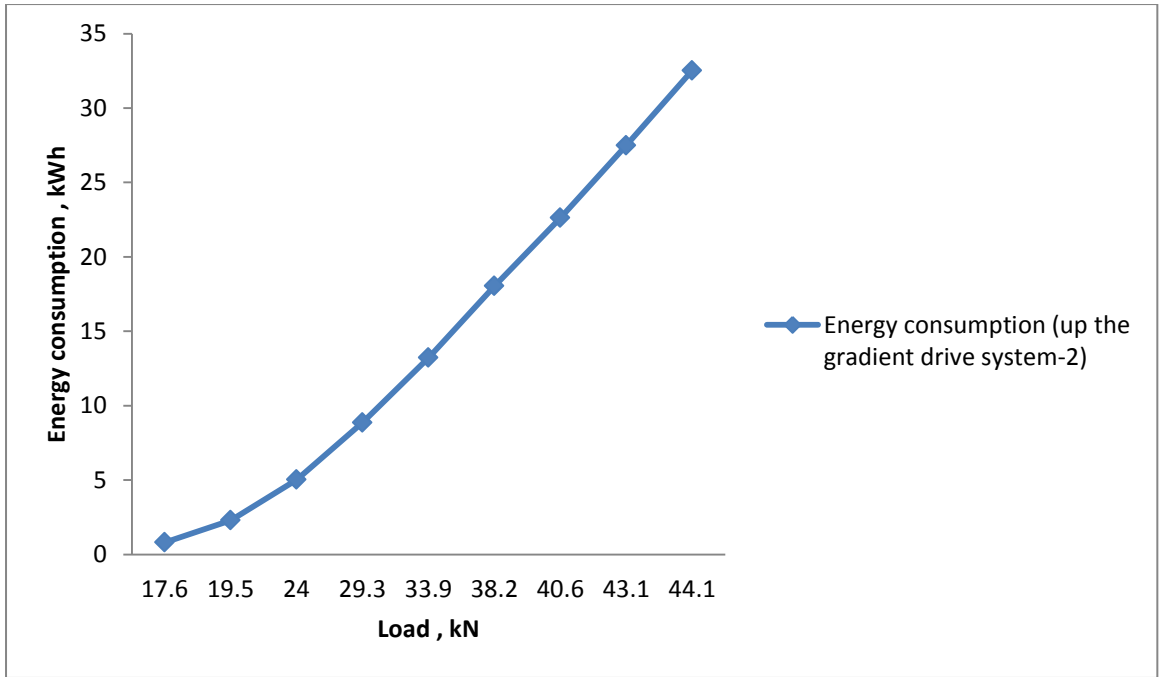
Figure 7.4(d) Influence of load on energy consumption for 150hp haulage drive
system -2 for up the gradient
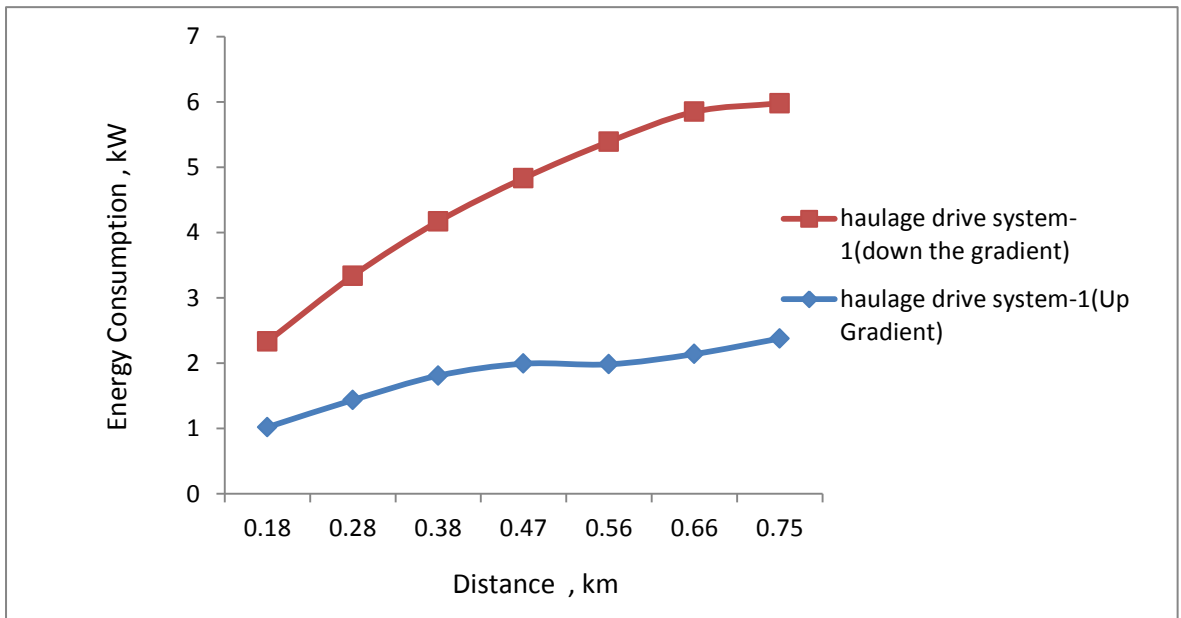
Figure 7.5 Influence of distance (km) on energy consumption of 150hp haulage drive
system-1 (Up the gradient and down the gradient)
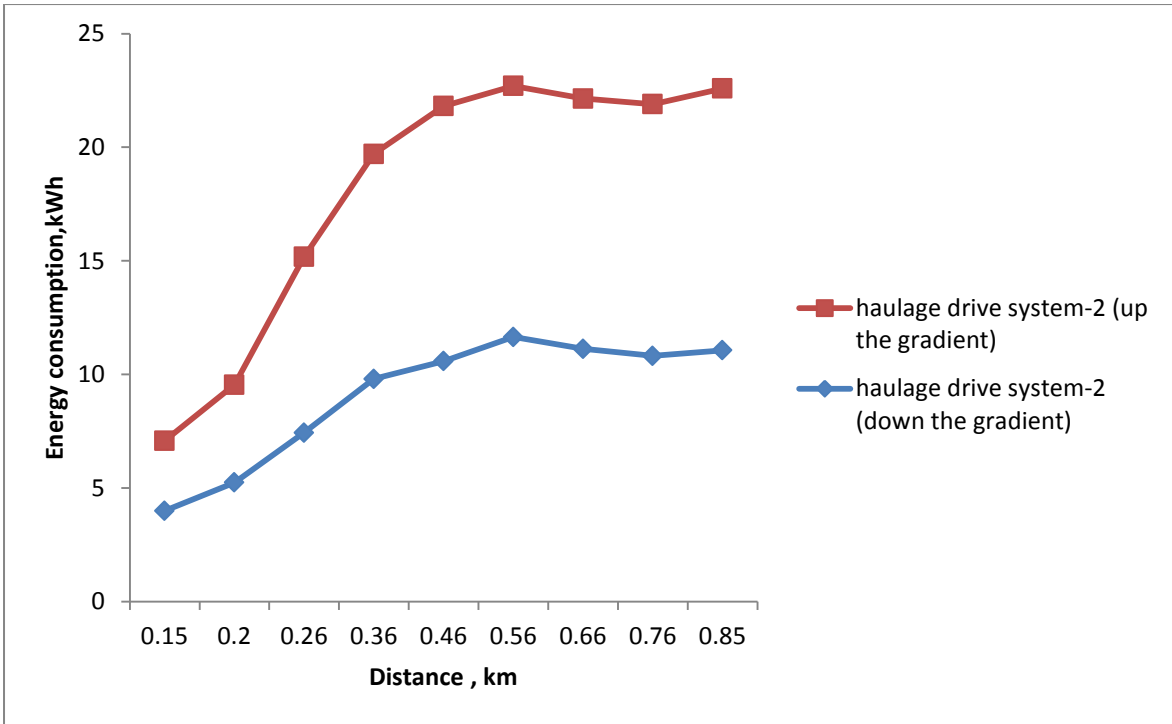
Figure 7.6 Influence of distance (km) on energy consumption of 150hp haulage drive
system-2 (Up the gradient and down the gradient)

.
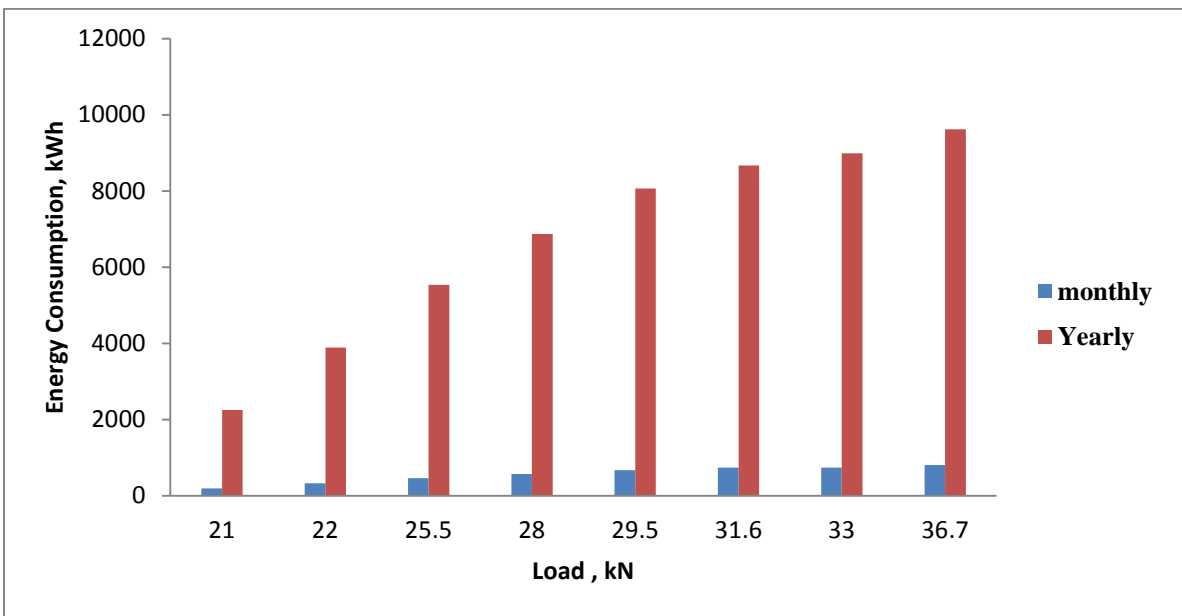
Figure 7.7(a) Variation of energy consumption with load for down the gradient (8th
level to 42nd level) of haulage drive system-2
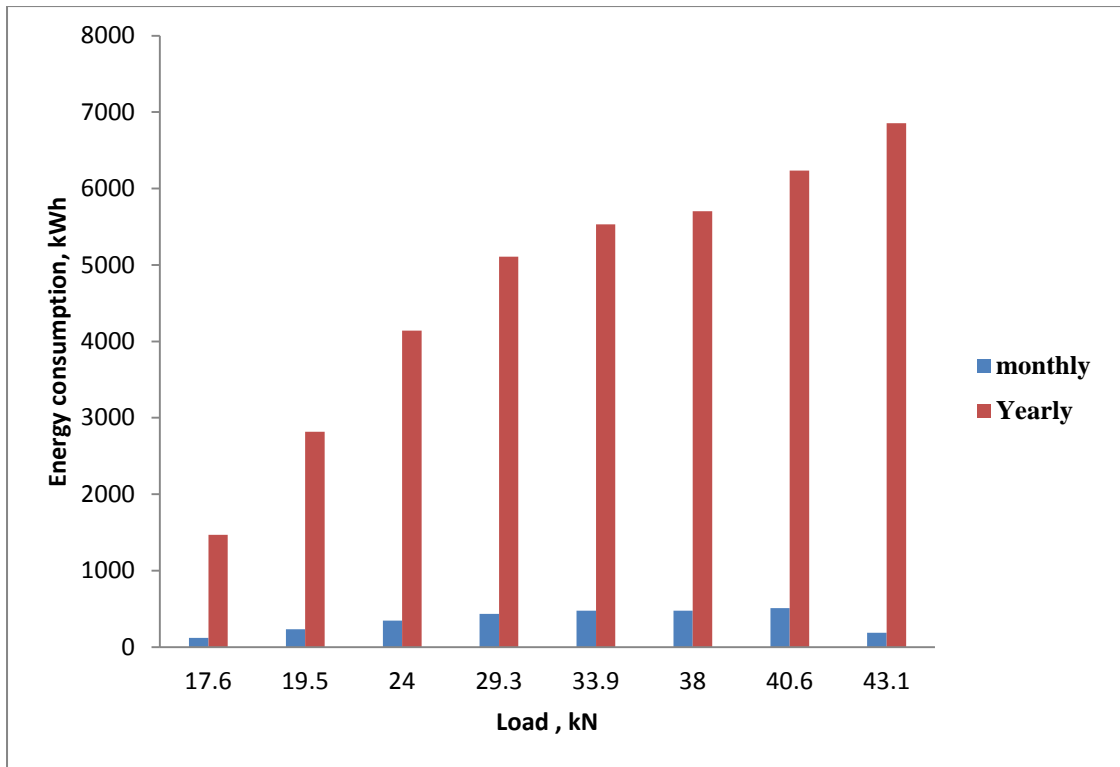
Figure 7.7(b) Variation of energy consumption with load for up the gradient (42nd to 8th level) of haulage drive system-2

7.2 COMPARATIVE STUDIES OF HAULAGE DRIVE SYSTEM
7.2.1 Introduction

In this section the comparative results for simulation study and conventional method are compared with field study results of 150hp underground haulage drive system-1 and haulage drive system-2.The comparative study are made on slip power recovered for 3hp conventional experimental and microcontroller haulage drive systems and also simulation study with experimental and field study of both haulage drive system.

The main objective of this comparative study is to calculate the difference of power output of both haulage drive system and percentage slip power recovery obtained from the conventional and micro controller based (field study and simulation on both methods) experimental method. The 3hp laboratory experimental (both conventional and micro controller) set-up for energy conservation studies on both the drive systems are explained in Chapter 4. Energy calculation and cost analysis are made based on the results obtained from field study on 150hp haulage drive system

and 3hp laboratory experimental study on conventional and micro controller based methods.

7.2.2 Comparative simulation study of 150hp underground haulage drive system

Comparisons were made on important electrical, mechanical parameter such as efficiency, speed, power output and torque for simulation results, field study and experimental study results were discussed. These parameters were mainly influence on the energy consumption of haulage drive system .Field study and simulation study results on energy consumption for both 150hp underground haulage drive system -1 and drive system-2 results obtained are compared with main parameter Such as efficiency, speed and torque.

Field study data collected from the 150hp underground haulage drive system-1 and haulage drive system-2 has been compared with simulated conventional method results with field study results of 150hp underground haulage drive system -1 and 150hp haulage system-2.Comparative results of simulation and field study results (conventional method) of 150hp underground haulage drive system -1 on energy consumption from surface to 8L for down the gradient (i.e. surface to 8th Level) and from 8L to surface up the gradient are presented in Table 7.1 and Table 7.2 respectively.

Similarly the comparative results of Simulation and field study results on energy consumption for conventional method 150hp underground haulage drive system-2 for down the gradient (i.e.8L to 42L) and up the gradient (42L to 8L) are presented in Table 7.3 and Table 7.4 respectively. The simulation field study results along with field study datas are simulated by using MATLAB/ SIMULINK software package. The simulation results for field study (conventional and micro controller method) on energy consumption results was varied from8.5% to 9 %.

Table 7.1 Simulation and field study results (conventional method) of150hp underground haulage Drive

system -1 on energy consumption for down the gradient(i.e. surface to 8L)

		Simulation results (conventional method)					Field study results(conventional method)				
Sl.No	Load (kN)	N_1 (rpm) (Actual speed)	Torque (Nm)	Output Power (kW)	Efficiency (%)	Energy consumption (kWh)	N_1 (rpm) (Actual speed)	Torque (Nm)	Output power (kW)	Efficiency (%)	Energy consumption (kWh)
1	39.2	410	6668	97.500	67.71	0.507	400	6668	97.7853	67.90	0.509
2	36.2	415	6521	96.738	69.56	1.008	410	6521	98.0404	70.49	1.021
3	34.8	425	6081	92.337	67.09	1.437	415	6081	92.4366	69.10	1.437
4	32.6	432	5641	87.034	66.63	1.813	420	5641	86.8955	66.74	1.810
5	30.4	437	4908	76.697	66.36	1.898	425	4908	76.3602	66.06	1.993
6	28.2	449	4028	64.636	56.31	2.020	430	4028	63.4962	55.30	1.984
7	23.0	430	3734	60.474	53.34	2.200	430	3734	59.8616	51.91	2.141
8	20.2	456	3539	57.487	51.7	2.403	440	3539	57.0961	51.16	2.379

Table 7.2 Simulation and field study results of energy consumption for conventional method 150hp underground haulage drive system-1 for up the gradient (i.e. from 8L to surface)

		Simulation results (conventional method)					Field study results(conventional method)				
Sl.No	Load (kN)	N_1 (rpm) (Actual speed)	Torque (Nm)	Output power (kW)	Efficiency (%)	Energy consumption (kWh)	N_1 (rpm) (Actual speed)	Torque (Nm)	Output power (kW)	Efficiency (%)	Energy consumption (kWh)
1	36.7	400	7943	113.541	70.80	0.729	400	7943	116.483	70.03	0.728
2	33.0	409	7153	104.466	69.70	1.315	400	7153	104.9398	69.67	1.311
3	31.6	414	6837	102.573	67.91	1.899	405	6837	101.5275	68.23	1.903
4	29.4	423	6363	96.347	65.3	2.368	405	6363	94.4887	65.78	2.362
5	27.9	425	6047	91.926	66.04	2.852	410	6047	90.9146	66.05	2.841
6	25.7	425	6047	91.926	69.8	3.408	410	6067	90.91406	69.91	3.409
7	22.0	427	5573	85.112	67.45	3.732	415	5573	84.81785	67.54	3.710
8	21.0	441	4572	72.098	59.1	3.605	430	4572	72.07167	59.07	3.603

Table 7.3 Simulation and field study results of energy consumption for conventional method 150hp

underground haulage drive system-2 for down the gradient (i.e.8L to 42L)

Sl.No	Simulation results (conventional method)						Field study results(conventional method)				
	Load (kN)	N₁ (rpm) (Actual speed)	Torque (Nm)	Output power (kW)	Efficiency (%)	Energy consumption (kWh)	N₁ (rpm) (Actual speed)	Torque (Nm)	Output power (kW)	Efficiency (%)	Energy consumption (kWh)
1	39.2	418	7841	118.532	78.5	2.726	415	7841	119.174	78.81	2.780
2	36.2	414	7254	109.333	74.5	5.239	420	7254	111.742	74.61	5.245
3	34.8	413	6961	102.578	74.4	7.409	415	6961	105.799	74.60	7.435
4	32.5	412	6521	97.497	71.10	9.204	410	6521	98.040.	71.22	9.205
5	30.4	406	6081	91.460	67.32	10.53	405	6081	90.301	67.42	10.585
6	28.1	411	5641	83.826	63.33	11.62	400	5641	82.724	63.74	11.650
7	23.0	412	4614	71.813	55.3	11.27	400	4614	67.663	55.09	11.126
8	19.8	409	3979	64.003	50.0	10.01	400	3941	57.794	50.00	10.82
9	18.6	413	3734	59.052	48.2	11.10	405	3734	55.448	48.13	11.06

Table 7.4 Simulation and field study results of energy consumption for conventional method

150hp underground haulage drive system-2 for up the gradient (i.e. 42L to 8L)

		Simulation results (conventional method)					Field study results(conventional method)				
Sl.No	Load (kN)	N_1 (rpm) (Actual speed)	Torque (Nm)	Output power (kW)	Efficiency (%)	Energy consumption (kWh)	N_1 (rpm) (Actual speed)	Torque (Nm)	Output power (kW)	Efficiency (%)	Energy consumption (kWh)
1	17.64	457	3834	62.619	45.3	0.825	440	3834	61.816	45.42	0.824
2	19.50	452	4235	68.537	47	2.299	435	4235	67.411	47.08	2.303
3	24.01	437	5204	81.333	54.86	5.042	430	5204	81.767	54.95	5.042
4	29.30	421	6342	99.287	67	8.869	428	6342	99.517	66.88	8.873
5	33.90	414	7332	108.36	67.5	13.20	420	7332	112.944	68.18	13.23
6	38.22	403	8259	118.92	73.3	18.11	415	8259	125.697	73.25	18.05
7	40.67	395	8786	124.01	76.93	22.25	410	8786	132.093	76.97	22.63
8	43.12	387	9313	128.72	78.54	27.60	405	9313	138.295	78.80	27.50
9	44.10	379	9523	128.80	79.54	32.55	400	9523	139.653	79.57	32.53

The 150hp underground haulage drive system for different combinations loads and gradient for both up the gradient and down the gradient are given in tabulation. Using the tabulation results, the graphical representations are given for different electrical parameters variation with different combinations of loads is presented. It is observed that the simulation results values are similar with experimental results and it observed that very small percentage error in few cases i.e. from Table 7.1 3hp laboratory haulage drive simulation value is 0.2 variations of experimental values.
The simulation and experimental comparisons of variation on energy consumption with load are as shown in Figure 7.8(a).

The results plotted is related to simulation and experimental is showing similar variation in few values i.e. energy consumption, efficiency and power output vary with load for 150hp underground haulage drive system −1 and haulage drive system-2 for conventional haulage drive for down the gradient and up the gradient are given in this thesis. Similarly other parameters like percentage efficiency, torque, ect care also presented in Figure 7.8(b) and Figure 7.8(c), respectively. Similarly the comparative study results of 150hp underground haulage drive system -1 up the gradient influence of load on % efficiency are shown in Figure 7.8(d).The comparative study results of influence of load on energy consumption forof150hp underground haulage drive system -2 down the gradient are given Figure 7.9 (a).

Figure 7.8(a) Comparative study results of 150hp underground haulage drive
    system −1 on energy consumption for down the gradient(i.e. surface
    to 8L)influence of load on energy consumption
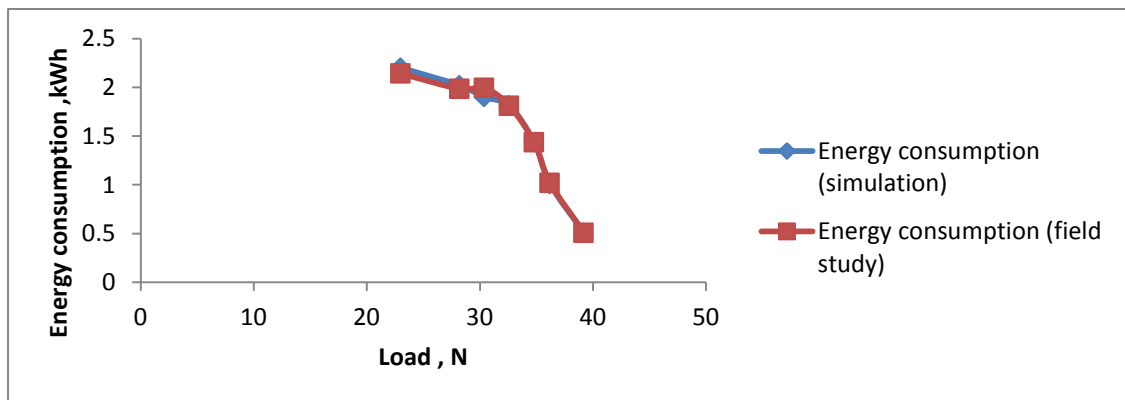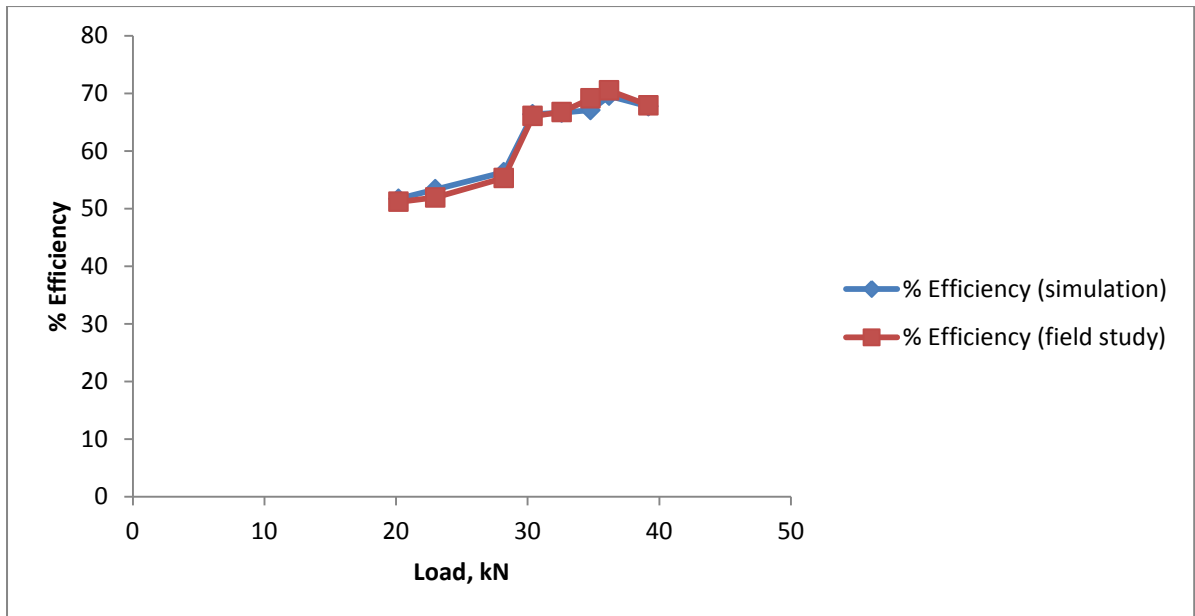
Figure 7.8(b) Comparative study results of haulage drive system -1 on energy
consumption for down the gradient(i.e. surface to 8L) influence of
load on % efficiency.
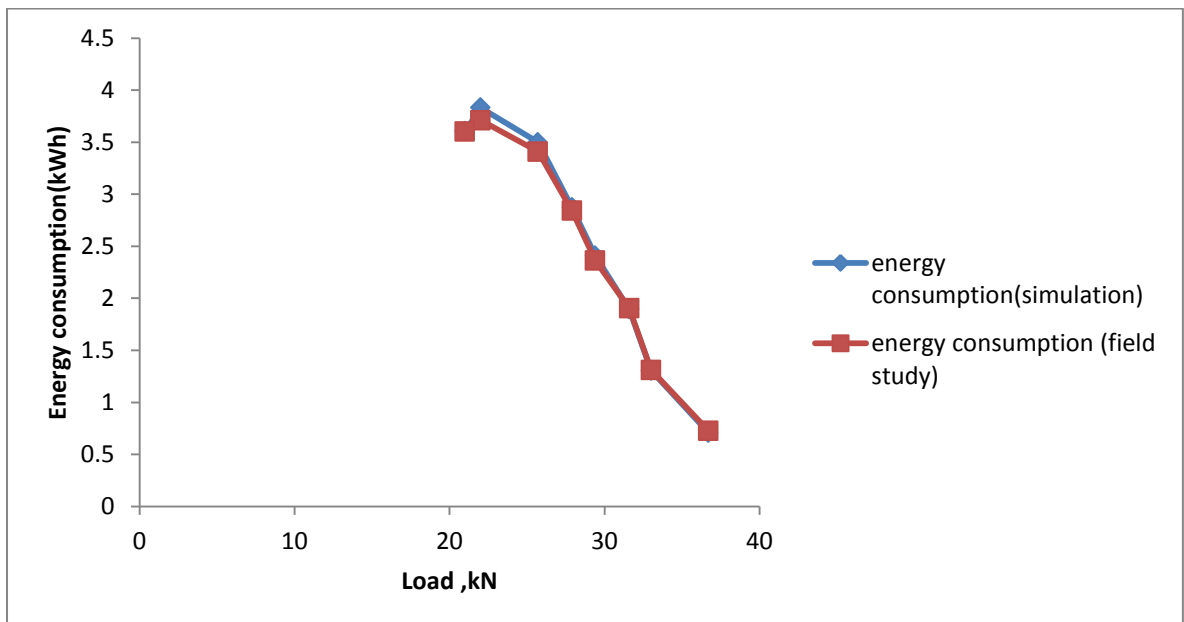
Figure 7.8(c) Comparative study results of 150hp underground haulage drive
system -1 up the gradient influence of load on energy consumption.
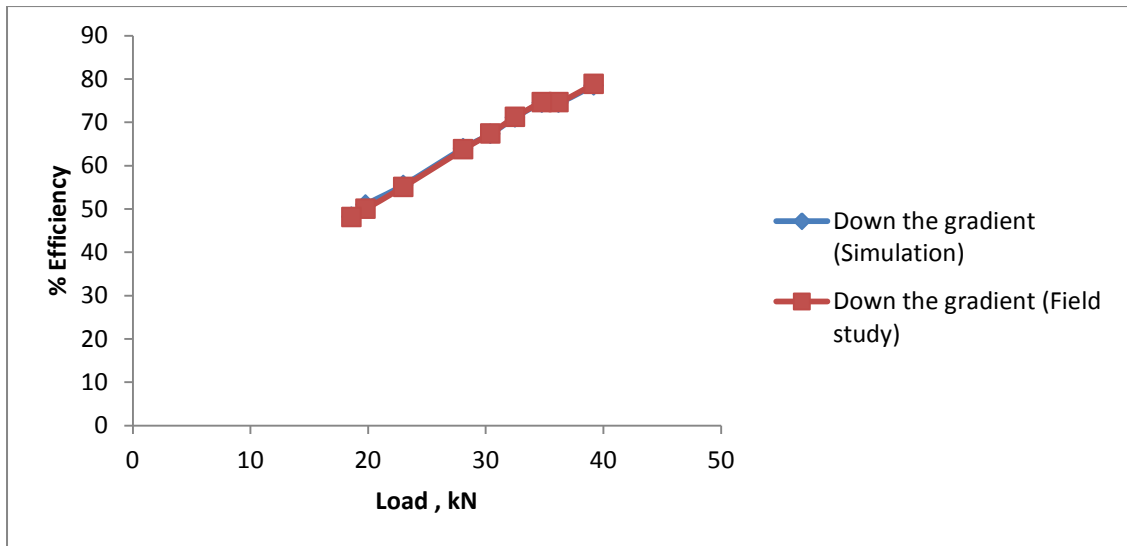
Figure 7.8(d) Comparative study results of 150hp underground haulage drive system -1
up the gradient influence of load on % efficiency.

Figure 7.9 (a) Comparative study results of influence of load on energy consumption
for 150hp underground haulage drive system -2 down the gradient

The comparative results of150hp underground haulage drive system -2 down the
gradient for influence of load on efficiency are shown in Figure 7.9 (b). Efficiency of
drive haulage system is very close to the simulation and field study values it observed
from the Table 7.3.Similarly comparative study results on influence of energy
consumption on load of 150hp underground haulage drive system-2 for up the gradient
(i.e. 42L to 8L)are shown in Figure7.10(a) and Figure7.10(b) .
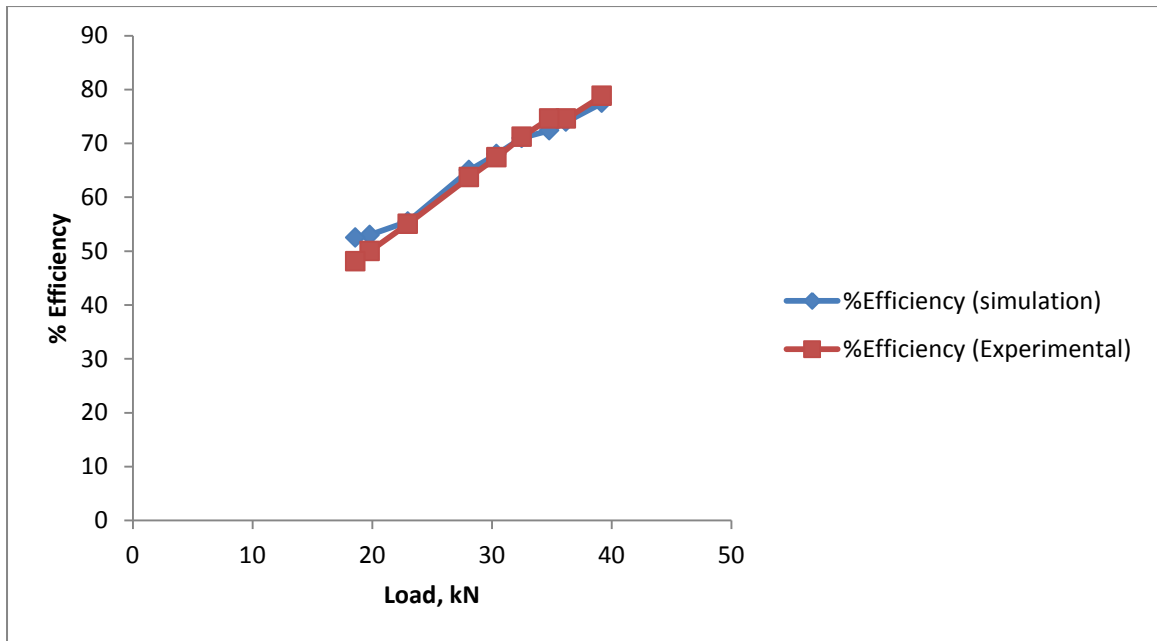
Figure 7.9 (b) Comparative study results of influence load on efficiency
150hp underground haulage drive system -2 down the gradient.
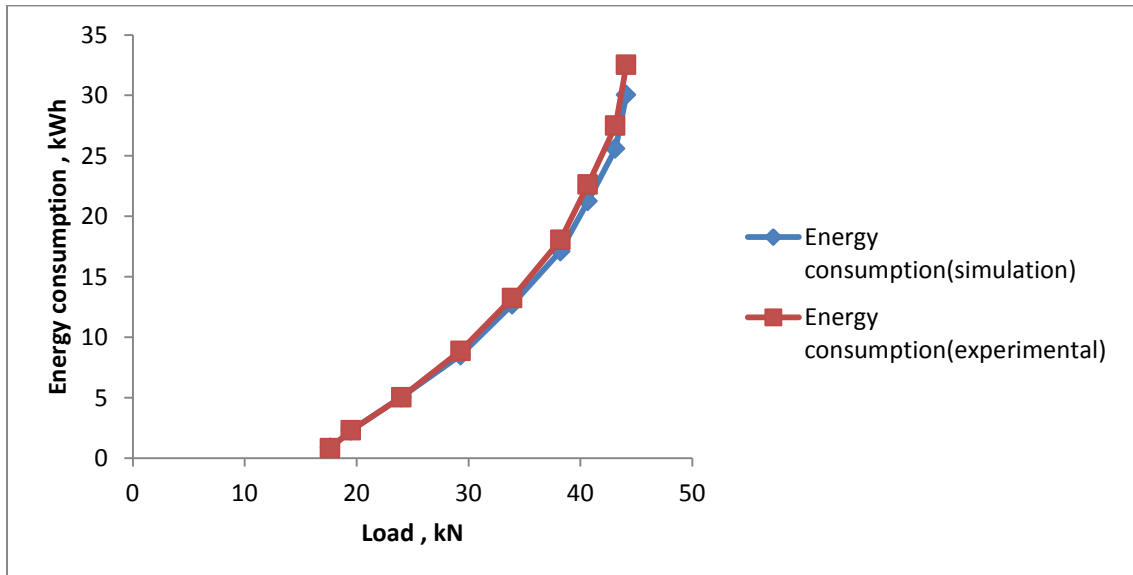
Figure 7.10(a) Comparative study results on influence of load on energy consumption
150hp underground haulage drive system-2 for up the gradient
(i.e.42L to 8L).
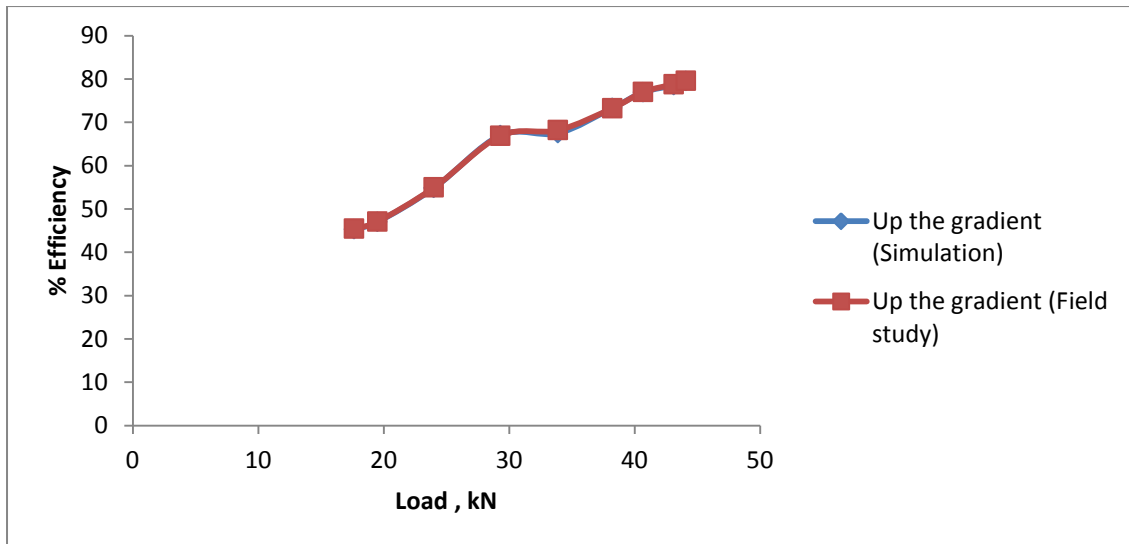
Figure 7.10(b) Comparative study results of 150hp haulage drive system-2 for up the gradient.
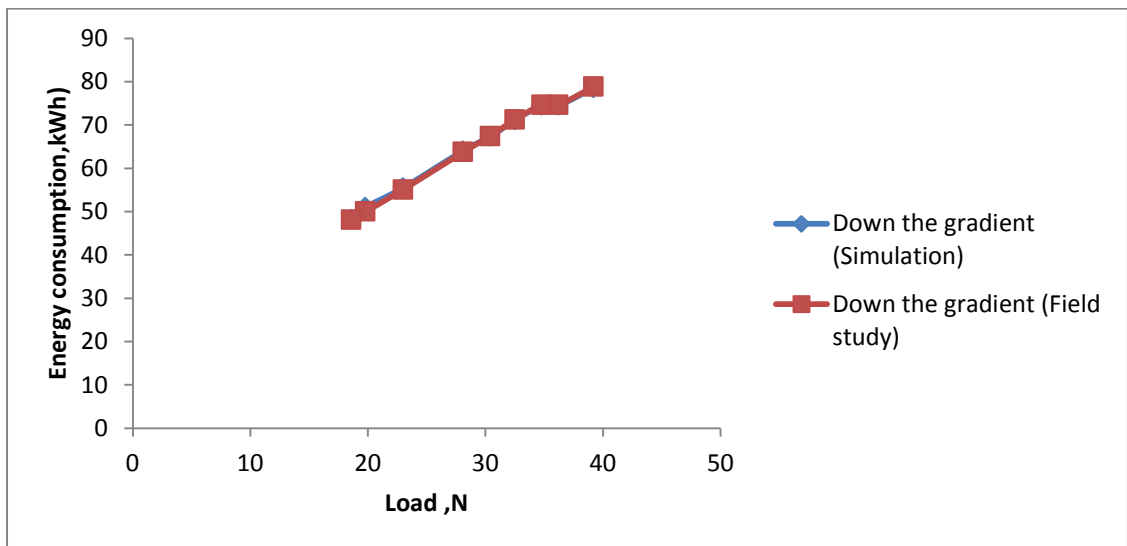
7.2.3 Cost analysis of 150hp underground haulage drive system.

The cost analysis is done based on the results obtained in the field study results from underground coal mine for haulage drive system-1 and haulage drive system -2 by considering present tariff. The total energy consumption of two drive system is 702801.64 kWh. The annual energy consumption charge for two drive system is. Rs.49,19,611/-The total energy consumption chart of both drive system are shown in Chart 7.11(a) which includes the daily, monthly and annually energy consumption of direct rope haulage system of underground coal mines.

The cost analysis of both drive haulage system has been shown in Figure 7.11(b). The total energy consumption per year and total cost of energy per year for drive system are 702801.64 kWh and Rs.49,19,611/-respectively. The procedure for calculations is as follows:

Maximum demand charges 150hpdrive system -1 110.25KVA@ Rs.150KVA

$$= Rs.16,537 /-$$

Maximum demand charges 150hp drive system -2 110.25 KVA@Rs.150KVA

$$= Rs.16, 537/-$$

Energy charges for two drive system Total kWh 702801.64 kWh @Rs.7.00kWh

$$= Rs.49, 19,611/-$$

.

Total Annual cost of energy consumption for two drive system is Rs.49,19,611/- .

	monthly	yearly	
■ Energy consumption kWh	58566	702801.64	

Figure 7.11(a) Total energy consumption chart

	monthly	yearly
■ Energy cost	409967.58	4919611

Figure 7.11(b) Cost analysis chart

7.3 3HP EXPERIMENTAL CONVENTIONAL METHOD

7.3.1 Conventional method:

Energy consumption for different combination loads and gradients is calculated. The energy consumption is calculated using the following assumptions. The numbers of trips per day are 12. The length of the track is 5m.

The influence of angle with horizontal on energy consumption for both up the gradient (forward direction)and down the gradient (reverse direction) are shown in Figure7.12(a) and Figure 7.12(b). It 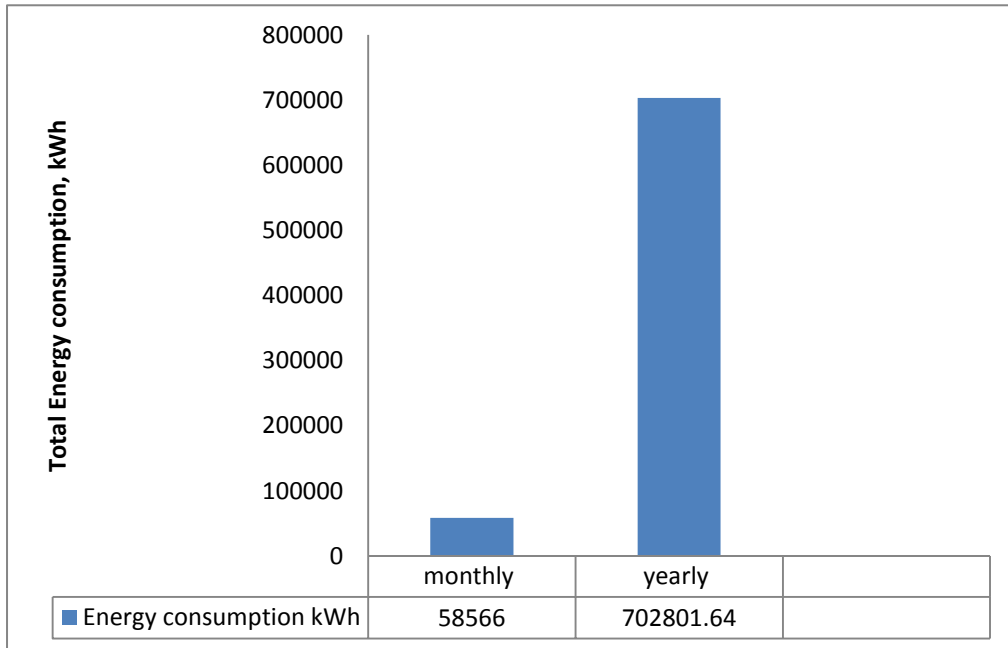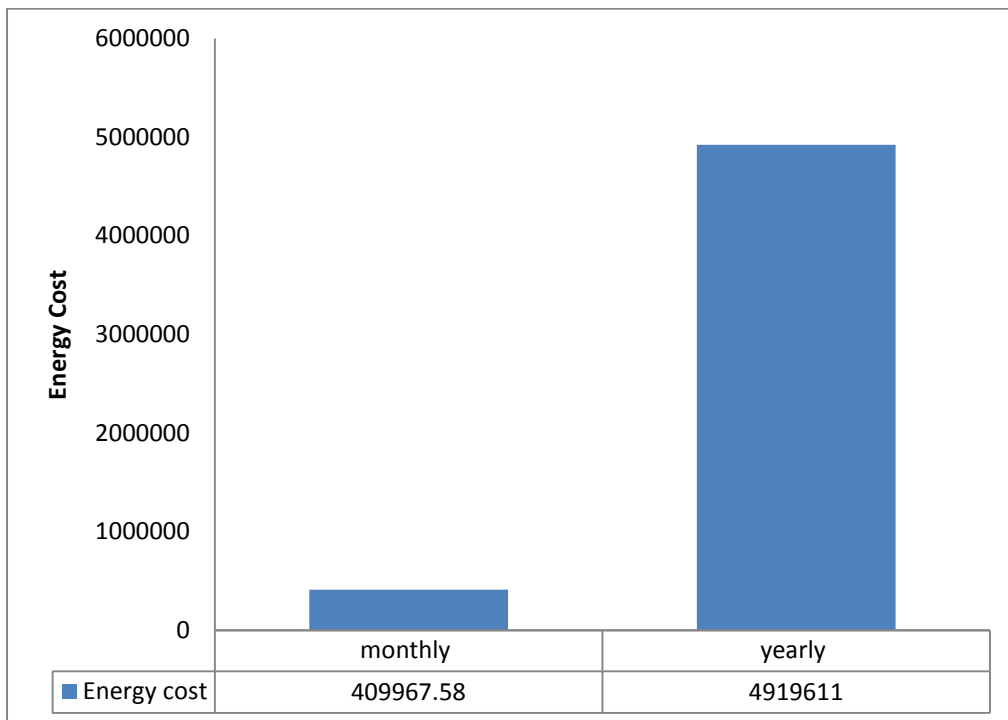is observed that Figure 7.12(a) shows down the gradients of drive system which requires less energy compared to up the gradient drive system, for all the combinations of loads and gradients.

According to tabulated experimental study results the energy consumption is varies 41.73% (from 0.00652 kWh to 0.01119 kWh) for up the gradient and 43.90% (from 0.005856 kWh to 0.01044 kWh) for down the gradient as the load is varies (from 1079 N to 1765.8 N). Similarly, energy consumption varies 11.39% (from 0.00754 kWh to 0.00851kWh) for up the gradient and 10.95% (from 0.00691 kWh to 0.00776 kWh) down the gradient, as the gradient varies from 27° to 35°.Influence of load on energy consumption at one gradient (27°with horizontal), when load is varies and gradient also presented.

Variation of energy consumption response for different combination loads and gradients for both up the gradient and gradient are observed for haulage drive system, from the graphical response it is concluded that conventional drive system requires more energy being wasted during up the gradient drive than down the gradient drive.

Normalized electrical parameters show the variation in the energy consumption for forward and reverse direction of the drive system. For a given load (i.e. at 1079N), it is observed that energy consumption is varies non linearly (as the gradient varies from 27° to 35°) and shown in Figure 7.13.For a given gradient (i.e. at 27°with horizontal) it is observed that energy consumption is also varies nonlinearly (as load varies from 1079 N to1765 N) and shown in Figure 7.14.

The energy consumption curves are plotted for various cases like up the gradient and down the gradient with different combinations of loads and gradients. Similarly, in Figure 7.15 (a) shows the torque variation with output power at 27^{0} for

down the gradient and figure 7.15 (b) shows the efficiency variation with output power at 27^0 for down the gradient. Figure 7.16 represents the energy consumption chart for different angle with horizontal for up the gradient and down the gradient. Chart for energy consumption variation with load and angle with horizontal are presented in Figure 7.17. Above experimental studies indicates how conventional control system effects on energy consumption for haulage drive system.
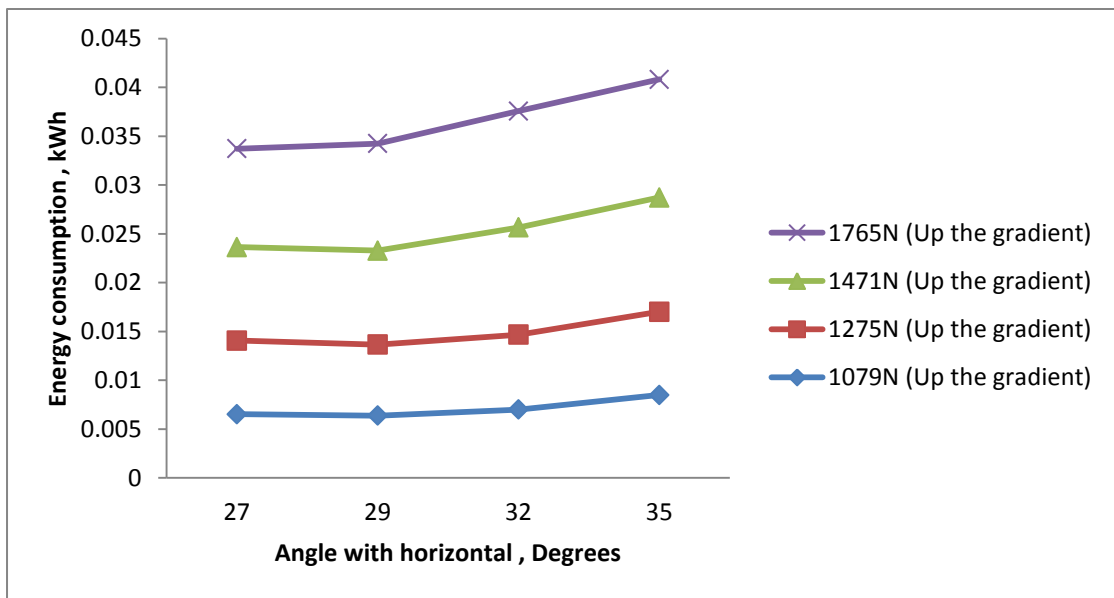
Figure 7.12(a) Influence of gradient (angle with horizontal) on energy consumption for up

the gradient for 3hp drive with conventional method

From these observations, it is concluded that conventional drive requires more energy and was varied 11.39% (from 0.00754 kWh to 0.00851kWh) during up the gradient than down the gradient.

The 3hp laboratory experimental studies the following observation are drawn. The energy consumption for different combination of loads and gradients is calculated. In conventional method the power output varies 97.17% (from 1614.8 W (maximum load (1765N) gradient (35°) to 57096.1 W (minimum load (1079N)) and gradient (27°) for down the gradient of haulage drive system. Similarly the power output varies 41.92% (from 937.1 W (minimum load (1079N) to 1613.5 W (maximum load (1765N) gradient (35°) and gradient (27°) for up the gradient haulage drive system.
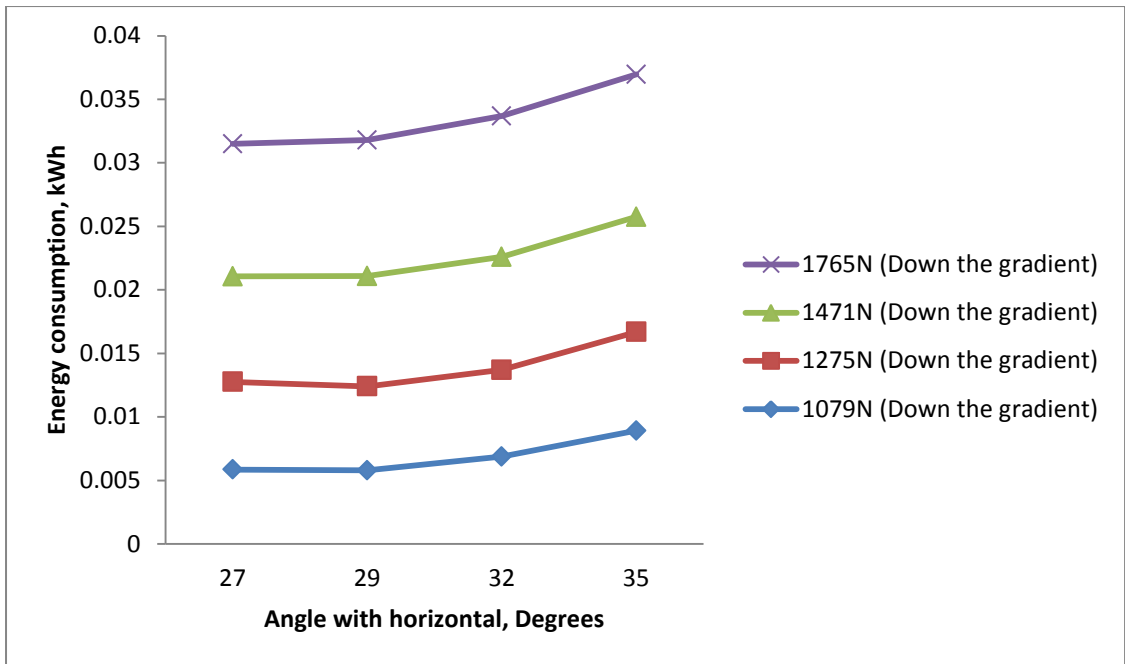
Figure7.12 (b) Influence of gradient (angle with horizontal) on energy consumption for

down the gradient for 3hp drive with conventional method
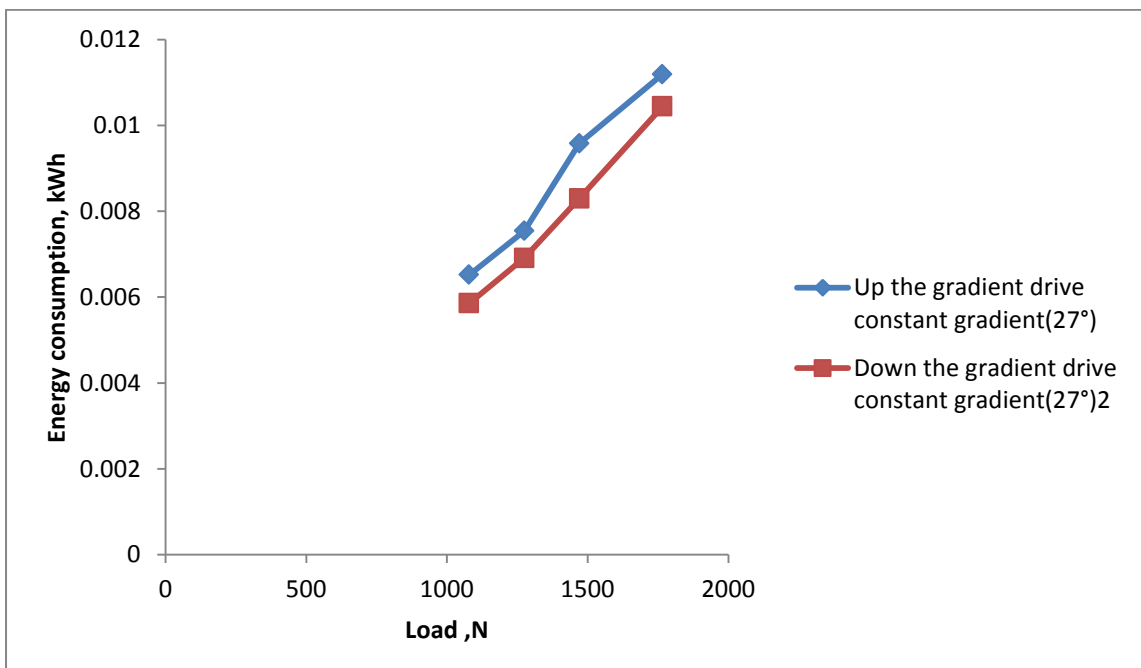
Figure 7.13 Influence of gradient on energy consumption for conventional method
using 3hp haulage drive system for up the gradient
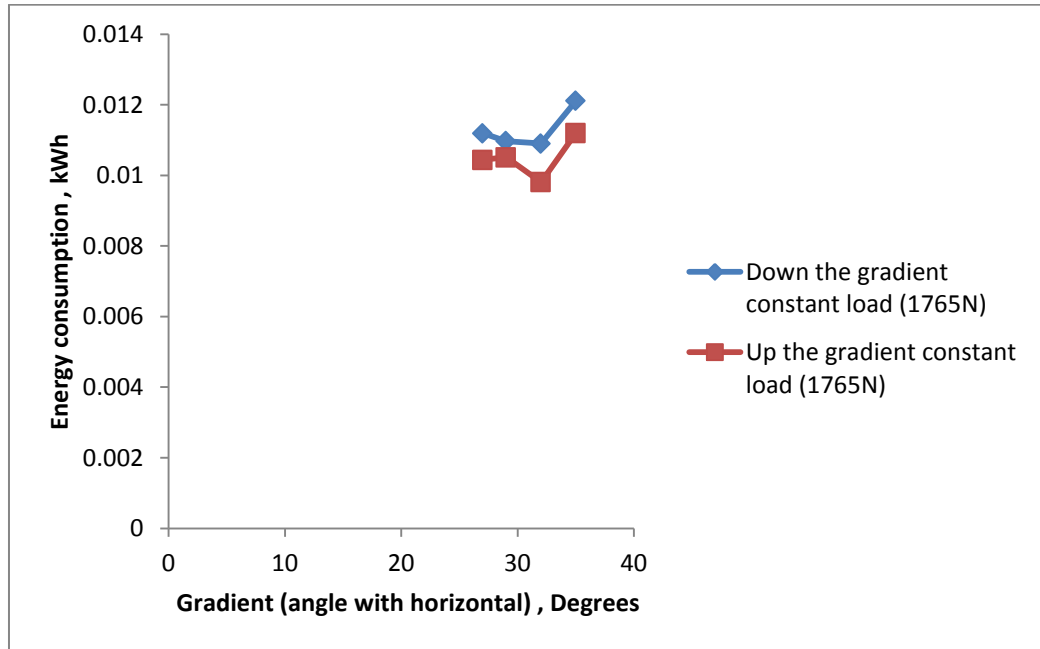
Figure 7.14 Influence of gradients on energy consumption for constant load (1765N)
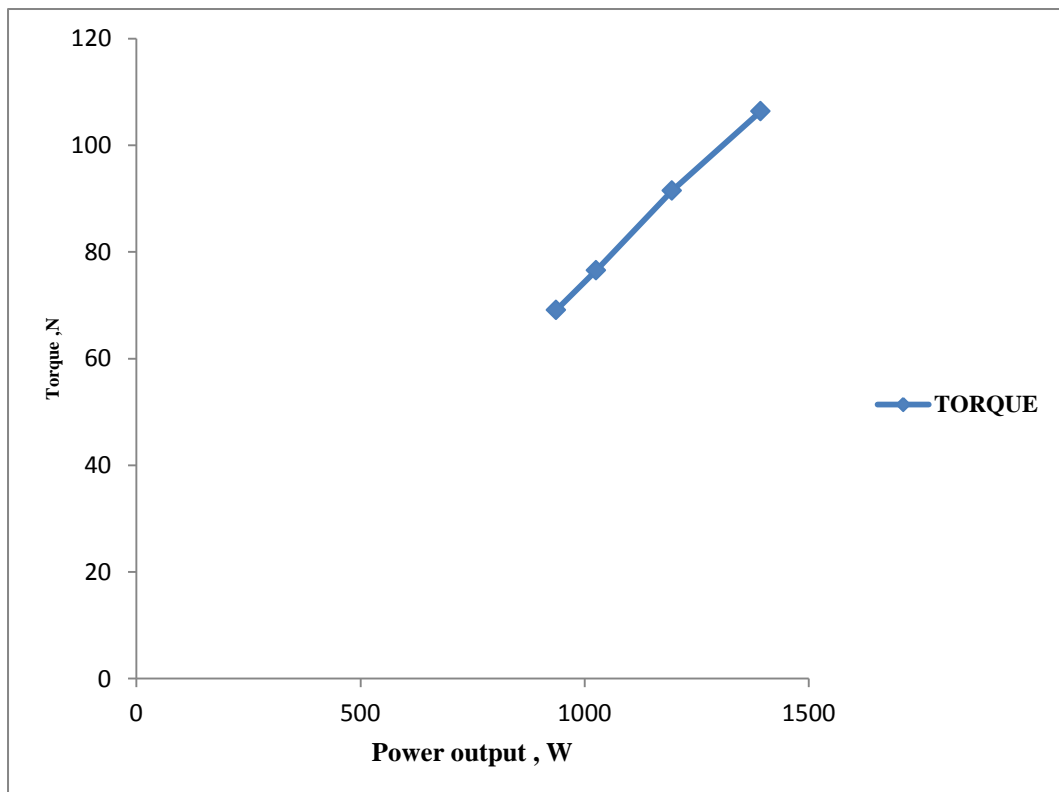
Figure 7.15(a) Influence of power output on torque and efficiency at 27^0 for down the gradient
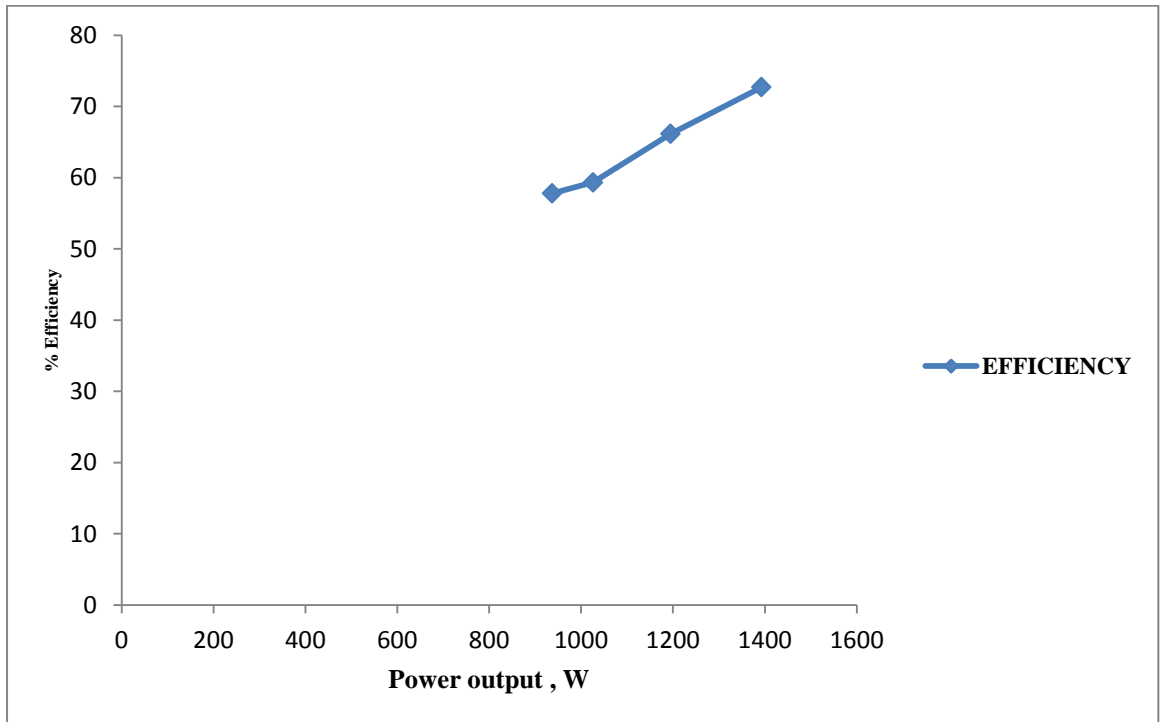
Figure 7.15(b) Influence of power output on efficiency at 27^0 for down the gradient

	Yearly
■ Up the gradient	506.46
■ Down the gradient	460.69
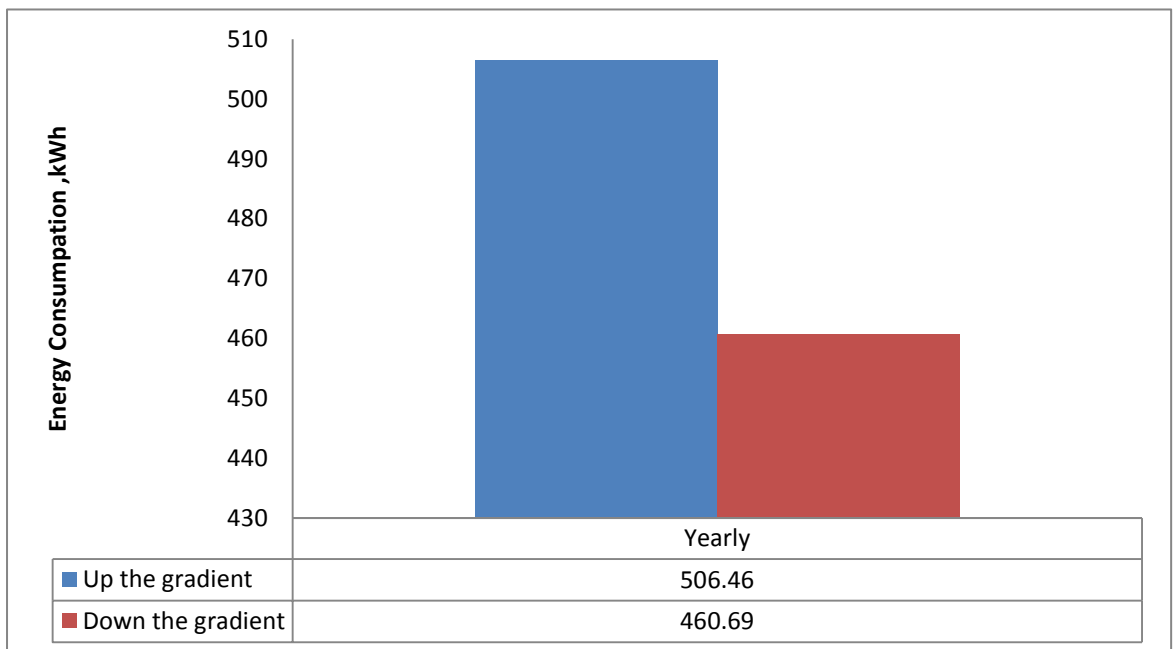
Figure 7.16 Annually energy consumption chart for conventional 3hp experimental
haulage drive system for up the gradient and down the gradient
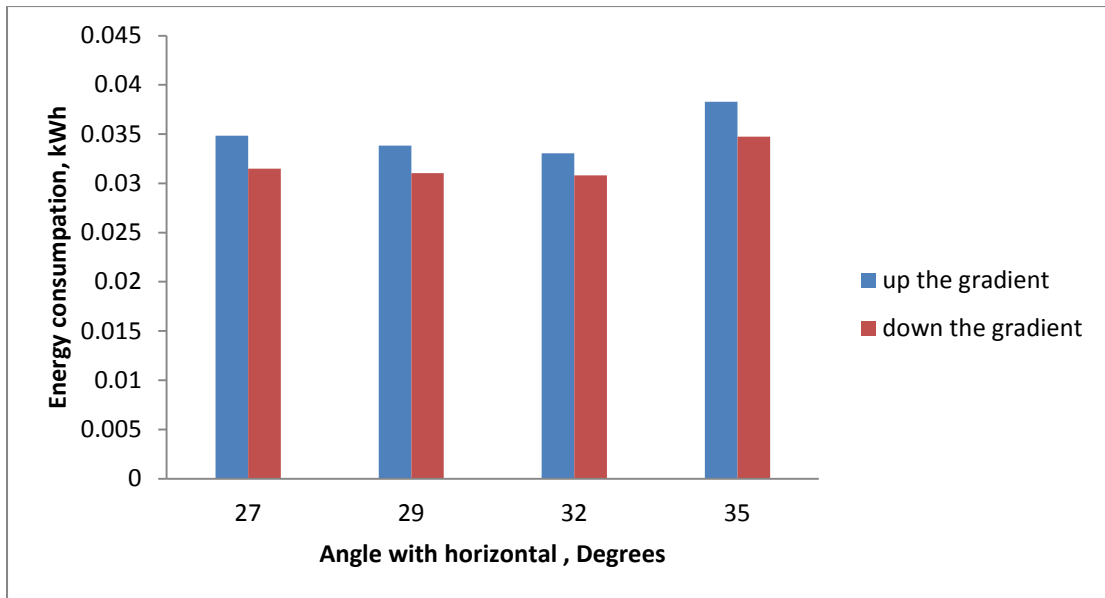
Figure 7.17 Energy consumption chart for different angle with horizontal for up and
down the gradient(3hp conventional experimental haulage drive system)

7.3.2 Comparative simulation study of 3hp laboratory experimental conventional haulage drive

Comparisons made on important electrical, mechanical parameter such as efficiency, speed, power output and torque for simulation results, field study and experimental study results are discussed which influence on the energy consumption of haulage drive system.   The experimental studies and simulation studies results on energy consumption are obtained and compared with main parameter such as efficiency, speed and torque.

Similarly the comparison are made on simulation and experimental study results for 3hp laboratory experimental (conventional and micro controller method) haulage drive system on energy consumption. The comparative results for simulation study and experimental study on energy consumption of 3hp conventional experimental results for both down the gradient and up the gradient are given in Table 7.5 and Table 7.6.

Table 7.5 Simulation and experimental results of energy consumption for 3hp conventional experimental haulage drive system for down the gradient

	Simulation results							
Angles with horizontal	Load (N)	N_1 (rpm) (Actual speed)	Torque (Nm)	Output power (W)	Efficiency (%)	Energy consumption (kWh)	N_1(rpm) (Actual speed)	Torque (Nm)
27^0	1079	549	69.13	949	58.53	0.00593	528	69.13
	1275	543	76.58	1040	60.14	0.00690	522	76.58
	1471	533	91.49	1220	67.53	0.00827	514	90.56
	1765	521	106.4	1387	72.4	0.01042	510	106.4
29^0	1079	546	73.34	1012	57.8	0.00564	540	73.34
	1275	539	82.04	1105	60.15	0.00661	530	81.35
	1471	528	98.00	1294	65.7	0.008276	515	98.00
	1765	518	114	1475	71.92	0.01054	502	113.9
32^0	1079	542	78.42	1062	57.8	0.005685	540	77.6
	1275	537	86.87	1166	60.86	0.006831	530	86.05
	1471	526	103.8	1364	68.34	0.008482	510	103.8
	1765	512	119.6	1545.5	75.35	0.009804	500	119.6
35^0	1079	541	82.19	1111.0	57.9	0.006730	565	81.7
	1275	535	91.04	1218	61.05	0.007763	540	90.5
	1471	522	108.7	1418	67.35	0.009056	510	108.1
	1765	510	126.4	1612	73.81	0.01119	500	125.7

Table 7.6 Simulation and experimental results on energy consumption for 3hp
experimental conventional haulage drive system for up the gradient.

	Simulation results				Experi			
Angles with horizontal	Load (N)	N_1 (rpm) (Actual speed)	Torque (Nm)	Output power (W)	Efficiency (%)	Energy consumption (kWh)	N_1 (rpm) (Actual speed)	7
27^0	1079	548	70.65	967.8	56	0.00655	540	
	1275	542	78.22	1060	57.6	0.00755	532	
	1471	531	93.38	1240	64.8	0.00957	521	
	1765	520	108.5	1410	68.7	0.0119	510	
29^0	1079	546	75.4	1028.7	56.95	0.00630	550	
	1275	541	83.5	1129	60	0.00727	540	
	1471	529	99.69	1317.8	67.93	0.00925	518	
	1765	523	115.9	1514	71.17	0.01091	512	
32^0	1079	541	79.6	1076	56.9	0.00600	538	
	1275	537	88.14	1184	59.36	0.00714	540	
	1471	524	105.2	1380	66.3	0.00900	510	
	1765	516	122.3	1577	74	0.01091	500	
35^0	1079	541	83.18	1126	60.01	0.00749	550	
	1275	537	92.12	1231	64.2	0.00851	540	
	1471	521	110.4	1432	66	0.01013	510	
	1765	509	127.8	1627.4	74.4	0.01212	501	

The 3hp laboratory experimental conventional haulage drive system for different combinations of loads and gradients for both up the gradient and down the gradient with various parameters are given in Table 4.3 and Table 4.4. Using the tabulation results, graphical representations are given in different electrical parameters variation with different combination of loads (Figure 7.12(a), Figure 7.12(b), Figure 7.13 and Figure 7.14).

It is observed that the simulation results values are in good agreement with experimental results and it is also observed that very small percentage error in few cases i.e. from Table 7.5 3hp laboratory haulage drive simulation value is 0.2 variations of experimental values. This error may be due to observation while taking reading from the experimental or may be simulation run time error.

Simulation and experimental study results variation on energy consumption with load are shown in Figure 7.18(a) .Plot related to simulation and experimental is showing similar variation in few values i.e. energy consumption vary with load for 3hp laboratory conventional haulage drive for down the gradient. Energy consumption varies 1.24% (from0.005856 kWh to 0.00593 kWh) for simulation and experimental. Similarly other parameters like percentage efficiency, torque, etc are also presented in Figure 7.18(b) and Figure7.18(c) respectively.

Figure 7.18(a)

Figure 7.18(b)

Figure 7.18(C)

Figure 7.18 (a), (b) and(c) Comparative study results of 3hp laboratory
          experimental conventional method haulage for down the gradient

Simulation and experimental study results variation on energy consumption with load are shown in Figure 7.19(a). Plot related to simulation and experimental is showing similar variation in few values i.e. energy consumption vary with load for 3hp laboratory conventional haulage drive for down the gradient. Energy consumption is varies 1.24% (from 0.005856 kWh to 0.00593 kWh) for simulation and experimental. Similarly other parameters like percentage efficiency, torque, etc are also presented in Figure 7.19(b) and Figure7.19(c), respectively.
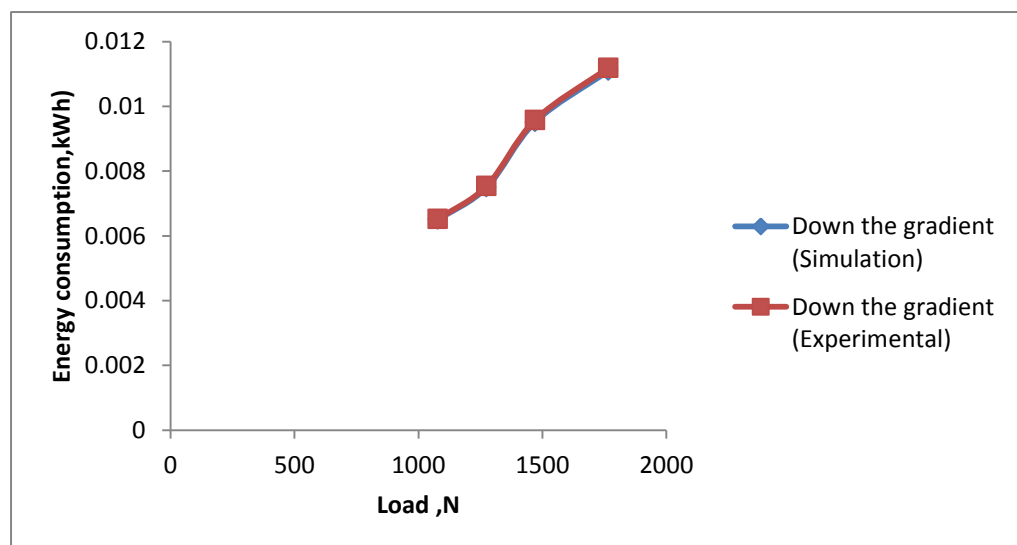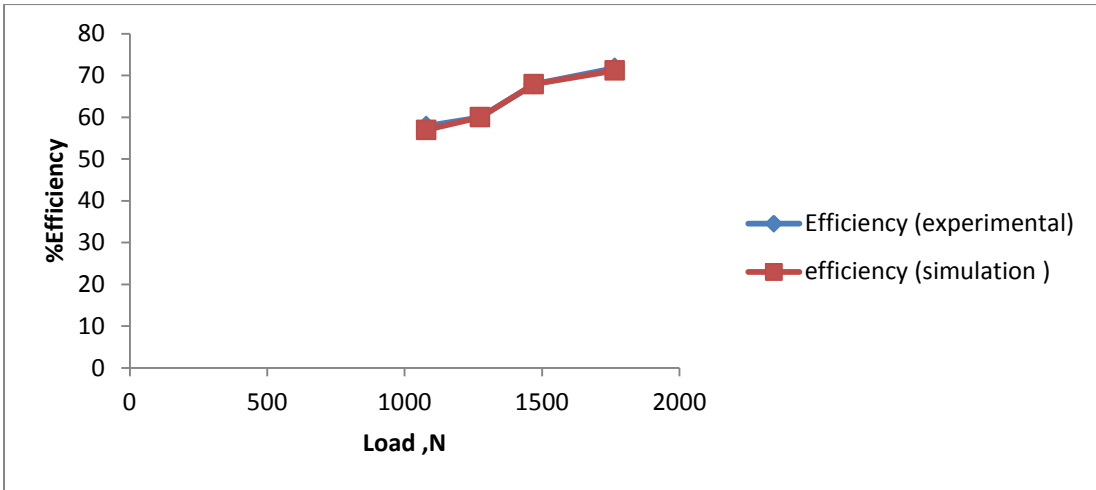
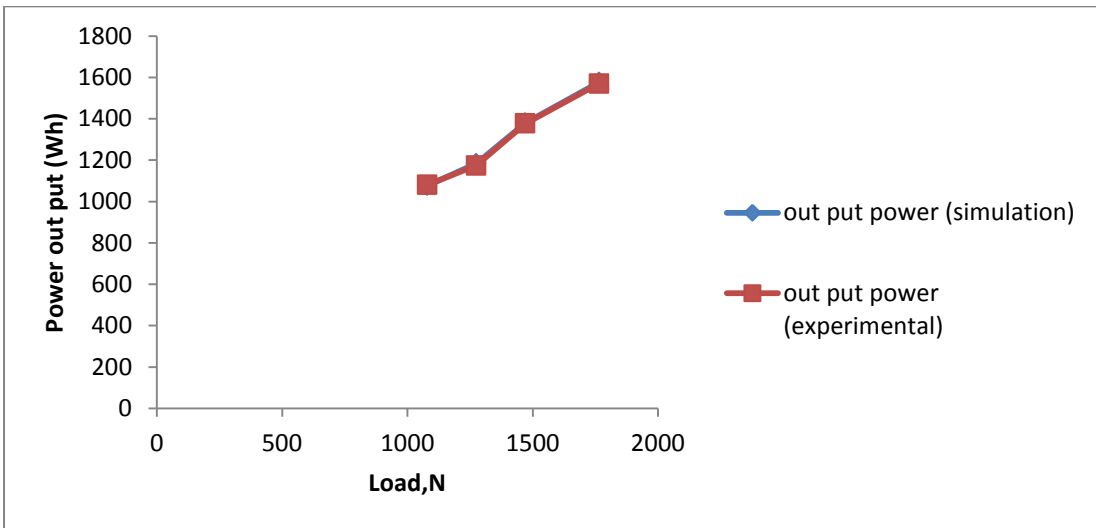170
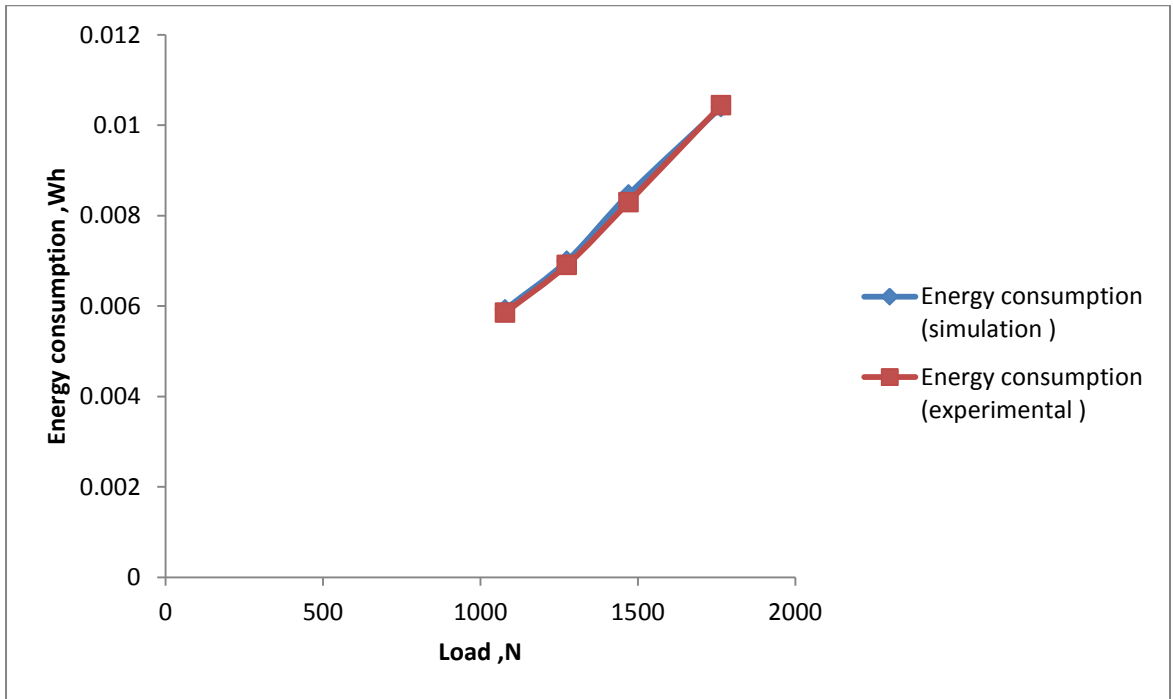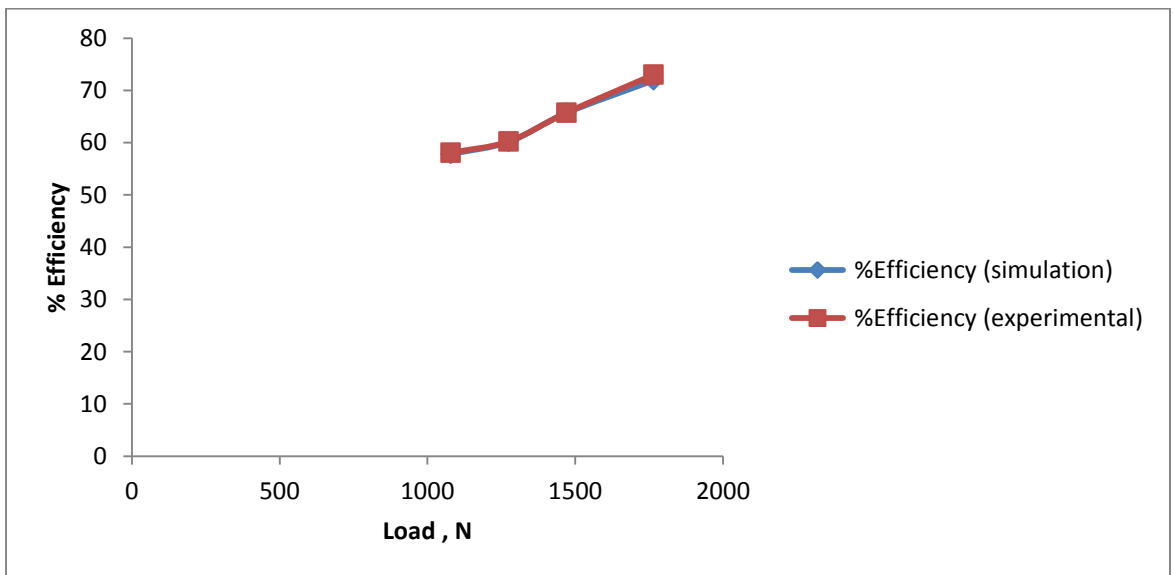
Figure 7.19(a)

Figure 7.19(b)
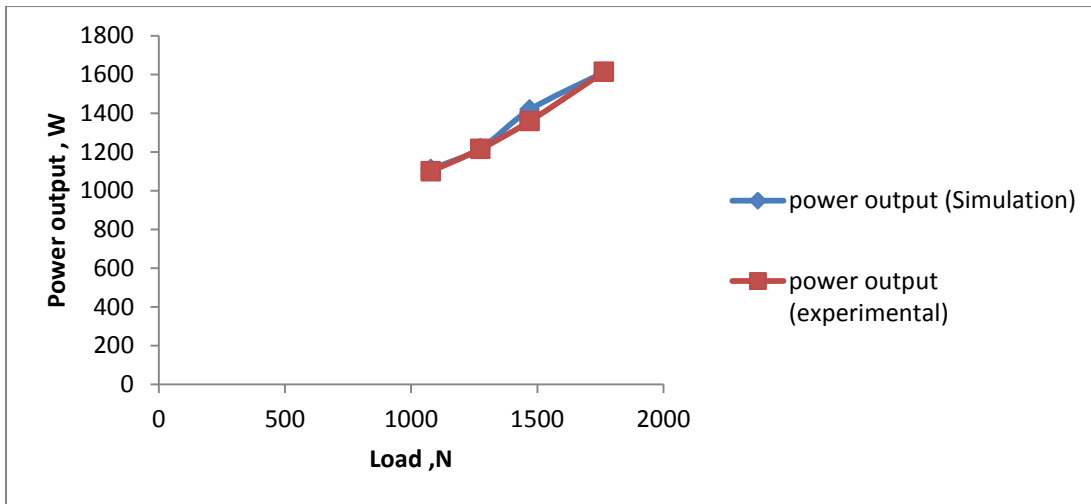
Figure 7.19(C)

Figure 7.19 (a), (b), (c) and (d) Comparative study results of 3hp laboratory

experimental conventional method haulage system for up the gradient

7.3.3 Cost analysis of 3hp laboratory experimental haulage drive system

Cost analysis is done based on the results obtained in the laboratory from3hp haulage drive system by considering present tariff. The total energy consumption of drive system is = 1158.23 kWh (604.8 kWh+553.43 kWh). The total energy consumption per year and total cost of energy per year for drive system are 1158.23 kWh and Rs.8437.61/- respectively. The procedures for calculation are as follows:

Maximum demand charges 3hp drive system 2.2KVA @ Rs.150KVA = Rs.330/-

Energy charges for 3hp drive system Total 1158.23kWh @Rs .7 kWh = Rs. 8107.61/-

Total annual cost of energy consumption for 3hp drive system is Rs. 8437.61/- .

7.4 3HP MICRO CONTROLLER METHOD

7.4.1 Micro controller method

Study of energy consumption using the micro controller method with different combinations loads and gradients for up the gradient and down the gradient the efficiency, output power, input power ,energy consumption per trip, yearly energy consumption and torque is calculated and given in tabular form and their influence on energy consumption are shown in figures. From the micro controller laboratory experimental study results the following observation are made on power output of haulage drive system.

In micro controller method the power output varies 42.42% (from to 1017.2 W (minimum load (1079N)) to 1766.87W (maximum load (1765N) and gradient (35°) and gradient (27°) of down the gradient of haulage drive system. Similarly the power output varies 44.21% from 1007 W (minimum load (1079N) and gradient (27°) 1805W to (maximum load (1765N) gradient (35°) for up the gradient haulage drive system (Table 4.5 toTable4.6).

Influence of angle with horizontal on energy consumption for up the gradient and down the gradients are given in Figure7.20 and Figure7.21, respectively. It is observed that energy consumption increases nonlinearly as load is increased for both up the gradient and down the gradient of drive system.

Experimental study on energy consumption using micro controller is varies 48.16% (from 0.00565 kWh to 0.0109 kWh) for up the gradient and from 0.00503kWh to 0.0926kWh for down the gradient as the load varies (from1079 N to 1765.8 N) (Table 4.5 toTable4.6).

Similarly the energy consumption varies from0.006864 kWh to 0.00805 kWh for up the gradient and from 0.00619 kWh to 0.00696 kWh down the gradient, as the gradient is varied (from27° to 35°).For a given load (i.e.at 1079N), it is observed that energy consumption varies non linearly (as the gradient varies from 27°to 35°) and shown in Figure7.22. For a given gradient (i.e.at 27°with horizontal) it is observed that energy consumption is also varies nonlinearly (as load varies from 1079 N to1765 N) and shown in Figure 7.23.The plotted graphs will clearly indicate consumption of energy will depend on the influence load acting on the movement of tub or car.

The energy consumption is calculated using the following assumptions. The numbers of trips per day are 10. The length of the track is 5m.From the above observations, it is concluded that 3hp laboratory experimental micro controller drive requires 11.06% energy (from 0.00619 kWh to 0.00696 kWh) for down the gradient and up the gradient. Total Energy consumption chart are presented in Figure 7.24.Total consumption charts for monthly and yearly are presented in Figure 7.25.

The energy consumption chart also indicates the micro controller based haulage drive system which requires less consumption compared to conventional haulage drive system. The procedure followed to calculate energy consumption is the same as experimental procedure of conventional method haulage drive system.

The plotted results are related to energy consumption, angle with horizontal and total energy consumption of   3hp experimental micro controller based haulage drive system. These results are in good agreement with simulation results as well as conventional experimental haulage drive system.

Similarly cost analysis for 3hp experimental haulage drive system for both methods (i.e. conventional and micro controller) is done by using experimental data and compared with cost analysis done based on simulation results.
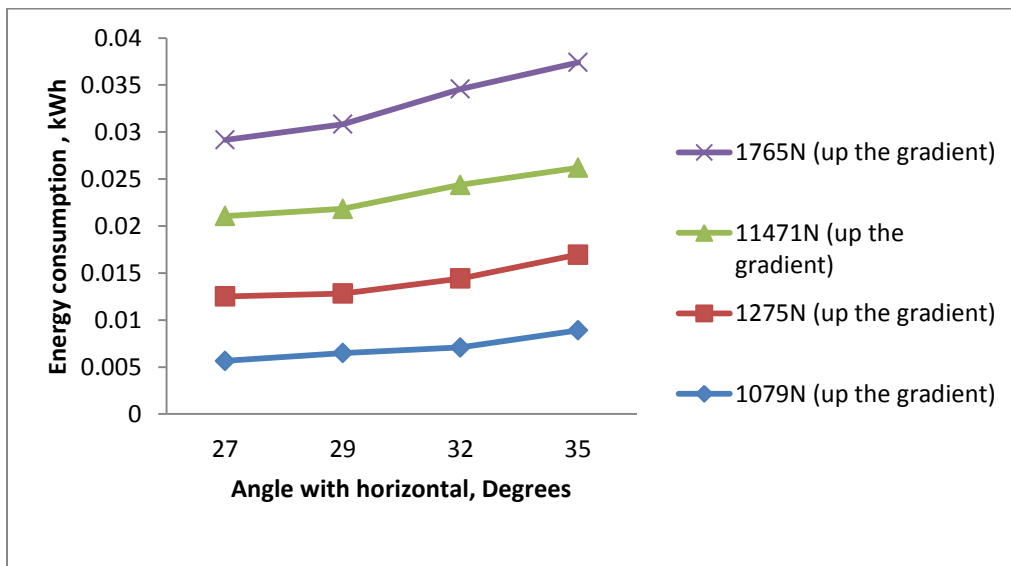
Figure 7.20 Influence of gradient (angle with horizontal) on energy consumption for up the gradient for 3hp haulage drive with microcontroller
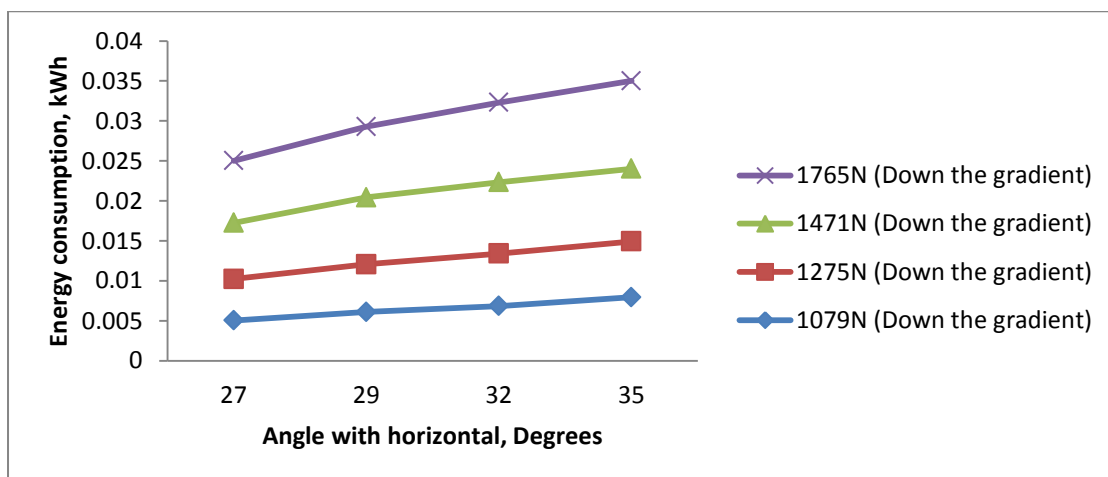
Figure7.21 Influence of gradient (angle with horizontal)on energy consumption for down the gradient for 3hp haulage drive with microcontroller
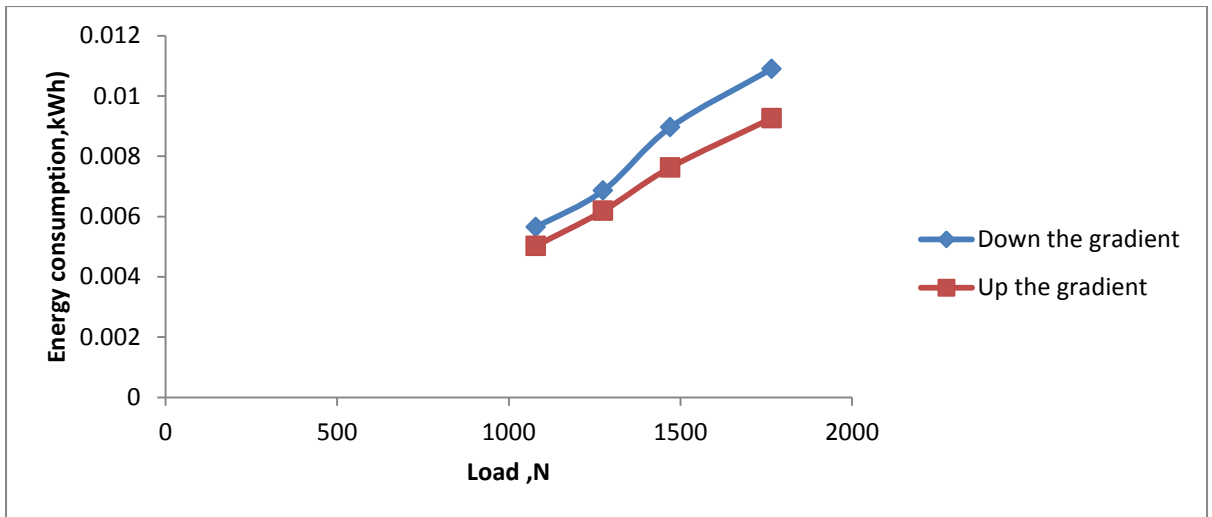
Figure 7.22 Influence of load on energy consumption when gradient constant (27°)

　　　　for 3hp haulage drive with microcontroller
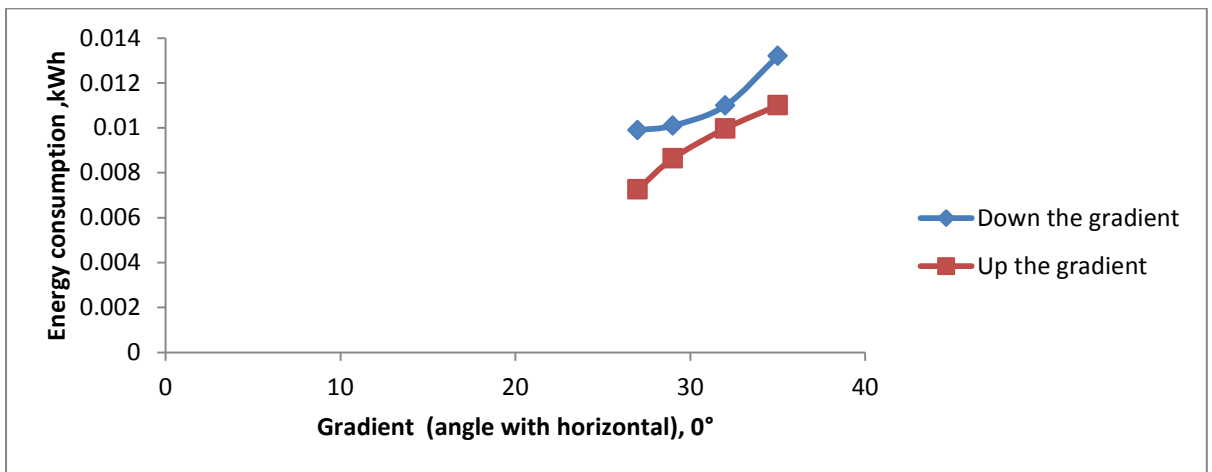
Figure 7.23 Influence on gradient on energy consumption when load constant

　　　　(1765N) for 3hp haulage drive with microcontroller

7.4.2 Experimental results

The graphs correspond to energy consumption variation with angle with horizontal up the gradient drive and down the gradient drives are presented in results and discussion. Graphical representation are indicates the energy variation with all possible combination of loads and gradients (angle with horizontal). The total consumption charts for monthly and yearly are presented and energy consumption variation in angle with horizontal chart for up the gradient and down the gradient are also presented.

The energy consumption calculation procedure is same as the experimental procedure of conventional method haulage drive system. The experimental calculated value of energy consumption shows the good results as compared to conventional method of drive system.
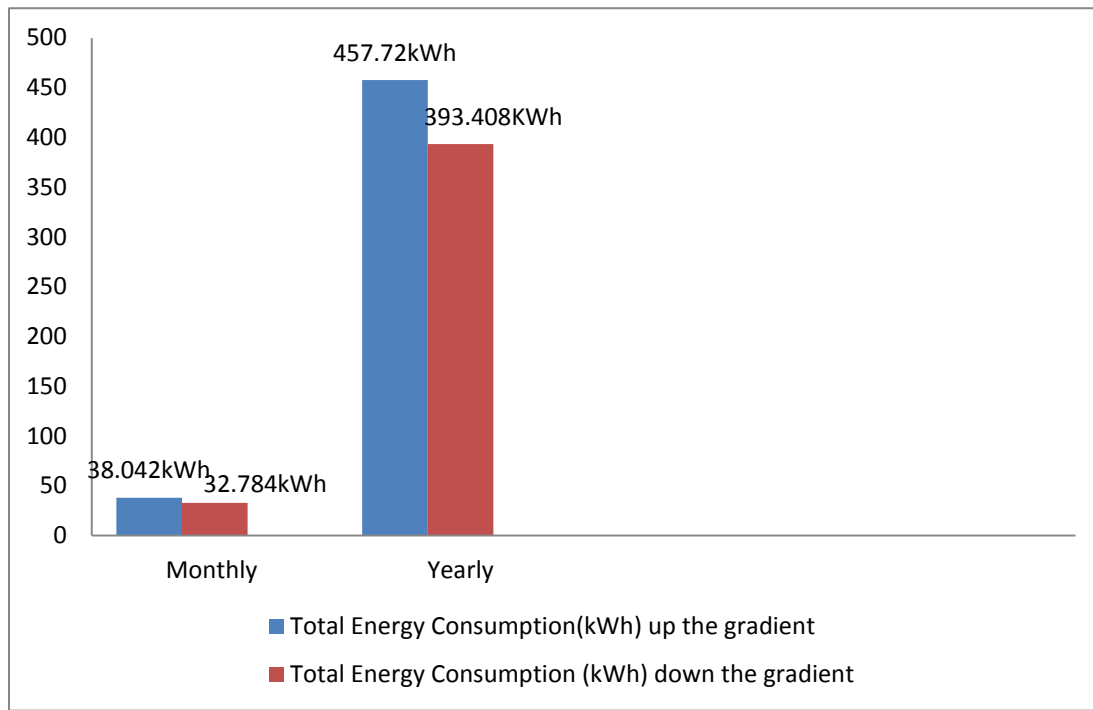
Figure 7.24 Total energy consumption chart 3hp laboratory experimental micro controller based haulage drive system
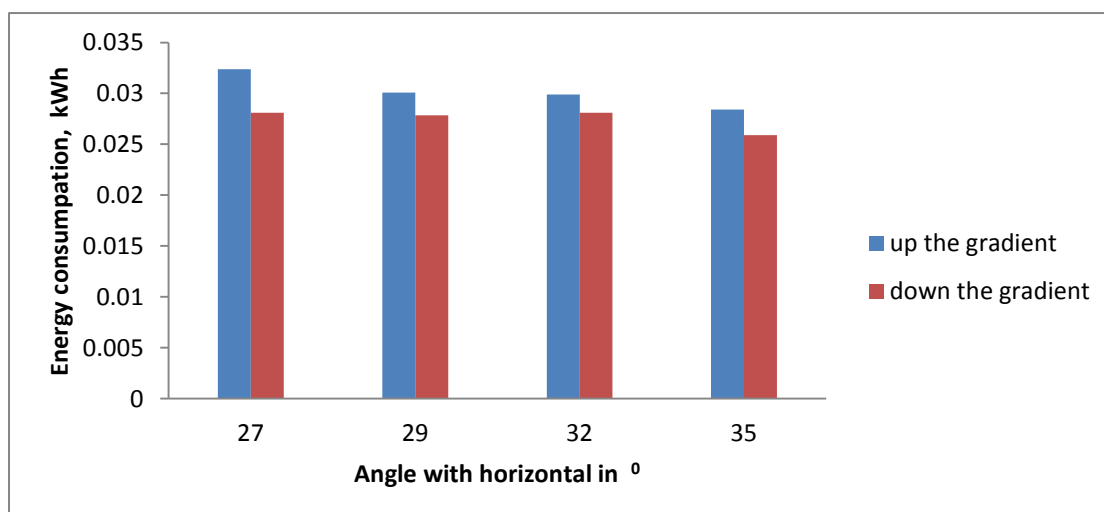
Figure 7.25 Energy consumption chart for angle with horizontal of 3hp experimental haulage drive system

From the literature it is concluded that in damper control, around 20% of the power is lost in speed variation but by rotor resistance control, around 10% to15% of the power is lost as heat. Hence, micro controller based experimental study results indicate that conservation of energy is possible up to 8 % to 9% obtained from 3hp laboratory experimental haulage drive system. The micro control based method is suitable in underground mine drive haulage system for energy conservation process, because the amount of energy lost due to conventional control method of drive system can be recovered by replacing the conventional control method of drive.

7.4.3 Comparative simulation study of 3hp laboratory experimental microcontroller based haulage drive system

The comparisons study on important electrical, mechanical parameter such as efficiency, speed, power output and torque for both simulation results, and experimental study results are discussed which influence on the energy consumption of haulage drive system. The results obtained are compared with main parameter such as efficiency, speed and torque. The comparison study on simulation and experimental study results for 3hp laboratory experimental micro controller method haulage drive system on energy consumption. The comparative results for simulation and experimental results on energy consumption 3hp microcontroller method for both down the gradient and up the gradient are presented in Table 7.7 and Table 7.8 respectively.

Table 7.7 Simulation and experimental results of energy consumption for 3hp micro controller

experimental haulage drive for down the gradient

Angles with horizontal	Load (N)	N$_1$ (Actual speed ,rpm)	Torque (Nm)	Output power (W)	Efficiency (%)	Energy consumption (kWh)	N$_1$ (Actual speed,rpm)	Torque (Nm)	Output power (W)	Efficiency (%)	Energy consumption (kWh)
				Simulation results					Experimental results		
27^0	1079	570	69.13	1010	66.75	0.00505	568	69.10	1007	64.75	0.00503
	1275	566	76.58	1101	68	0.00615	560	77.50	1114.6	69.00	0.00619
	1471	565	91.49	1327	78.2	0.00770	562	91.44	1309.4	77.74	0.00763
	1765	557	106.4	1521	87	0.00923	554	106.2	1516	86.57	0.00926
29^0	1079	568	73.34	1079	65.7	0.00475	562	75.30	1071	65.49	0.00476
	1275	567	82.04	1194	69	0.00597	565	82	1193.2	69	0.00596
	1471	564	98.00	1419	78.5	0.00748	563	97.80	1418.2	78.2	0.00748
	1765	561	114	1642	84.7	0.00957	560	115	1653.4	85.22	0.00964
32^0	1079	567	78.42	1141	66	0.00507	564	78.32	1134.8	65.59	0.00504
	1275	565	86.87	1262	69	0.00621	562	86.8	1252.4	68.5	0.00626
	1471	563	103.8	1500	77.4	0.00823	560	103.2	1483.7	78.73	0.00824
	1765	560	119.6	1735.3	86	0.0100	559	119.1	1709.3	84.61	0.00997
35^0	1079	567	82.19	1196.4	66	0.00598	564	82.1	1188.8	65.64	0.00594
	1275	565	91.04	1320	70	0.00696	562	90.44	1319.3	70	0.00696
	1471	562	108.7	1568.5	78.6	0.00904	560	108.3	1557	78.00	0.00908
	1765	560	126.4	1792	86.3	0.0109	558	126	1805	86.95	0.0110

Table 7.8 Simulation and experimental results of energy consumption for 3hp experimental micro controller haulage drive system for up the gradient

Angles with horizontal	Load (N)	Simulation results					Experimental results				
		N (rpm)(Actual speed)	Torque (Nm)	Output power (W)	Efficiency (%)	Energy consumption (kWh)	N (rpm) (Actual speed)	Torque (Nm)	Output power (W)	Efficiency (%)	Energy consumption (kWh)
27^0	1079	570	70.13	1024	63.17	0.00566	566	70.00	1017.2	62.75	0.00565
	1275	567	77.66	1129.6	65.5	0.00690	564	77.56	1123	67.0	0.00686
	1471	565	93.38	1344.7	72.3	0.00896	563	93.18	1344.7	74.43	0.00896
	1765	561	108.5	1551	81	0.01098	548	108.0	1519.2	79.32	0.0109
29^0	1079	574	75.4	1105	63	0.00552	570	75.1	1099	62.74	0.00549
	1275	567	83.5	1208	66	0.00637	564	83	1202	65.71	0.00634
	1471	564	99.69	1433.5	76	0.00816	562	99.3	1470.5	78	0.00816
	1765	562	115.9	1659	80.1	0.0103	558	115.4	1653.2	80	0.0101
32^0	1079	567	79.6	1153	62.75	0.00512	565	79.1	1147.4	62.45	0.00509
	1275	565	88.14	1272	65.6	0.00633	563	88.0	1267.5	65.33	0.00633
	1471	563	105.2	1513.3	75.85	0.00793	560	105.0	1509.6	75.65	0.00796
	1765	561	122.3	1754	83.3	0.00974	559	122.0	1751	85.6	0.00972
35^0	1079	568	83.18	1208	64.18	0.00691	570	85.0	1243.9	64.5	0.00691
	1275	566	92.12	1339	69	0.00798	566	94	1380.5	70.41	0.00805
	1471	562	110.4	1580	79.19	0.00930	562	109	1515	78	0.00925
	1765	558	127.8	1824	87.87	0.0113	555	124	1766.8	85.10	0.0112

The Comparative study results obtained from conventional and micro controller based methods (3hp experimental laboratory haulage drive system) are discussed. The comparative study results of (simulation and experimental) 3hp laboratory conventional experimental haulage drive system for variation of energy consumption , efficiency and power output with load for up the gradient drive system are given in Figure7.26 (a), Figure7.26(b) and Figure7.26(c), respectively.

The variation of energy consumption in simulation and experimental results are observed from this study. The comparative study results of simulation and experimental on energy consumption, efficiency, power output variations with load are given for both drive systems. It is observed that the simulation result varies from 0.2% to 0.5% compared to experimental values. This can be represented as graphical observation. Similarly the same study was carried out for 3hp laboratory experimental microcontroller method haulage drive system for both up the gradient and down the gradient and comparative results is given in the above section.

Figure 7.26(a) Comparative study results of 3hp laboratory experimental microcontroller method haulage drive system (constant gradient (27^0) variable load) for up the gradient

Figure 7.26(b) Comparative study results of 3hp laboratory experimental
microcontroller method haulage drive system (constant gradient (29^0)
variable load) for up the gradient

Figure 7.26(c) Comparative study results of 3hp laboratory experimental
microcontroller method haulage drive system (constant gradient (35^0)
variable load) for up the gradient

The comparative study results on energy consumption , efficiency and power
output variation load of 3hp laboratory experimental microcontroller method haulage
drive system (constant gradient (29^0) variable load) for down the gradient are given in
Figure 7.27.

Figure 7.27 Comparative study results of 3hp laboratory experimental microcontroller
method haulage drive system (constant gradient (29^0) variable load) for
down the gradient

The same comparative study results of 3hp laboratory experimental
microcontroller method haulage drive system (constant gradient (29^0) variable load)
for both down the gradient and up the gradient are given in Figure 7.28(a) and Figure
7.28(b) for comparative study results of simulation and experimental for down the
gradient . Similarly constant gradient (35^0) variable load is also shown in Figure 7.29.
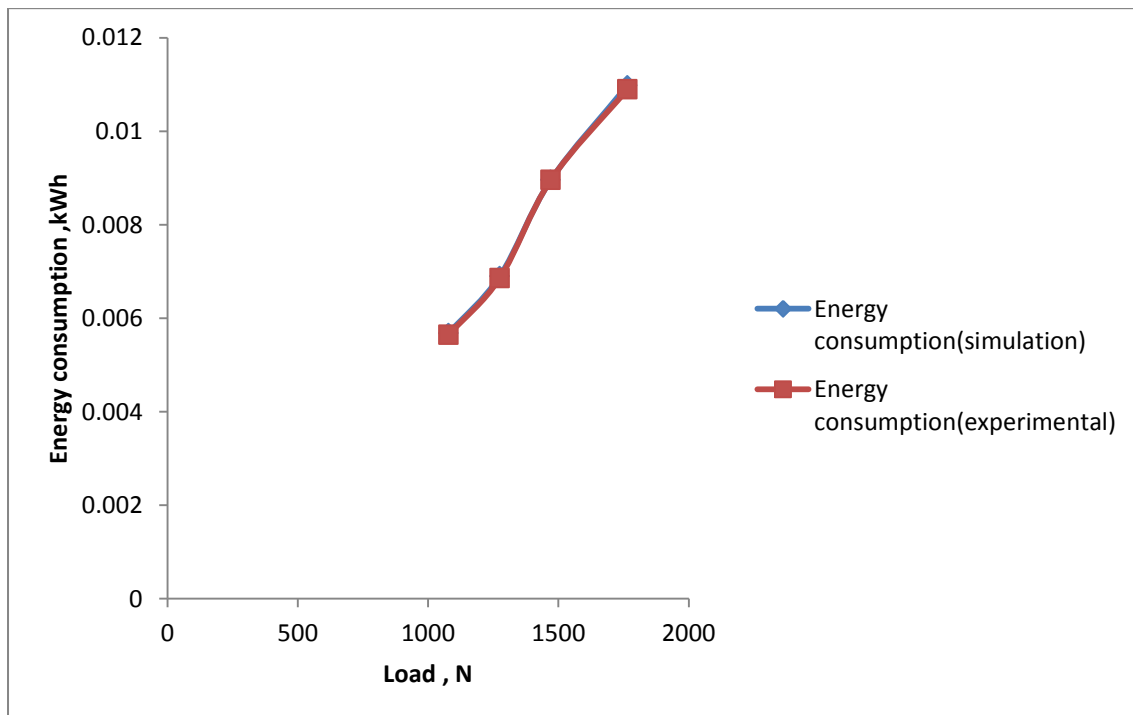

Figure 7.28(a) Comparative study results of 3hp laboratory experimental
microcontroller method haulage drive system (constant gradient (29^0)
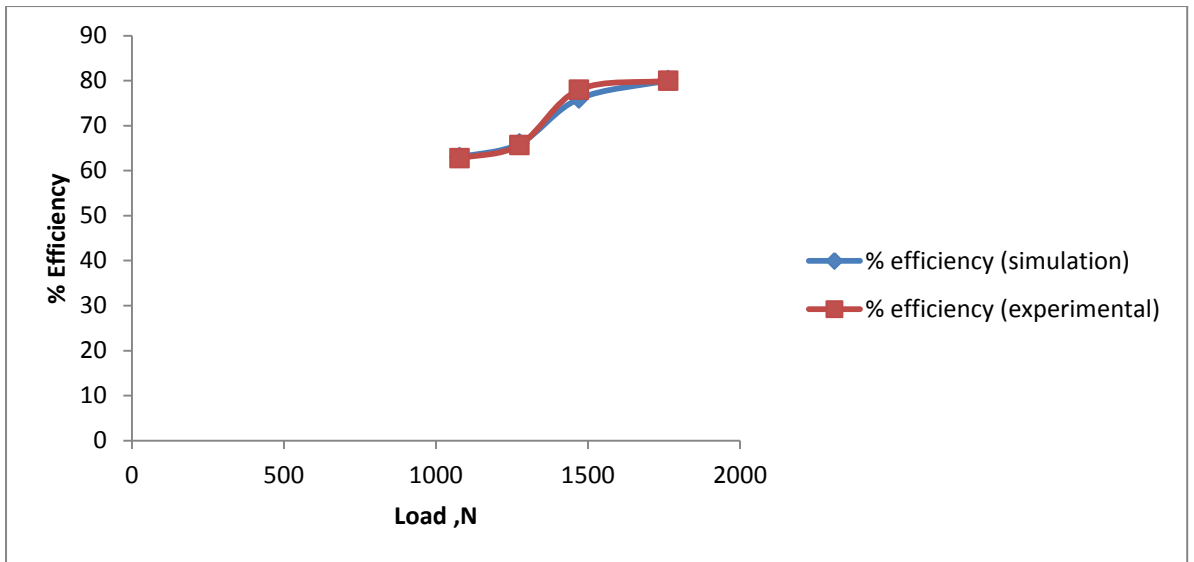variable load) for both down the gradient and up the gradient

Figure 7.28(b) Comparative study results of 3hp laboratory experimental
microcontroller method haulage drive system (constant gradient (29^0)
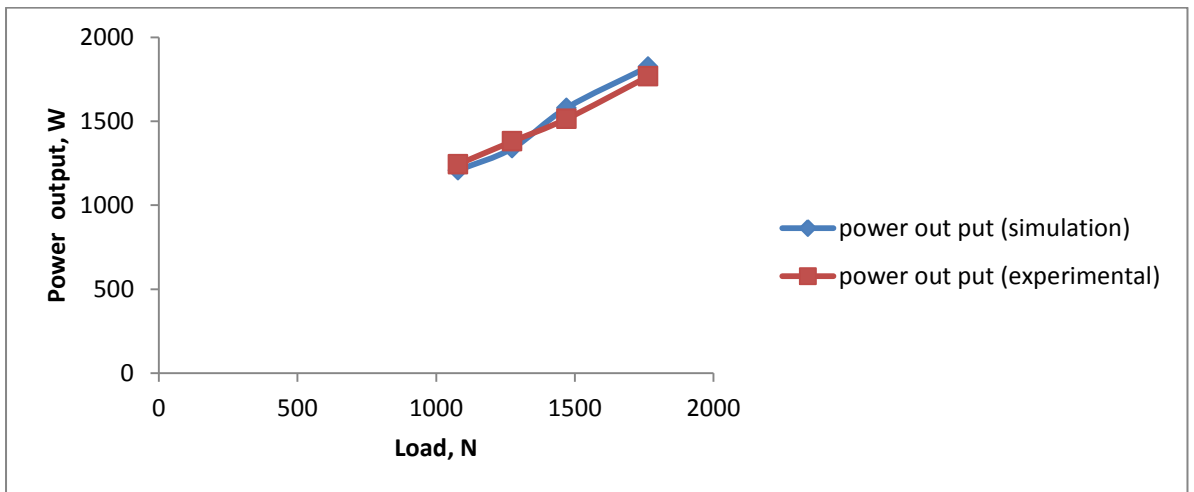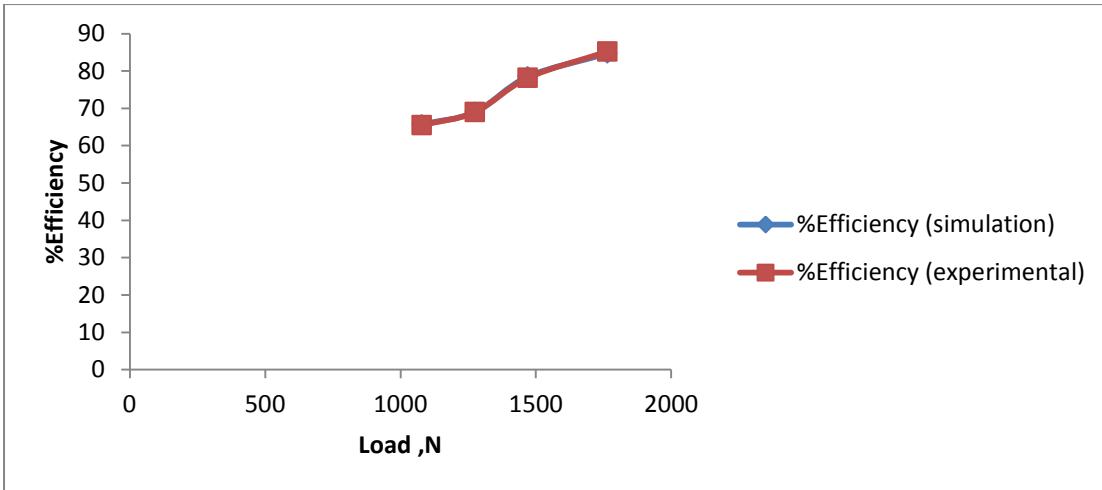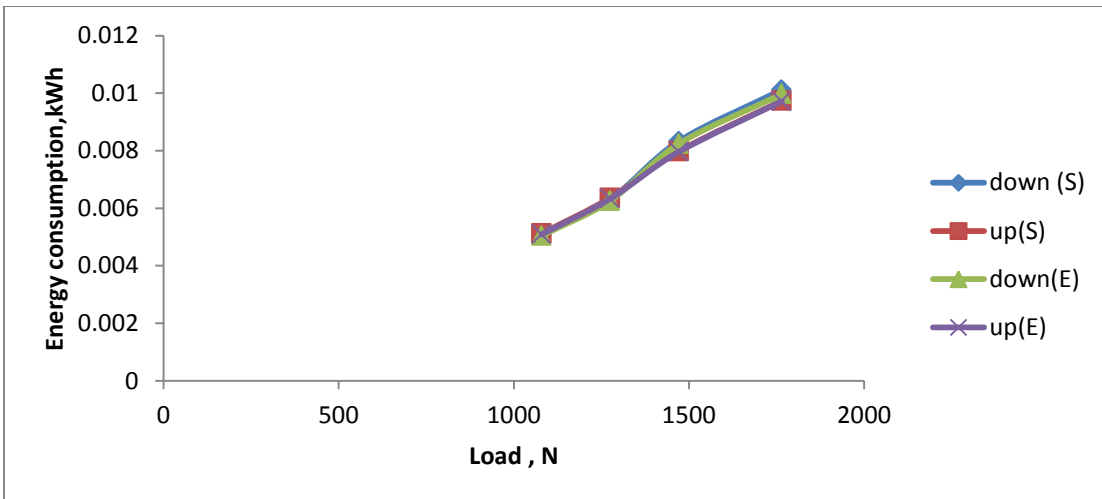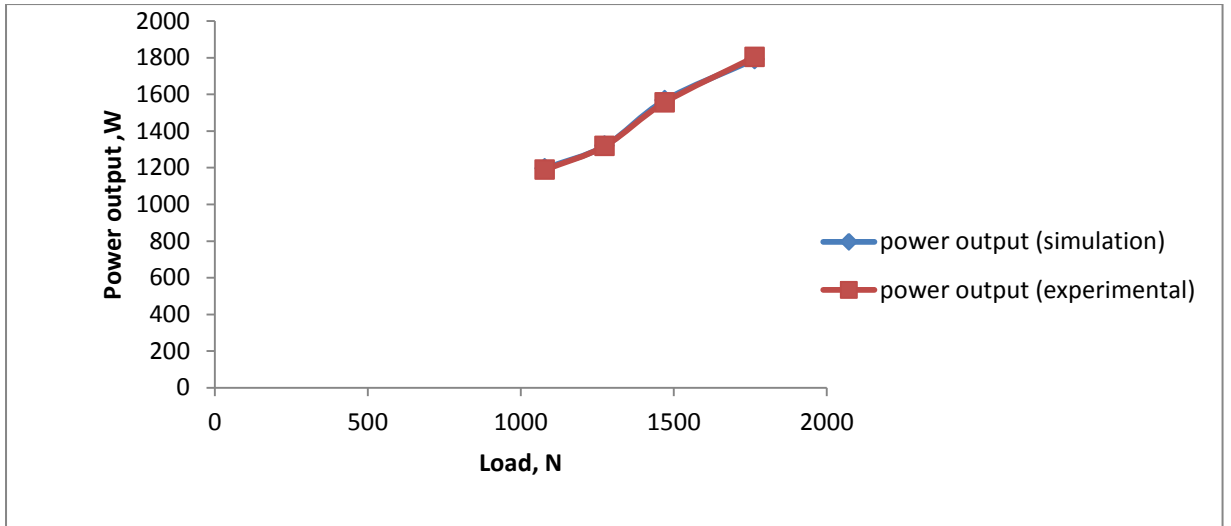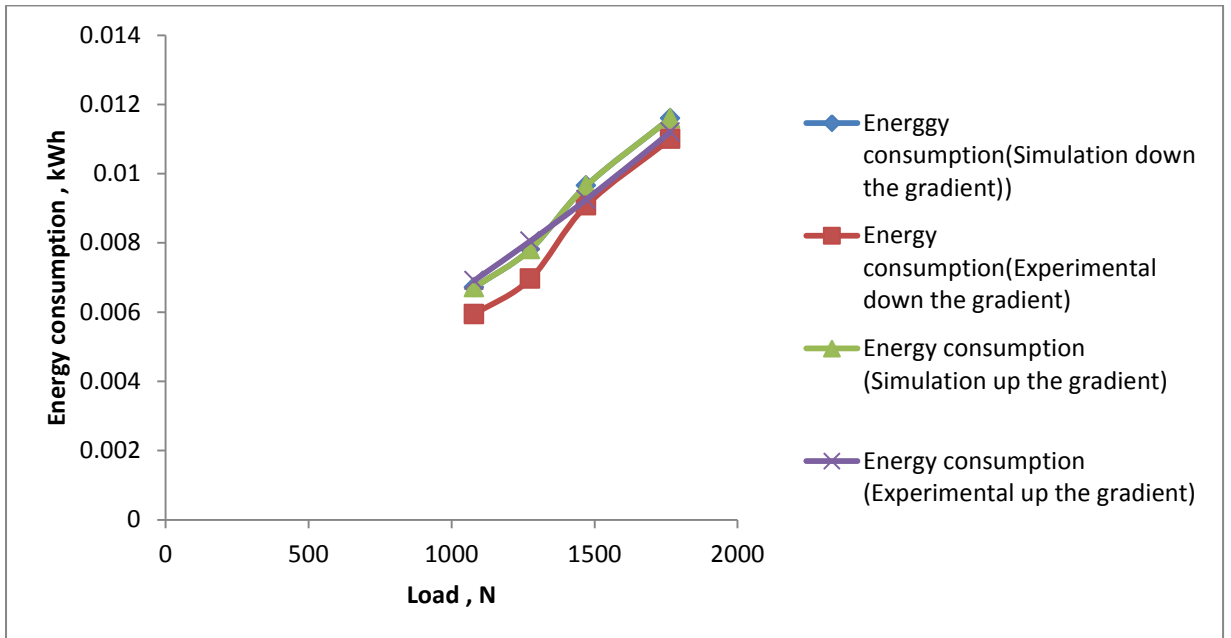variable load) for down the gradient

Figure 7.29 Comparative study results of 3hp laboratory experimental microcontroller
method haulage drive system (constant gradient (35^0) variable load) for
both down the gradient and up the gradient

7.4.4 Cost analysis of 3hp laboratory experimental micro controller based haulage drive system

The cost analysis is done based on the results obtained in the laboratory from 3hp micro controller based haulage drive system by considering present tariff. The total energy consumption of drive system is = 1023.159 kWh (501.653 kWh + 521.506 kWh).

The total energy consumption per year and total cost of energy per year for drive system are 1023.159 kWh and Rs.7492.113/- respectively. The procedures for calculation are as follows:

Maximum demand charges 3hp drive system 2.2 KVA @ Rs.150 KVA = Rs.330/- .Energy Charges for 3hp drive system total 1023.159 kWh @Rs.7 kWh

$$= \text{Rs. } 7162.113/-$$

Total annual cost of energy consumption for drive system is Rs .7492.113/-.

7.4.5 Comparison between conventional and micro controller method in Laboratory experimental studies

Comparative study results of conventional and micro controller method (3hp experimental laboratory haulage drive system) were presented. Power output obtained from both methods (i.e. conventional and micro controller method) were calculated. The difference of power is considered for calculation of percentage power from two drive systems. The slip power obtained from these results was drawn in graphs and is shown for different combinations of loads and gradients. Experimental study in micro controller method when compared to conventional method, the power (saving) vary 68.53% (from 0.0129 kW to 0.041kW), for up the gradient and 64.23% (from 0.00691kW to 0.007766 kW), for down the gradient. Similarly, the power (saving) varies 11.86% (from 0.078 kW to 0.0885 kW) for up the gradient and 18.76% (from 0.088 kW to 0.143 kW)for down the gradient, as the load varies. Influence of gradient on energy consumption for conventional method and micro controller method using 3hp haulage drive system at a 1079 N load is shown in Figure 7.30.Similarly, influence of load on energy consumption at one gradient (27°with horizontal) for conventional method and micro controller method using 3hp haulage drive system is shown in Figure 7.31.
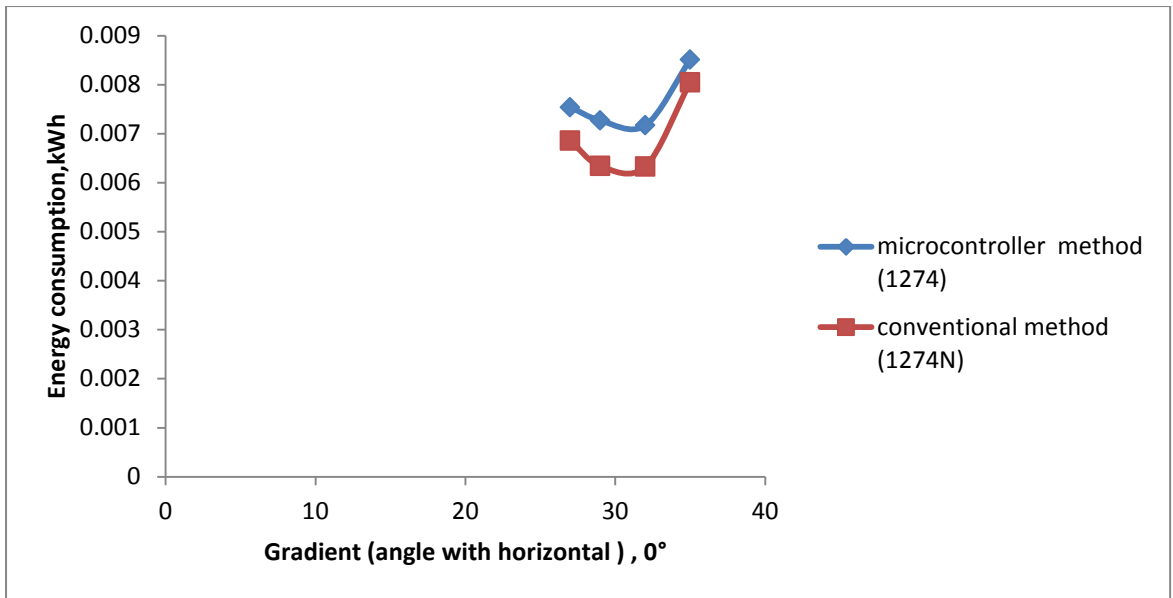
Figure 7.30 Influence of gradient on energy consumption for constant load (1274N)
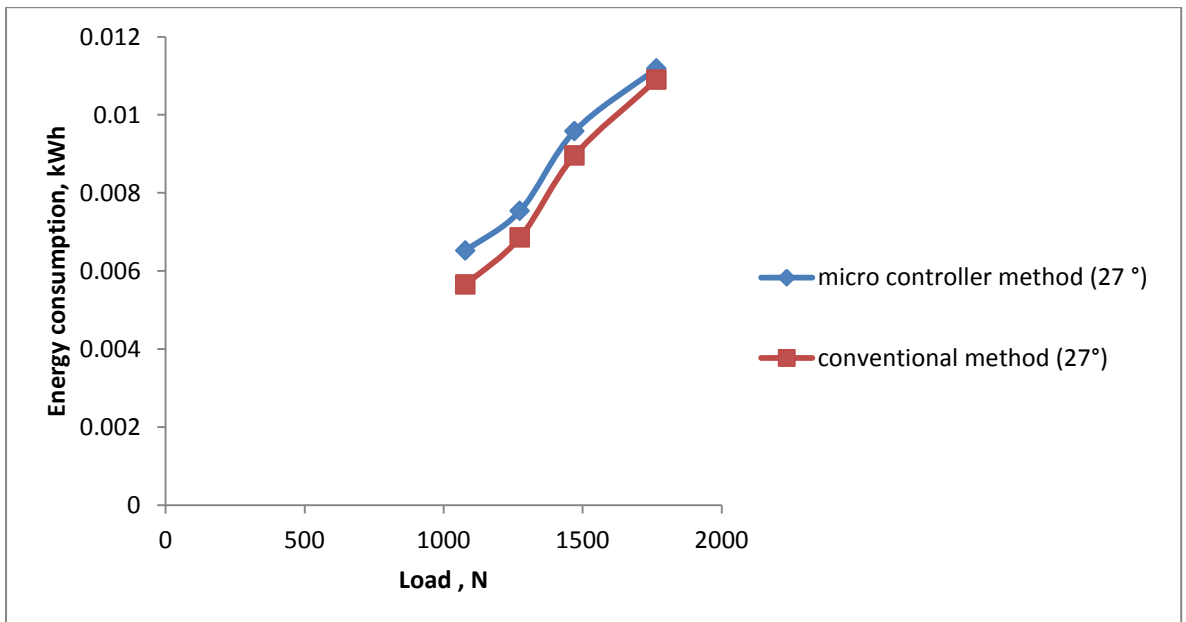
Figure 7.31 Influence of load on energy consumption at 27°with horizontal

Slip power recovery for 3hp laboratory experimental haulage drive system (conventional and micro controller) method are shown in Figure 7.32. The slip power recovery for 3hp laboratory experimental haulage drive system (conventional and micro controller) method is shown in Figure 7.33. Comparison between the results of

conventional method and micro controller method are obtained from field and simulation study are presented in Table 7.5 to Table 7.6.

The 150hp underground haulage drive system -1 the slip power recovered from haulage drive system – 1 for up the gradient and down the gradient are shown in Figure 7.34. Similarly 150hp underground haulage drive haulage drive -2 the slip power recovered from haulage drive system – 2 for up the gradient and down the gradient are shown in Figure7.35 and Figure7.36 respectively.

The slip power recovery from drive system -1 and drive system-2 the power increases non linearly in up the gradient drives and decreases non- linearly in down the gradient of the drive system-2. The energy conservation (saving) for down the gradient and up the gradient for 150hp haulage drive system -1 (i.e. serving from surface to 8th level and 8th level to surface) varies 63.31% (from 4.5 kWh to 12.265 kWh) and 49.57% (from 1.644 kWh to 3.260 kWh) respectively.

Similarly the energy conservation (saving) for 150hp haulage drive system-2 (i.e. serving from 8th level to 42nd level and 42nd level to 8th level) varies 57.5% (from 8.32 kWh to 8.799 kWh) and 69% (from 3.852 kWh to 12.435 kWh) respectively. 150hp underground haulage drive system from simulation (micro controller method) results the following observation are made on power output of haulage drive system.

1) The field study results on conventional method the power output was varied 44.41% (from 60357 W (minimum load, 17.64 kN)) to 108583 W (maximum load , 32.65kN) of down the gradient of haulage drive system-1 . Similarly the power output was varied 49.59% (from 73716 W (minimum load, 21.0kN) to 129639W (maximum load, 36.7kN)) to for up the gradient haulage drive system-1.

2) Similarly the power output was varied 50.23% (from 63682 W (minimum load, 19.8kN) to 127974W (maximum load, 39.2 kN) for down the gradient of haulage drive system-2. Similarly the power output was varied 39.06% (from 65669W (minimum load, 17.6kN) to 152088W (maximum load, 44.1kN) to for up the gradient haulage drive system-2. From the graphical results the energy consumption can be reduced in microcontroller based drive method.
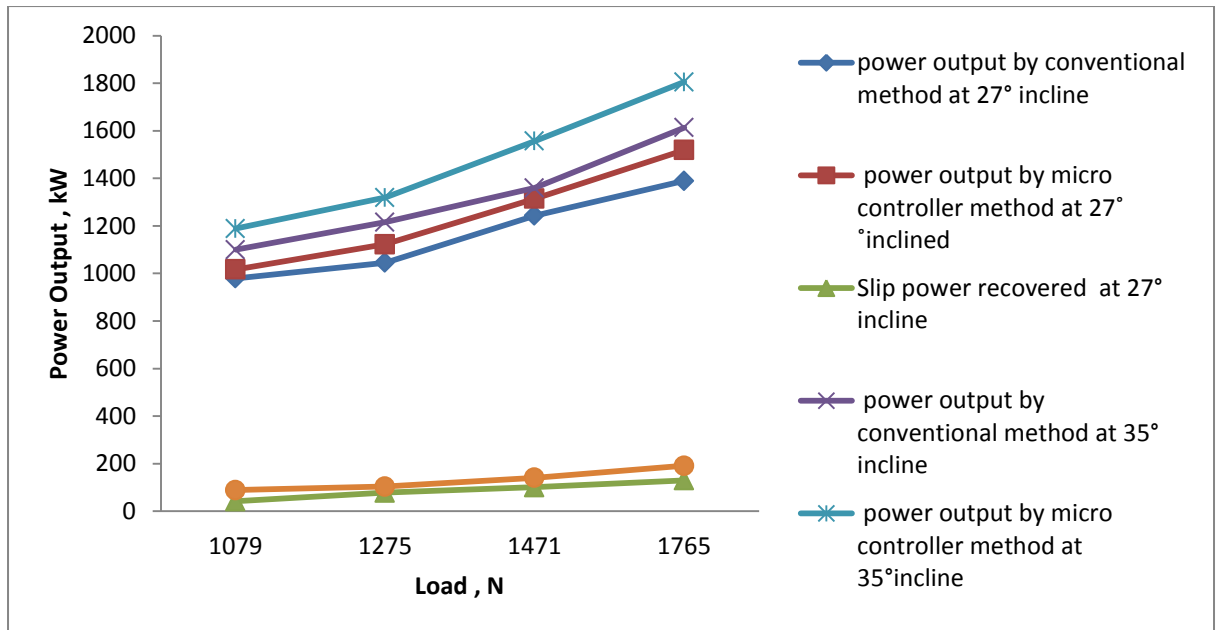
Figure 7.32 Slip power recovery for 3hp laboratory experimental haulage drive
system (Conventional and micro controller) method
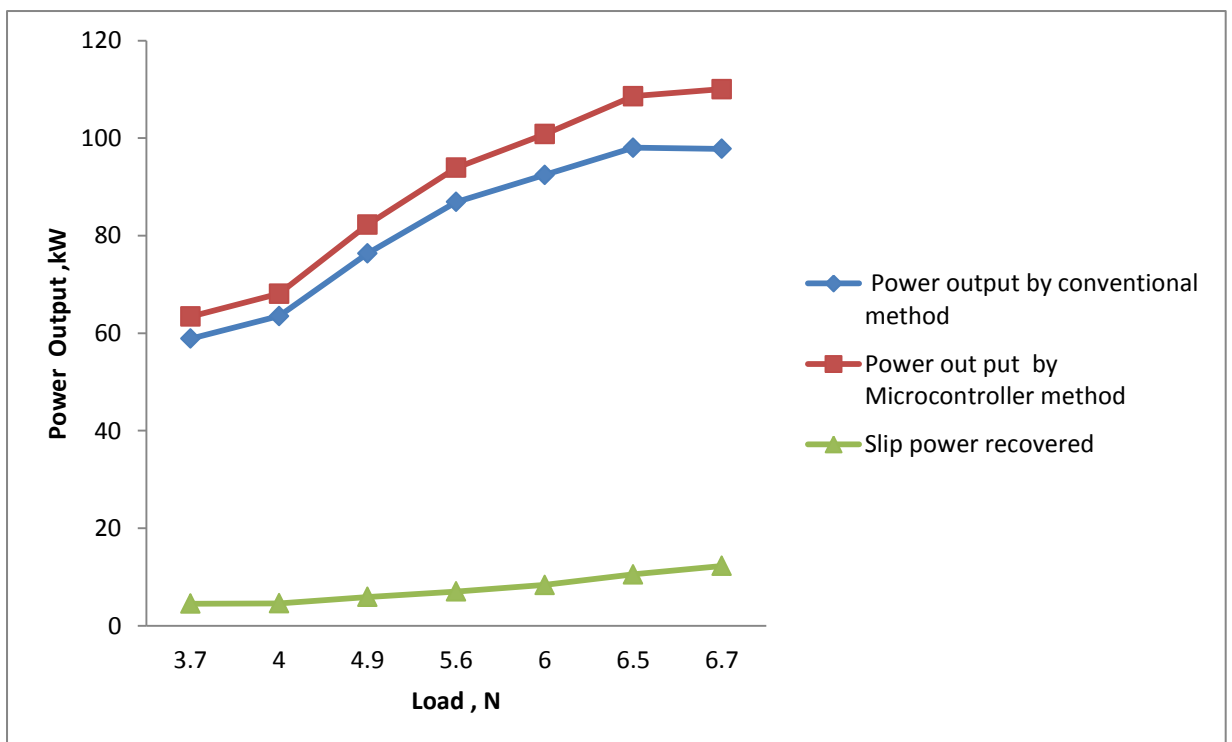
Figure 7.33 Slip power recovery by haulage drive system -1 down the gradient
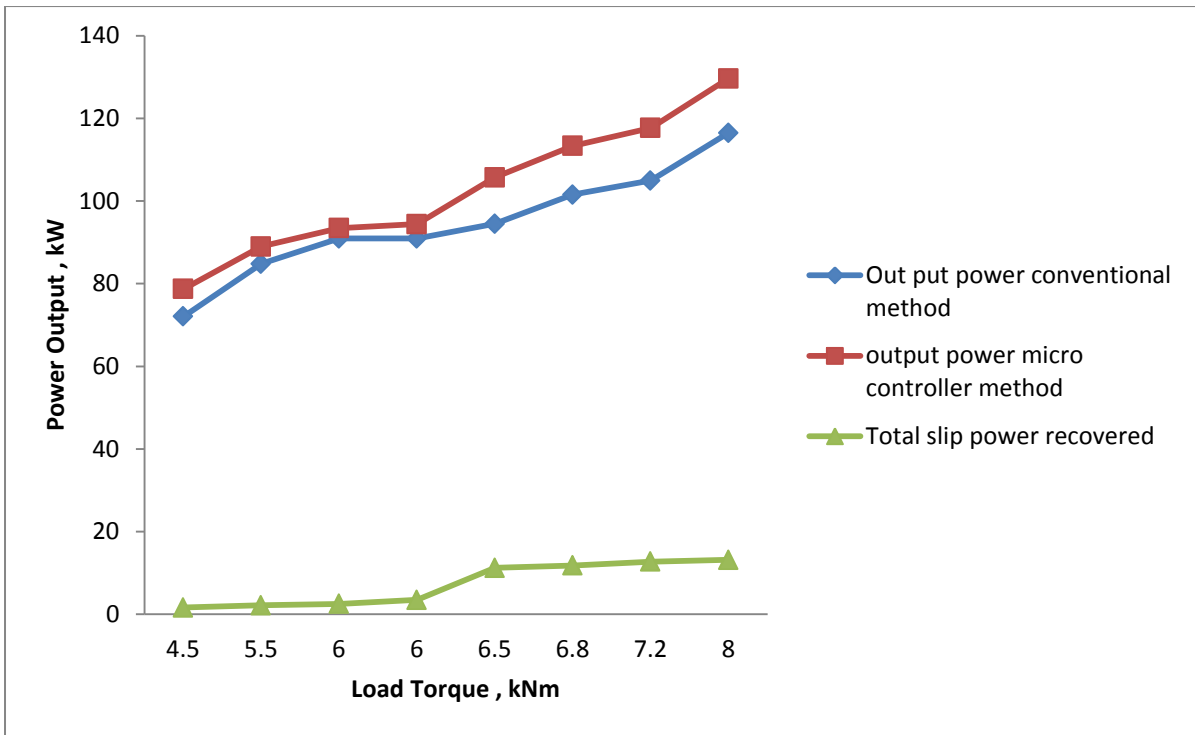
Figure 7.34 Slip power recovery by haulage drive system- 1 up the gradient
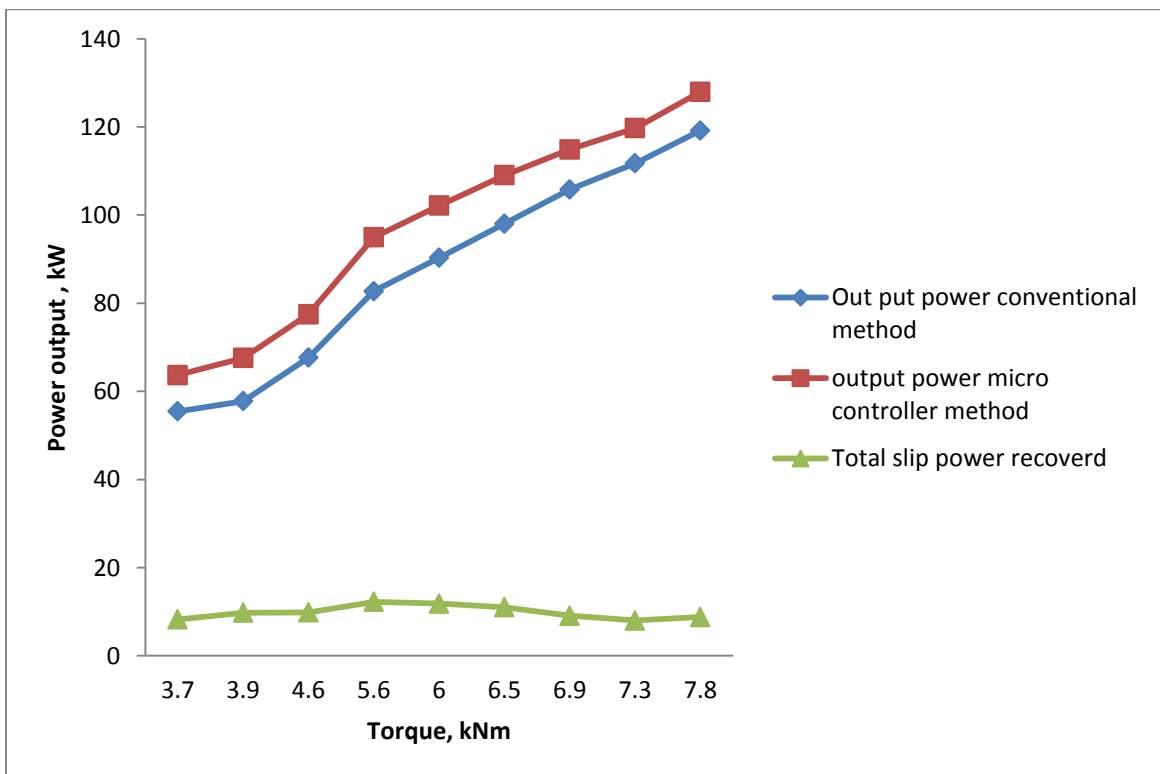
Figure 7.35 Slip power recovery by haulage drive system- 2 for down the gradient
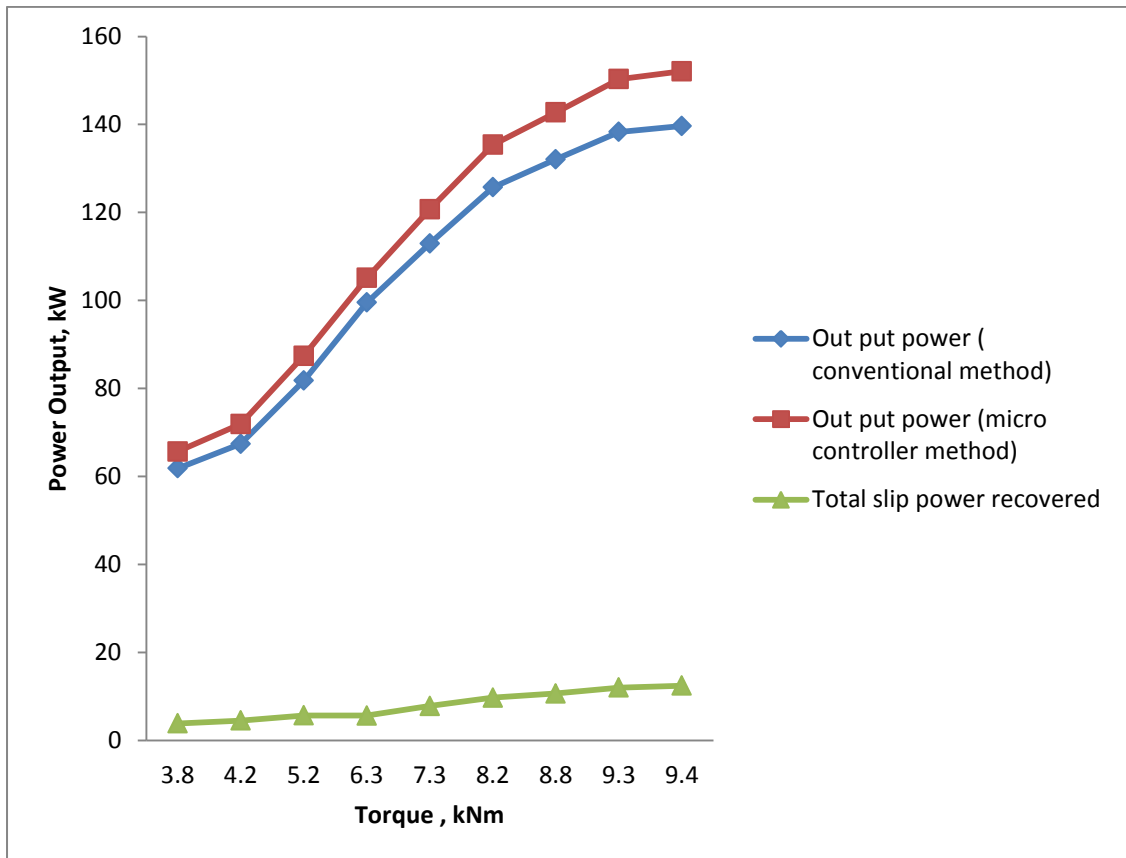
Figure 7.36 Slip power recovery by haulage drive system- 2 for up the gradient

The actual energy conservation is obtained from the field study on conventional method of drive and micro controller (static) method of drive system. For simulation of 150hp underground haulage drive total energy consumption is calculated. The calculation procedure is illustrated in APPENDIX VI.

The same procedure is adopted in 3hp laboratory experimental haulage drive on both methods of control. Total energy consumption of 3hp laboratory experimental study on conventional and micro controller method haulage drive system is shown in Figure 7.37.
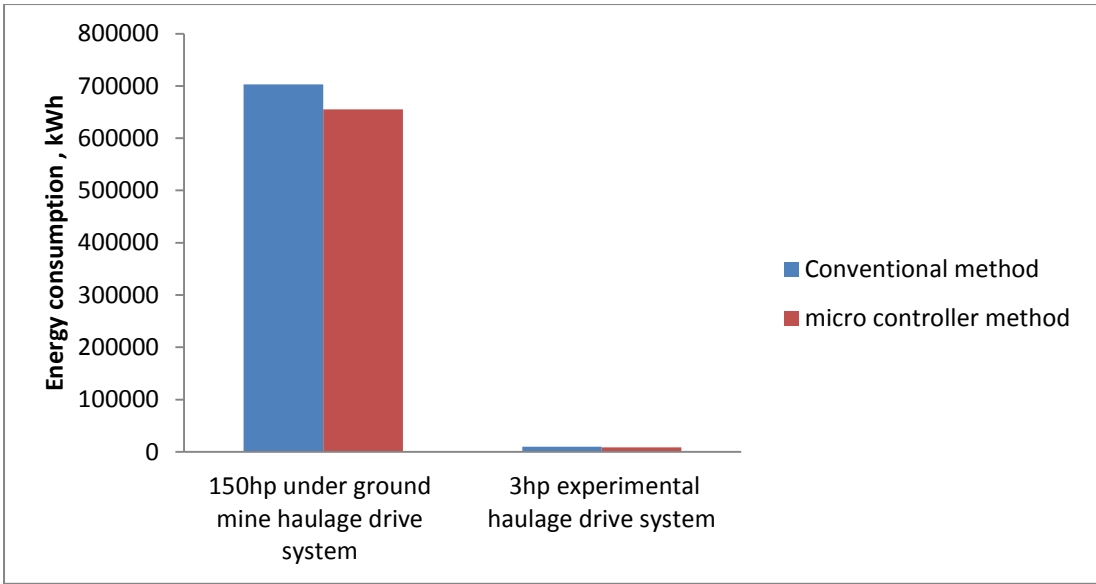
Figure 7.37 Total energy consumption of conventional and micro controller method drive

The comparative study of simulation, experimental study on conventional and micro controller based method on energy consumption study results with graphical results as well calculated results are presented. The energy conservation can be improved in the concerned mine by using the same technique to 150hp underground haulage drive system in GDK 10A incline mine.

7.5 Mathematical modelling (Results and discussion)

7.5.1 Power requirement of the motor to run haulage

The force equation 5.3 is gives the total force required up the gradient and down the gradient of the drive system. The force equation is used for modeling mechanical load in simulation process. Simulation studies are presented in Figure 6.2 Simulink model for mechanical load arrangement of 3hp and 150hp haulage drive system. The values are entered by creating MATLAB md.file and clik the run menu .The output are appeared on the MATLAB work space.

The torque equation of the experimental model pertaining to both up the gradient and down the gradient along with simple mechanics force diagram are presented in the above diagram.

Load torque equation of the experimental model for both up the gradient and down the gradient by using force diagram simple mechanics of load is T_L = Total Force × radius of the drum = F×R .The load toque equation decides pattern speed torque curve for different levels haulage drive system. The behavior of the characteristics curves different drive system are represented in simulation of conventional system of haulage drive system. The corresponding results are also given in Figure 7.38(a) Power loss of 150hp haulage drive system under no-load condition and Figure 7.38(b) Power loss of 3hp experimental haulage drive system under load condition.

7.5.2 Slip ring induction motor (conventional method)

A stator flux oriented model has been derived for the wound rotor induction machine. Current Controllers designed in the field reference frame comprise proportional or proportional-integral controllers with subsequent addition or subtraction of the compensating terms. The design method is simple as it directly follows from the rotor voltage equations. The front end converter is modeled in the stator voltage reference frame.   The structure of the current loops is similar to that of the rotor side control. The front end converter is simulated in both directions of power flow.

Formulate a mathematical model of the doubly-fed grid-connected wound rotor induction machine and the front end converter. A design methodology is evolved for developing the current controllers. Simulation results are presented to confirm the modeling. The implementation of field oriented control and experimental results are given in the simulation study results and discussion section 7.6.

The voltage controller indicates transient results during unexpected effect of load on the forward and reverse direction of drive haulage system. And proportional integral (PI) controller will show energy consumption of 150hp underground haulage drive system and 3hp laboratory experimental haulage drive system. The mathematical model is used for simulating the entire haulage drive system.

7.5.3 Rotor resistance starter design of Equation (5.23) It shows that the value of the torque can be varied for a particular speed of the rotor by varying the external rotor resistance. The value of the maximum torque is independent of the rotor

resistance and the speed at which the T_{max} occurs can be adjusted using the rotor resistance. The starting torque also increases.

7.5.4 Modelling of Static Drive System

From the Eqn.(5.35) we obtain the T_L which depends on the proposed drive load system.Shaft output of the proposed drive system: The output shaft power Equation (5.18) is used for calculating the power in proposed drive system. Determining the power to be regenerated starts with recognizing the stator power passes to the rotor. Based above equation used for obtaining power for haulage drive system. The proposed simulink model presented in Figure

7.5.5 Pulse Width Modulation (PWM)

The recovered slip power calculated is given as, Total Power recovered = Shaft output power conventional method – Output power micro controller method The other electrical parameters are calculated as per simulation output and data obtained from conduction of 3hp laboratory experimental on conventional method haulage drive system and micro controller based haulage drive system also the field study on 150hp underground haulage drive system-1 and haulage drive system-2.

7.5.6 IGBT inverter

The state space modelling of the IGBT is given in Eqn. (5.49). It is found to be non-linear in α. Here the control task taken up is to keep m (mc) constant since α is related to qc of the IGBT inverter. This control task is best achieved through small signal model of the IGBT inverter. The active power (losses plus change of steady state) is indirectly controlled by controlling the dc-link voltage. It may be noted that a controller is able to perform the control task. The simulink model for IGBT are given Figure 6.8.

7.5.7 CONTROLLERS FOR ROTOR (voltage and current controller)

So Eqn.(5.50) is multi input mu lti output (MIMO) system, its input and output are given in Eqn.(5.52). Both active and reactive currents are coupled with each other, through reactance of coupled inductor, so it is very essential to decouple both active and reactive current from each other and design the controller for tracking the required value.

Closed loop control system

With closed loop regulation, a transducer is used to continuously monitor an operating parameter. The measured value of the parameter provides a Feedback signal that is compared with the desired value called the Set point or Reference. Any measured

Error is used to increase or decrease the output to match the set point.

Figure 7.3 is a diagram of a closed loop speed regulating system for 150hp haulage drive system. With a closed loop regulating system, the steady state regulation accuracy is primarily determined by the measurement and comparison accuracy. The input vs. output characteristics of the process becomes less important.

The closed loop speed regulator compensates for any changes in the characteristics

of the drive caused by changes in load or by outside influences such as line voltage and ambient temperature. With a closed loop speed regulator, the most important characteristic of the drive is its ability to rapidly respond to changes in requirements for torque.

In Eqn.(5.55) the gain of K can be adjusted in such a way that if it is increased too high then the system behaves as second order, otherwise responses are very slow.

Hence the numerical values for k_p and k_i are decided from the circuit parameters L_s and R_s from the required value of K. So the parameters of PI controller are defined a $K_P = K$ and $K_i = KR_s / L_s$

7.6 SIMULATION STUDY

7.6.1 Conventional method of Simulation results and discussion

The detailed technical specifications for both the drive system are given in APPENDIX I. As per available data on 150hp underground haulage drive system and laboratory 3hp experimental haulage drive system using the MATLAB/SIMULINK software package the haulage drive system model was developed.

The entire system is simulated by experimental data obtain from the 3hp laboratory experimental haulage drive system. It is developed with the different combinations of loads and gradients for both up the gradient and down the gradient of haulage drive system. The simulation of conventional method (i.e. Rotor resistance) is

also discussed in the chapter 4. In the simulation study the opening time of circuit breaker is fixed as 4 sec, 6 sec, 7 sec., 9 sec and 12sec.

The various parameters for simulation results of 3hp laboratory experimental haulage drive system are discussed and presented. In the simulation study the response of motor speed, rotor current, power loss in resistance starter of the drive during the loaded and unloaded condition of drives are observed. The power loss of rotor resistance is very high during the start period and is illustrated in Figure 7.38 (a).

The 150hp underground haulage drive shows the power loss during time step of 1sec the response observed from the Figure7.38 (a) as per the observation first 0.5sec it reaches maximum power loss and for the next 0.5sec power loss reaches minimumvalue.3hp laboratory experimental haulage drive system consumes minimum power compared to high capacity drive system as shown in Figure7.38(b). The 150hp underground haulage drive system power loss varies from 200 W to 45000 W during the start period of the motor.

The power loss variations of 3hp laboratory experimental haulage drives are shown in Figure 7.38(b) and Figure 7.38 (c), and it also depends on the opening of circuit breaker of resistance starter. 3hp laboratory experimental haulage drive the power variations are observed from 20 W to 1500 W during starting period of the motor.

The Energy consumption variation with time for 1764 N up the gradient load at 32° and efficiency variation with time for 1764 N up the gradient load at 32° angle with horizontal are plotted and presented in Figure7.39 (a) and Figure 7.39(b) respectively.
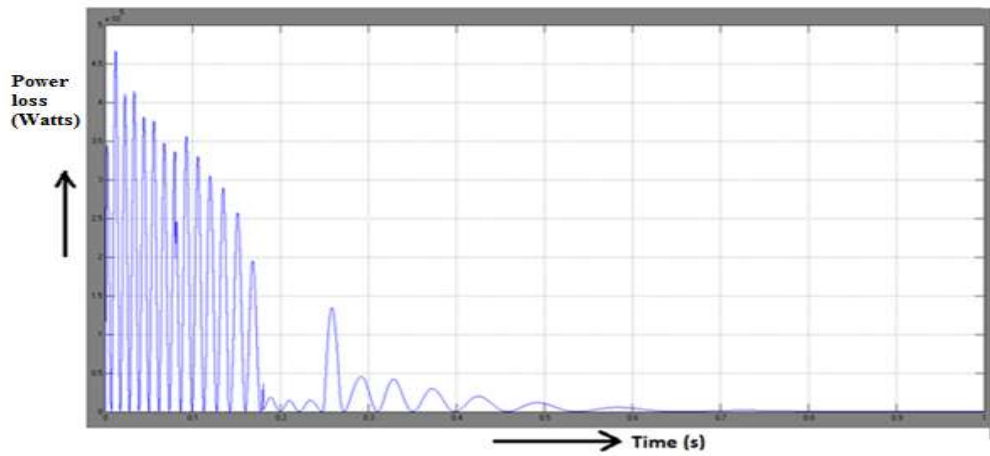
Figure 7.38(a) Power loss of 150hp haulage drive system under no-load condition
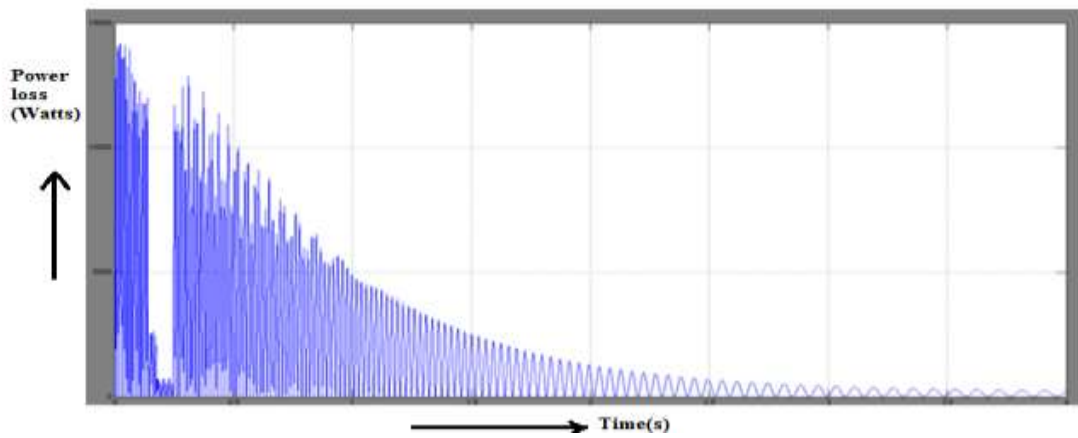
Figure 7.38(b) Power loss of 3hp experimental haulage drive system under load
condition
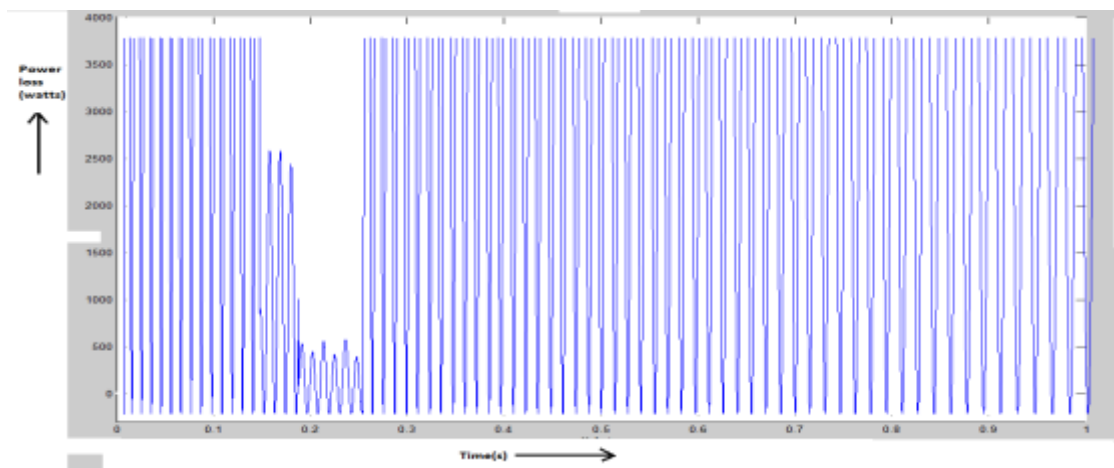
Figure 7.38(c) Power loss variation with time for1764N up the gradient at 35^0
inclined plane

Similarly energy consumption is calculated and plotted for various loads for the both drive system which is presented in Figure 7.40(a). In this figure the energy consumption is zero at the starting point and after time interval of 2seconds the consumption reaches a maximum for load of 1764 N up the gradient with 32° (angle with horizontal). As per the simulation study the energy consumption depends on the load as well as on the gradient. If gradient is more, the energy consumption is less for down the gradient of the drive system and energy consumption more for up gradient drive. In Figure 7.40(b) the efficiency variation with time is plotted for the same load and angle with horizontal.
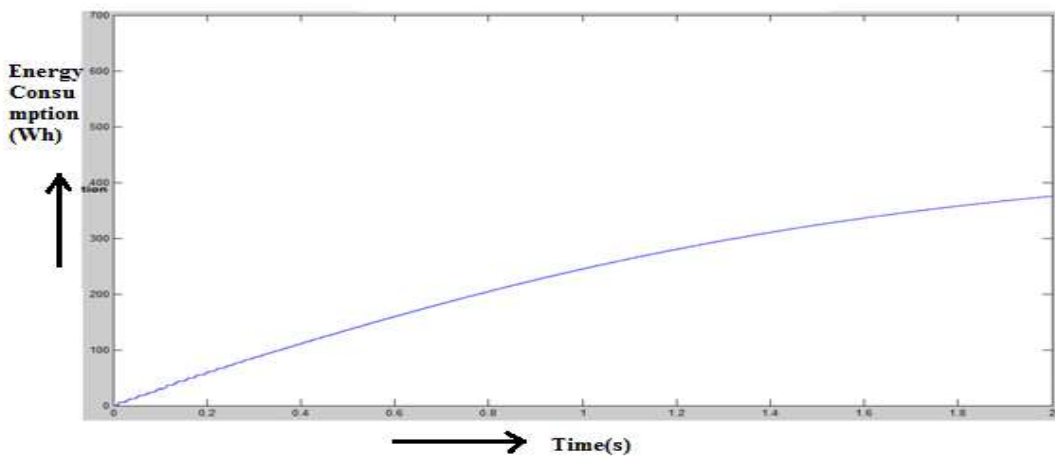
Figure 7.39(a) Energy consumption variation with time for 1764 N up the gradient load at32^o
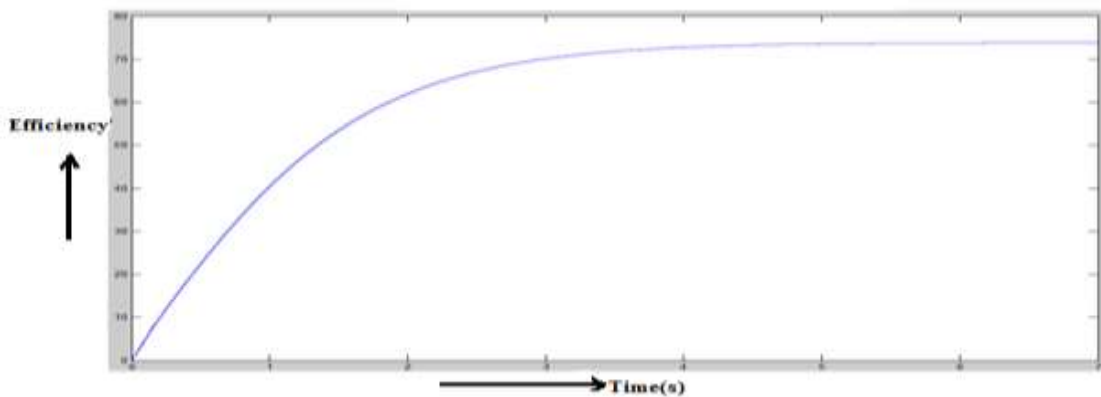
Figure 7.39(b) Efficiency variation with time for 1764 N up the gradient load at 32° angle with horizontal

196

Other normalized electrical parameters of electromagnetic torque of motor for no load condition and loaded condition, current variation with time for both stator and rotor are presented in Figure 7.40 (a), Figure7.40 (b), Figure7.40 (c) and Figure7.40 (d).

The response of torque is high at 0.1 sec with a value of 1000 Nm and after a few seconds, the machine torque comes to stable value.

The stator and rotor current is high at 0.5sec and after 3sec it comes to steady state value. Similarly the other electrical response is also investigated when the machine is loaded at different conditions. In this section the parameters of speed variation with time plot for 1764N up the gradient load of 3hp experimental haulage drive system at 32^0 inclined planes are presented in Figure7.41, Figure 7.42(a) and Figure 7.42(b). The speed variation with time for down the gradient load 150hp haulage drive system -2 and the effect of change of rotor resistance influence on speed with respect time are studied and simulation response results are discussed.

The Speed and change of resistance variation at no-load and with loaded condition for 3hp Laboratory mine haulage drive system are presented in Figure7.43(a) and Figure7.43(b), respectively. The percentage efficiency and output power variation with time plot for150hp haulage drive system-2down the gradient load are shown in Figure 7.44(a) and Figure 7.44(b). In this section conventional methods of simulation study for drive system are discussed and presented.
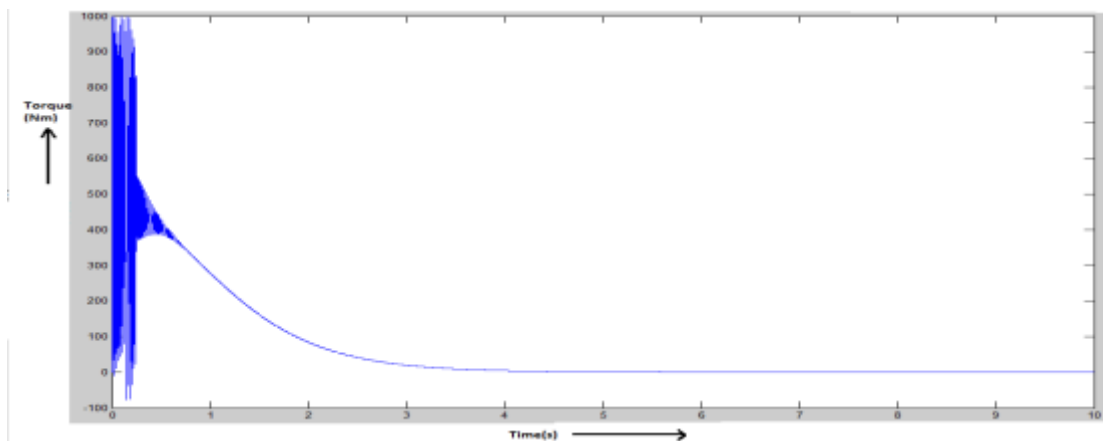
Figure7.40(a) Torque variation with time at no load
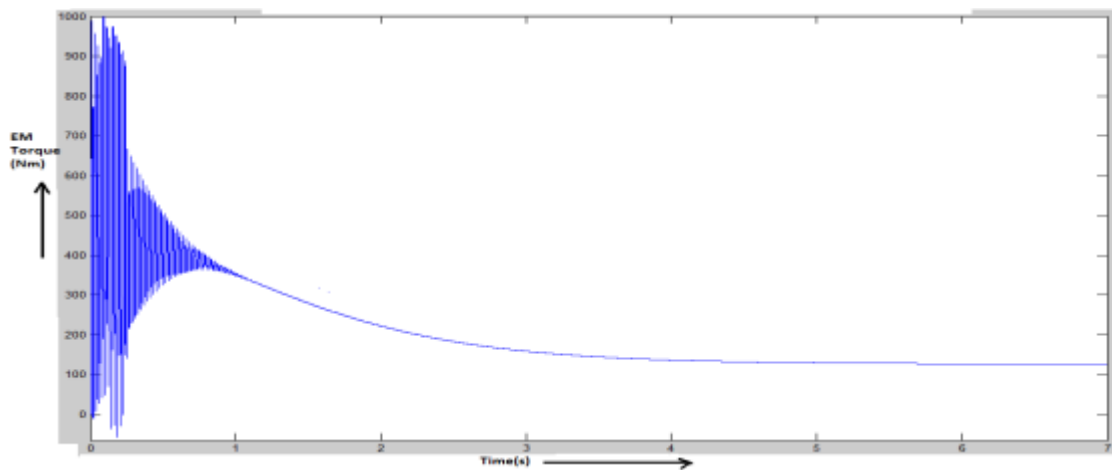
Figure 7.40(b) Torque variation with time for motor loaded condition
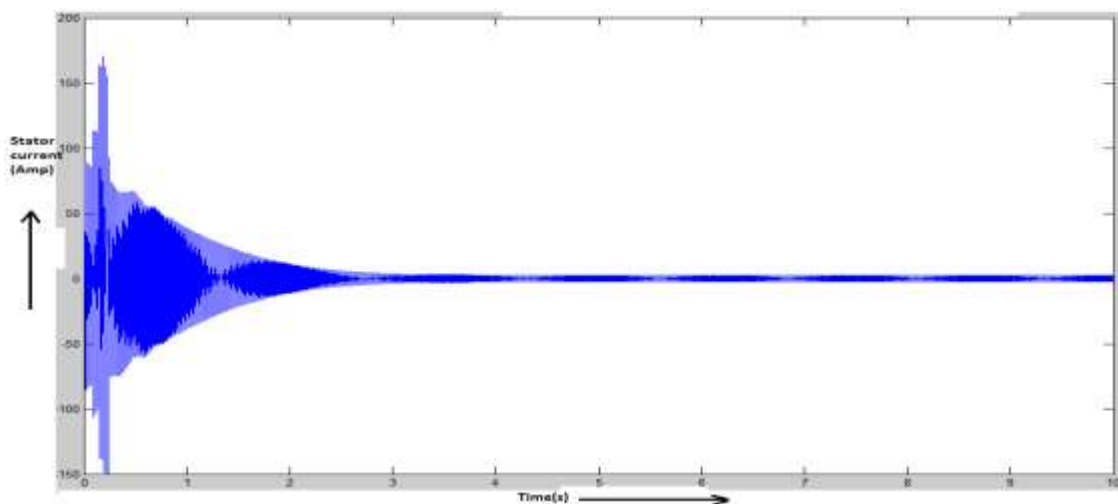
Figure 7.40(c) Stator current variation with time for motor loaded condition
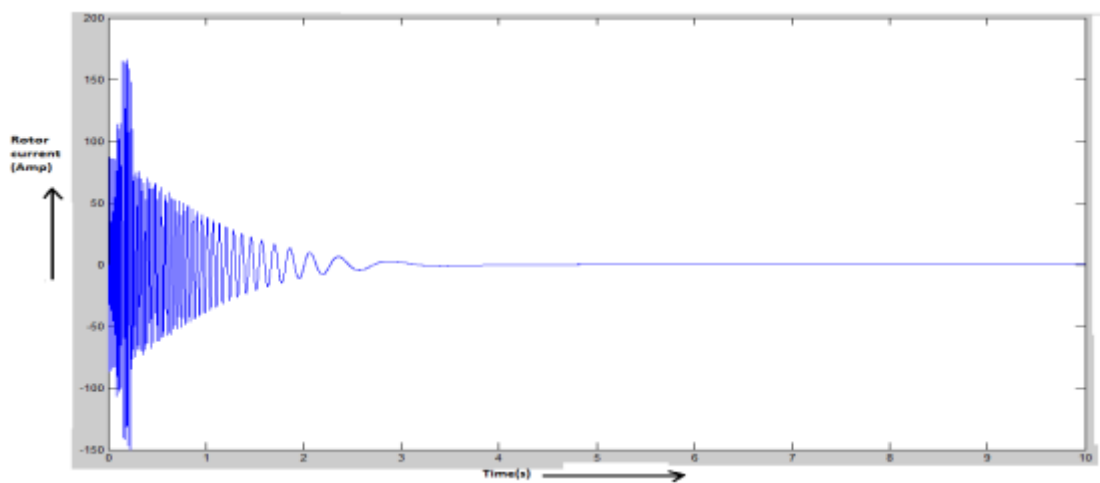
Figure 7.40(d) Rotor current variation with time for no load condition
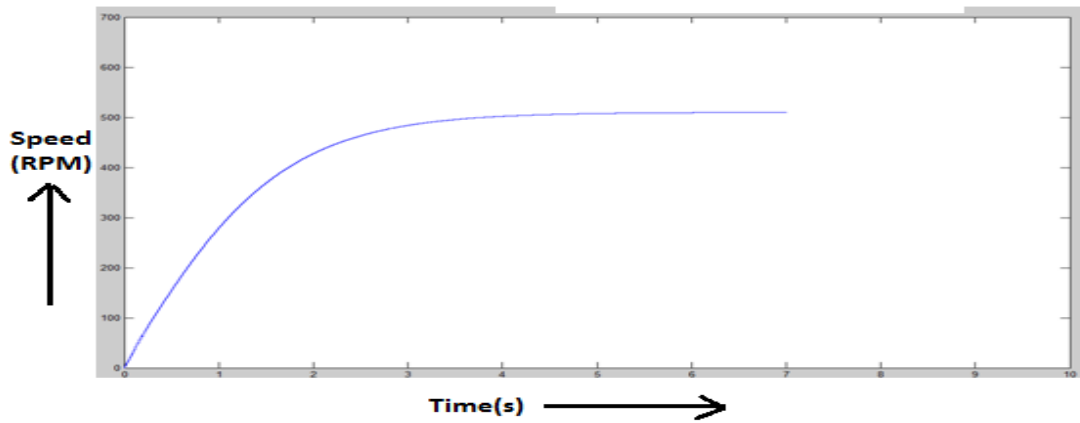
Figure 7.41 Speed variation with time for 1764N up the gradient load condition
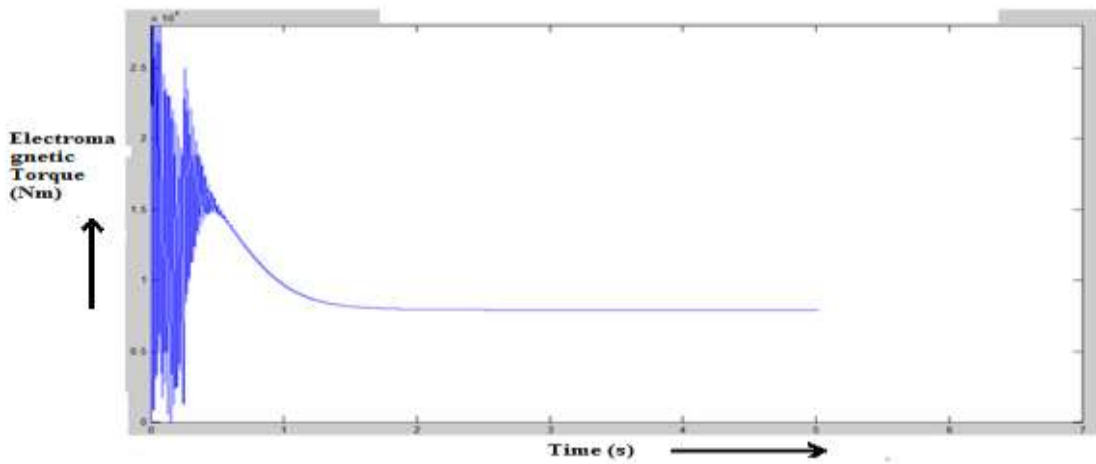
Figure 7.42(a)
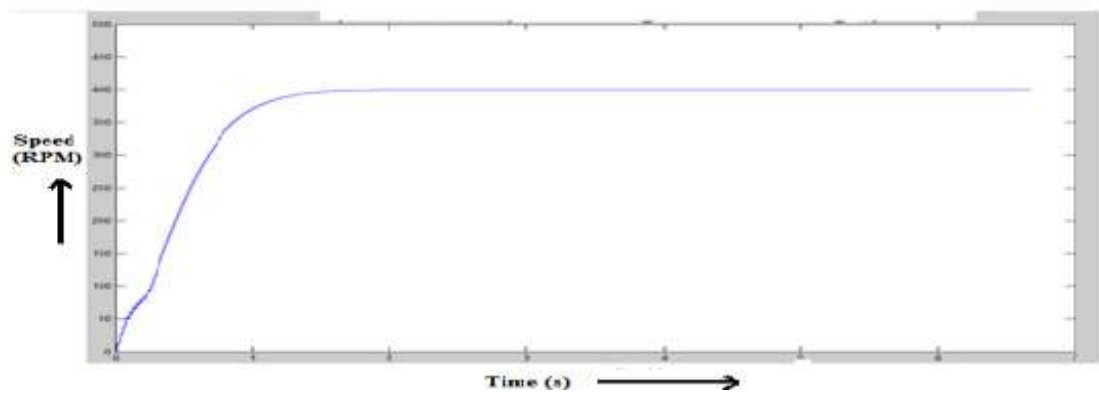
Figure 7.42(b)

Figure 7.42 (a) and (b) The electromagnetic torque and speed versus time for down the gradient load at150 hp haulage drive system -2
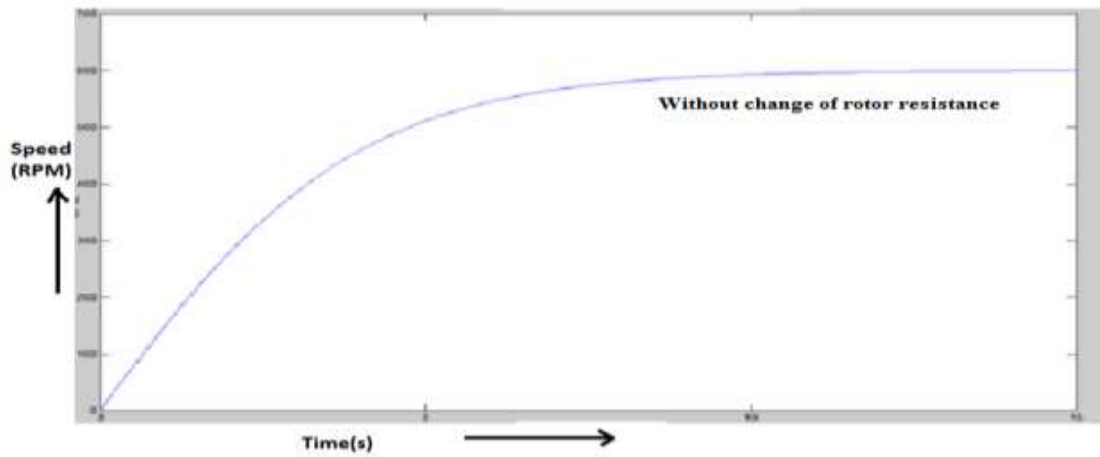
Figure 7.43(a) Variation of speed without change of the rotor resistance
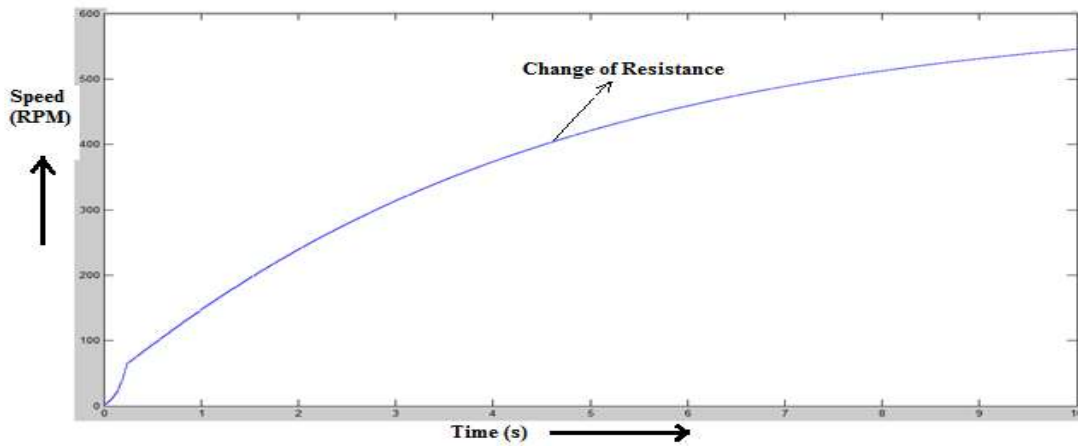
Figure 7.43(b) Variation of speed with change of rotor resistance

Figure 7.43(a) and (b) Speed variation with time for down the gradient
load 150hphaulagedrive system -2
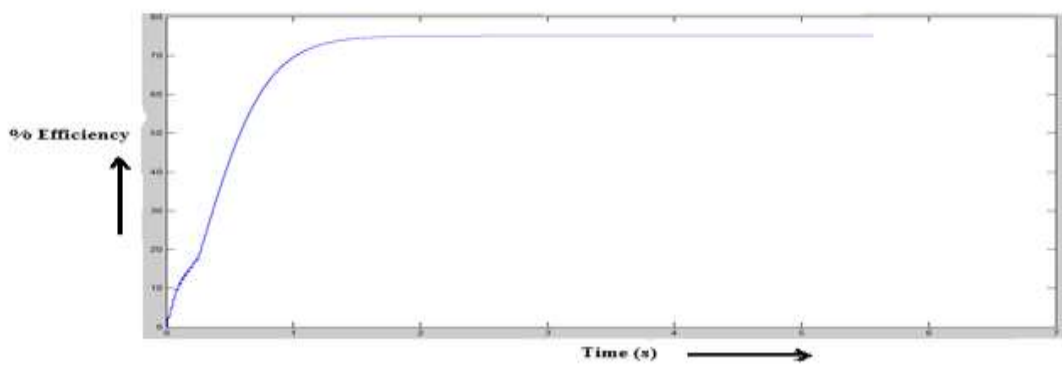
Figure 7.44(a)
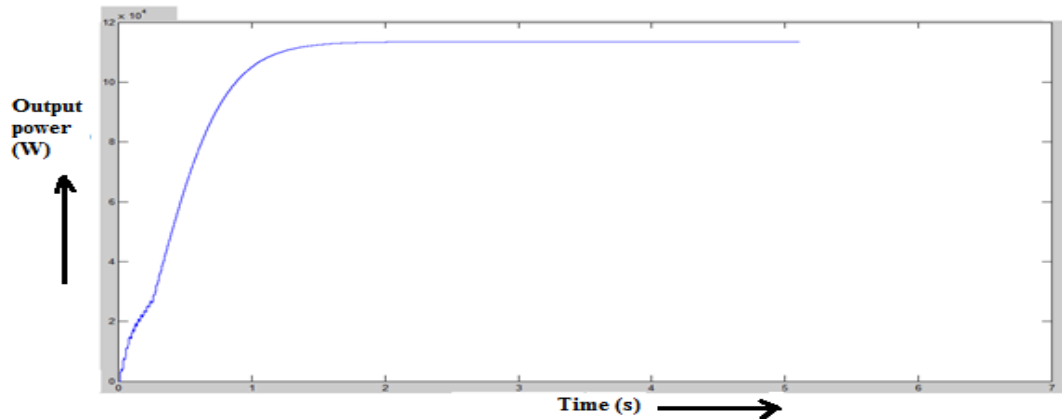
Figure 7.44(b)

Figure 7.44(a) and (b) % Efficiency and output power variation with time for down the gradient load 150hp underground haulage drive system-2

7.6.2 Micro controller drive system

The simulation results for open loop variable frequency control and closed loop control of both mine haulage drive system with the variation of energy, efficiency, Electromagnetic (EM) torque and speed with time are discussed. The simulation electrical parameter results obtained from open loop control of underground haulage drive system-2 for up the gradient are presented in Figure 7.45(a) and Figure 7.45(b). Similarly the Closed loop control simulation electrical parameters of 150hp underground haulage drive system-1 for up the gradient are shown in Figure 7.46 (a), Figure 7.46(b) and Figure 7.46(c) respectively.

The total energy consumption chart of 150hp underground haulage drive system-1 and haulage drive-2 are presented in Figure 7.47.The following observations are made in open and closed loop control drive system.

    i.   The system is stable in closed loop control because of feedback and well design of pi controller.

    ii.   Open loop system is unstable because accuracy in drive system is not good.

201

iii.   In closed loop variable frequency (v/f) controller simulation study results vary with 0.2 to 0.5 percent when compared to open loop control method simulation studies parameters.

iv.   The design of closed loop system is complicated and expensive when compared to open loop control drive.

All the above mentioned observations are also observed in simulation results related to open loop and closed loop control systems of 3hp and 150hp underground haulage drive systems.
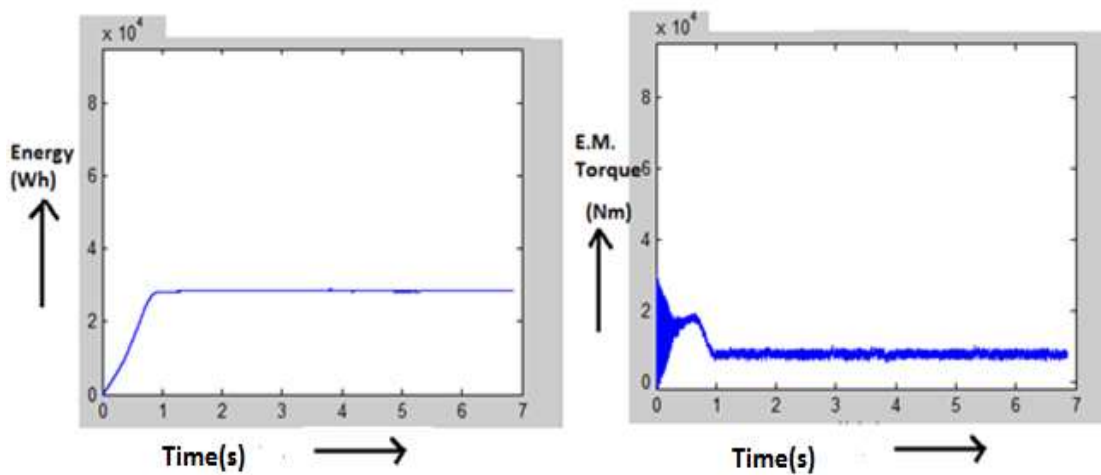
Figure 7.45 (a)
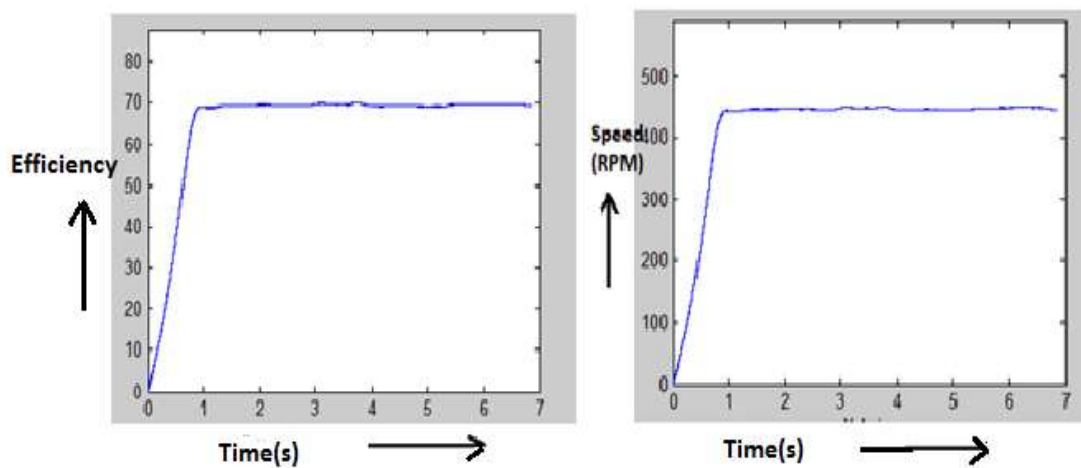
Figure 7.45 (b)

Figure 7.45(a) and (b) Open loop control simulation electrical parameters of 150hp underground haulage drive system-2 for up the gradient
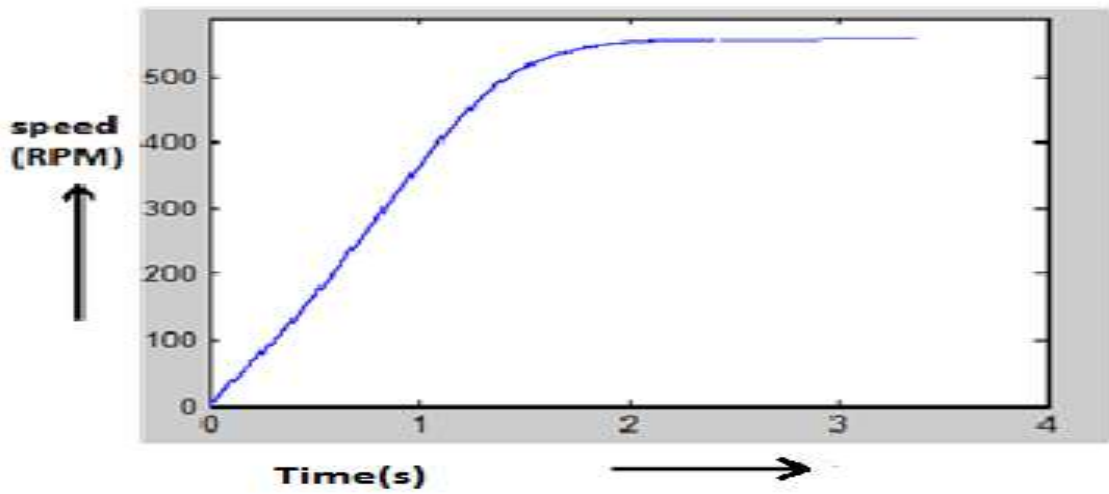
Figure 7.46(a)
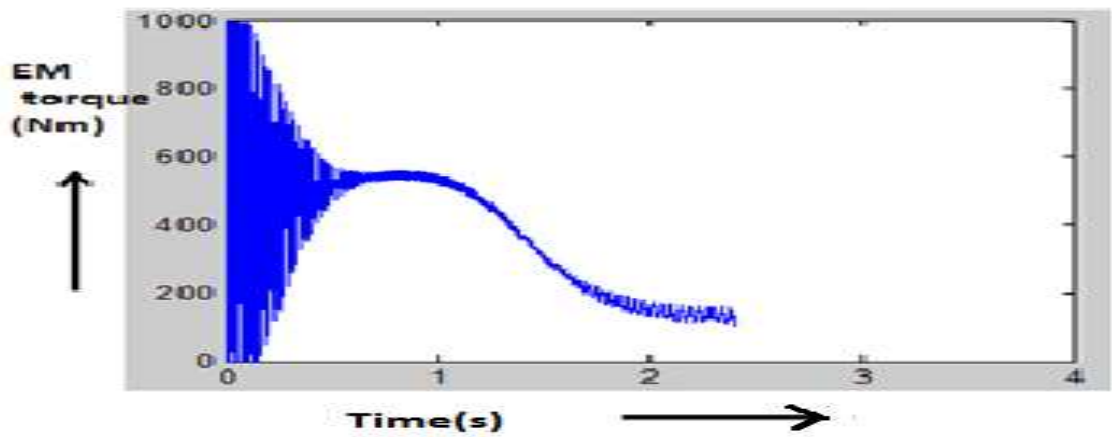
Figure 7.46(b)
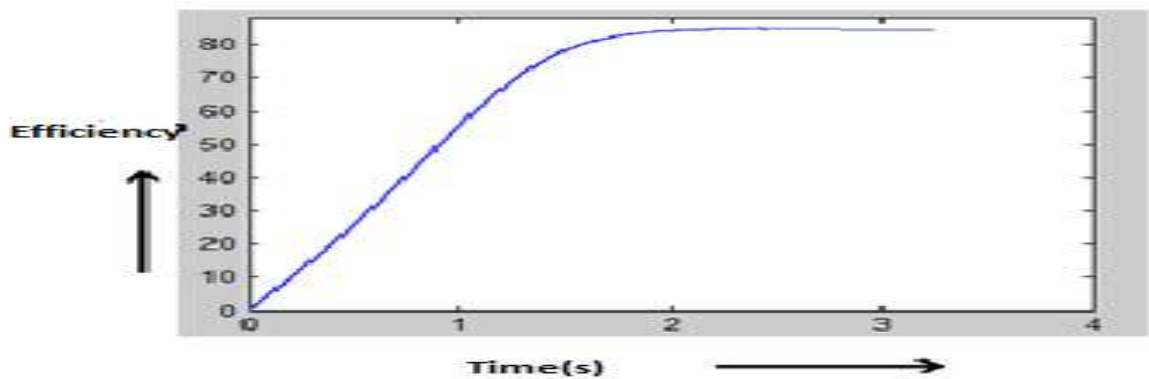
Figure 7.46(c)

Figure7.46 (a), (b) and (c) Closed loop control simulation electrical parameters of

150hp Underground haulage drive system-1

(up the gradient)

	Monthly	Yearly		
■ Drive system- 1 Down	2994.9	35938.8		
■ Drive System-1 Up	4222.86	50674.82		
■ Drive System -2 Down	20983.9	50674.82		
■ Drive System -2 Up	33110.16	397321.92		
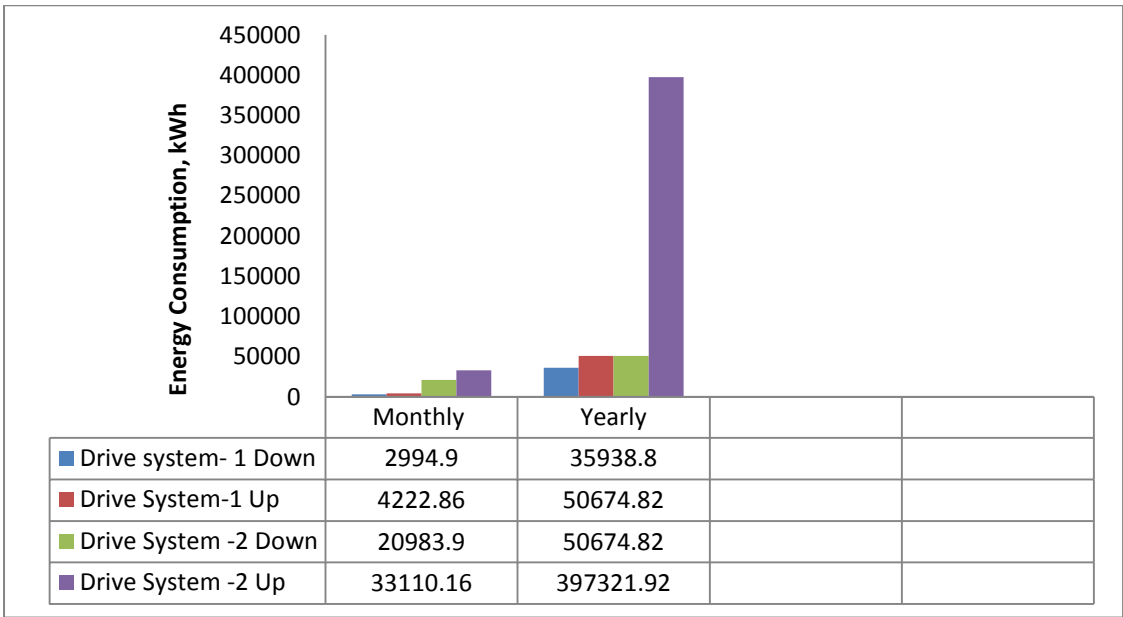
Figure 7.47 Total energy consumption chart for 150hp underground haulage drive

system-1 and haulage drive system – 2

The simulation study has been carried out according to the data obtained from the 150hp underground mine haulage drive GDK -10A (visited mine) and design of 3hp laboratory experimental haulage drive system. The obtained result clearly shows that the effect of energy consumption and power loss analysis for both the haulage drive system. From the simulation study results, it is observed that the amount of energy consumption is more in conventional control method of drive.

This method is useful with high starting torque and at below synchronous speed control. Simulation study for the micro controller (static) drive system on slip power recovery method (Krammer method of control) by using with controller and without controller simulated response results are studied and presented.

The slip power recovered of both methods of haulage drive systems by simulation, using the data obtained from field study of 150hp underground haulage drive system and 3hp laboratory experimental haulage drive system and observed that power conservation is improved by 8.5% to 9% when compared to conventional method of control. Therefore, micro controller (static control) method is very much suitable for haulage drive system in an underground coal mine application. With this

study it is concluded that microcontroller based slip power recovery slip ring induction motor drive is required for energy conservation.

In the simulation study of 3hp laboratory experimental haulage drive system by changing the angle of horizontal, effects of power consumption are observed on down the gradient and up the gradient of drive systems. In simulation results we observed that down the gradient drive requires less power when compared to up the gradient drive system.

7.6.3 Comparative results of 3hp laboratory experimental and 150hp underground mine haulage drive system (comparison of power recovery)

The comparative experimental results of conventional and micro controller method are presented in Table 7.9 and Table 7.10. The comparison study of experimental conventional and micro controller haulage drive system results shows that the micro controller based method gives 8 % to 9 % of power recovered from each level of drive system for up the gradient and down the gradient. The simulation study results of 150hp underground haulage drive and 3hp experimental haulage drive (conventional and micro controller) system 8.5 % to 9 % the slip power recovered from each level of drive system for up the gradient and down the gradient.

The 150hp underground haulage drive system field study results and comparative result of simulation and experimental studies on energy consumption for different combination of loads and gradients for up and down the gradients are presented in this section. The observation is mainly on the comparative slip power recovery for 150hp underground haulage drive system; 3hp laboratory experimental conventional and micro controller methods are presented.

Table 7.9 Comparative slip power recovery for experimental 3hp haulage drive conventional and micro controller method.

Angle with horizontal	Load (N)	Up the gradient				Down the gradient			
		Conventional method(output power (W)	Micro controller method(output power) (W)	Slip power Recovered (W)	% Power recovered	Conventional method output power (W)	Micro controller output power (W)	Slip Power Recovered (W)	%Power recovered
27^0	1079	979.45	1017.2	41.75	3.87	937.1	1007	69.9	6.94
	1275	1045	1123	78	7.46	1026.3	1114.6	88.3	8.6
	1471	1243.0	1344.7	101	8.18	1195.0	1309.4	114.4	9.57
	1765	1389.3	1519.2	129.9	9.35	1393.1	1516	122.9	9.97
29^0	1079	1045.3	1099	53.7	5.13	1016.8	1071	54.2	5.33
	1275	1114.4	1202	87.6	7.86	1106.9	1193.25	86.35	7.80
	1471	1325.7	1470.5	144.8	9.84	1295.7	1418.2	122.5	9.45
	1765	1490.7	1653.21	162.5	10.90	1497.2	1653.4	156.13	10.43
32^0	1079	1080.5	1147.4	70	6.19	1076.3	1134.80	58.5	5.43
	1275	1174.1	1267.5	93.4	7.95	1170.9	1252.4	81.5	6.96
	1471	1377.4	1509.6	132.2	9.59	1359.1	1483.73	124.63	9.17
	1765	1570	1751	181	11.52	1535.2	1709.3	174.1	10.18
35^0	1079	1174.8	1243.9	69	5.88	1100.1	1188.80	88.7	8.06
	1275	1277.4	1380.5	88.5	8.07	1215.6	1319.35	103.75	8.53
	1471	1408.5	1515	106.5	8.56	1359.9	1557	140.9	12.65
	1765	1614.8	1766.87	152	9.41	1613.5	1805	191.5	11.86

Table 7.10 Comparative slip power recovery for 150hp underground mine haulage drives system conventional and micro controller method.

Torque (Nm)	Haulage drive system -1				Torque (Nm)	Haulage drive system -2			
	Conventional method output power (W)	Micro controller method output power (W)	Slip power Recovered (W)	% slip power recovered		Conventional method(output power) (W)	Micro controller method output power (W)	Slip power Recovered (W)	%Slip power recovered
6668	97785.3	110052	12265.7	11.14	7841	119174.4	127974	8799.6	7.38
6521	98040.4	108583	10542.6	9.70	7254	111742.6	119724	7981.4	7.14
6081	92436.6	100810	8373.4	9.05	6961	105799.4	114888	9088.6	8.59
5641	86895.5	93930	7034.5	8.09	6521	98040.45	109061	11020.5	11.24
4908	76360.2	82264	5903.8	7.73	6081	90301.15	102149	11847.8	11.59
3734	58861.6	63408	4546.0	7.72	4614	67663.7	77506	9842.3	12.69
3539	57096.1	60357	3260.9	5.71	3979	57789	67569	9780	10.20
7943	116483.0	129639	13156.0	11.29	3734	55448.86	63682	8233.14	8.9
6363	94488.7	105.719	11230.3	11.88	5204	81767.1	87416	5648.9	6.68
6047	90914.06	94391.6	3477.54	3.82	6342	99517.5	105137	5619.5	5.64
6067	90914.06	93.457	2542.94	2.8	7332	112944	120742	7798	6.90
					9313	138295	150292	11997	9.61
					9403	139653	152088	12435	10.42

The energy conservation(saving)are obtained from the 150hp underground haulage drive system for both methods (conventional and simulation results (micro controller methods) are shown in Table 7.11 and the energy conservation (saving) are obtained from 3hp laboratory experimental(conventional and micro controller) haulage drive system are also shown in Table 7.12. It is observed that the 150hp underground haulage drive stsyem-1 and haulage drive system-2 based on microcontroller method control (simulation studies) the energy consumption reduced to 655237.3 kWh. Similarly in Table 7.12 energy conservation of 3hp laboratory experimental haulage drive system the consumption reduced to 47564.3 kWh.

Table 7.11 Energy conservation of 150hp underground haulage drive system in an underground coal mine

Conventional method(field study)		Micro control method (simulation study)		Energy consumption (kWh)
Drive system -1	Drive system -2	Drive system -1	Drive system-2	
95444.8kWh	607356.8 kWh	86517 kWh	568720.3 kWh	
Total energy consumption (kWh)				
702801.6 kWh (Addition of annual energy for up and down the gradient)		655237.3 kWh (Addition of annual energy for up and down the gradient)		(702801.6-655237.3)= 47564.3 kWh

Table 7.12 Energy conservation of experimental 3hp laboratory haulage drive system

Conventional method	Micro controller method	Energy consumption (kWh)
Total energy consumption (kWh)		
1158.23 kWh(Addition of annual energy for up and down the gradients)	1023.159 kWh (Addition of annual energy for up and down the gradients)	(1158.23- 1023.15)= 135.23 kWh

7.6.4 Conventional method 3hp haulage drive system (Simulation results and discussion)

Simulation results of conventional method of 3hp haulage drive system are represented in graphical form in Figure 7.48, considering the influence of angles on energy consumption when the load is constant. In Figure 7.49, the influence of load

on energy consumption when the angle is constant for up the gradient and down the gradient of the drive system is considered. The graphical observation of simulated results clearly indicates the variation of energy is depends mainly the angle with horizontal, also the up the gradient and down the gradient of drive system of Figure 7.49. Also the up gradient drive consumes more than the down gradient system can be observed in the present graphical simulation results.
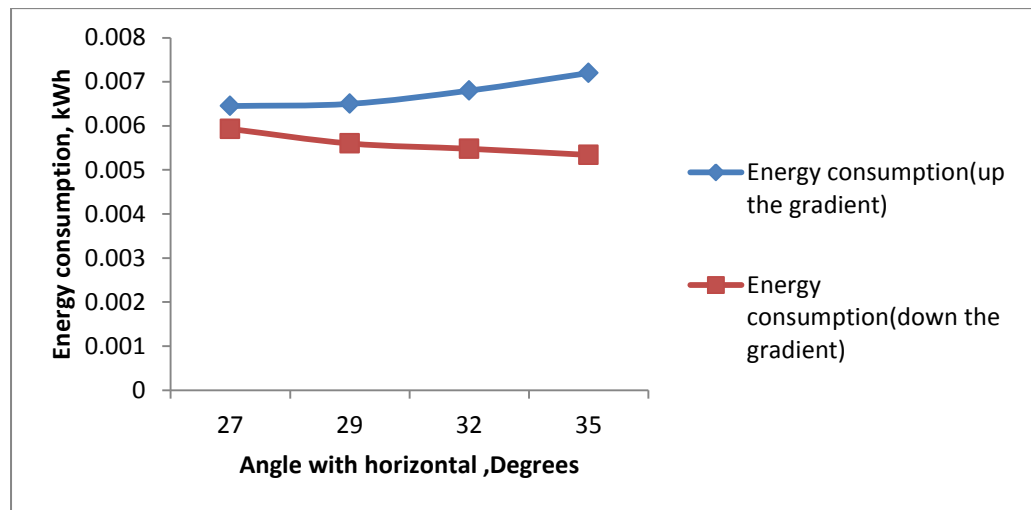
Figure 7.48 Influence of angles on energy consumption (constant load of 1079) for both gradients of the drive (simulation)
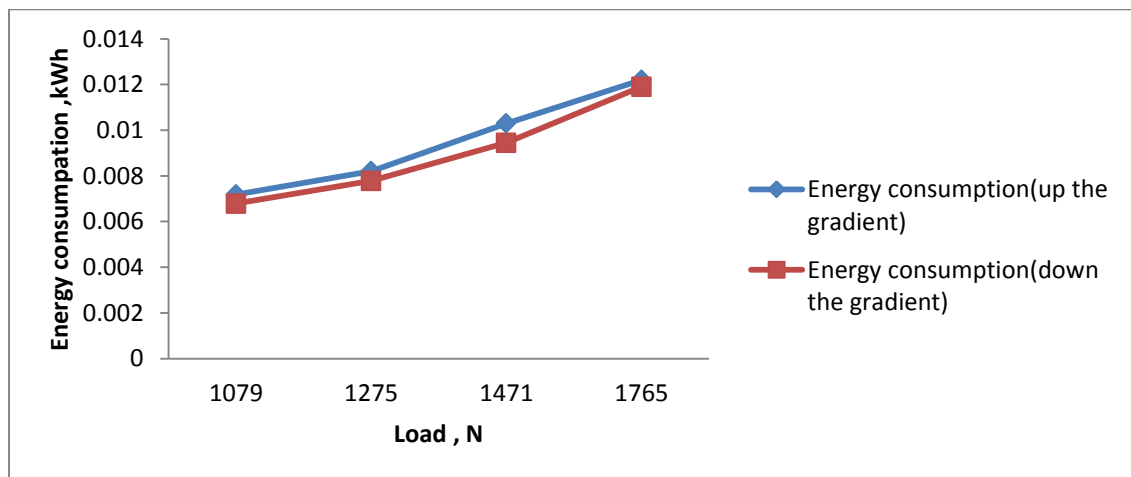
Figure 7.49 Influence of load on energy consumption (constant angle 35^0) for both gradients of the drive (simulation)

Influence of load on energy consumption by considering two variables can be observed by the following inference i) when load is constant and angle is variable, then the energy consumption increases linearly for up the gradient and down the gradient, ii) When the angle is constant and load is variable, then the energy consumption increases linearly for up the gradient and down the gradient.

7.6.5 Micro control method 3hp haulage drive system (Simulation results and discussion)
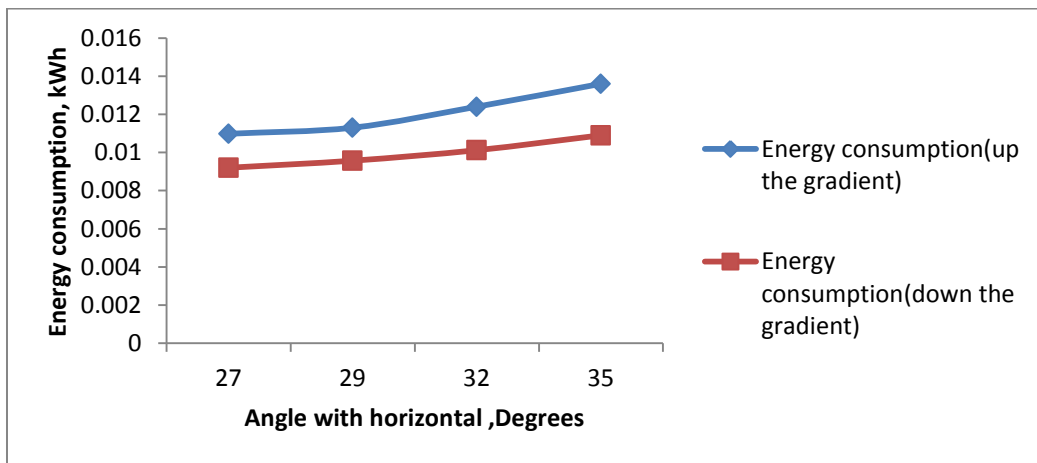
Figure 7.50 Influence of angles on energy consumption (constant load of 1765 N) for both gradients of the drive (simulation)
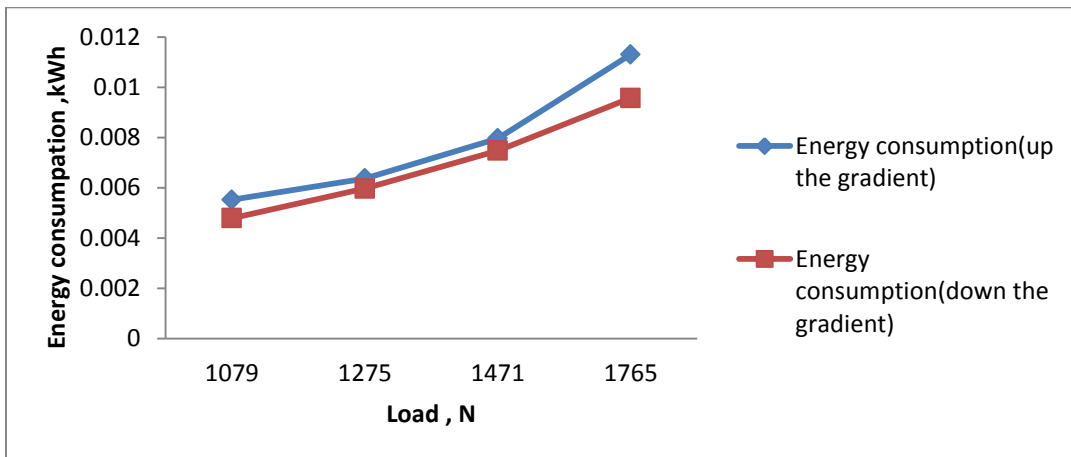
Figure 7.51 Influence of load on energy consumption (constant angle 29^0) for both gradients of the drive (simulation)

Similarly Simulation results of micro controller method of experimental 3hp haulage drive system are represented in graphical form in Figure 7.50 , considering the influence of angles on energy consumption when the load is constant (1765 N). In

Figure 7.51, the influence of load on energy consumption when the angle is constant (29^0) for up the gradient and down the gradient of the drive system is considered. The graphical observation of simulated results clearly indicates the variation of energy is depends mainly the angle with horizontal, also the up the gradient and down the gradient of drive system.

7.6.6 Conventional method 150hp haulage drive system (Simulation results and discussion)

The gradient of the coal seam is 1 in 4 (i.e.14.04^0) .Therefore coal seam is considered as 14.04^0 the same gradient used for entire simulation as well calculation purpose in this thesis. The 150hp underground haulage drive system the influence of angle on energy consumption is not variable because the coal seam fixed. The only influence of load on energy consumption is considered for up the gradient and down the gradient of the haulage drive system.

Simulation results of conventional method of 150hpunderground haulage drive system represented graphical form as shown in Figure7.52. Influence of load on energy consumption for down the gradient and up the gradient   for150hp haulage drive system -1 drive system-2 are shown in Figure 7.53. As per simulation study load was increases and the energy consumption was decreases linearly because the energy depends on the power and time. Therefore the same observation noticed in the field study results also and discussed in section 7.1.
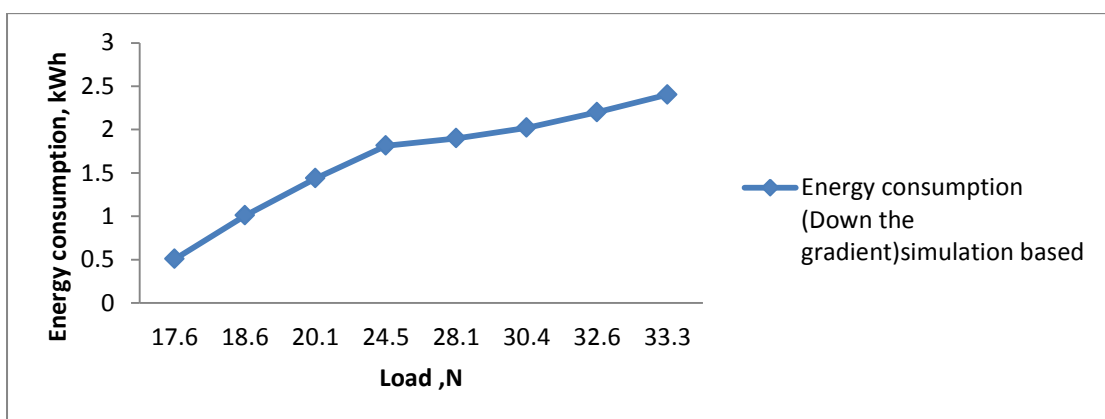
Figure 7.52 Influence of load on energy consumption (constant angle 14^0) for 150hp haulage drive system -1 for down the gradient (simulation)
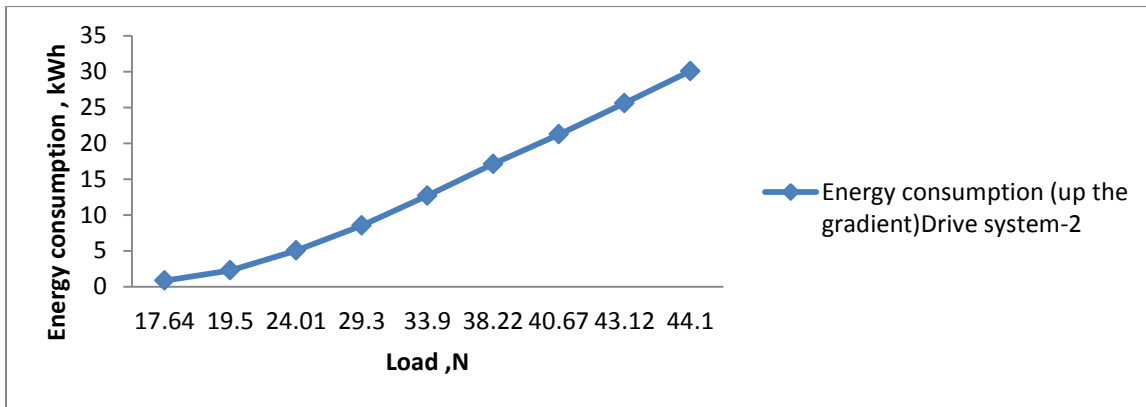
Figure 7.53 Influence of load on energy consumption (constant angle 14^0) for 150hp

haulage drive system – 2 for down the gradient (simulation)

7.6.7 Micro controller method 150hp haulage drive system (Simulation results and discussion)
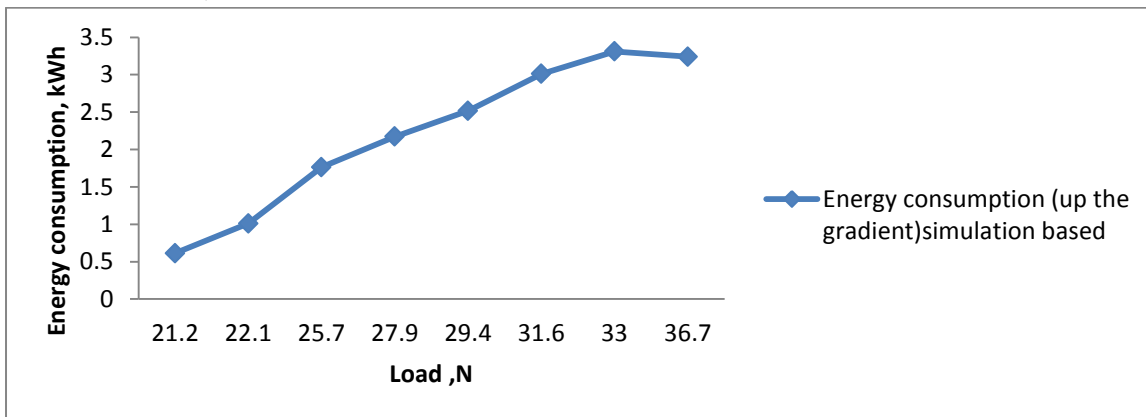
Figure 7.54 Influence of load on energy consumption (constant angle 14^0) for 150hp

haulage drive system -1 for up the gradient (simulation)
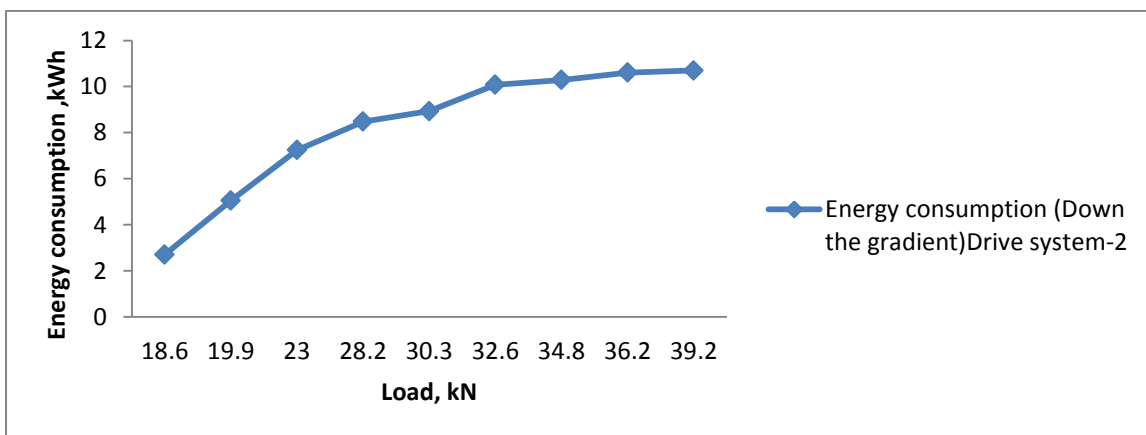
Figure 7.55 Influence of load on energy consumption (constant angle 14^0) for 150hp
haulage drive system – 2 for down the gradient (simulation)

Simulation results of micro controller method of 150hp underground haulage drive system represented graphical form as shown in Figure 7.54. Influence of load on energy consumption for down the gradient and up the gradient for 150hp haulage drive system -1 and down the gradient drive system-2 are shown in Figure 7.55.

As per simulation study load was increases and the energy consumption was decreases linearly because the energy depends on the power and time. And also some level consumption of energy is decreases because of load on haulage are decreases. Therefore the same observation noticed in the field study results also and discussed in section 7.1.

7.6.8 Cost analysis of 150hp underground micro controller based haulage drive System.

The cost analysis is done based for the results obtained from micro controller based simulation studies of 150hp underground haulage drive system -1 and haulage drive system-2 by considering present tariff. The total energy consumption of drive system in mine is 65, 52, 37.3kWh. The total energy consumption per year and total cost of energy per year for drive system are 655237.3kWh and Rs.45, 86,661/-, respectively. Maximum demand charges for 150hp underground haulage

drive system -1 110.25KVA @ Rs.150KVA = Rs.16, 537.00

Maximum demand charges for 150hp underground haulage

drive system -2 110.25KVA @ Rs.150KVA = Rs.16, 537.00

Energy Charges for two drive system Total kWh 655237.3kWh @ Rs.7.00 kWh

= Rs.45, 86,661/-.

CHAPTER 8

CONCLUSIONS AND SCOPE FOR FUTURE WORK

8. 1 CONCLUSIONS

The conclusions drawn from the current study are:

➤ **FIELD STUDIES**

1. The energy consumption for down the gradient and up the gradient for 150hp haulage drive system -1 (i.e. serving from surface to 8th level and 8th level to surface, distances of 0.75 km and time from 19(s) to 180(s)) was varied 78.60% (from 0.509 kWh to 2.379 kWh) and 79.79% (from 0.728 kWh to 3.603 kWh) respectively (Table 3.1 to Table 3.2).

2. Similarly, the energy consumption for 150hp haulage drive system -2 for down the gradient and up the gradient (i.e. serving from 8th level to 42nd level and 42nd level to 8th level, distance of 4.25 km and time period of 84(s) to 840(s)) was varied 74.86% (from 2.780 kWh to 11.06 kWh) and 97.64% (from 0.824 kWh to 32.53kWh) respectively (Table 3.3 to Table 3.4).

3. The power output was varied 41.76% (from 57096.1W (minimum load, 17.64N) to 98040.4W (maximum load, 32.65 kN)) of down the gradient of haulage drive system-1. Similarly the power output was varied 38.12% (from 72071.67 W (minimum load, 21.0kN) to 116483.0 W (Maximum load, 36.7 kN)) to for up the gradient haulage drive system-1(Table 3.1 to Table 3.2).

4. Similarly the power output was varied 53.47% (from 55448.86 W (minimum load, 19.8 kN) to 119174.4 W (maximum load, 39.2 kN)) for down the gradient of haulage drive system-2. Similarly the power output was varied 55.73% (from 61816.1W (minimum load, 17.6 kN) to 139653.0 W (Maximum load, 44.1kN) for up the gradient haulage drive system-2 (Table 3.3 to Table 3.4).

The field study results on energy consumption the suggestions are provided for replacement of various conventional methods in the regions where electrical energy is being wasted. Conventional haulage drive system consumes more power and hence it should be replaced by energy efficient drive system.

To reduce the power consumption static speed control method should be implemented such as slip energy recovery system for closed loop control, chopper controlled slip ring induction motor control etc. Instead of rheostatic method, the gadget speed control method should be implemented thereby saving the energy of about 10% to 15% or more by providing micro controller based drive system for the 150hp underground incline coal mine haulage drive system.

> **EXPERIMENTAL STUDIES WITH 3HP HAULAGE DRIVE SYSTEM**

a) Conventional control method.

1. The energy consumption was varied 48.07% (from 0.00652 kWh to 0.01119 kWh for up the gradient and 43.90% (from 0.005856 kWh to 0.01044 kWh for down the gradient as the load was varied (from 1079 N to 1765 N)) at a distance of 5 m (Table 4.2 to Table 4.3).

2. The energy consumption was varied 33.09% (from 0.00750 kWh to 0.011211kWh) for up the gradient and 33.10% (from 0.006722 kWh to 0.01120 kWh) for down the gradient as the load was varied (from 1079 N to 1765 N) at a distance of 5 m (Table 4.2 to Table 4.3).

3. The energy consumption was varied 11.39% (from 0.00754 kWh to 0.00851 kWh) for up the gradient and 11.27% (from 0.00691 kWh to 0.00776 kWh) down the gradient, as the gradient was varied (from 27º to 35º) (Table 4.2 to Table 4.3).

4. The power output was varied 71.71% (from 1614.8 W (maximum load (1765N) gradient (35°) to 5709.61W (minimum load (1079N) and gradient (27°)) of down the gradient of haulage drive system. Similarly the power output was varied 41.92% (from to 937.1 W (minimum load (1079N) to 1613.5W (maximum load (1765N) gradient (35°) to 937.1 W (minimum load (1079N) and gradient (27°) for up the gradient haulage drive system (Table 4.2 to Table 4.3).

b) Micro controller method

1. The energy consumption was varied 48.16% (from 0.00565 kWh to 0.0109 kWh) for up the gradient and 51.03% (from 0.00568 kWh to 0.0116 kWh)for down the gradient as the load was varied 38.86% (from1079 N to 1765 N) (Table 4.5 to Table 4.6).

2. The energy consumption was varied 37.85% (from 0.00691 kWh to 0.01112 kWh) for up the gradient and 46% (from 0.00594 kWh to 0.0110 kWh) for down the gradient as the load was varied 38.86% (from1079 N to 1765 N) (Table 4.5 to Table 4.6).

3. The energy consumption was varied 41.63% (from 0.00509 kWh to 0.00972 kWh) for the up gradient and 49.44% (from 0.00504 kWh to0.00997 kWh) for down the gradient as the load was varied 38.86% (from1079 N to 1765 N) (Table 4.5 to Table 4.6).

4.The energy consumption was varied 14.73% (from 0.006864 kWh to0.00805 kWh) for up the gradient and 11.06% (from 0.00619 kWh to 0.00696 kWh) down the gradient, as the gradient was varied (from 27° to 35°) (Table 4.5 to Table 4.6).

5. The power output was varied 42.42% (from 1017.2 W (minimum load (1079N) to 1766.87W (maximum Load (1765N) gradient (35°) and gradient (27°)) of down the gradient of haulage drive system. Similarly the power output was varied 45.16% (from 1007 W (minimum load (1079N) to 1805 W (maximum Load (1765N) gradient (35°) and gradient (27°) for up the gradient haulage drive system (Table 4.5 to Table 4.6).

> **COMPARISION BETWEEN CONVENTIONAL AND MICRO CONTROLLER METHOD IN LABORATORY EXPERIMENTAL STUDIES**

EXPERIMENTAL STUDIES

(Comparison between conventional results and micro controller method (3hp experimental laboratory haulage drive system).

1. The slip power recovered (saving) was varied 66.02% (from 0.04175 kW to 0.1229 kW) for up the gradient and 43.12% (from 0.0699 kW to 0.1229 kW) for down the gradient as the load was varied. In micro controller method when compared to conventional method (Table 7.9).

2. The slip power recovered (saving) was varied 11.86% (from 0.078 kW to 0.0885 kW) for up the gradient and 14.84% (from 0.0883 kW to 0.10373 kW) for down the gradient, as the gradient was varied In micro controller method when compared to conventional method (Table 7.9).

➢ **SIMULATION STUDY**

FIELD STUDIES

(150hp underground haulage drive system and 3hp experimental drive haulage system)
a) Conventional control method

    1. The energy consumption is generally was varied for (down the gradient and up the gradient) for 150hp haulage drive system -1 (i.e. serving from surface to 8th level and 8th level to surface) was varied 78.9% (from 0.507 kWh to 2.403 kWh) and 80.33% (from 0.709 kWh to 3.605 kWh) (down the gradient and up the gradient) respectively (Table 6.4 to Table 6.5).

    2. Similarly the energy consumption for 150 hp haulage drive system -2 (i.e. serving from 8th level to 42nd level and 42nd level to 8th level) was varied 78.35% (from 2.62 kWh to 12.104 kWh) and 32.85% (from 0.835 kWh to 30.05 kWh) respectively (Table 6.6 to Table 6.7).

 b) Micro controller method

    1. The energy consumption down the gradient and up the gradient for 150hp haulage drive system -1 (i.e. serving from surface to 8th level and 8th level to surface) was varied 77.46% (from 0.489kWh to 2.17kWh) and 80.83% (from 0.612kWh to 3.194kWh) respectively (Table 6.11to Table 6.12).

    2. Similarly energy consumption for 150hp haulage drive system -2 (i.e. serving from 8th level to 42nd level and 42nd level to 8th level) was varied 78.91% (from 2.17 kWh to 10.70 kWh) and 97.79% (from 0.693 kWh to 31.47kWh) respectively (Table 6.13 to Table 6.14).

c) Comparison between the results of conventional method and micro controller method obtained from field and simulation study.

    1. The slip power recovered (saving) for down the gradient and up the gradient for 150hp haulage drive system -1 (i.e. serving from surface to 8th level and 8th level to surface) was varied 62.49 % (from 4.6 kW to12.265 kW) and 80.67% (from 13.156 kW to 2.542 kW) respectively (Table 7.10).

    2. Similarly the slip power recovered (saving) for 150hp haulage drive system-2 (i.e. serving from 8th level to 42nd level and 42nd level to 8th level) was

varied 36.84% (from 7.730 kW to 12.239 kW) and 58.17% (from15.208 kW to 6.36 kW) respectively (Table 7.10).

3.The power output was varied 44.41% (from 108583 W (maximum load) to 60357 W (minimum load))of down the gradient of haulage drive system-1.Similarly the power output was varied 43.13% (from 129639 W (Maximum load) to 73716 W (minimum load, 21.0 kN)) for up the gradient haulage drive system-1(Table 7.10).

4. The power output was varied 50.74% (from 63682 W (minimum load) to 127974 W (maximum load) for down the gradient of haulage drive system-2. Similarly the power output was varied 56.82% (from 65669 W (minimum load, 17.6kN) to 152088 W (Maximum load)) for up the gradient haulage drive system-2 (Table 7.10).

➢ **EXPERIMENTA STUDIES WITH 3HP HAULAGE DRIVE SYSTEM**
a) Conventional control method

1. The energy consumption was varied 42.98% (from 0.00593 kWh to 0.0104 kWh) for up the gradient and 52.50% (from 0.00645 kWh to 0.01358 kWh) for down the gradient as the load was varied (Table 6.2).

2. The energy consumption was varied 6.8% (from 0.00765 kWh to 0.00821 kWh) for up the gradient and 10.01% (from 0.00700 kWh to 0.00778 kWh) for down the gradient, as the gradient was varied (Table 6.3).

b) Micro controller method

1. The energy consumption was varied 48.16% (from 0.00567 kWh to 0.0116 kWh) for up the gradient and 60% (from 0.00503 kWh to 0.0126 kWh) for down the gradient as the load was varied (Table 6.9).

2. The energy consumption was varied 14.73% (from 0.006864 kWh to 0.00805 kWh) for up the gradient and 11.06% (from 0.00619 kWh to 0.00696 kWh) down the gradient, as the gradient was varied (Table 6.10).

The simulation field study results along with field study datas are simulated by using MATLAB/ SIMULINK software package. The simulation results for field study (conventional and micro controller method) and 3hp laboratory experimental (conventional and micro controller method) haulage drive system study on energy consumption results was varied from 8.5 % to 9 %.

8.2 SCOPE FOR FUTURE WORK

This thesis successfully demonstrates the potential of conventional and micro controller based energy conservation study on mine haulage drive system. Doubly-fed wound rotor induction motor schemes of operation can also be used in high power drives. The closed loop control haulage drive system directly connected to grid so that the drive system can run without operator. The operation of car to different level by using remote sensing technique to control is also possible by implementing the software so that whole drive system automatically operated.

The entire haulage drive can be designed for closed loop control by using same micro controller technique. However, with the stator connected to a constant frequency source, the speed cannot be further increased. Moreover, it is not possible to obtain speed reversal with the present arrangement. Instead of connecting the stator to the grid which is fed from a voltage source inverter, the speed range of the system can be further extended and speed reversal can also be achieved. This scheme will be attractive in high speed, high torque applications. Direct torque control algorithms can be developed for such doubly-controlled machines. It simultaneously opens many possibilities for selecting the switching states of the inverters.

There is a growing awareness for power electronic systems need to be modularized, so that systems of larger ratings can be developed by integrating low power modules. High frequency IGBT inverters are now commercially available up to a rating of 250 kW. A doubly-controlled induction machine may be designed with split-phase rotor and stator windings, each being fed from a standard inverter module.

The number of split phase windings used will depend on the required power rating of the drive.. The micro controller based slip power recovery drive haulage system with automatic controlled man riding car, by using wireless technique to control the car to different level of the mine without operator can be implemented by conserving the energy of the rope haulage system of the underground mines.

REFERENCES

Ajay Kumar., Aggarwal, S. K., Saini, L. M. and Ashwani K. (2011). "Performance analysis of a microcontroller based slip power recovery drive." International Journal of Engineering, Science and Technology., 3(8), 25-35.

Akplnar.E and Pillay, P. (1990). "Modeling and Performance of Slip Energy Recovery Induction Motor Drives ", IEEE Transactions on Energy Conversion, 5(1), 612-618.

Annual report of SCCL, Ministry of coal. April , 2009.

Brig,A.R. (2012). "Constant v/f induction motor drive with synchronized space vector pulse width modulation", IET Power Electron., 5 , 1446-1455.

Bose, B.K. (1987). "Microcomputer control of power electronics and drives." IEEE Press, 235-267.

Bose, B.K. (1997). " Power Electronics and Variable Frequency Drives." IEEE Press, 134-176.

Bose,B.K.(1982)."Adjustable Speed Ac Drive-A Technology Status Review". IEEE Proceedings.,70, 2-6.

Chattopadhyay,A.(1978). "An Adjustable-speed induction motor drive with a Cycloconverter-Type Thyristor-Commutator in the Rotor," IEEE Trans. Ind. Appl., 12(2), 116-122.

Chakrabarti,P.K. and Shrivastava .1992). "Energy Management in Mechanized Mines in India" ,Proc. of Management of Mine Mechanization ,MGMI publication, 1-16.

Chandan,PardhiAbhishek,Yadavalli Swati , and G. Arunkumar. (2014). "A Study of Slip-Power Recovery Schemes with a Buck DC Voltage Intermediate Circuit and Reduced Harmonics on the Mains by various PWM Techniques" 2014 IEEE International Conference on Power and Advanced Control Eng., 297-302

Cunha, B. S., Camacho, J. R. Bissochi, C. A. (2001). "Single phase induction motor speed control through a PIC controlled Sinusoidal PWM inverter", IEEE Porto Power Tech Conference, September, 7803-7139.

Dhaval D. Mer, Rakeshkumar, Patel,A. and Manish G. (2014)."Comprehensive Study of Speed Control And Power Loss Analysis Using Rotor Resistance And Slip

Power Recovery Method." International journal of innovative research in electrical, electronics, instrumentation and control Eng ., 2(3), 214-221.

Doradla, S. R., Chakravorty, S. and Hole, K. E. (1988). "A new slip power recovery scheme with improved supply power factor." IEEE Transaction on Power Electronics, 3(2), 200-207.

Deepali, shirk, Haripriya, Kulkarni,H.(2013). "Microcontroller Based Speed Control of Three Phase Induction Motor Using V/F Metod", International Journal of Scientific and Research Publications, 3 , 2250-3153.

EI-Samathy, A.A., Amin, M.A., EI-Tanaby, E.T. and Sayed, A. A. (1969). "Modeling and speed control scheme for the static kramer drive." Proc. of IEEE Transactions on industry and general applications, 584-588.

Erlicki, M.S.(1965). "Inverter Rotor Drive of an Induction Machine," IEEE Trans. Pow. App. and Sys, 84(11), 1011-1016.

Energy Audit Report for HOCL by CPRI, Bangalore, April 2007.

Gajare, A M., Nitin ,R., Bhasme. (2012). "A Review on Speed Control Techniques of Single Phase Induction Motor", International Journal of Computer Technology and Electronics Engineering (IJCTEE)., 2, 33-39.

Ghani.S.N.,(1988). "Digital Computer Simulation of Three-Phase Induction Machine Dynamics - A Generalized Approach." IEEE Trans Industry Appl., 24(1), 106–114.

Guru Deep singh. (1994). "Augmentation of underground Pumped out water for potable purpose from coal mines of Jharia coalfield". Proceedings 5th international mine water congress, Nottingham (U,K). 125-139.

Giesselmann,M .Salehfar, H.. Toliyat, H.A and. Rahman T.U ,(2002). "Modulation Strategies,"CRC Press LLC, 235-253.

Guru Deep singh. (1994). "Augmentation of underground Pumped out water for potable purpose from coal mines of Jharia coalfield". Proceedings 5th international mine water congress, Nottingham (U,K). 125-139.

Heising, C. R. (1982). "Quantitative Relationship between Scheduled Electrical Preventive Maintenance and Failure Rate of Electrical Equipment." IEEE Transactions on Industry Applications, 18(3), 268-272.

Jagendrasingh, Swati Rani, Rohini. (2010). "Slip Power recovery system in Three Phase Slip Ring Induction motor." IOSR Journal of Electrical and Electronics Eng., 43-46.

Kawabata, Y. Ejiogu, E. and Kawabata, T.(1999). "Vector-Controlled Double-Inverter-Fed Wound-Rotor Induction Motor Suitable for High-Power Drives," IEEE Trans. Power Electronics, 35(5), 1058-1066.

Kumar, K.V. Michael, P.A. John, J.P. and Kumar, S.S. (2010). "Simulation and Comparison of SPWM and SVPWM control for Three Phase Inverter," Asian Research Publishing Network, 5(7), 61-74.

Krause, P. C. (1965). "Simulation Of Symmetrical Induction Machinery', IEEE T rans. Power Apparatus Systems., 84(11), 1038–1053.

Lavi, A. and Polge, R. J. (1966). "Induction Motor Speed Control With Static Inverter in The Rotor." IEEE Transaction on Power Apparatus and Systems, 85 (1), 76-84.

Liao, F. JI Sheng and Thomas, A. L. (1991)."A New Energy Recovery Scheme For Doubly Fed, Adjustable-Speed Induction Motor Drives." IEEE Transaction on Industry Applications, 27(4), 728-733.

Long, W.E .and Schmitz, N.L. (1971). "CycloconverterControl Of The Doubly Fed Induction Motor," IEEETrans. Ind. and Gen. Appl., 7(1), 95-100.

Mahto,T. (2009). "Energy Management in Underground Mines –A Case Study" ,Coal Mining Technology &Management, 23-32.

Nehrir, M. H. Fatehi, F. and Gerez, V. (1995) ."Computer Modeling For Enhancing Instruction Of Electric Machinery," IEEE Transactions on Education, 38(2), 166–170.

NGEF Ltd., (1995) Standard Induction Motors Catalogue.

Pradhan,G.K. and Chakraborti,A.(2010). "Energy Conversation in Mines- The Indian initiatives." J.The Indian Mining &Eng., 49(11), 213-230.

Rimifriu, Lucanu, M. Aghion, C. Ursaru, O. (2003). "Control With Microcontroller For PWM Single-Phase Inverter," IEEE, "Gh. Asachi" Technical University of Iasi, Faculty of Electronics and Telecommunications, Bd. Carol I, no. 11, Iasi, 700537 Romania.

Sen, P.C.and K.H.J.Ma.(1975). "Rotor Chopper Control for Induction Motor Drive: TRC Strategy,"IEEE Trans. Ind. Appl., 11(1), 43-49.

Sen, P.C.(1990). "Electric Motor Drives And Control-Past, Present & Future" IEEE Transaction of industrial Electronics, 37(6), 317-328.

Semikron,(1997/1998) Power Electronics Data Manual,

Shepherd, W. and Stan way, J. (1969). "Slip Power Recovery in an Induction Motor by the use of A Thyristor Inverter." IEEE Transaction on Industry and General Applications, 5(1), 74-82.

SimPowerSystems for Use with Simulink, MathWorks Inc., MATLAB7.10, "Simulink 7.10 /SimPowerSystems," The Math Works Inc.,1984-2010.

Singh, B. K. and Naik, K. B. (2001). "Design Of Microprocessor Based Closed-Loop Slip Power Recovery Control Of Slip Ring Induction Motor Drive." Proc.Of PowerSystemsand ControlDrive,1, 49-52.

Smith,G.A. and Nigim, K.A. (1981). "Wind-energy recovery by a static Scherbius induction generator,"IEE Proc., 128(6), 317-324.

Smith,R. L. and Stratford, R. P. (1984). "Power System Harmonics Effects From Adjustable –Speed Drives."IEEE Trans. Industrial Appl., 20 (4), 973-77.

Srichander, R. and Datta, K. B. (1994). "Design of a microprocessor based slip power recovery drive." Journal of Electrical Machine and Power System, 22, 339-354.

SrinivasulaTadisetty and Gupta, R. N. (2006). "Frequency Control System For Improving Efficiency Of Conventional Coal Mine Hauler Efficiency." Proc. of 1st Asian Mining Congress, India the Mining Geological and Metallurgical institute of India (MGMI), Kolkata, 141-145.

Srivatsa. G, Prashanth. V. Joshi (2015) "Review on Energy Efficient Drive of an Induction Motor",India International Journal for Technological Research in Eng, 2(6), 218-227.

SaffetAyasun and Chika O. Nwankpa,(2005). "Induction Motor Tests UsingMATLAB/Simulink And Their Integration Into Undergraduate ElectricMachinery Courses," *IEEE Transactions on Education*, 48(1), 165-169.

Takahashi,I and Ohmori, Y.(1989). "High Performance Direct Torque Control of an Induction Motor,"IEEE Trans. Ind. Appl., 25(2), 257-264.

Texas Instruments,(1981) The Interface Circuits Data Book for Design Engineers

U.S Energy Information Administration. International Energy Outlook 2009: World Energy and economic Outlook; 2009,179-189.

Weiss,H.W.(1974)."Adjustable Speed AC Drive Systems for Pump and Compressor Applications." IEEE Trans. Ind. Appl., 10(1), 162-167.

Wani, N. S. (1978). "ThyristorController For Slip Ring Induction Motor." Ph.D. Thesis, Department of Electrical Engineering, IIT Kanpur.

Wakabayashi,T. Hori, N. Shimzu, K. and Yoshioka, T. (1976). "Commutatorless Kramer Control System for Large Capacity Induction Motors for Driving Water Service Pumps," Conf. Rec. IEEE/IAS Anual Meet, 822-828.

Wakabayashi,T. Hori, N. Shimzu, K. and Yoshioka, T. (1976). "Commutatorless Kramer Control System for Large Capacity Induction Motors for Driving Water Service Pumps," Conf. Rec. IEEE/IAS Anual Meet, 822-828.

BOOKS

Bhimra,P.S.(2004)." Slip recovery schemes – electrical drives power electronics" khanna publication. 201-204.

Krishnan, R. (2001). "Electric motor drives modeling analysis and control", Prentice Hall PTR, Prentice-Hall, Inc., 282–308.

Kereline, N.T .(1999). "Mining Transport Engineering" IIT khragpur. 189-193.

Leonharn, W. (1985) "Control of electrical drives." Springer-Verlag, Berlin, 245–259.

Mohammad Salah .(2002). "Mechatronics Engineering" .Khanna publication.98-99

Muhammad H. Rashid.(2008). "Pulse Width Modulated Inverters," Power Electronics: Circuits, Devices, and Applications, 3rd Edition, New Delhi, Prentice Hall of India Private Limited, 224-301.

Parlos,AG. (2001). Introduction to Simulink, In: Department of Mechanical Engineering Student Information Retrieval System Texas A&M University.

Paul C.Krause,OlegWasynczuk, Scott D.Sudhoff,(1998)"Analysis of Machinery and Drive System", second Edition, AJohnwileyandsons.Inc.Publicationw, 198-201

PutriZalilaYaacob and Dr. Abdullah AsuhaimlMohd.Zin,(1993) "Electrical Energy Management in Small and Medium Size Industries", FEE, UTM, K. Lumpur, IEEE TENCON'93/ Beijing.

Rashid ,M.H. (1994)."Power Electronics - Circuits, Devices, with application" . Printice Hall ,India , New delhi.200-208.

Sawhney,A.K. (1992)."A course in electrical machine design", Dhanpatpai & Son.

Tripathy, S. C. (1991). "Electric energy utilization & conservation."Publisher-Tata McGraw-Hill, London.

WEBSITES

Website of BEE, SCCL, Ministry of coal, Ministry of power.

http://www.mathworks.com.

http://www.eia.doe.gov/oiaf/ieo/world.html

http://www.eia.doe.gov/oiaf/ieo/

http://www.eia.doe.gov/oiaf/ieo/industrial.html,

http://www. eia.doe.gov/emeu/aer/eh/total.html [Accessed 20.04.10].

(http://www.planningcommission.nic.in/plans/planrel/fiveyr/welcome.html).

APPENDIX I

TECHNICAL DETAILS OF 150hp SLIP RING INDUCTIONMOTOR:

Type: slip ring induction motor, rpm: 496, Stator voltage: 3.3 kV, rotor voltage: 210 V, Stator current: 33.6 A, Rotor current: 327 A.
TECHNICAL DETAILS OF 150 hp HAULER:

Speed: 8kmph, drum dia: 1600 mm , drum width:1200 mm,Rope dia:26mm ,drum rope capacity: 1500 m,gear ratio:1:28.

TECHNICAL DETAILS OF 3hp SLIP RING INDUCTIONMOTOR:

Stator voltage: 415 V, stator current 6.5 A, (2.25 kW), rpm: 600, Frequency: 50Hz,

Pole: 10, And mechanical specification reduction gear ratio 1:40.

APPENDIX II

FIELD STUDY PROCEDURE FORCALCULATION OF ENERGY

CONSUMPTION OF 150hpUNDERGROUNDHAULAGE DRIVE SYSTEM

(FIELD STUDY)

Case 1: up the gradient drive (Table 3.2).

1) μ_t = coefficient of friction between the car and incline surface is taken as 0.01.

μ_r = coefficient of friction between the rope and incline surface is taken as 1.

2) Weight includes train weight plus weight of man (i.e. weight of the train is 14700 N

+weight of workers 22050 N= 36750 N).

3) The gear ratio of the motor is 1:29.

4) The distance of the train 0.10 km.

5) The cost of electricity is Rs.7 per unit.

6) The radius of the drum: 1600mm, drum width: 1200mm, Rope dia: 26mm
For θ=14.04° (1 in 4)   up the gradient 8th level to 1st level. Mt =36750N, g =9.81 m/s^2,

M_r =294N, μ_t=0.01, μ_r =0.1. Diameter of drum =1600mm.

The total force acting along the inclined plane up the gradient F= 794.3 Nm.

1. Torque $\quad$ = $\quad$ T $\quad$ = $\quad$ F × r = 7943 Nm

2. Shaft Output of motor in kW $\quad$ = $\dfrac{2\pi NT \times 735.5}{4500}$

$$= \dfrac{2\pi \times 14.28 \times 7943 \times 735.5}{4500}$$

$$= 116483.0 W.$$

3. Input power $\qquad\qquad\qquad$ =166320 W.

4. % Efficiency $\quad$ = $\dfrac{output power}{Input power}$x100= 70.03%

5. Energy consumption = 116483.0×22.5 = 0.728 kWh

6. Annual energy consumption = No. of trips per day × No. of days × No. of months

= (8×30×12) ×0.728 k = 2880 ×0.728 k = 2096.6 kWh

Case 2: Down the gradient drive energy consumption calculation 1st level to 8th level drive system (Table 3.1).

For θ=14.04º (1in4) $\quad$ Mt =33320 N, g =9.81 m/s, M_r =294N, μ_t=0.01, μ_r =0.1. Diameter of drum =1600mm.

1. Torque $\quad$ = $\quad$ T $\quad$ = $\quad$ F × r = 6668Nm

2. Shaft Output of motor in kW $\quad$ = $\dfrac{2\pi NT \times 735.5}{4500}$

$$= \dfrac{2\pi \times 14.28 \times 6668 \times 735.5}{4500}$$

$$= 97785.3.0 W.$$

3. Input power $\qquad\qquad\qquad$ = 144000W.

4. % Efficiency $\quad$ = $\dfrac{output power}{Input power}$x100= 67.90%

5. Energy consumption = 144000.0× 18.75 = 0.509kWh

6. Annual energy consumption = (8×30×12) ×0.509k = 2880 × 0.509k = 1465.8 kWh

APPENDIX III

PROCEDURE FORCALCULATION OF ENERGY CONSUMPTION OF 3HP
LABORATORY EXPERIMENTAL HAULAGE DRIVE SYSTEM

1) μt = coefficient of friction between the tub and incline surface is taken as 0.001.

μr = coefficient of friction between the rope and incline surface is taken as 0.1.

2) Weight includes train weight plus load weight (i.e. weight of the tub 392 N + load
is 392 N= Total weight 784 N)

3) The gear ratio of the motor is 1:40 (i.e.N_1 = 530 rpm and N_2= 530/40=13.25 rpm)

4) The distance of the train track remains same i.e. 5m

5) The cost of electricity is Rs.7 per unit.

6) The radius of the drum is0.1 m and 0.2m.

Case 1:For θ=35º up the gradient (Table 4.3).

M_t =1764N, g =9.81 m/s^2, M_r=9.81N, μ_t=0.001, μ_r =0.1.Diameter of drum = 200mm.

The total force acting along the inclined plane up the gradient F= 127.8 Nm.

2. Shaft Output of motor in kW $= \dfrac{2\pi NT \times 735.5}{4500}$

$= \dfrac{2\pi \times 12.7 \times 127.8 \times 735.5}{4500}$

$= 1614.8W.$

3. Input power $= 2188.8W.$

4. % Efficiency $= \dfrac{output power}{Input power} \times 100 = 73.77\%$

5. Energy consumption $= \dfrac{1614.8 \times 27}{3600} = 0.01211kWh.$

6. Annual energy consumption = (Number of trip× number of days × number of

months) $= 10 \times 30 \times 12 \times 0.01211k = 3600 \times 0.01211k = 43.596$ kWh.

Case 2: For θ=35° Down the gradient (Table 4.2). M_t =1764N, g =9.81 m/s^2, M_r =1kgs, μ_t=0.001, μ_r =0.1. Diameter of drum = 200mm.

The total force acting along the inclined plane up the gradient F= 126.4 Nm.

2. Shaft Output of motor in kW $= \dfrac{2\pi NT \times 735.5}{4500}$

$= \dfrac{2\pi \times 12.74 \times 126.4 \times 735.5}{4500}$

$= 1613.5\text{W}.$

3. Input power $= 2188.6\text{W}.$

4. % Efficiency $= \dfrac{outputpower}{Inputpower} \times 100 = 73.72\%$

5. Energy consumption $= \dfrac{1613.8 \times 25}{3600} = 0.01120\text{kWh}.$

6. Annual energy consumption = 10x30x12 =3600 ×0.01120k = 40.32 kWh.

APPENDIX IV

PROCEDURE FORCALCULATION OF ENERGY CONSUMPTION OF 3HP LABORATORY MICRO CONTROLLER BASED EXPERIMENTAL HAULAGE DRIVE SYSTEM.

1) μ_t = coefficient of friction between the tub and incline surface is taken as 0.001.

μ_r = coefficient of friction between the rope and incline surface is taken as 0.1.

2) Weight includes train weight plus load weight (i.e. weight of the tub 392N +

load 392 N=Total weight 784N)

3) The gear ratio of the motor is 1:40 (i.e.N_1 = 530rpm then N_2 = 530/40=13.25rpm)

4) The distance of the train track remains same i.e. 5m

5) The cost of electricity is Rs.7 per unit.

6) The radius of the drum is 0.1m and 0.2m.

Case 1: For θ=27° up the gradient (Table 4.2).
M_t =1074N, g =9.81 m/s^2, M_r =9.8N, μ_t=0.001,
μ_r =0.1 diameter of drum = 200 mm.

The total force acting along the inclined plane up the gradient F= 70.0 Nm.

2. Shaft Output of motor in kW $= \dfrac{2\pi NT \times 735.5}{4500}$

$$= \dfrac{2\pi \times 14.15 \times 70 \times 735.5}{4500}$$

$$= 1017.2 \text{ W.}$$

3. Input power $= 1621\text{W.}$

4. % Efficiency $= \dfrac{output\,power}{Input\,power} \times 100 = 62.75\%$

5. Energy consumption $= 1621 \times 20 = 0.00565$ kWh.

6. Annual energy consumption $= 3600 \times 0.00565 \text{ k} = 20.3\,4$ kWh.

7. Annual energy cost $= 20.34$ kWh$\times 7 =$ Rs.142.8

8. Power recovered $= 41.7$ W

Case 2: For $\theta = 27^{\circ}$ Down the gradient.(Table 4.4)

Mt $=1078$N, g $=9.81$ m/s^2, Mr $=9.8$N,
$\mu_t = 0.001$,

$\mu_r = 0.1$ Diameter of drum $= 200$mm.

The total force acting along the inclined plane up the gradient F$= 69.10$ Nm.

2. Shaft Output of motor in kW $= \dfrac{2\pi NT \times 735.5}{4500}$

$$= \dfrac{2\pi \times 14.2 \times 69.10 \times 735.5}{4500}$$

$$= 1007\text{W.}$$

3. Input power $= 1567\text{W.}$

4. % Efficiency $= \dfrac{output\,power}{Input\,power} \times 100 = 64.75\%$

5. Energy consumption $= 1567 \times 18 = 0.00503$ kWh.

6. Annual energy consumption $=$ (Number of trip$\times$ number of days $\times$ number of months)

$$= 10 \times 30 \times 12 = 3600 \times 0.00503\text{k} = 18.12 \text{ kWh.}$$

7. Annual energy cost $= 18.12$ kWh $\times$ Rs.7 $=$ Rs.126.84

8. Power recovered $=$ Micro controller method power output - Conventional method

Power output $= 1007.00 - 937.10 = 69.9$ W (Table 7.9).

APPENDIX V

The block diagram of AT Mega32 (AVR) – 8 – bit Microcontroller

Block Diagram - ATmega32(AVR) - 8-bit Microcontroller

www.CircuitsToday.com
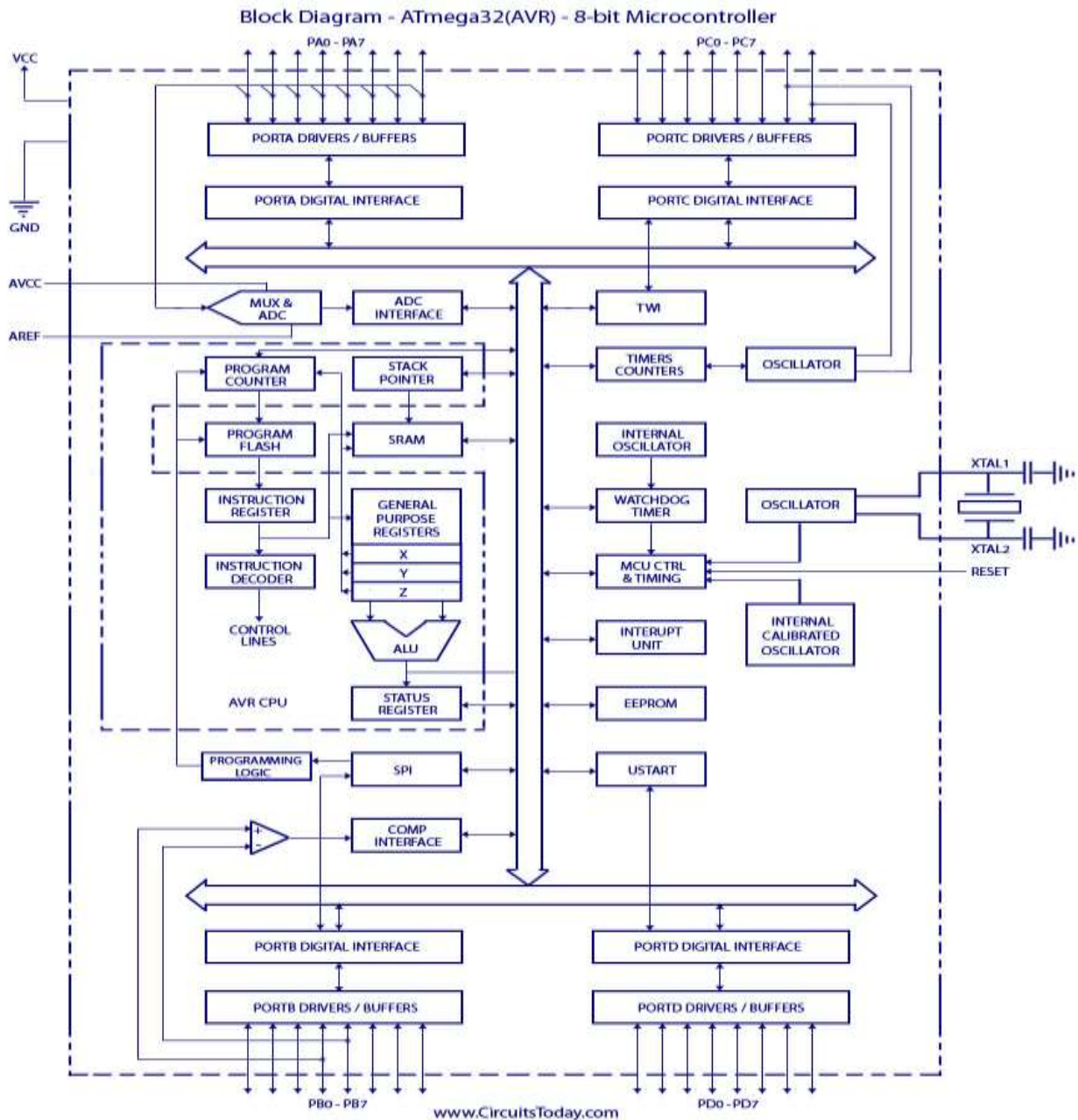
Case 1: PWM GENERATION CODE PROGRAMMING IGBT INVERTER

```
/* Pseudo Code */
flag=0;
//pwm initialization code
while(flag!=1)
{
//pwm code
pwm_value+=delta //delta is the steps of increase in speed
//motor running at pwm value
for(i=0;i<10;i++)
{
//check if switch pressed, if pressed set flag=1 and exit for loop
//small delay loop
}
final_pwm=pwm_value;
}
//run motor at final_pwm
```

Let me know in case of any more doubts

```
II./* Program used for bidirectional motor drive
* Motor is connected between PB0 and PB1 through proper buffers
 * If PD0 is made high, the motor will rotate forward, else it rotates backwards */
#include <avr/io.h> //standard include for ATMega32
#define sbi(x,y) x |= _BV(y) //set bit
#define cbi(x,y) x &= ~(_BV(y)) //clear bit
#define tbi(x,y) x ^= _BV(y) //toggle bit
#define is_high(x,y) (x & _BV(y)) == _BV(y) //(for input) checks if the input is high
(Logic 1)
int main(void)
{
    DDRB=0xff; //PORTC as OUTPUT
```

```c
    PORTB=0x00;

    DDRD=0x00; //PORTD as INPUT

    PORTD=0xff; //To enable internal pullups
while(1==1) //Infinite loop

    {
if(is_high(PIND,PD0))

        {
sbi(PORTC,PB0); //  Motor runs forward when tub reach the dead end
cbi(PORTC,PB1);

        }
else

        {
sbi(PORTC,PB1); //Now runs backwards with time delay  of 5 minutes
cbi(PORTC,PB0);

        }

    }
return 0; }
```

Case 2: C CODE FOR MOTOR RUNNING BI-DIRECTIONAL

```c
* Motors are connected to PORTB (PB0-PB3)

*/#include <avr/io.h>                    //standard i/o functions for ATMega32

#include <util/delay.h>        //delay functions for ATMega32

voidfun_delay(void)

{             for(int i=0;i<5;i++)

_delay_s(300);

}

int main(void)

{

DDRB=0xff;                     //All pins of PORTC assigned as OUTPUT

PORTC=0x00;                    //All pins made to exhibit LOW state initially

while(1)                 //Infinite loop

{

//BOT Moves Forward – Motors in Forward Direction
```

```
PORTC=0x0A;              //0b00001010
fun_delay();
//BOT Moves Backward – Motors in Backward Direction
PORTC=0x300;             //0b00000101
fun_delay();
//BOT Moves Right – LM-Forward and RM-Stop
PORTB=0x02;              //0b00000010
fun_delay();
//BOT STOPS
PORTC=0x00;              fun_delay();
}
return 0;
}
//end of code
```

III. Code for Reading the Sensor Inputs

* Sensors are connected to PORTA (PA0-PA7)

* LEDs are connected to PORTB (PB0-PB3)

*/

```
#include <avr/io.h>                    //standard i/o functions for ATMega 32
#include <util/delay.h>       //delay functions for ATMega32
int main(void)
{
DDRA=0x00;
PORTA=0xff;                      //enabling the pull-ups
DDRB=0xff;                       //All pins of PORTB assigned as OUTPUT
while(1)                  //Infinite loop
{
PORTB=PINA;          // displays all 8 pin values from PORTA on PORTB
}
return 0;
}
//end of code
```

RF TRANSMITTER AND RF RECEIVER DETAILS
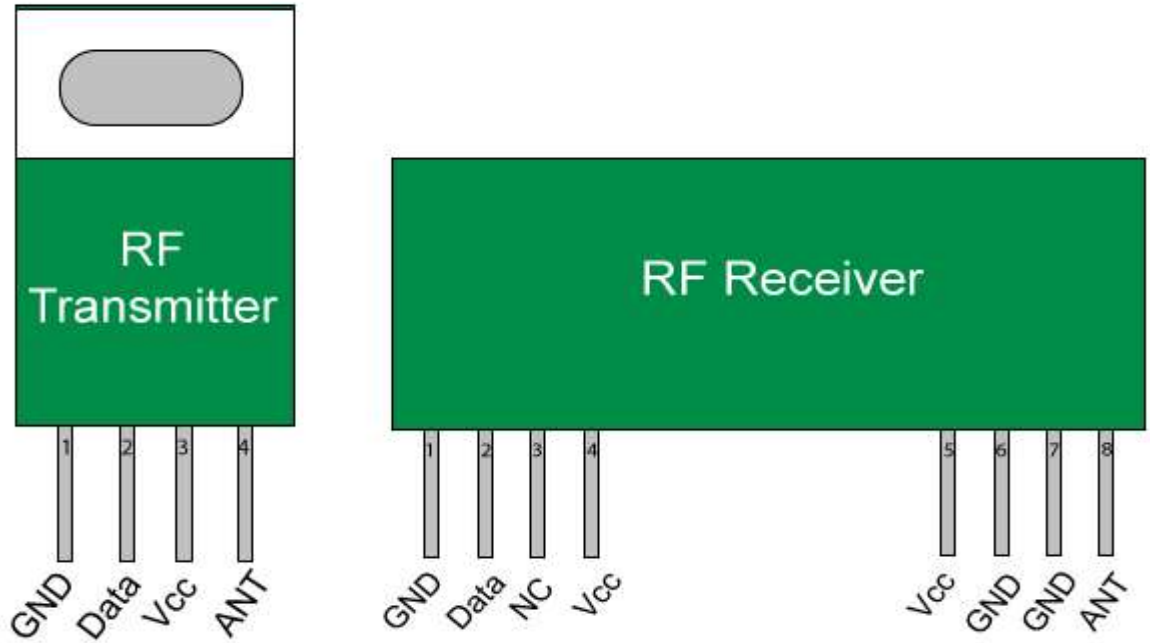
Features

- Distance in open place (Standard Conditions) : 100 Meters
- RX Receiver Frequency : 433 MHz
- RX Typical Sensitivity : 105 Dbm
- RX Supply Current : 3.5 mA
- RX IF Frequency : 1MHz
- Less Energy Consumption
- Usage is easy
- Operating Voltage Of RX : 5V
- Frequency Range of TX: 433.92 MHz
- Rating of Voltage supply : 3V ~ 6V
- Power Out Put of TX : 4 ~ 12 Dbm

APPENDIX VIII

THE SERIAL FLOW DATA PROCESS FOR BI -DIRECTIONAL MOTOR.

RF Transmitter 433 MHz	→ Serial Data →	RF Receiver 433 MHz
↑		↓
Serial Data		Serial Data
↑		↓
Encoder IC HT12E		Decoder ICHT12E
↑		↓
Parallel Data (Control)		Parallel Data
		↓
		Not Gate (7404)
		↓
		Bi Directional Motor Driver
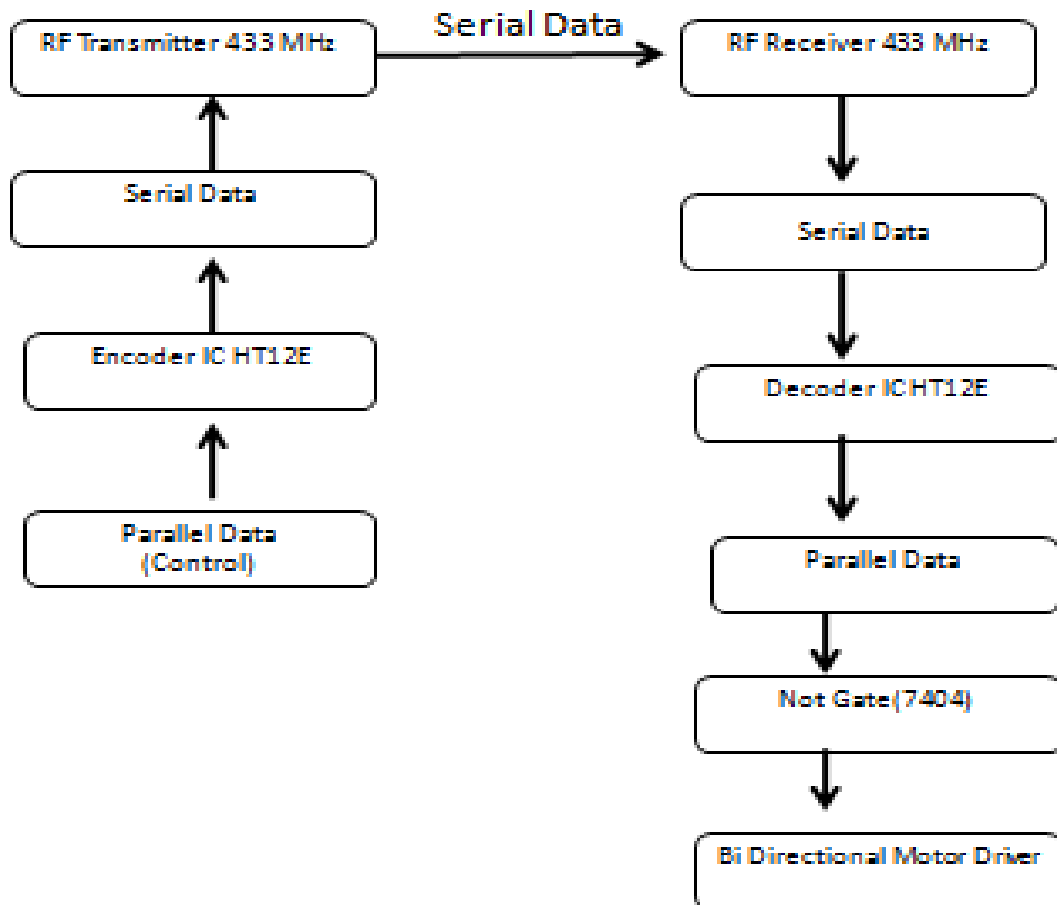
APPENDIX IX

MATLAB DATA FILES
C.1 Machine Parameters used for Simulation
%%%%%%%%%%%%%%%%%%%%%%%%%%%%%%%%
% %
% Data file for simulation of 3hp experimental haulage drive system
% of wound rotor induction motor with stator connected %
% %%%%%%%%%%%%%%%%%%%%%%%%%%%%%%%
% 3ph Source
%%%%%%%%%%%%%%%%%%%%%%%%%%%%%%%%
% Supply to stator of WRIM and rotor is connected by resistance stator
%
%%%%%%%%%%%%%%%%%%%%%%%%%%%%%%%%
% Wound Rotor Induction Machine Parameters.
%%%%%%%%%%%%%%%%%%%%%%%%%%%%%%%%
3HP EXPERIMENTAL WOUND ROTOR INDUCTION MOTOR HAULAGE

DRIVE SYSTEM INPUT PARAMETER FOR SIMULATION.

Rating 2.2 kW, speed 600rpm, 50 Hz frequency, No of pole 10, speed reduction 1:40

Matlab data file for 3hp Experimental haulage drive system with.

M_t=1372N;   % weight of car + weight of material%

θ=35˚;   % angle with horizontal %

M_r=29N;   % weight of rope%

Q_r=0.1;   % coefficient of friction between the tub and incline surface %

R_t=0.01;   % coefficient of friction between the rope and incline surface %

g=9.81m/s^2;   % gravitational force %

V=405 V;   % supply voltage %

 I=3.7 A;   % stator current %

T=24 Nm;   % Time taken to complete each level trip %

150hp underground haulage drive system input parameter for simulation

M_t= 36750N;   % weight of car + no of person%

θ=14.04˚;   % angle with horizontal %

M_r=294N;   % weight of rope%

Q_r=.1;   % friction between track and tub%

   R_t=0.001;   % coefficient of friction between the rope and incline surface %

g=9.81 m/s^2;   % gravitational force %

V=3150 V;   %Input voltage %

I=23.5 A;   % Input current %

 T=830 Nm;   %Load torque N-m %

APPENDIX X

PROCEDURE FORCALCULATION OF ENERGY CONSUMPTION OF 150HP UNDERGROUND CONVENTIONAL METHOD HAULAGE DRIVE SYSTEM (simulation study).

Case 1: Up the gradient drive (Table 6.5).

1) μ_t = coefficient of friction between the car and incline surface is taken as 0.001.

μ_r = coefficient of friction between the rope and incline surface is taken as 1

2) Weight includes train weight plus weight of man (i.e. weight of the train is 14700 N +   weight of person 22050 N=total weight 36750 N)

3) The gear ratio of the motor is 1:29

4) The distance of the train 0.10 Km

5) The cost of electricity is Rs.7 per unit.

6) The radius of the drum diameter: 1600mm, drum width: 1200mm, Ropedia: 26mm

Case1: Simulated experimental case study results from surface to 8L. Down the gradient.

For $\theta = 14.04°$ (1 in 4)   up the gradient 8th level to 1st level. $M_t = 33320$ N,

$g = 9.81 \text{m/s}^2$, $M_r = 294$N, $\mu_t = 0.01$, $\mu_r = 0.1$. Diameter of drum $= 1600$mm.

The total force acting along the inclined plane up the gradient F= 6668 Nm.

1. Torque   =   T   = $F \times r = 6668$ Nm

2. Shaft Output of motor in kW $= \dfrac{2\pi NT \times 735.5}{4500}$

$= \dfrac{2\pi \times 14.28 \times 7943 \times 735.5}{4500}$

$= 97500.0$ W.

3. Input power $= 144000$ W

4. % Efficiency $= \dfrac{output power}{Input power} \times 100 = 67.71\%$

5. Energy consumption $= 116483.0 \times 22.5 = 0.507$ kWh

6. Annual energy consumption $= 2880 \times 0.507k = 1464.216$ kWh

Case 2: Simulated field study results 150hp surface hauler (up the gradient) from 8l to surface level.

For $\theta = 14.04°$ (1 in 4) $M_t = 36750$ N, $g = 9.81 \text{ m/s}^2$, $M_r = 294$N, $\mu_t = 0.01$, $\mu_r = 0.1$. Diameter of drum $= 1600$mm.

The total force acting along the inclined plane up the gradient F= 666.8 Nm.

1. Torque   =   T   = $F \times r = 7943$Nm

2. Shaft Output of motor in kW $= \dfrac{2\pi NT \times 735.5}{4500}$

$= \dfrac{2\pi \times 14.29 \times 7943 \times 735.5}{4500}$

$= 113541$W.

3. Input power $= 153846$W.

4. % Efficiency $= \dfrac{output power}{Input power} \times 100 = 73.80\%$

5. Energy consumption $= 113541 \times 22.5 = 709.64$kWh **(Table 6.5)**

6. Annual energy consumption $= 8 \times 30 \times 12 \times 709.64 = 2880 \times 709.64k = 2043763.2$Wh

NO LOAD SIMULATION PARAMETERS FOR 150HP SLIP RING INDUCTION MOTOR.

The 150Hp slip ring induction motor machine simulated electrical parameter
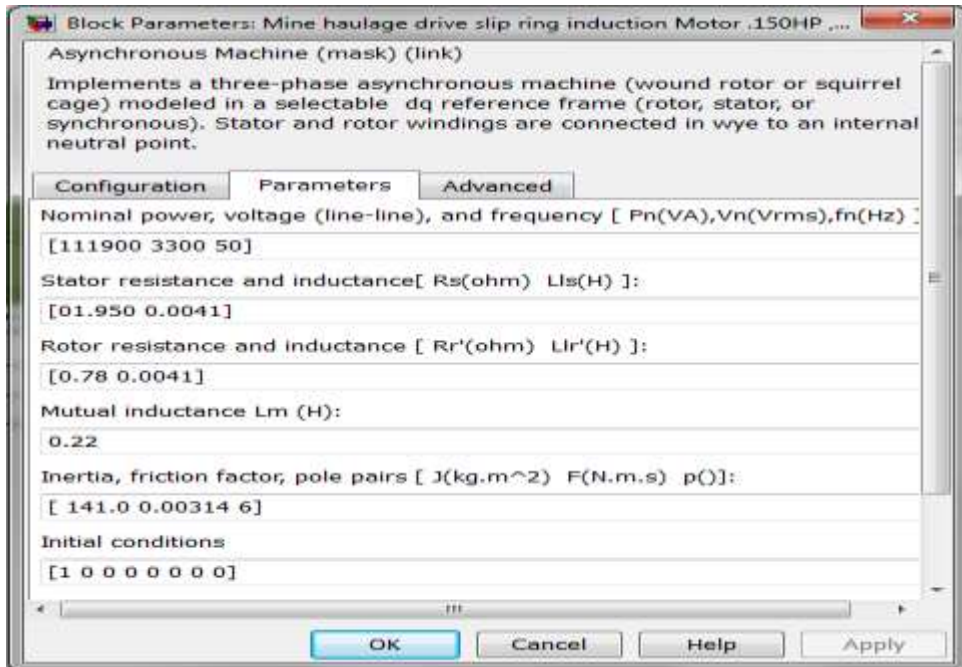
The 3hp slip ring induction motor machine simulated electrical parameter

3hp experimental diode bridge simulated electrical parameter

3hp experimental recovery transformer simulated electrical parameter

150hp micro controller study recovery transformer simulated electrical parameter

Block Parameters: recovery transformer

Three-Phase Transformer (Two Windings) (mask) (link)

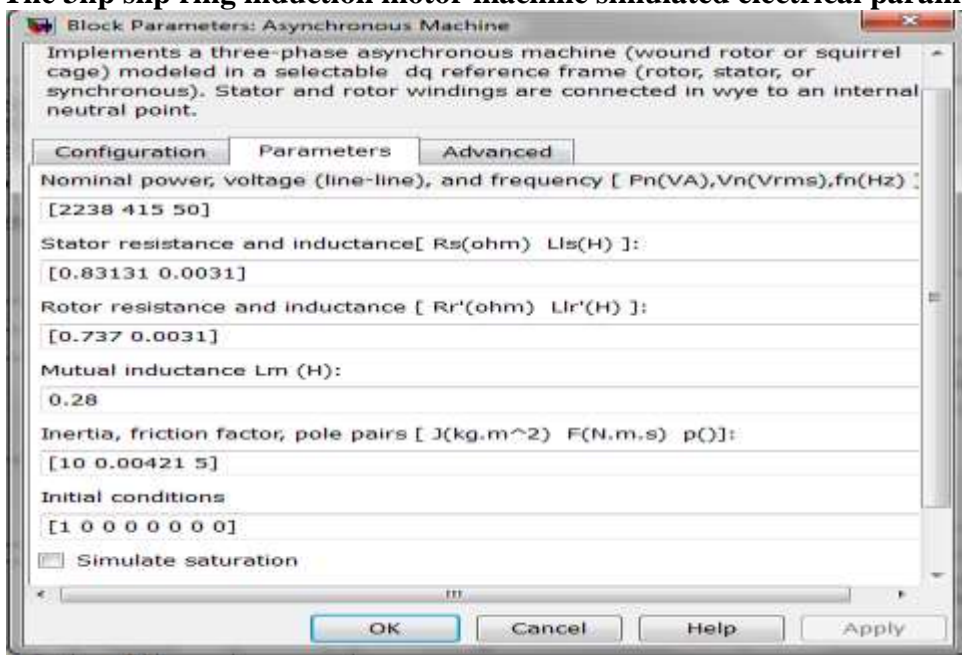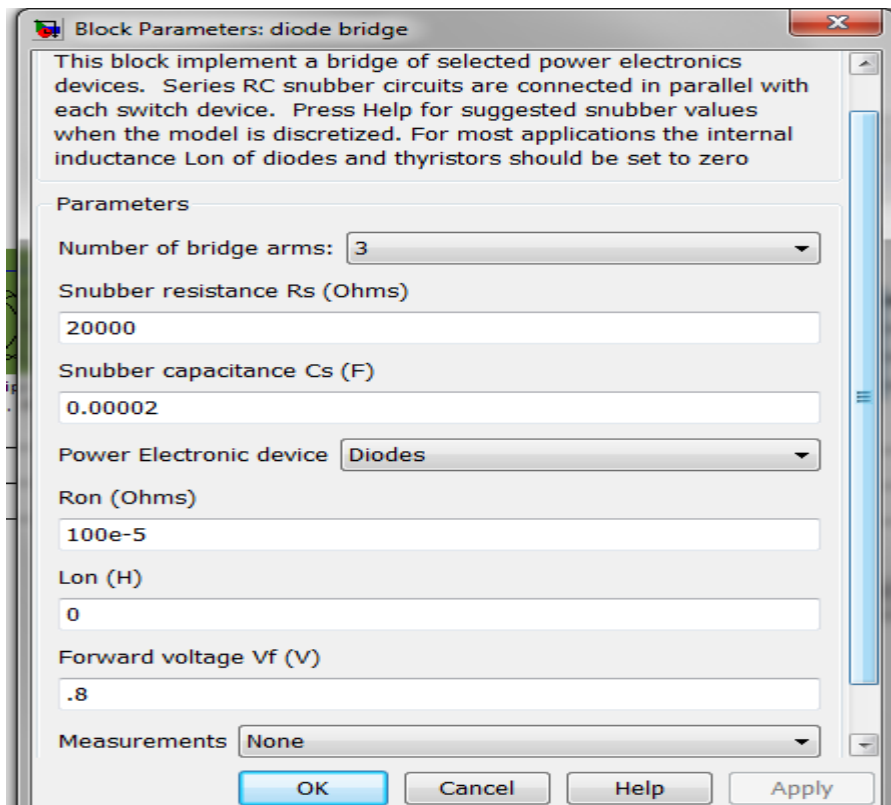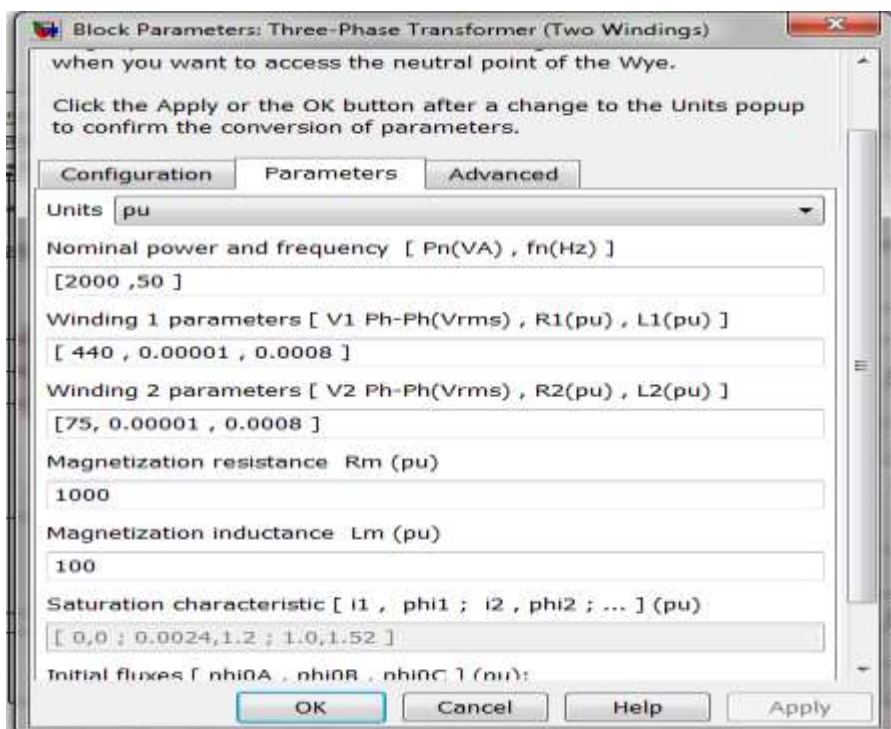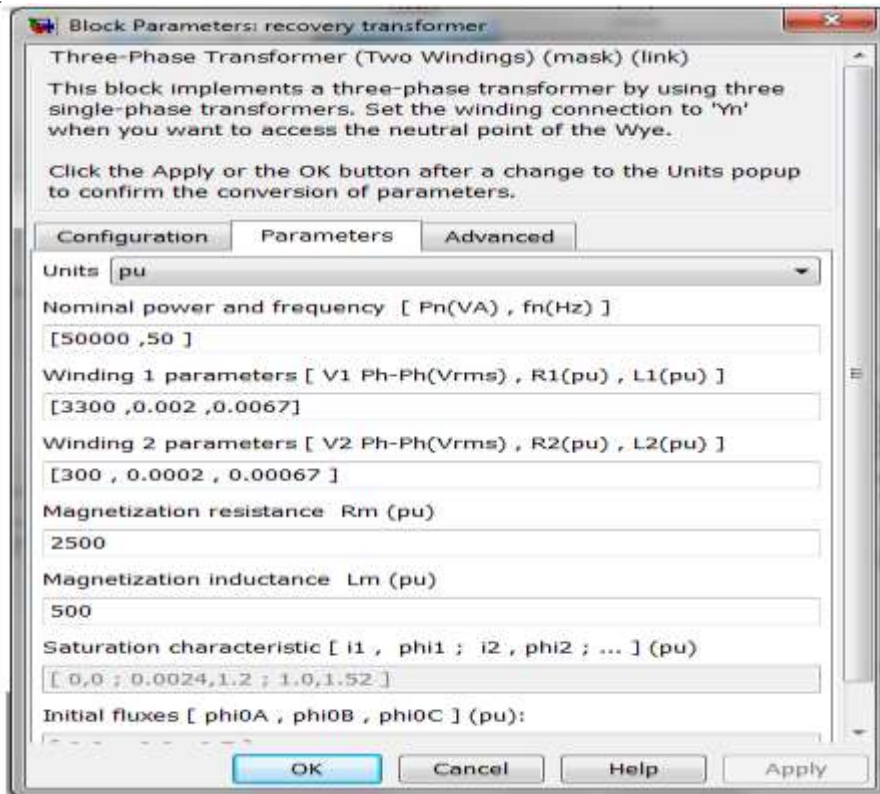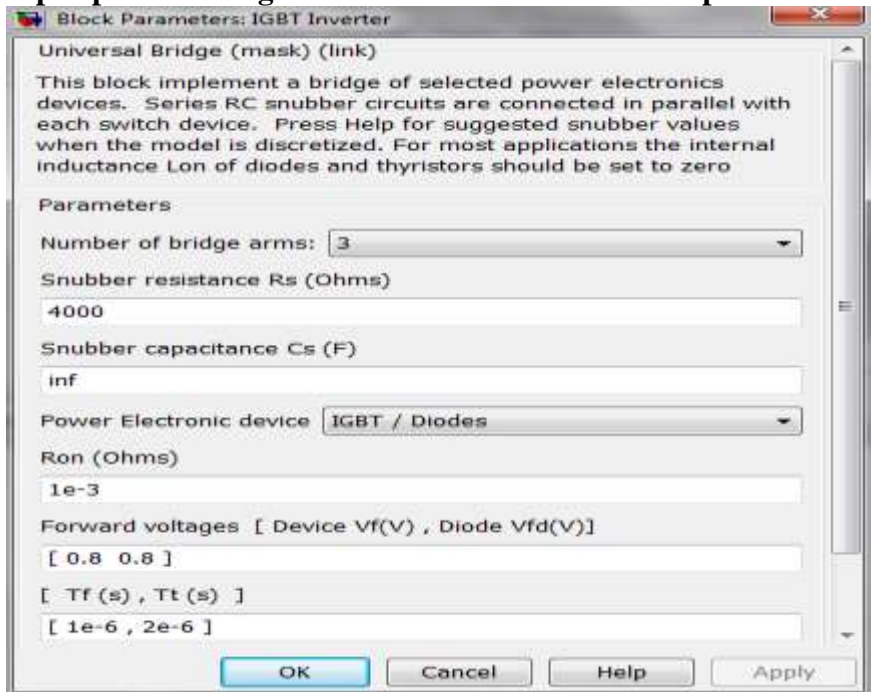This block implements a three-phase transformer by using three single-phase transformers. Set the winding connection to 'Yn' when you want to access the neutral point of the Wye.

Click the Apply or the OK button after a change to the Units popup to confirm the conversion of parameters.

| Configuration | Parameters | Advanced |

Units [pu]

Nominal power and frequency [Pn(VA) , fn(Hz)]
[50000 ,50]

Winding 1 parameters [V1 Ph-Ph(Vrms) , R1(pu) , L1(pu)]
[3300 ,0.002 ,0.0067]

Winding 2 parameters [V2 Ph-Ph(Vrms) , R2(pu) , L2(pu)]
[300 , 0.0002 , 0.00067]

Magnetization resistance Rm (pu)
2500

Magnetization inductance Lm (pu)
500

Saturation characteristic [i1 , phi1 ; i2 , phi2 ; ...] (pu)
[0,0 ; 0.0024,1.2 ; 1.0,1.52]

Initial fluxes [phi0A , phi0B , phi0C] (pu):

[OK]   [Cancel]   [Help]   [Apply]

3hp experimental igbt inverter simulated electrical parameter

Block Parameters: IGBT Inverter

Universal Bridge (mask) (link)

This block implement a bridge of selected power electronics devices. Series RC snubber circuits are connected in parallel with each switch device. Press Help for suggested snubber values when the model is discretized. For most applications the internal inductance Lon of diodes and thyristors should be set to zero

Parameters

Number of bridge arms: [3]

Snubber resistance Rs (Ohms)
4000

Snubber capacitance Cs (F)
inf

Power Electronic device [IGBT / Diodes]

Ron (Ohms)
1e-3

Forward voltages [Device Vf(V) , Diode Vfd(V)]
[0.8 0.8]

[Tf (s) , Tt (s)]
[1e-6 , 2e-6]

[OK]   [Cancel]   [Help]   [Apply]

APPENDIX XII

PROCEDURE FORCALCULATION OF ENERGY CONSUMPTION OF 150HP UNDERGROUND MICRO CONTROLLER METHOD (SIMULATION STUDY) HAULAGE DRIVE SYSTEM

Case 1: Up the gradient drive.

1) μ_t = coefficient of friction between the car and incline surface is taken as 0.01.

μ_r = coefficient of friction between the rope and incline surface is taken as 1

2) Weight includes train weight plus weight of man (i.e. weight of the train is 14700

N + weight of workers is18620N= Total weight 33320 N)

3) The gear ratio of the motor is 1:29

4) The distance of the train 0.10 Km

5) The cost of electricity is Rs.7 per unit.

6) The radius of the drum is drum diameter: 1600mm, drum width: 1200mm, Rope Diameter: 26mm

**Case 1: 150 hpunderground haulage drive system from surface to 8L.
(Down thegradient) (Table 6.11).**

For θ=14.04º,M_t =33320 N, g=9.81 m/s^2,M_r =294 N, μ_t=0.01, μ_r =0.1.

Diameter of drum =1600mm.

The total force acting along the inclined plane up the gradient F= 6668 Nm.

1. Torque $\quad = \quad$ T $\quad = \quad$ F × r $\quad = \quad$ 6668 Nm

2. Shaft Output of motor in kW $\quad = \quad \dfrac{2\pi NT \times 735.5}{4500}$

$$= \dfrac{2\pi \times 14.28 \times 7943 \times 735.5}{4500}$$

$\quad = 11005$W (Table 6.11).

3. Input power $\qquad\qquad = 136800$W (Table 6.11).

4. % Efficiency $= \frac{outputpower}{Inputpower}$ x100 $= 80.44\%$ (Table 6.11)

5. Energy consumption $= 11005 \times 16 = 0.489$ kWh (Table 6.11)

6. Annual energy consumption = No. of trips per day $\times$ No.of days $\times$ No.of months

$$= 8 \times 30 \times 12$$

$$= 2880 \times 0.489k = 1408kWh \text{ (Table 6.11)}$$

7. Power recovered = (Conventional method output power − Micro control

Method output power) = (110052 W- 97785.30 W)

$$= 12265W \text{ (Table 7.10)}$$

Case 2: 150hp underground surface hauler (up the gradient) from 8th to surface level.

For $\theta = 14.4°$ $M_t = 36750N$, $g = 9.81$ m/s^2, $M_r = 274N$ $\mu_t = 0.01$, $\mu_r = 0.1$.
Diameter of drum $= 1600$mm.

The total force acting along the inclined plane up the gradient F= 794.3 Nm.

1. Torque $=$ T $= F \times r = 7943Nm$

2. Shaft Output of motor in kW $= \frac{2\pi NT \times 735.5}{4500}$

$$= \frac{2\pi \times 14.28 \times 7943 \times 735.5}{4500}$$

$$= 129639.0W \text{ (Table 6.12)}.$$

3. Input power $= 15120$ W (Table 6.12).

4. % Efficiency $= \frac{outputpower}{Inputpower}$ x100$= 85.74\%$ (Table 6.12).

5. Energy consumption $= 144000.0 \times 18.75 = 0.612$ kWh (Table 6.12).

6. Annual energy consumption $= 2880 \times 0.509$ k $= 1763$ kWh (Table 6.12).

7. Power recovered = (Conventional method output power − Micro control

Method output power)

$$= (129639 \text{ W- } 116483.0 \text{ W}) = 13156 \text{ W (Table 7.10)}.$$

BIODATA

1. Name :Ganapathi.D.Moger

2. Father's Name :Devajji.M.Moger

3. Date of Birth :22-07-1968

4. Nationality : Indian

5. Marital Status : Married

6. Present Position :Associate professor .

7. Address for Communication: Department of Electrical and Electronics Engineering,East point college of Engineering,BangaluruK.R.Pura,K Karnataka, India.

 8. Mobile : +91-9449193943

9. E-mail :mogergdm@gmail.com

10. Academic Qualifications:

Degree	University/ Board	Year of awarding degree
Ph.D in Mining Engineering	N.I.T.K, Surathkal	Pursuing
M.Tech (Power and nergy system)	N.I.T.K, Surathkal (K.R.E.C)	2001
B.E ,Electrical& Electronics Engg.	N.I.T.K, Surathkal (K.R.E.C)	1992

11. Publications: Total No.

National Journals:2

National Seminars: 5

International Conferences: 2

International Journals: 4